

PERMEABILITY PATHWAYS IN THE CANADIAN
RIVER ALLUVIUM ADJACENT TO THE
NORMAN LANDFILL, NORMAN,
OKLAHOMA

By

KELLI LYNN COLLINS

Bachelor of Science

Oklahoma State University

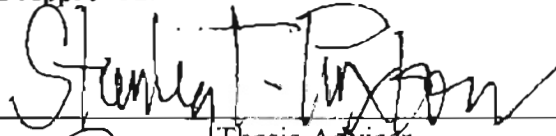
Stillwater, Oklahoma

1998

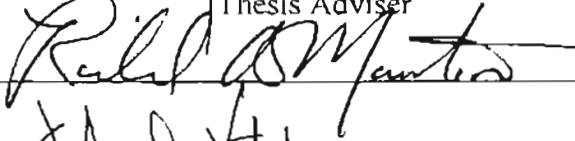
Submitted to the Faculty of the
Graduate College of the
Oklahoma State University
in partial fulfillment of
the requirements for
the Degree of
MASTER OF SCIENCE
December, 2001

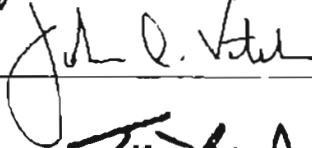
PERMEABILITY PATHWAYS IN THE CANADIAN
RIVER ALLUVIUM ADJACENT TO THE
NORMAN LANDFILL, NORMAN,
OKLAHOMA

Thesis Approved:



Thesis Adviser







Dean of the Graduate College

ACKNOWLEDGMENTS

I would like to thank the U.S. Geological Survey, Oklahoma District Office, and the Environmental Institute/Oklahoma Water Resources Research Institute at Oklahoma State University for providing funding for this project. The funds were awarded under the 2000-2001 Annual Cooperative Program of the Oklahoma Water Resources Research Institute.

A major contributor to the success of this project was Scott Christenson, Project Manager with the U.S. Geological Survey, Oklahoma District Office. Scott provided training and technical support on the Geoprobe®, the main piece of equipment used in the study. Scott also collected and provided GPS data for all of the sample sites at the Norman Landfill. Scott was always available to provide assistance and current information about research at the site. Dale Ferree also provided valuable field support and helped with data collection.

A huge thanks goes to my main thesis advisor, Dr. Stanley Paxton, who provided guidance and untiring support. Without his intelligent supervision this project would not have been such a success. My sincere appreciation extends to my other committee members Dr. Richard Marston and Dr. John Vitek, whose constructive guidance and encouragement greatly aided me in the completion of this project.

Important field assistance with acquiring cores and conductivity logs was provided by Tom Kropatsch, Jerrod Smith and Barbara Pickup. Barbara also assisted

with core descriptions and data analysis. Her support is truly appreciated. Marlene Collins and Coleman Smith performed the sieve analyses. Brian DeHay helped create some of the maps and figures for the project. Brian also spent numerous hours working on corrections and helping reformat the figures. His help has been invaluable.

A special thanks goes to my family who have always supported me. My mother, Jan Collins, provided emotional support and was always available to help when I needed her. I would like to dedicate this thesis to my father, Tony Collins, who never stopped believing in me. His encouragement through the years will never be forgotten.

TABLE OF CONTENTS

Chapter	Page
I. Introduction.....	1
Goals and Objectives.....	2
Study Area.....	3
II. Literature Review.....	5
Investigations at the Norman Landfill.....	5
Direct Push Technology.....	6
Resistivity Study of Alluvial Deposits.....	6
Permeability Equations and Size Distribution Parameters.....	7
III. Methodology.....	8
Obtaining Conductivity Logs and Cores.....	8
Conductivity Logs.....	8
Continuous Core.....	13
Core Description.....	15
Texture Analysis of Core Samples.....	16
Texture-Permeability Equations.....	19
Interpretation of Conductivity Logs for Texture and Generation of 3-D Block Diagrams.....	19
IV. Results and Discussion.....	23
Description of Sedimentary Features.....	23
Criteria for Correlation the Conductivity Logs.....	30
Cross Sections of Conductivity Logs.....	43
Vertical Profiles and Interval Units for Correlation.....	46
Calculated Permeabilities Relative to Stratigraphic Intervals.....	53
Permeability and Fining Upward Profile of Fluvial Sediments.....	58
Block Diagrams.....	64
V. Conclusions.....	75
Recommendations.....	77

References.....	80
Appendix A: Core Descriptions.....	82
Appendix B: Core Photos.....	102
Appendix C: Cumulative Grain Size Curves.....	164
Appendix D: Cross Sections.....	184
Appendix E: Sieve Sample Depths.....	198



LIST OF FIGURES

Figure	Page
1. Location of data collection sites at Norman Landfill.....	4
2. Schematic showing truck with tool.....	9
3. The USGS Geoprobe in action.....	11
4. Cross-section lines of conductivity logs.....	12
5. Schematic showing mc core catcher with liner, macrocore piston rod sample.....	14
6. Examples of cumulative curves used for estimating graphic mean and standard deviations for use in the permeability prediction equations.....	17
7. Plot of porosity vs permeability based on raw data of Beard and Weyl	21
8. Cores from well #1 showing sand / mud layers and mud clasts.....	24
9. Cores from well #3 showing layers, mud clasts, and the underlying Hennessey Formation.....	26
10. Cores from well #7 showing sand / mud layers and gravel at the basal contact with the Hennessey.....	28
11. Cores from well #46 showing sand / mud layers, trough cross bedding, fining upward cycles, and gravel intervals that have high calculated permeability.....	31
12. A portion of the Canadian River Floodplain that has been incised and abandoned.....	36
13. Ripples on the surface of a series of large advancing dunes	

in the Cimarron River of Oklahoma.....

14. Cross bedding in a stacked unit bar that has migrated right to left in the Canadian River near Norman, O.....
15. Subtle topographic lows on the margins of the main channel accumulate muds that form the discontinuous mud layers seen in the subsurface cores and depicted in the cross sections.....
16. The onlap of sand or mud layers onto stratal surfaces that exhibit relief suggests the basal contact of each correlation unit in the point bar is erosional.....
17. Mudclasts or “rip-ups” commonly occur at or near the base of many of the major sand beds in the Norman Landfill point bar.....
18. Example cross section running perpendicular to the point bar.....
19. Example cross section running parallel to the point bar.....
20. Type conductivity log from the Norman Landfill.....
21. Frequency distributions of mean grain size from sieve data.....
22. Frequency distributions of mean grain sorting from sieve data.....
23. Profiles of calculated permeability from measurement grain size / sorting in the Norman Landfill point bar subsurface intervals.....
24. Frequency distribution of mean permeability calculated from sieve data.....
25. Calculated hydraulic conductivity compared to measured hydraulic conductivity.....
26. Rate of plume movement based upon calculated hydraulic conductivity of each of the sand intervals.....
27. Vertical profiles of grain size, sorting and calculated permeability in Norman Landfill well #1.....
28. Vertical Profiles of grain size, sorting and calculated permeability in Norman Landfill well #2.....

permeability in Norman Landfill well #15.....	63
29. Block diagram of the alluvium intervals. View is from the southwest corner of the study area.....	65
30. Block diagram of the alluvium intervals. View is from the southeast corner of the study area.....	66
31. Block diagram of conductivity values. View is from the southeast corner of the study area.....	67
32. Block diagram of conductivity values. View is from the southwest corner of the study area.....	68
33. Conductivity map of the 100 unit slice.....	69
34. Conductivity map of the 200 unit slice.....	70
35. Conductivity map of the 300 unit slice.....	71
36. Conductivity map of the 400 unit slice.....	72
37. Conductivity map of the 500 unit slice.....	73

LIST OF TABLES

Table	Page
1. Grain size and sorting controls on pre-burial porosity and permeability.....	20
2. Testing for grain size differences between layers in the NLF point bar.....	51
3. Testing for sorting differences between layers in the NLF point bar.....	52
4. Testing for permeability differences between layers in the NLF point bar.....	57

CHAPTER 1

INTRODUCTION

An estimated 50,000 inactive municipal solid waste landfills exist in the United States today. These landfills were typically sited along floodplains because floodplains were areas with high groundwater tables which limited their economic use. Many of the inactive landfills were established in the early 1900's and were not subject to regulation. They were operated as open dumps with no historical record of the substances dumped in them. Also many of these landfills were not lined. Without a liner, substances leached from the landfills could move through the alluvial sediments toward the rivers (Lee & Jones-Lee, 1995).

The former municipal landfill for the city of Norman, Oklahoma, received solid wastes from 1922 to 1985. In 1985 the landfill was closed and capped with a clay, sand, and silt mixture (Scholl & Christenson, 1998). The landfill was never lined, and a leachate plume developed and now extends down gradient from the landfill. The landfill is situated adjacent to the Canadian River and the plume is moving southward into the floodplain alluvium in the direction of regional groundwater flow. The floodplain of the Canadian River consists of an unconfined alluvial aquifer. The aquifer is 10 to 15 meters (32 to 48 feet) thick and composed of unconsolidated sediments ranging from clay to gravel. The aquifer is underlain by the Hennessey Shale, which acts as a confining unit.

The sedimentologic characteristics of the Canadian River Floodplain adjacent to the Norman Landfill have not been documented. These characteristics control the permeability of the floodplain and the migration potential of the leachate plume. Because the sedimentology has not been studied extensively, a study was proposed for the purpose of establishing a 3-D model of the vertical and horizontal texture of the floodplain alluvium. This exercise establishes the permeability pathways in the floodplain of the Canadian River. A textural analysis of the floodplain can provide the U.S.G.S. with an understanding of how the landfill leachate will move through the alluvium. The research methods employed for this site can also be used to help other scientists working in similar environments.

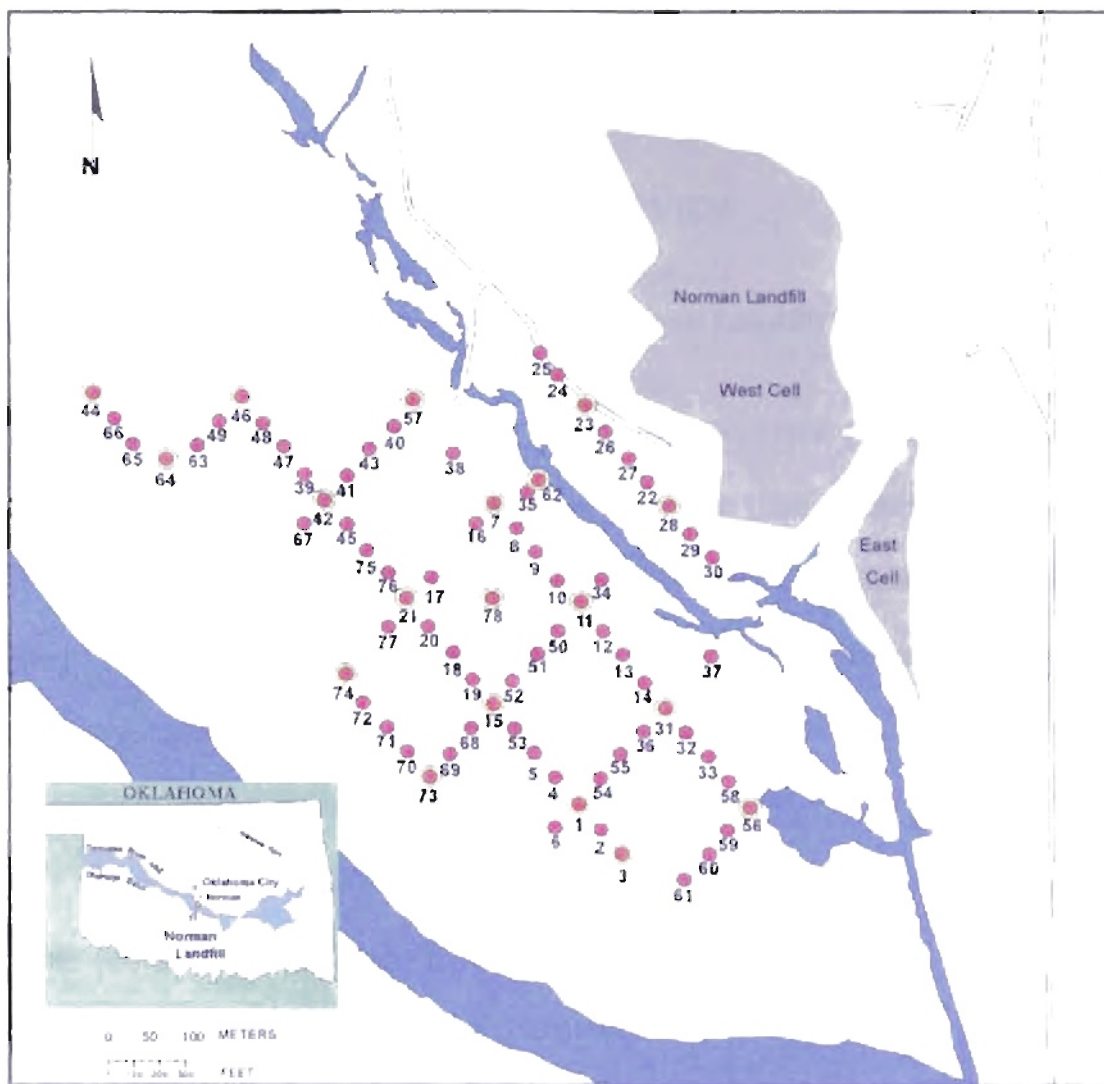
Goals and Objectives

The project entailed eight major tasks:

- 1) collect cores and conductivity logs from the floodplain alluvium;
- 2) describe and photograph the cores;
- 3) perform textural analysis on each core based on lithofacies;
- 4) determine the relationship between texture and permeability using established equations;
- 5) inspect the conductivity logs to establish relationships between conductivity and lithofacies;
- 6) correlate the conductivity logs;
- 7) create a 3-D model of subsurface permeability; and
- 8) make recommendations based on findings.

Study Area

The Canadian River begins in the Sangre de Cristo Mountains of southeastern Colorado and flows 1460 km to its confluence with the Arkansas River in eastern Oklahoma. In the vicinity of the Norman Landfill, the Canadian River is a low-sinuosity, sand-bed river that alternates between braiding and meandering in pattern. In central Oklahoma, the Canadian River Valley ranges in width from 2.5 to 6.5 km, and is composed of two geomorphic surfaces: a late Holocene valley fill and the modern floodplain. The Norman City Landfill is situated on the north side of the Canadian River, south of the city of Norman, between Chautauqua and Jenkins Avenues (Fig. 1). The base of the landfill is 3.5 meters (11 feet) above the thalweg of the river. The valley fill is approximately 10-15 meters (32 to 48 feet) deep and composed of unconsolidated sediments ranging from clay to gravel. The alluvial aquifer is underlain by the Hennessey Shale, which acts as a confining unit.



North American Datum of 1986
 Universal Transverse Mercator
 Projection Zone 14

○ Cores
 ● Conductivity Logs

Fig. 1- Location of Data Collection Sites at Norman Landfill. Map based on data by U. S. Geological Survey.

CHAPTER II

LITERATURE REVIEW

Investigations at the Norman Landfill

The Norman Landfill site is under investigation by several groups of researchers, including the Toxic Substances Hydrology program of the United States Geological Survey, the University of Oklahoma, and the United States Environmental Protection Agency (Scholl & Christenson, 1998). The focus of the research program has been to determine the microbiological, geochemical, and hydrological factors that control the transport of contaminants in the plume.

Scholl and Christenson (1998) performed slug tests in the alluvial aquifer to estimate the hydraulic conductivity of the area. These results showed two strata that appeared to be continuous across the site. The first unit was a layer of low hydraulic conductivity about 4 meters (13 feet) below the water table, and the second unit was a zone of high hydraulic conductivity about 1.5 meters (5 feet) above the base of the aquifer. This study provided indications of a permeability structure within the alluvium.

Lucius and Bisdorf (1995) performed electromagnetic induction (EM) surveys surrounding the Norman Landfill in January and February 1995. Electromagnetic induction surveys measure the electrical conductivity of the soils and fluids in the aquifer. This study determined the vertical and horizontal extent of the leachate plume. The

highest conductivities were found within 200 meters (656 feet) of the landfill. Moving laterally away from the landfill, little variation occurred in the alluvium conductivity, but changes were seen with depth. The EM methods, however, were unable to resolve the vertical changes in conductivity with precision, and the study noted the need for further data to describe the thickness and lithologic characteristics of the aquifer alluvium.

Direct Push Technology

Direct push (DP) technology was used to collect data at the Norman Landfill site. Direct push technology has recently seen more widespread use in aquifer assessment. The DP technology is popular because the systems are more mobile than conventional drilling systems, no drill cuttings are generated, and the subsurface is less disturbed.

Butler, et al. (1999) from the Kansas Geological Survey worked in cooperation with Geoprobe Systems to determine subsurface detail of the Kansas sites using Direct Push electrical logs. Electrical logs were collected at two sites in Kansas. Cores were also collected at both sites adjacent to the locations of the DP e-logs. The relative differences seen in the electrical conductivity logs were found to agree the cores. This article does not discuss how the conductivity would be affected in areas that may be contaminated with leachate or other fluids.

Resistivity Study of Alluvial Deposits

Klefstad (1973) used electrical resistivity equipment to detect landfill leachate in alluvial deposits in Iowa. Klefstad found that limitations exist in the use of electrical resistivity equipment to delineate contaminated zones in alluvial deposits. These limitations result from the lateral variation present in alluvial deposits. Because alluvial deposits exhibit vertical and horizontal heterogeneity, it is difficult to determine

contaminated materials from natural variation. Klefstad noted the need for establishing a stronger geologic framework within which to evaluate the log response.

Permeability Equations and Size Distribution Parameters

Beard and Weyl (1973) performed an investigation on the relationship between porosity, permeability, and the texture of artificially mixed and packed sand. They were concerned primarily with the effects of grain size and sorting on porosity and permeability. In the study, 48 samples of artificially mixed sand were prepared that covered eight grain size subclasses from upper coarse to very fine, and six sorting groups from extremely well to poorly sorted. The data show that permeability decreases as grain size becomes finer and sorting becomes poorer. Beard and Weyl also looked at the effect of grain shape and roundness on porosity and permeability. They found the effects of shape and roundness on permeability were far less pronounced than grain size and sorting.

Many parameters for describing size distribution of sedimentary particles have been devised. Krumbein (1936) and Trask (1930) defined size parameters based on quartile measurements. These measurements included the 25th, 50th, and 75th percentile of the cumulative size distribution. Folk (1957) defined particle size parameters based on these quartile measurements as well as on percentile measurements closer to the extremes of the distribution. These parameters are important in calculating the median diameter or average size, and the sorting of the grains, which is used in calculating the permeability of sediments based on Beard and Weyl's (1973) equation.

CHAPTER III

METHODOLOGY

Obtaining Conductivity Logs and Cores

A sampling grid was designed to obtain uniform coverage of the floodplain alluvium. The grid was composed of cross-lines, which ran parallel and perpendicular to the Canadian River (Fig.1). Geoprobe® conductivity logs were taken along these cross-lines to a depth of 10 to 12 meters (35 to 40 feet). The average distance between the sample locations was about 37 meters (110 ft). A total of 78 conductivity logs were taken, and continuous cores were taken in 19 of these wells. A hand-held GPS system and map were used to locate each of the sampling locations. This GPS system could locate the latitude and longitude to within 1 m (3 feet). After the samples were collected from each site, the site of each well on the floodplain was marked. A second GPS system was used by Scott Christenson from the USGS office in Oklahoma City to obtain more accurate readings. Christenson was able to measure the latitude (X), longitude (Y), and surface elevation (Z) of each well to within 2 cm. The set of readings taken by Christenson provided the X, Y, and Z data for each well in the project.

Conductivity Logs

Seventy-eight conductivity logs (Fig.2) were collected using a Geoprobe®. A Geoprobe® is a hydraulically powered, percussion soil probing instrument. The

Geoprobe Details

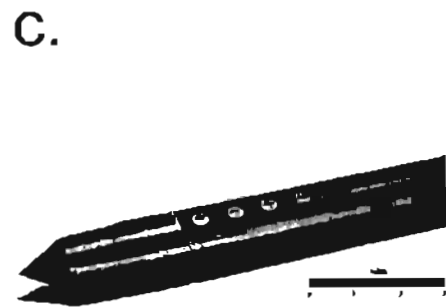
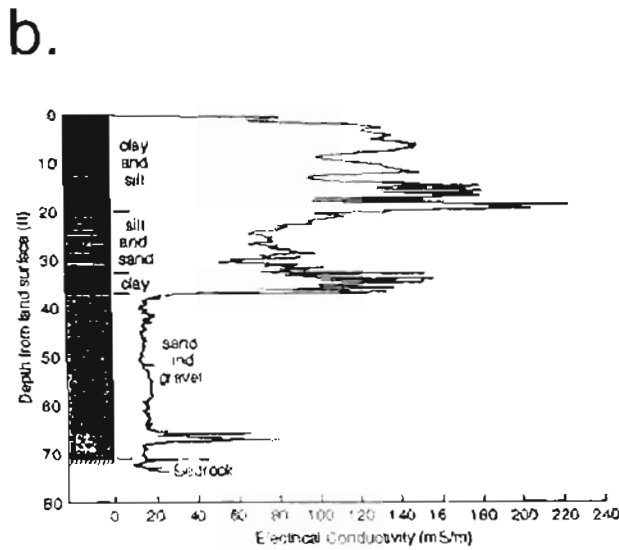
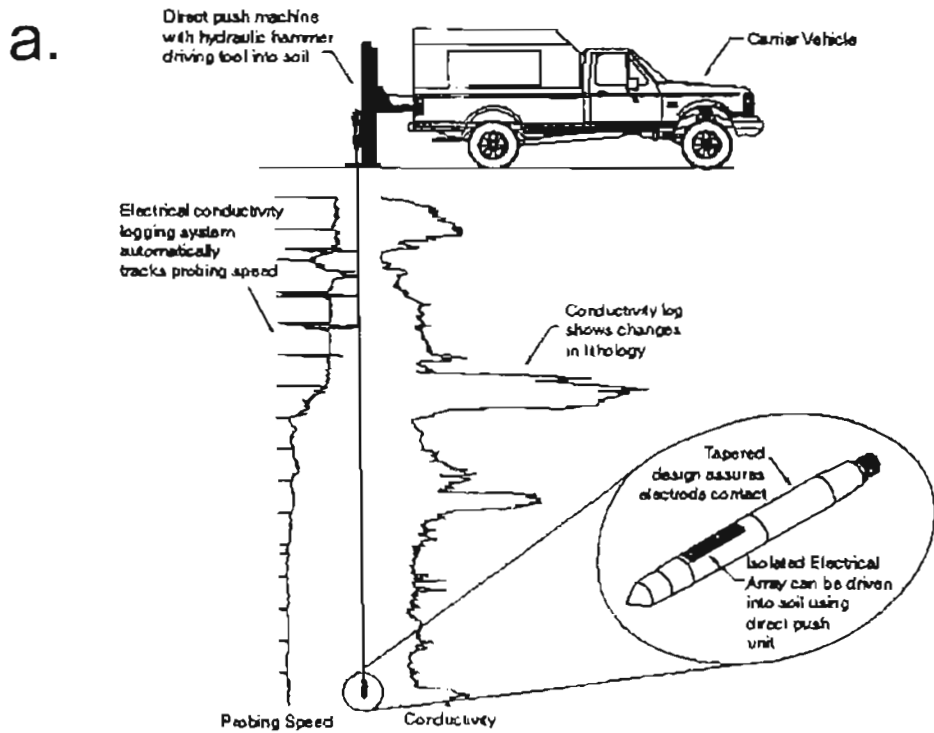


Fig. 2 – (a) Schematic showing truck with tool, (b) example log, (c) direct push (DP) e-logging probe (Illustrations courtesy of Geoprobe®).

Geoprobe® uses static weight and the percussion force of a soil probing hammer to advance a direct-push electrical-logging probe through the subsurface. The Geoprobe® is attached to a vehicle, which provides the static weight for the instrument. The direct-push e-logging probe is attached to the leading end of a tool string and advanced into the subsurface (Fig. 2, 3). The probe used is a Wenner array design that is 38 cm (15 inches) long with a maximum diameter of 3.8 cm (1.5 inches). The electrical conductivity data is transmitted to a field computer, which is attached to the Geoprobe® via a cable. The conductivity is measured in millisiemens/ft. Conductivity readings are taken every 1.5 cm (0.05 feet) and the computer displays a real-time log on its screen as the log is taken. In addition to conductivity, the system also records the rate of penetration (Geoprobe Systems). The data are discussed in feet and meters because the Geoprobe measurements are taken in feet.

After collection, the conductivity log data were imported to an Excel spreadsheet. Once in Excel, the log data were plotted as a curve with depth and printed out on oversize paper. The logs were pieced together to form the cross-sections of the study area (Fig. 4). These cross-sections were then correlated based on the following criteria:

- 1) vertical position of sands relative to mud layers
- 2) vertical variations in texture based on sieve analysis
- 3) depositional subenvironments

The macro-cores provided a check between the conductivity logs and the actual lithology. No age control was available for the cores that were collected. Therefore, the strata of the conductivity logs were matched based on similar lithologic characteristics as seen in the cores. The sieve data were also used to match similar strata based on the

The USGS Geoprobe in Action



Fig. 3 – Kelli Collins and Tom Kropatsch collect conductivity data in the Canadian River floodplain.

Cross-Sections of Study Area

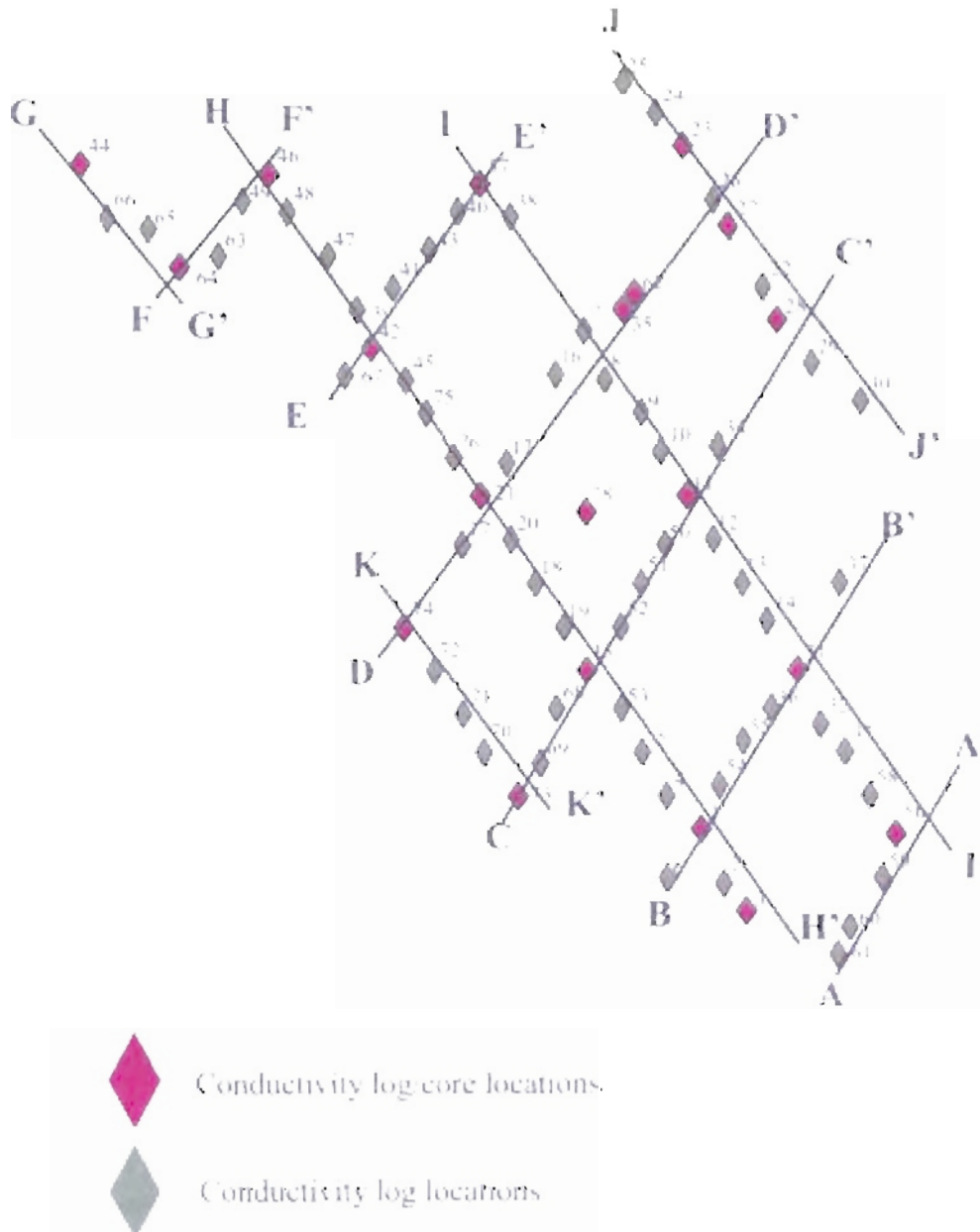


Fig. 4 - Cross-Section lines of conductivity logs. Refer to Fig. 1 to see position of wells relative to landfill.

premise that similar lithologies will exhibit similar texture. Missing sections in the cores, because of compaction and poor recovery, provided problems for correlation. It was impossible to check the conductivity log data against known lithology for the sections that were missing.

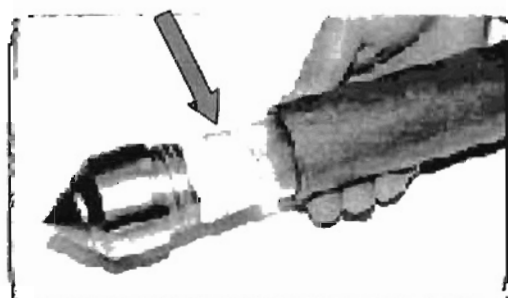
Continuous Cores

Nineteen continuous cores were collected using a Geoprobe®. The Geoprobe® yielded cores of alluvium in 1.2 meter (4 foot) depth intervals. The total depth of each cored well ranged from 11 to 12.2 meters (36 to 40 feet) encompassing the entire thickness of the floodplain alluvium. The Geoprobe® uses a macro-core piston rod soil sampler. The macro-core sampling tube is 122 cm (48 inches) long and 5 cm (2 inches) in diameter. The sampling tube contains a removable polycarbonate core liner that is 3.8 cm (1.5 inch) in diameter (Fig. 5). The sampling tube also contains a piston rod, which keeps the sampler sealed until the desired depth is reached for each sample interval. The piston rod sampler is designed to enhance the recovery of unconsolidated materials. Recovery of complete samples, however, proved difficult in the floodplain alluvium. When samples contained clay, the recovery was around 75%, but when samples were primarily sand the recovery was as low as 25%.

The Geoprobe® can only penetrate unconsolidated materials. Underlying the alluvium is the Permian Hennessey shale bedrock. Once the Geoprobe® reached the shale, the penetration slowed or stopped completely ensuring complete coverage of the alluvium.

Geoprobe Details

a.



b.

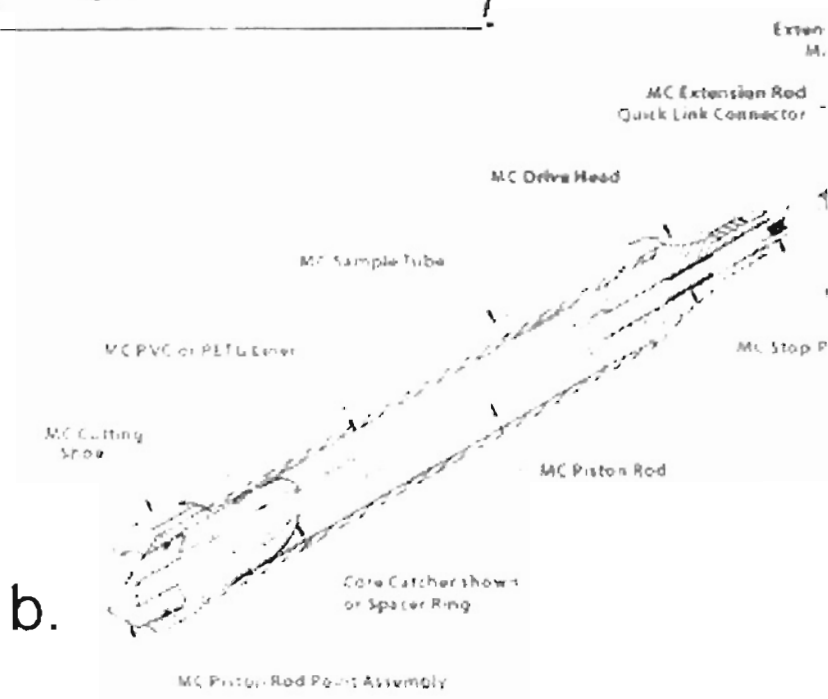


Fig. 5 – (a) Schematic showing MC core catcher with liner (arrow macrocore piston rod sampler. (Illustrations courtesy of Geoprobe Systems, www.geoprobesystems.com).

Core Description

The cores, described in the laboratory, were stored upright to prevent mixing of the sediments. The core liner was split open when the cores were described, but they were kept sealed until then to prevent dessication. The cores were described using a standard strip-log form. Core was described at a scale of 1 inch of strip log to 1 foot of core. The core descriptions included details about lamina and bed thicknesses, lithology, sedimentary structures, color, and estimates of texture (grain size, sorting). Color was determined using a visual comparitor (Exxon-Mobil). Sediment texture was estimated using a binocular microscope and a grain size/sorting visual comparitor. Grain size/sorting estimates were taken about every .45 meters (1.5 feet), and each sediment sample averaged about 1 to 2 grams. A range was recorded for the grain size of each sample. This range included the smallest to largest grain viewed in the sample. Then an average grain size was assigned to the sample based on the most frequent grain size seen in the sample. The core descriptions with grain size/sorting estimates are included in Appendix A.

After the description was complete for each well, the core was photographed with Kodak 100 speed film. Photographs of the core covered about six meters (20 feet) of the alluvial section, so a set of two photos was required to cover each well. In addition, photographs were taken of key features (texture, structures, bounding surfaces, lithoclasts) within the cores. The negatives from each core were scanned to create digital image files. The images were then inserted to Powerpoint, pieced together, and described (Appendix B).

Texture Analysis of Core Samples

Once the cores were described and photographed, they were divided into samples for mechanical sieving. Approximately 15 samples were taken from each of the 78 cores, and the average weight of each sample was about 150 grams. Samples were taken whenever an abrupt contact or change occurred in grain size within the core. The estimates of grain size, performed on the cores during the description process, helped to identify any key changes in grain size when decisions were made on where to collect samples for sieving.

The core samples were placed into labeled sample bags. Each sample was sieved through a set of thirty wire mesh sieves using a Ro-Tap machine. The sieves ranged in size from 1 to 230 according to the U. S. Standard Sieve number. This range is equivalent to -4.64 to 4.00 phi grain size (25.0 to 0.0625 mm). Each core sample was sieved for about 12 minutes. The amount of sediment collected in each mesh was weighed and recorded in grams using a digital scale.

The results from sieving were input to an Excel spreadsheet. The spreadsheet automatically calculates the weight percentages of the individual grain size fractions present in each core sample. These weight percentages were summed to form a cumulative weight percentage curve that was then plotted against phi grain size to form a standard grain size cumulative curve (Fig. 6). A cumulative curve was generated for each sample (Appendix C). Each curve was then used to determine a graphic mean and inclusive graphic standard deviation for that sample. The graphic mean is equivalent to a mean grain size and the standard deviation is equivalent to sorting. The equation used to calculate the graphic mean is:

Cumulative Curves for Samples in Well #1

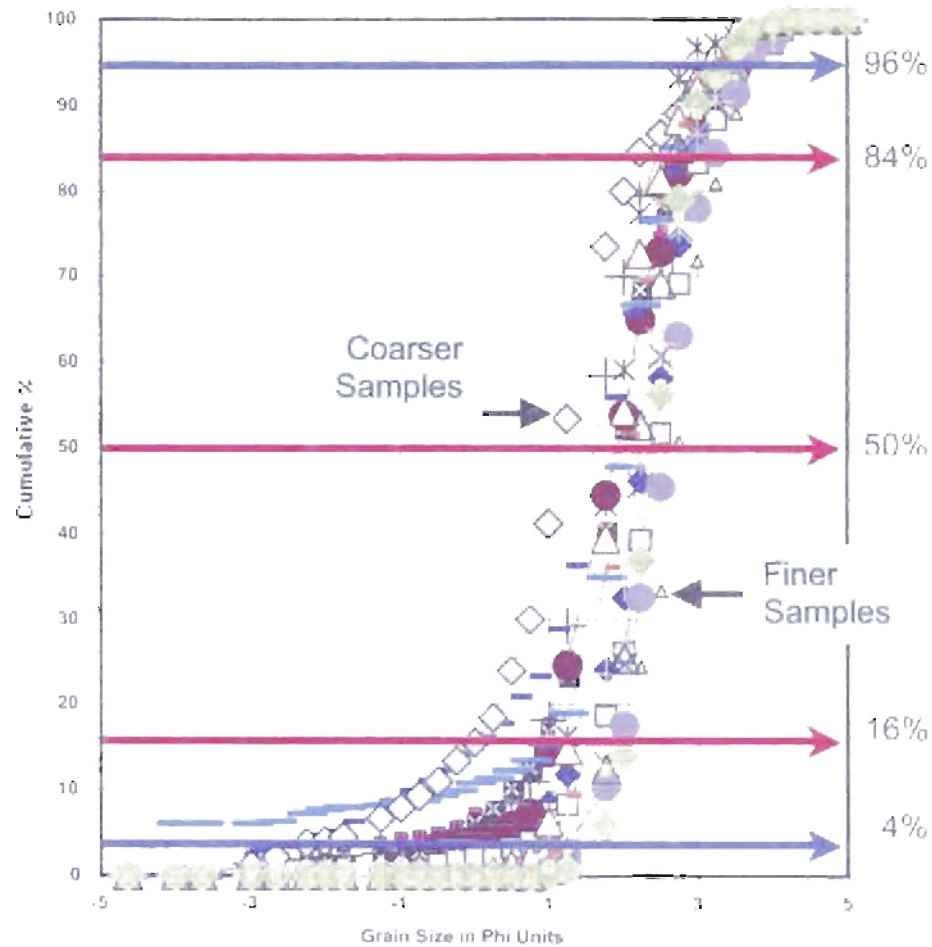


Fig. 6 Example of cumulative curves used for estimating graphic mean and standard deviations for use in the permeability prediction equation.

$$Mz = (\phi_{16} + \phi_{50} + \phi_{84}) / 3 \quad (\text{eq. 1})$$

The phi grain size was read from the cumulative curves at the 16%, 50%, and 84% marks. By reading the data from these intervals the central two thirds of the grain size data were encompassed. These three values were then averaged to provide a mean grain size for the sample. The inclusive standard deviation equation used to calculate the standard deviation is:

$$\sigma_1 = (\phi_{84} - \phi_{16}) / 4 + (\phi_{95} - \phi_5) / 6.6 \quad (\text{eq. 2})$$

For this equation the phi grain size was read at 5%, 16%, 84%, and 95% from each of the curves and input into the equation. The inclusive standard deviation is an average of the standard deviation calculated from ϕ_{16} and ϕ_{84} , and the standard deviation calculated from ϕ_5 and ϕ_{95} . This is the best overall measure of sorting because it includes 90% of the distribution (Folk, 1974). The mean grain size and sorting were then used to calculate the permeability.

The equations used to calculate the graphic mean and inclusive graphic standard deviation followed the recommendations of Folk (1974). These equations were used for this analysis because of inherent sensitivity to the “tails” of the grain size distribution. This sensitivity is important to determinations of sediment grain sorting, a major control on the porosity and permeability of sands.

Texture-Permeability Equation

The raw data (ϕ , K , grain size, sorting) from the classic Beard and Weyl (1973) paper was used to generate a permeability equation (Table 1, Fig. 7). These raw data were input to an Excel spreadsheet that was imported to SAS (v.8.01). SAS was used for analyzing the relationships among the variables. A step-wise multivariate statistical technique was used to evaluate the controls on the permeability log units. Permeability is a measure of the ease with which fluid can be transmitted through a porous medium. The effects of grain size and shape, and their interconnectedness are included in the measurement of permeability. In the SI system, permeability has units of m^2 . Another unit of permeability is the darcy, which was used in this study. The conversion factor to the SI system is $1 \text{ darcy} = 0.987 \times 10^{-12} m^2$ (Hermance, 1999)

The units of permeability were measured in Darcies (cgs). The results of the statistical analysis indicate the grain size was the most important to the permeability equation. Phi grain size explained 64% of the total variation, while sorting explained 32%. The r^2 value for the multiple regression was 0.97. This value is so high that one suspects that the Beard and Weyl raw data have been adjusted by some additional factor not listed in their paper.

The multivariate equation that was produced to calculate the permeability is:

$$\text{Log (10) of permeability} = 6.18660 - 0.49463 (S_0) - 0.57248 (\phi_{gs}) \quad (\text{eq. 3})$$

or

$$\text{Permeability} = 10^{6.18660 - 0.49463 (S_0) - 0.57248 (\phi_{gs})} \quad (\text{eq. 4})$$

where S_0 = sorting and ϕ_{gs} = phi grain size.

Raw Data

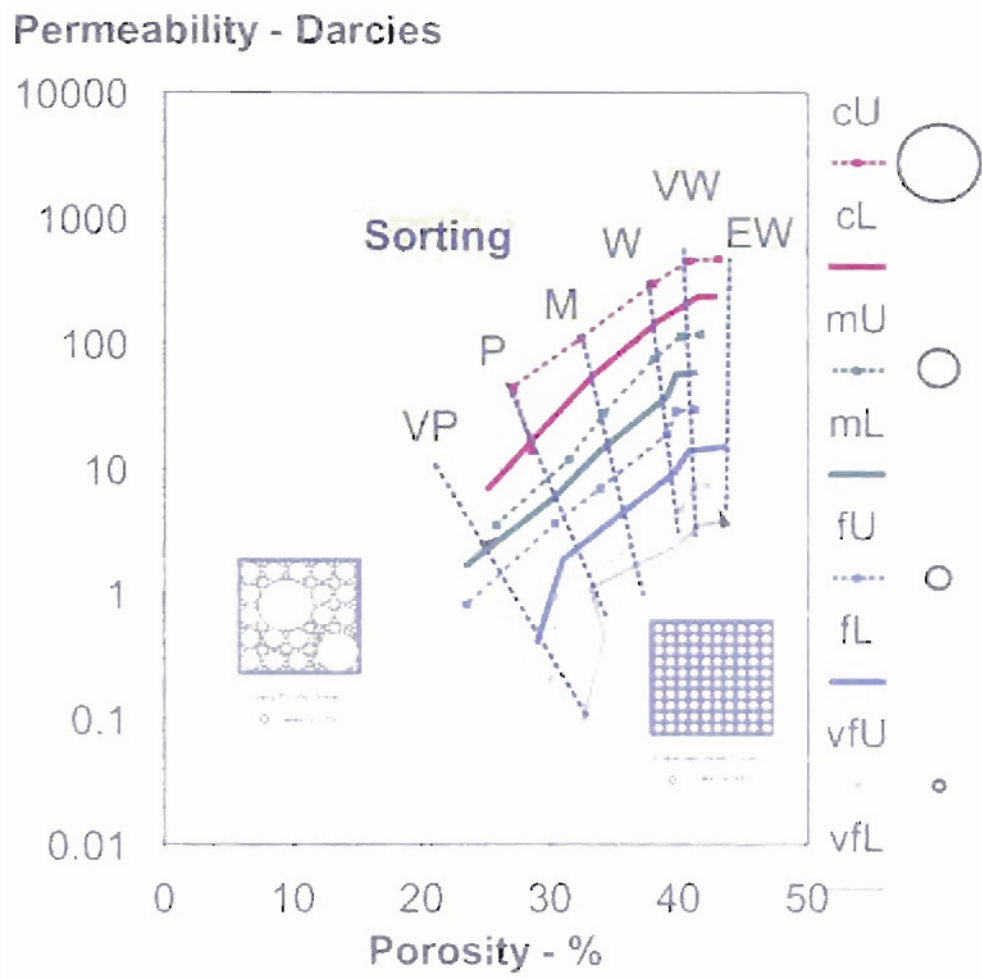
Table 1- Grain size and sorting controls on pre-burial porosity and permeability. These raw data were used for generating the permeability equation discussed in the text.

Data from Beard and Weyl (1973)

Sample	Sorting	Size	phiGS	Porosity	Permeability	Darcies	LogPerm
Sample 1	1.0500	0.8550	0.2260	43.10	475000	475	5.6767
Sample 2	1.0500	0.6050	0.7250	42.80	238000	238	5.3766
Sample 3	1.0500	0.4250	1.2345	41.70	119000	119	5.0755
Sample 4	1.0500	0.3000	1.7370	41.30	59000	59	4.7709
Sample 5	1.0500	0.2135	2.2277	41.30	30000	30	4.4771
Sample 6	1.0500	0.1510	2.7274	43.50	15000	15	4.1761
Sample 7	1.0500	0.1065	3.2311	42.30	7400	7.4	3.8692
Sample 8	1.0500	0.0660	3.9214	43.00	3700	3.7	3.5682
Sample 9	1.1500	0.8550	0.2260	40.80	458000	458	5.6609
Sample 10	1.1500	0.6050	0.7250	41.50	239000	239	5.3784
Sample 11	1.1500	0.4250	1.2345	40.20	115000	115	5.0607
Sample 12	1.1500	0.3000	1.7370	40.20	57000	57	4.7559
Sample 13	1.1500	0.2135	2.2277	39.80	29000	29	4.4624
Sample 14	1.1500	0.1510	2.7274	40.80	14000	14	4.1461
Sample 15	1.1500	0.1065	3.2311	41.20	7200	7.2	3.8573
Sample 16	1.1500	0.0660	3.9214	41.80	3600	3.6	3.5563
Sample 17	1.3000	0.8550	0.2260	38.00	302000	302	5.4800
Sample 18	1.3000	0.6050	0.7250	38.40	151000	151	5.1790
Sample 19	1.3000	0.4250	1.2345	38.10	76000	76	4.8808
Sample 20	1.3000	0.3000	1.7370	38.80	38000	38	4.5798
Sample 21	1.3000	0.2135	2.2277	39.10	19000	19	4.2788
Sample 22	1.3000	0.1510	2.7274	39.70	9400	9.4	3.9731
Sample 23	1.3000	0.1065	3.2311	40.20	4700	4.7	3.6721
Sample 24	1.3000	0.0660	3.9214	39.80	2400	2.4	3.3802
Sample 25	1.7000	0.8550	0.2260	32.40	110000	110	5.0414
Sample 26	1.7000	0.6050	0.7250	33.30	55000	55	4.7404
Sample 27	1.7000	0.4250	1.2345	34.20	28000	28	4.4472
Sample 28	1.7000	0.3000	1.7370	34.90	14000	14	4.1461
Sample 29	1.7000	0.2135	2.2277	33.90	7000	7	3.8451
Sample 30	1.7000	0.1510	2.7274	34.30	3500	3.5	3.5441
Sample 31	1.7000	0.1065	3.2311	35.60	2100	2.1	3.3222
Sample 32	1.7000	0.0660	3.9214	33.10	1100	1.1	3.0414
Sample 33	2.3500	0.8550	0.2260	27.10	45000	45	4.6532
Sample 34	2.3500	0.6050	0.7250	29.80	23000	23	4.3617
Sample 35	2.3500	0.4250	1.2345	31.50	12000	12	4.0792
Sample 36	2.3500	0.3000	1.7370	31.30	6000	6	3.7782
Sample 37	2.3500	0.2135	2.2277	30.40	3700	3.7	3.5682
Sample 38	2.3500	0.1510	2.7274	31.00	1900	1.9	3.2788
Sample 39	2.3500	0.1065	3.2311	30.50	930	0.93	2.9685
Sample 40	2.3500	0.0660	3.9214	34.20	460	0.46	2.6628
Sample 41	4.2000	0.8550	0.2260	28.60	14000	14	4.1461
Sample 42	4.2000	0.6050	0.7250	25.20	7000	7	3.8451
Sample 43	4.2000	0.4250	1.2345	25.80	3500	3.5	3.5441
Sample 44	4.2000	0.3000	1.7370	23.40	1700	1.7	3.2304
Sample 45	4.2000	0.2135	2.2277	28.50	830	0.83	2.9191
Sample 46	4.2000	0.1510	2.7274	29.00	420	0.42	2.6232
Sample 47	4.2000	0.1065	3.2311	30.10	210	0.21	2.3222
Sample 48	4.2000	0.0660	3.9214	32.60	100	0.1	2.0000

Beard and Weyl Data (1973)

Grain Size & Sorting - Controls on Pre-Burial Porosity & Permeability



*Artificial Sand Packs
Beard and Weyl (1973)*

Fig. 7 This plot of porosity vs. permeability is based on the raw data of Beard and Weyl (1973). These data were used to generate the permeability equation used for calculating the permeability of the NLF point bar layers.

Interpretation of Conductivity Logs for Texture and Generation of 3-D Block Diagrams

A database was set up in Rockworks 99 that contained the latitude (X), longitude(Y), and surface elevation (Z) for each of the sample locations. The files for the conductivity log curves were then associated with the sample locations in the database. Once these curve files were imported into Rockworks with the corresponding X, Y, and Z locations, the software was able to plot the conductivity logs as cross-sections and 3-D block diagrams. Digital strip logs for display were also created for each of the 19 cores based on the log form descriptions (Appendix A).

CHAPTER IV

RESULTS AND DISCUSSION

Description of Sedimentary Features

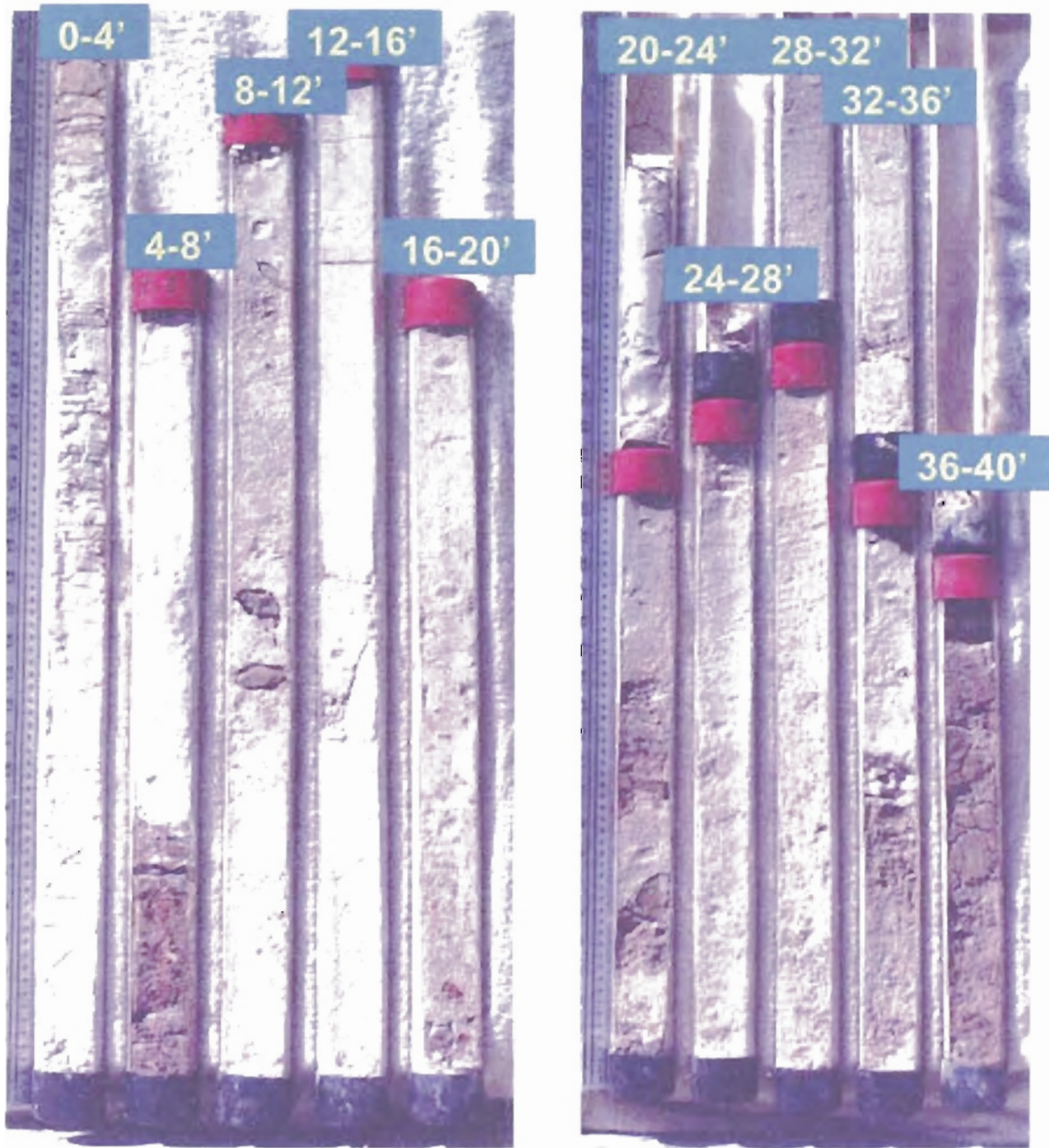
Figures 8, 9, 10, and 11 show excellent examples of the sedimentary features noted in the 19-cored wells. The depth units are expressed in English units rather than metric units as the Geoprobe probe rods are manufactured in increments of 4' lengths.

Fig. 8 - Well #1 Core has a thin, incipient soil (b), mud rip-up clasts (b), and a sharp contact of sands with the underlying mud layer (b). No cross bedding is obvious in the sand beds.

Fig. 9 - Well #3 Core shows an excellent example of an accumulation of silt and clay that has been carried past the piston by flowing water because of sudden pressure drop in the core barrel (b). This well also has mud clasts and a solid contact with the underlying Hennessey Fm.

Fig. 10 - Well #7 Core shows an excellent recovery of gravel near the base of the valley fill and a very sharp contact with the underlying Hennessey red bed (b). Mud in this core is red and black (organic-rich).

Well #1 – Canadian River Floodplain

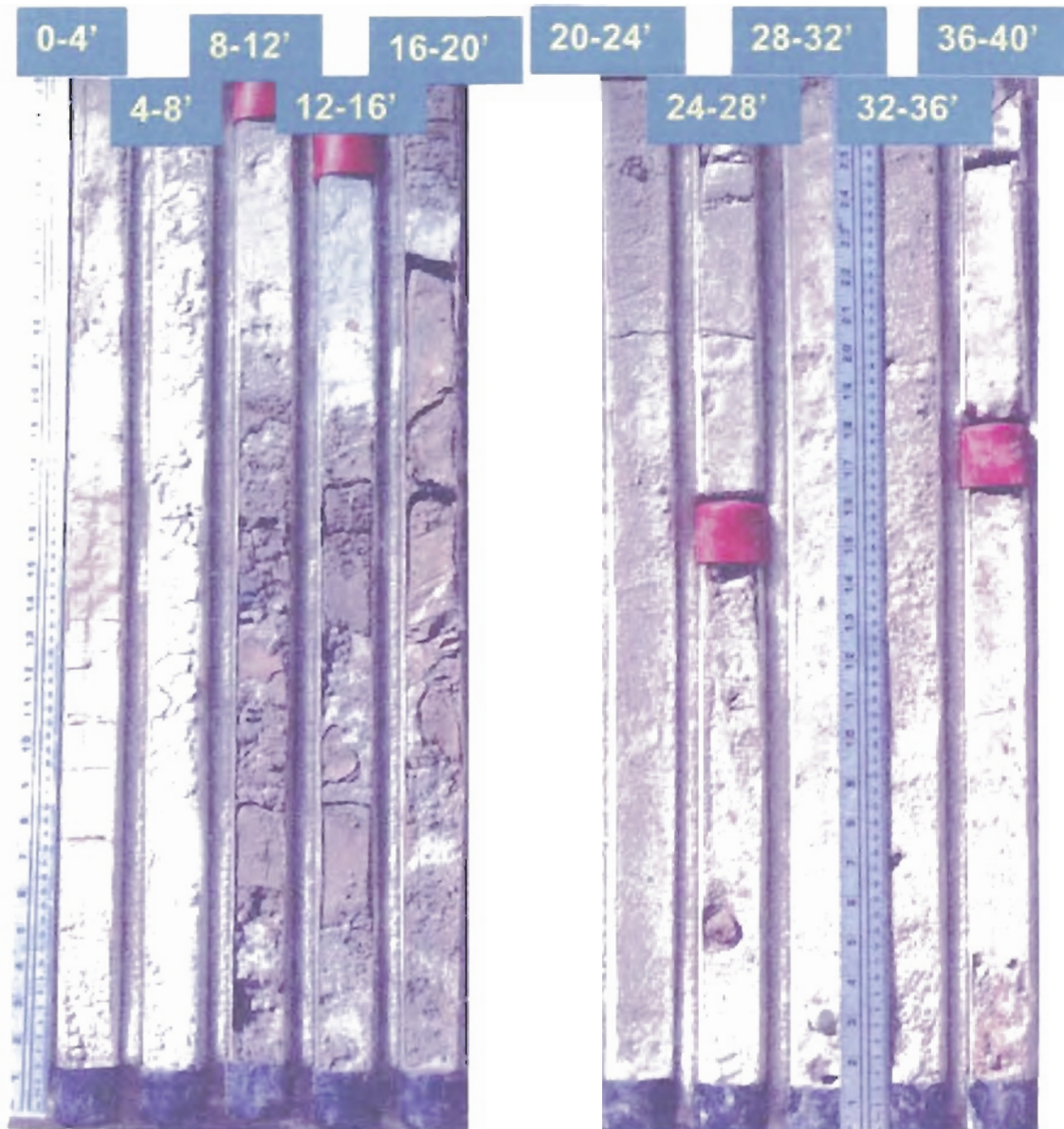


a.

Figs. 8a, b (next page) – Cores from Well #1 showing sand / mud layers and mud clasts. Each core segment is 4' in length though compaction of the sediment and loss of some materials (failure of core catcher?) always results in core length segments that are <4'.



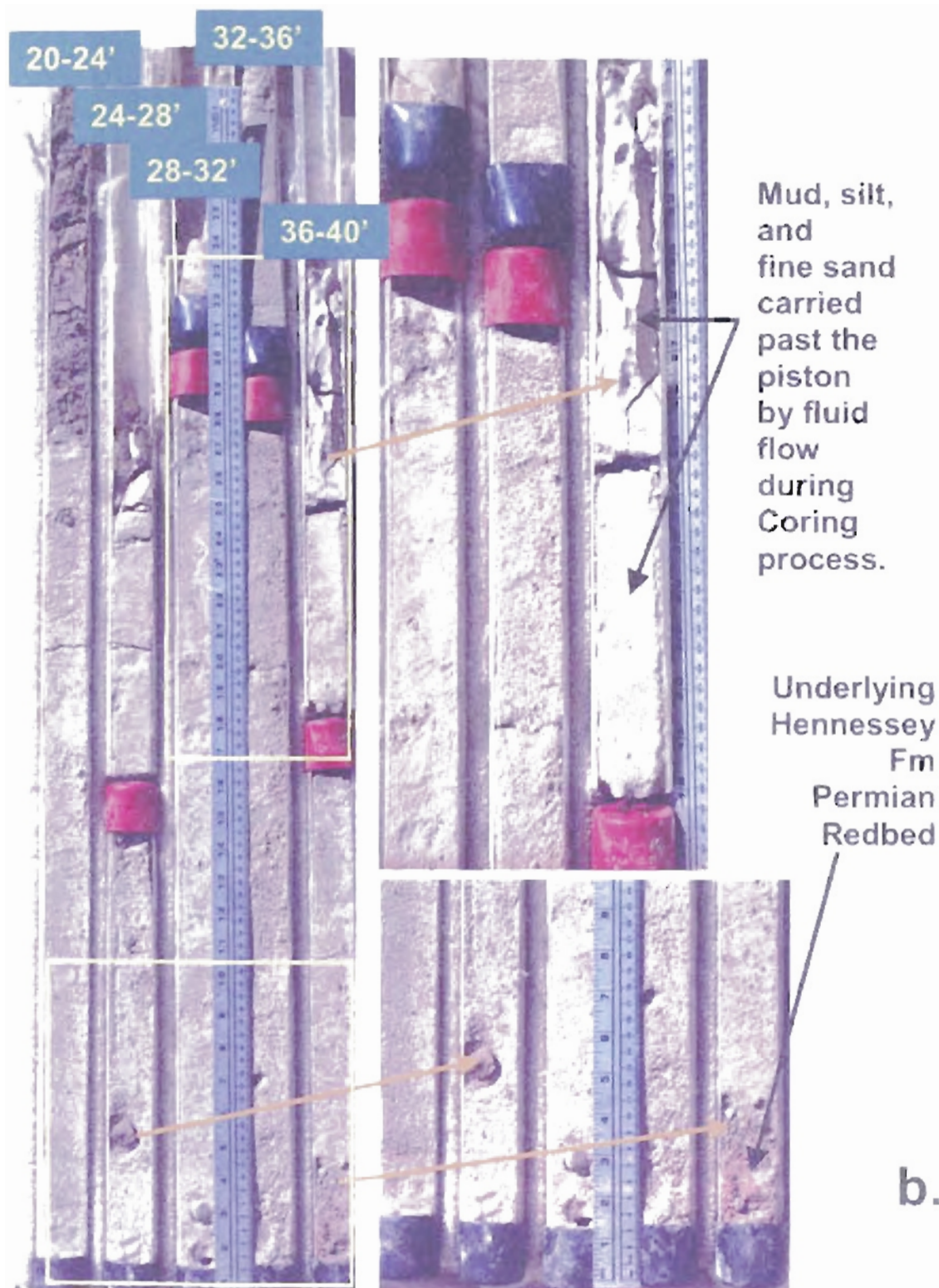
Well #3 – Canadian River Floodplain



a.

Figs. 9a, b (next page) – Cores from Well #3 showing layers, mud clasts, and the underlying Hennessey Fm. Due to movement of water into the well bore, some sediment is always transported up around the coring piston, accumulating in the upper portion of the core sleeve.

Well #3 – Canadian River Floodplain



Well #7 – Canadian River Floodplain



Figs. 10a, b (next page) – Cores from Well #7 showing sand / mud layers and gravel at the basal contact with the Hennessey Fm.

Well #7
Canadian
River
Floodplain

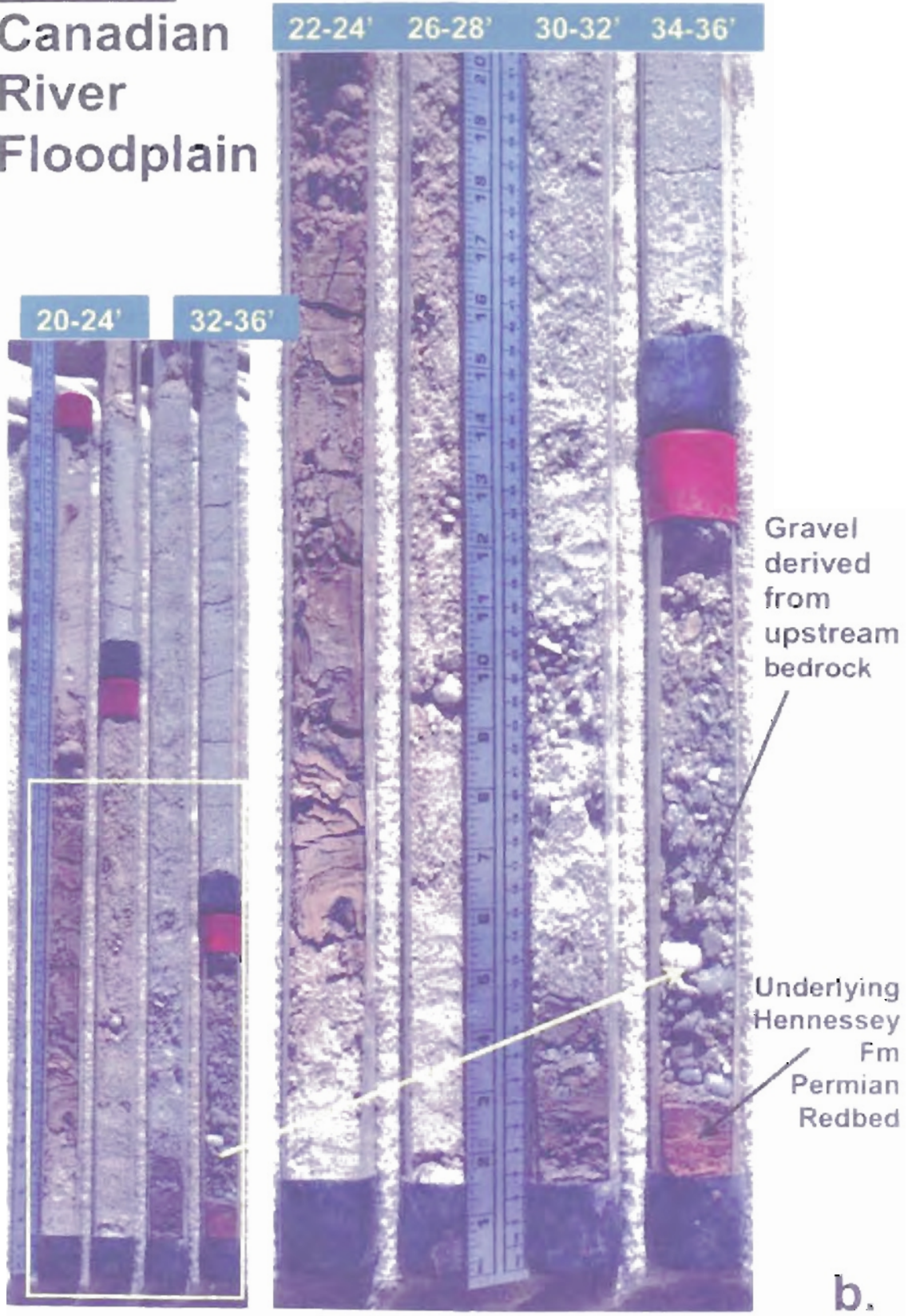


Fig. 11 - *Well #46 Core* has some of the best-preserved cross bedding in any of the 19 cored wells. Sedimentary structures were always absent or disturbed below the water table because of the rapid movement of water into the well bore during penetration of the probe. The preserved tough cross bedding in this well occurred above the water table (b). Disruption (doming) of layering because of water movement is apparent in images 11b and d. Poorly sorted gravels were recovered near the base of the well (c). Image 11e contains two fining upward cycles, each with gravel at the base.

Criteria for Correlating the Conductivity Logs

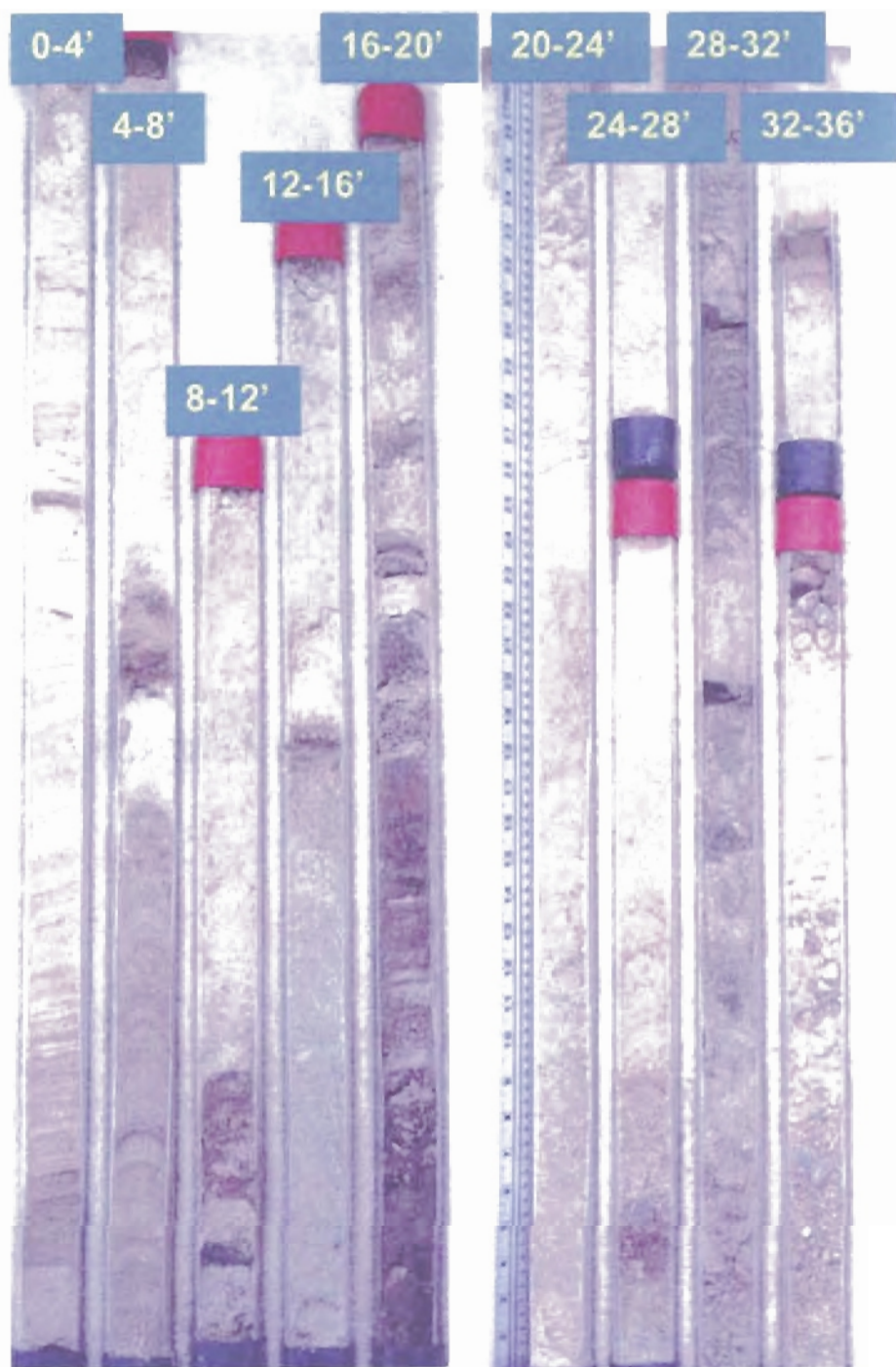
The vertical succession of the point bar from the basal contact with the underlying Permian Hennessey Fm. to the present day land surface was vertically subdivided on the basis of conductivity profiles, mud layers, and rapid changes in sediment texture (grain size, sorting). No strong independent age-control exists for the stratigraphy of the point bar. Consequently, the criteria used for correlating the conductivity logs were:

- (1) similarities in conductivity response patterns,
- (2) stratigraphic position (superposition), and
- (3) lithologic similarity.

The correlation style was strongly tempered by observations about the nature and distribution of the modern Canadian River floodplain sediments. Observations of the floodplain, sand bars, and mud layers are as follows:

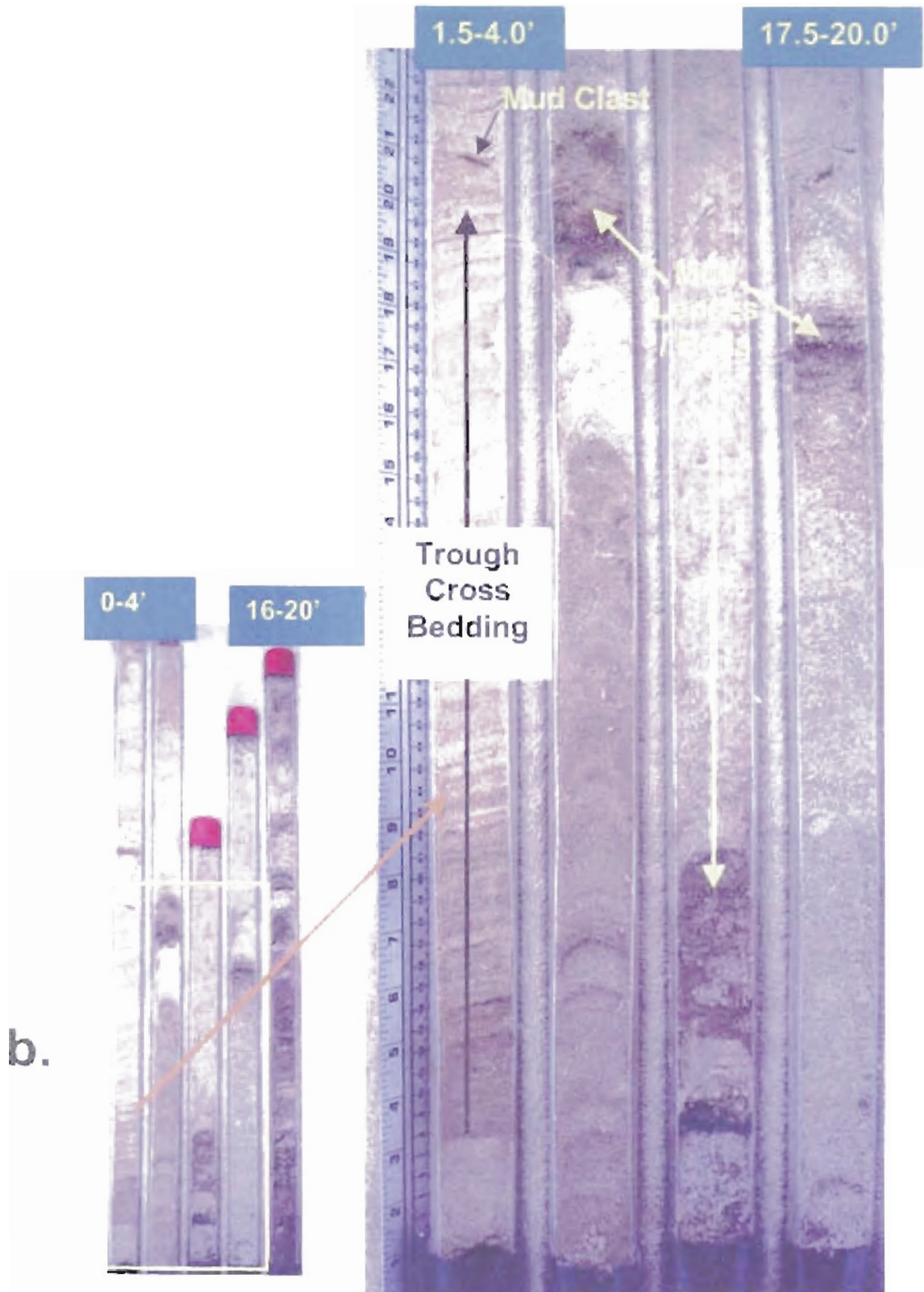
- (1) Floodplain: very flat with little relief (see Fig. 12)
- (2) Sand Bars:

Well #46 – Canadian River Floodplain



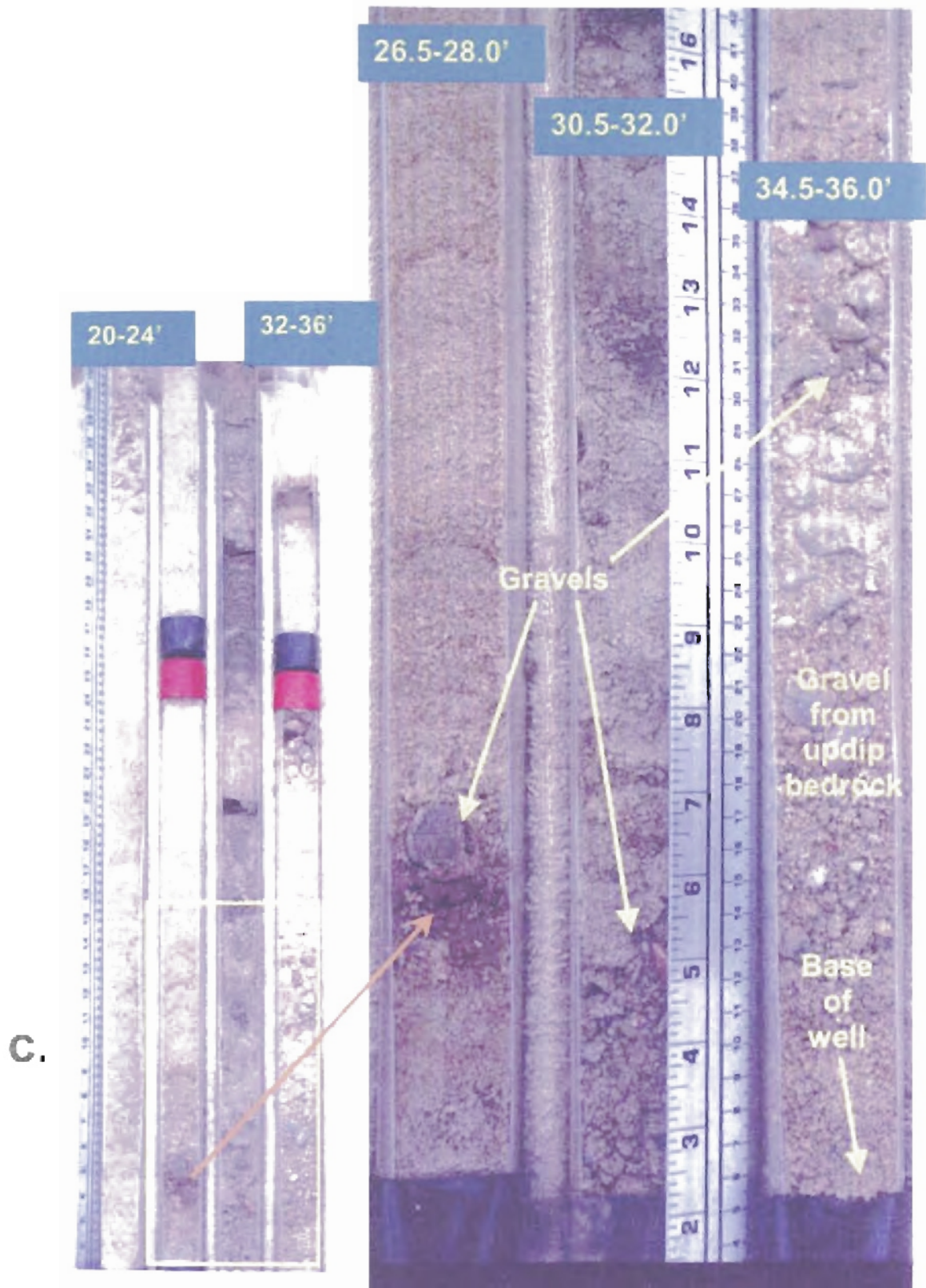
Figs. 11a-e (following pages) – Cores from Well #46 showing sand / mud layers, trough cross bedding, fining upward cycles, and gravel intervals that have high calculated permeability.

Well #46 – Canadian River Floodplain



b.

Well #46 – Canadian River Floodplain

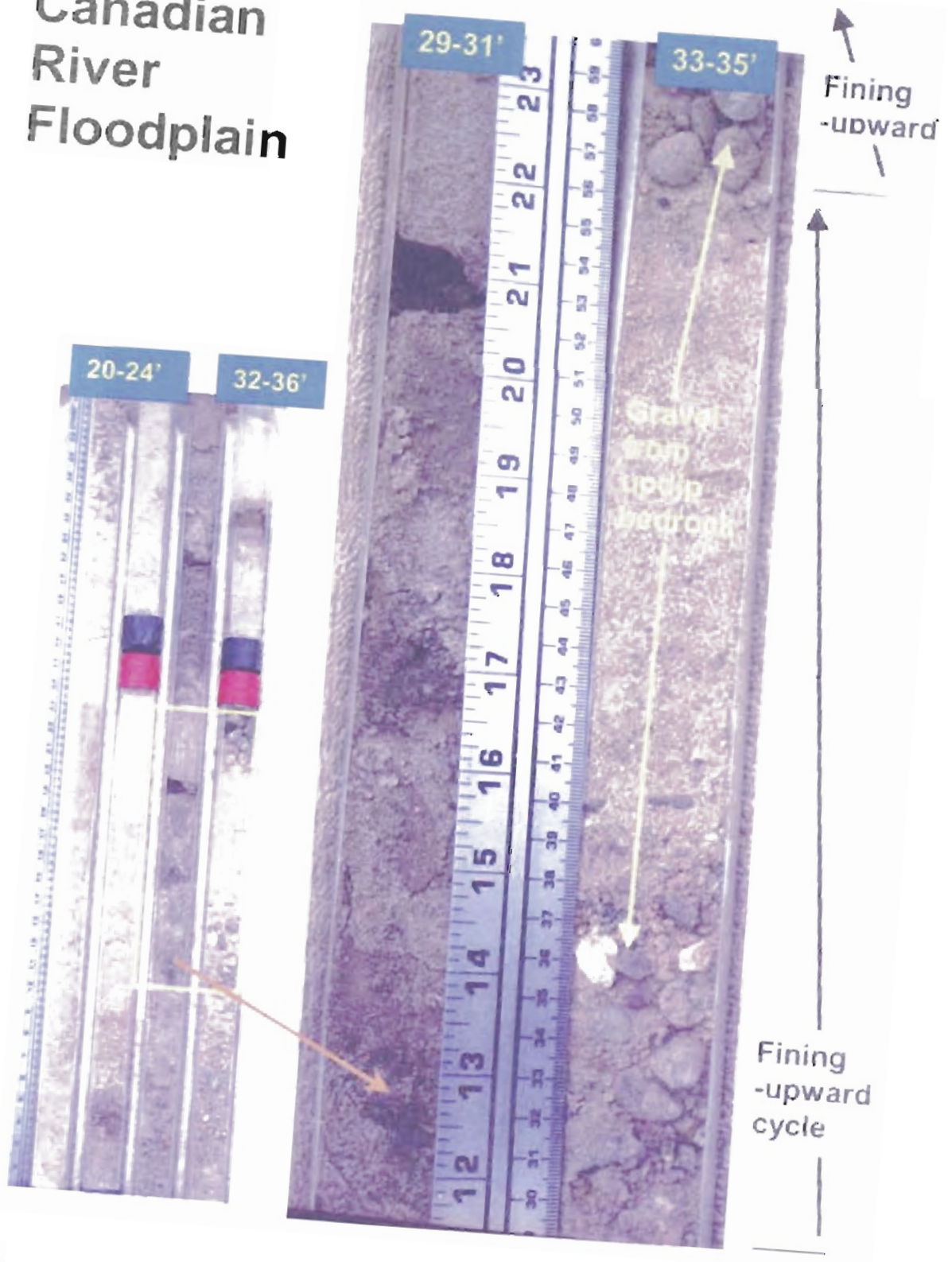


Well #46 – Canadian River Floodplain



d.

**Well #46
Canadian
River
Floodplain**



e.

Incised North Bank of the Canadian River, Norman, Oklahoma

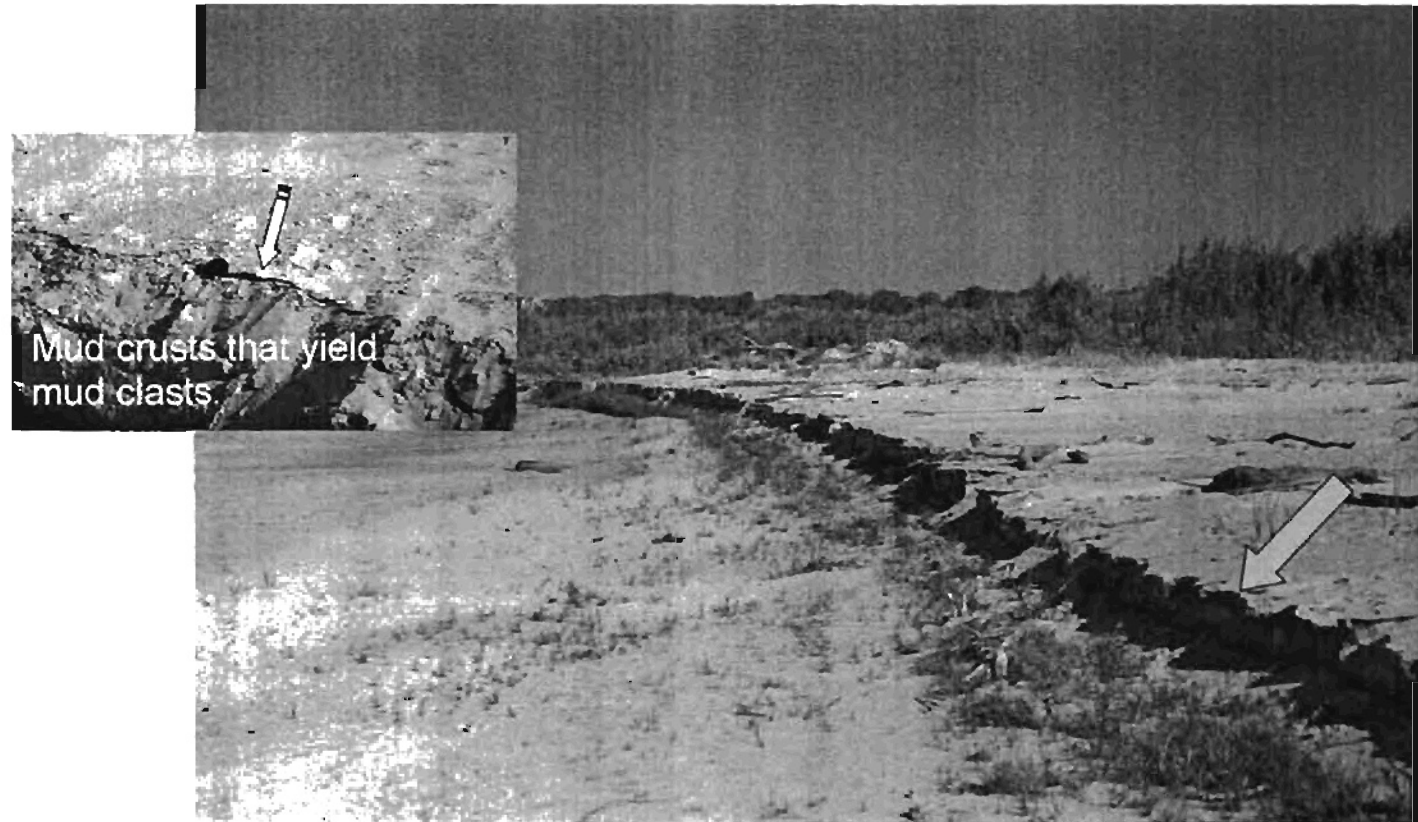


Fig. 12 - Pictured above is a portion of the Canadian River floodplain that has been incised and abandoned. Note the flat, horizontal nature of the floodplain. The inset photograph shows a thin, dried mud layer that will be eroded during the next major high discharge event. This mud layer was observed near the yellow arrow in the larger photograph.

- a) Initially sinuous-crested linguoid-shaped dunes that form during high discharge events (Fig. 13, 14).
- b) final morphology results from continuous dissection of the constructional bar forms by braids of channelized flow that accompany waning flow (Fig. 12)
- c) incision of the constructional bar forms continues until the occurrence of the next high discharge event

(3) Mud Layers

- a) Occur adjacent to main channels; are flat-topped, may onlap an erosional surface, are discontinuous (Fig. 15)
- b) mud layers develop as silt and clay settles from suspension each time high water (which has a high suspended load in the Canadian River) inundates the topographic lows on the floodplain
- c) the topographic lows are the erosional features mentioned above and are produced subsequent to a high-discharge event

Subsurface evidence confirms these observations with respect to bar form shape and relationship to mud layers. The contacts of some mud layers with underlying bar sands are observed in core to onlap erosional surfaces and vice versa (Fig. 16). In addition, mud clasts are found at the base of some of the sandbars (Fig. 17). The mud clasts were derived from the underlying mud layers as the river erodes surface sediments during a high discharge event.

Sand Bars in Oklahoma Rivers

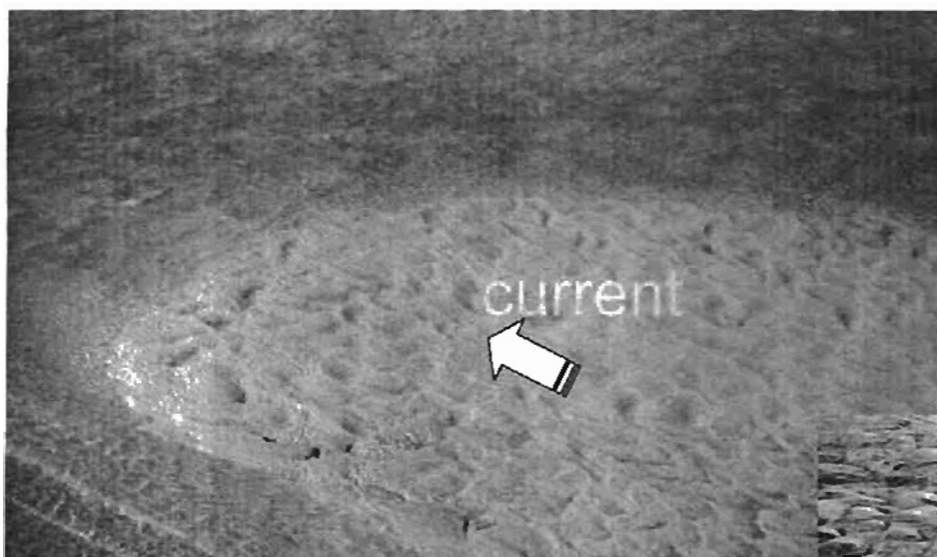


Fig. 13b - Migration of a thin unit bar down the Canadian River channel at low flow – linguoid ripples are advancing up the back of the bar form.

Foresets in an Exhumed Subaqueous Dune, South Bank of Canadian River



Development of Mud Layers in the Canadian River, Norman, Oklahoma

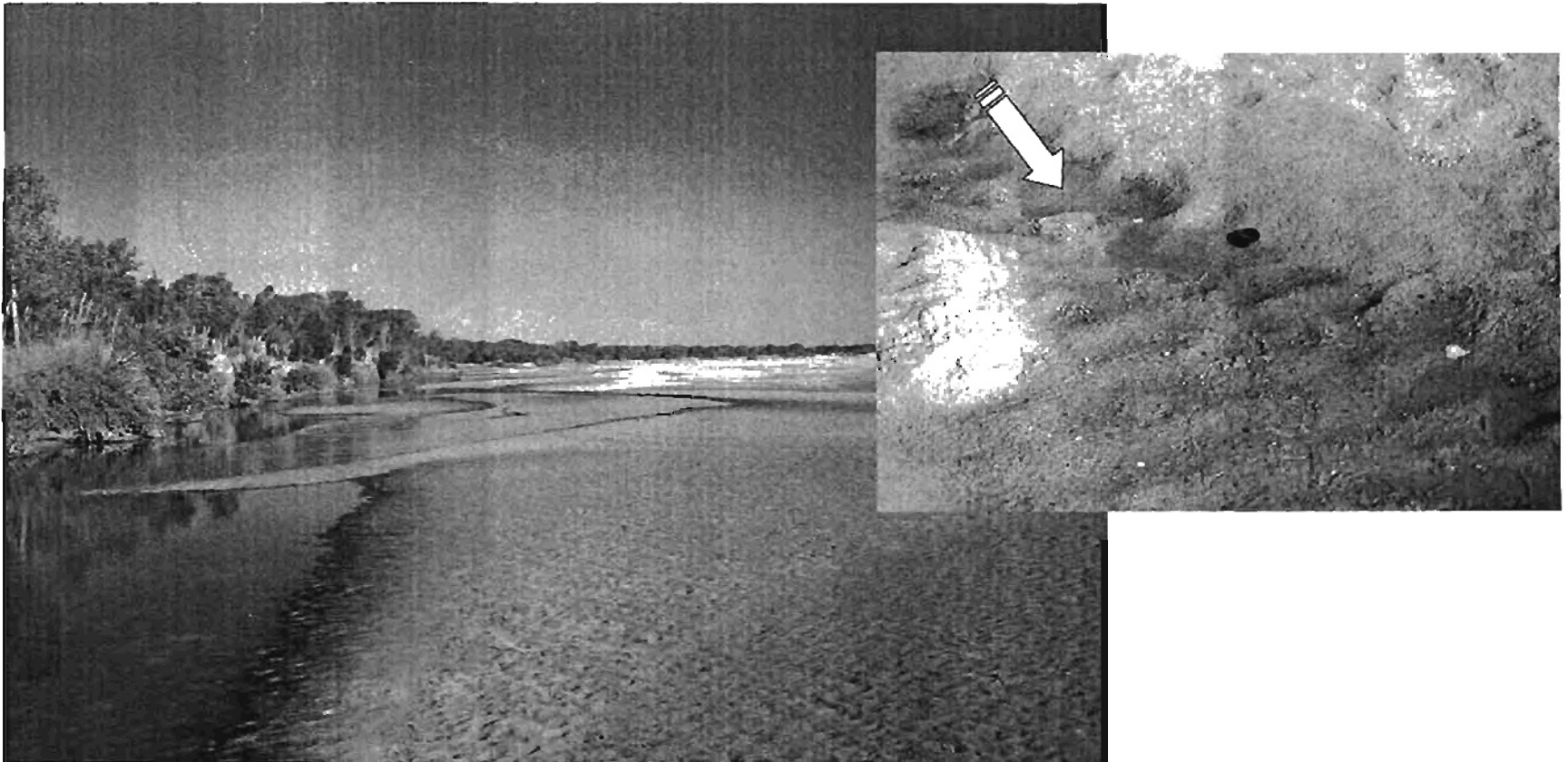


Fig. 15 - Subtle topographic lows on the margin of the main channel accumulate mud (and some algae) that forms the discontinuous mud layers seen in the subsurface cores and as depicted on the cross sections.

Evidence for Deposition on Erosional Surfaces within the Point Bar

11

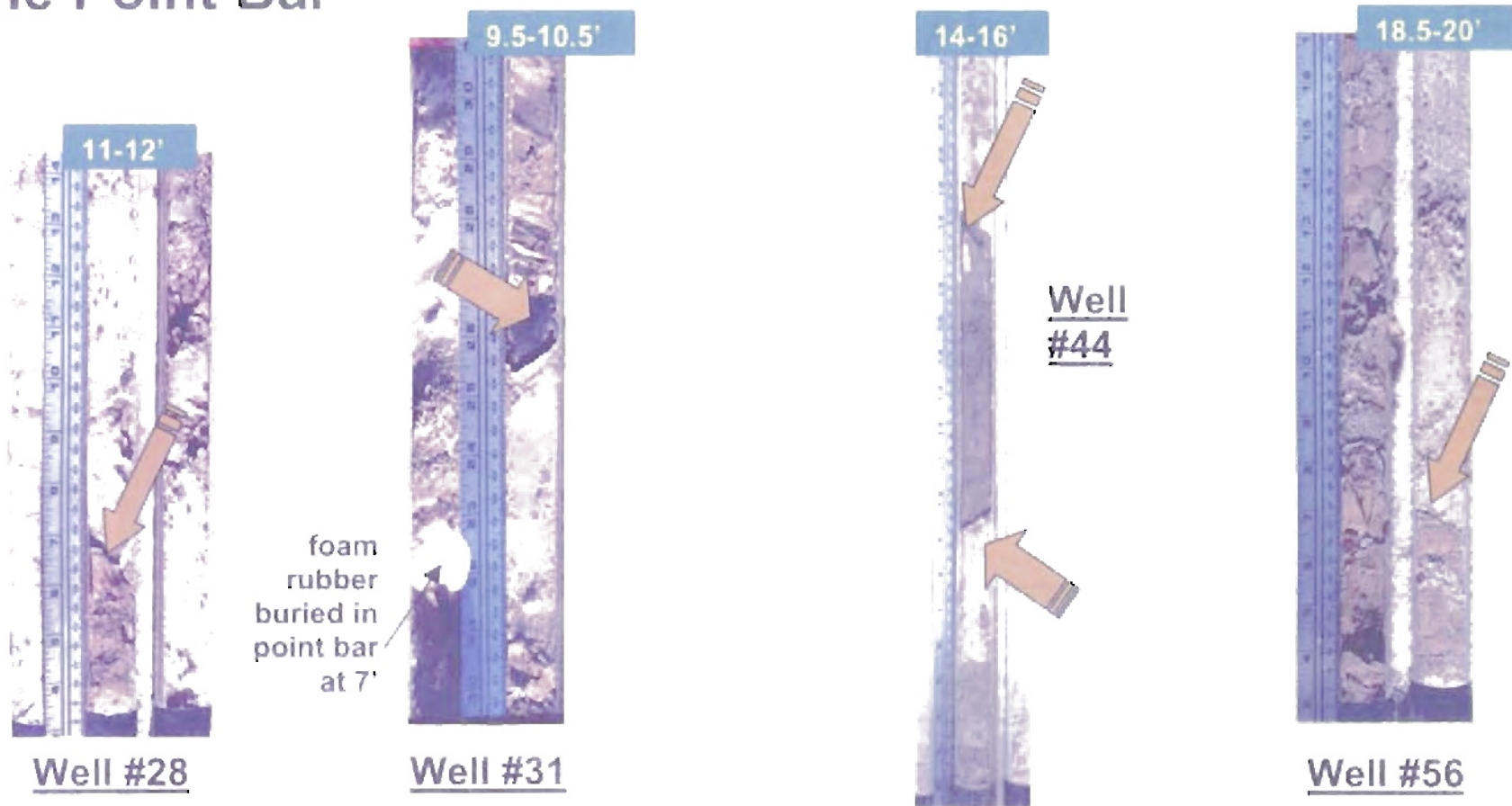


Fig. 16 The onlap of sand or mud layers onto stratal surfaces that exhibit relief suggests the basal contact of each correlation unit in the point bar (**Intervals 200-500**) is erosional (in part or entirely). The basal contact of the **100 Interval** with the underlying Hennessey is clearly erosional. This contact is highlighted in other core photos.

Well #11 – Canadian River Floodplain

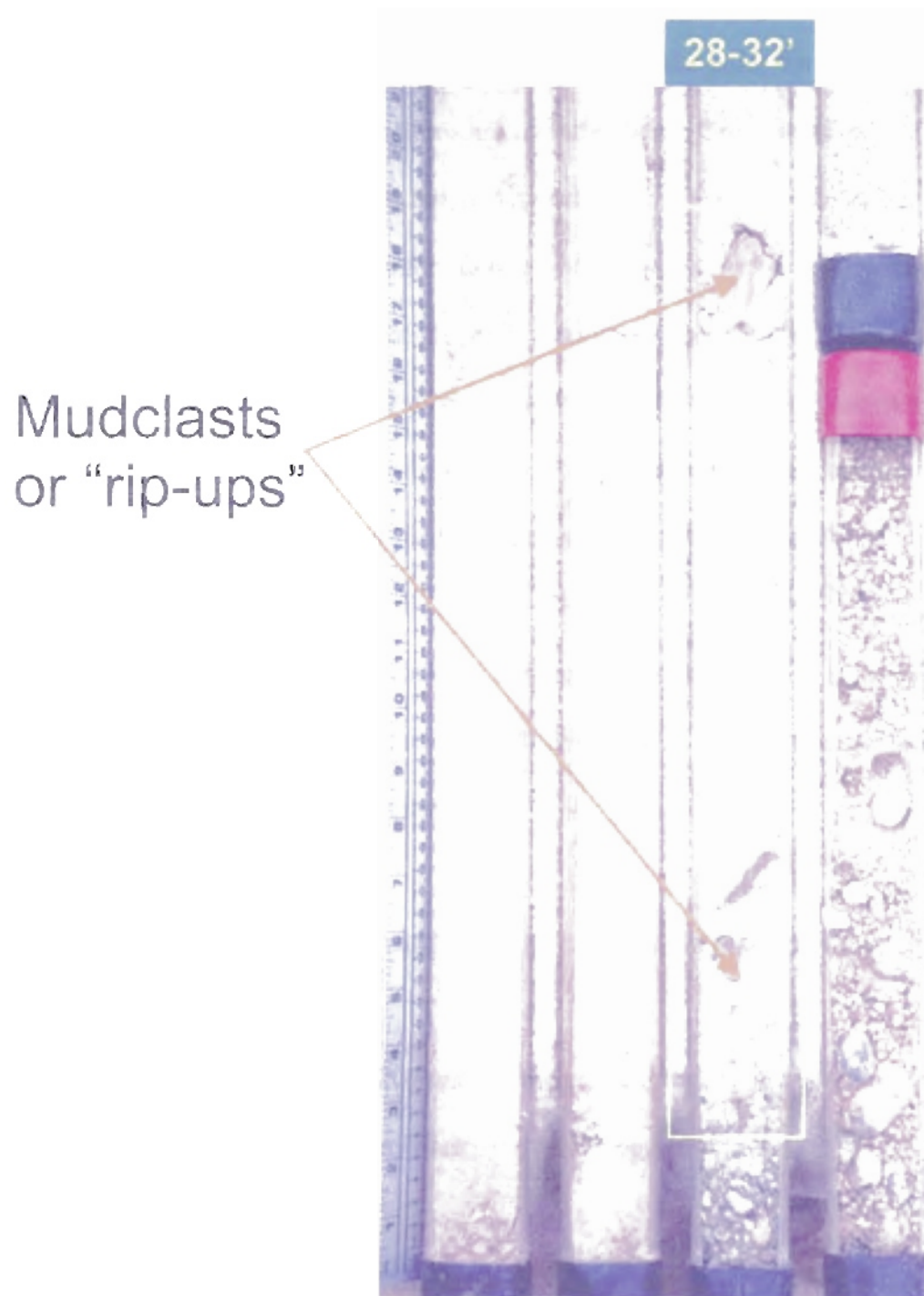


Fig. 17 – Mudclasts or "rip-ups" commonly occur at or near the base of many of the major sand beds in the Norman Landfill point bar.

Cross Sections of Conductivity Logs

Cross-sections of the conductivity logs were correlated across the study area. Eleven cross-sections were created; six run perpendicular to the point bar and five run parallel to the point bar. Two cross-sections are included here: Cross-section D-D' (Fig 18) runs perpendicular to the point bar, and a portion of cross-section I-I' (Fig 19) runs parallel to the point bar. The remaining cross-sections are shown in Appendix D.

The cross-sections indicate that the gross stratigraphy of the floodplain is essentially horizontal (layer-cake) and similar to flat floodplain topography seen today (Fig 12). The floodplain alluvium was broken up into 5 intervals that are labeled as Unit 100 through Unit 500. These units are identified on each of the cross-sections.

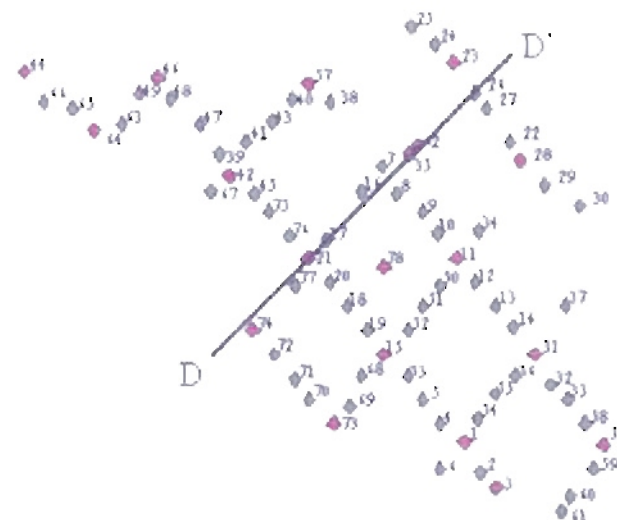
Unit 100- Basal layer of the alluvium. It ranges in thickness from 1.8 to 2.4 meters (6 to 8 feet) from the base of the alluvium. This unit is characterized by coarse grained sediments and gravels.

Unit 200- Sand overlying the basal layer. It is about 3 m (10 feet) thick.

Unit 300- Unit overlying the 200 unit. It ranges in thickness from 4.5 to 6 m (15 to 20 feet). This layer contains extensive mud layers and lenses.

Unit 400- Sand unit overlying the 300 unit. It is about 2.4 to 2.7 m thick (8 to 9 feet).

Norman Landfill Cross-Section D-D'



4

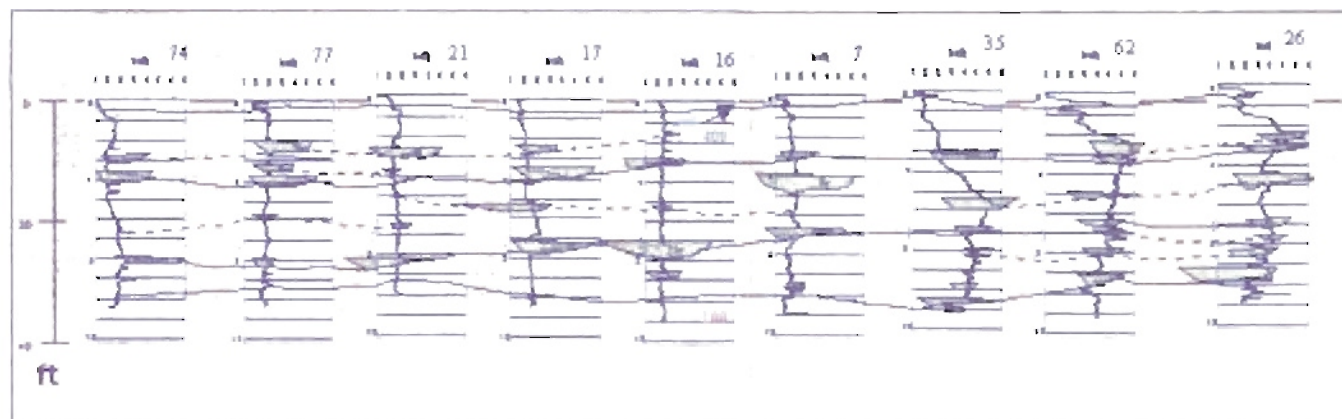


Fig. 18 Example cross-section running perpendicular to the point bar

Norman Landfill Cross-Section I-I'

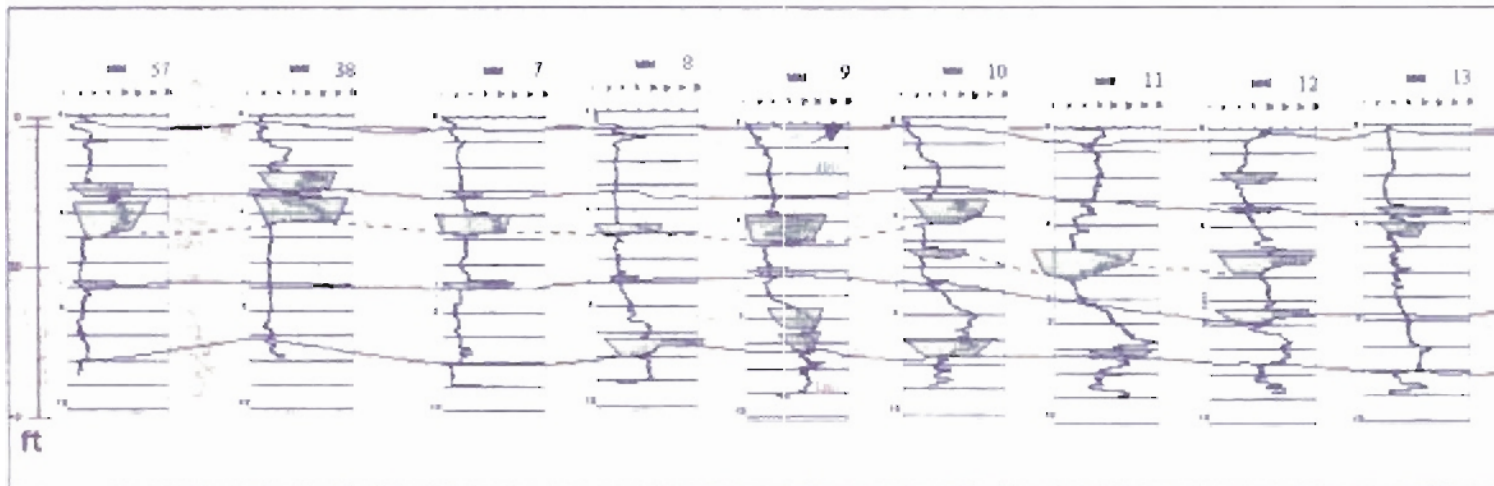
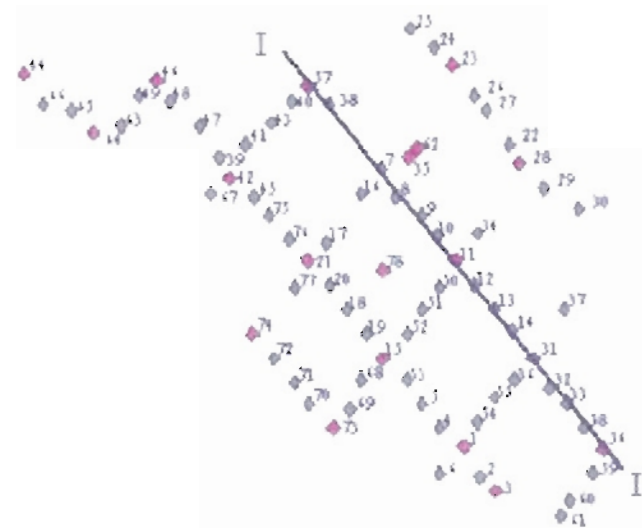


Fig. 19 Example cross-section running parallel to the point bar (complete cross-section is shown in Appendix D)

Unit 500- Unit extending from the surface down to about 1 m (3 feet). This unit is composed of very fine-grained sands.

These intervals have distinct texture (grain size/ sorting) and are bounded by mud layers. Mud layers were drawn on the cross-sections to illustrate the number and thickness of the muds in the floodplain alluvium. The cross-sections indicate that the number and thickness of muds increases toward the slough. The lateral extent of the mud layers throughout the alluvium is as follows:

- 1) Mud layers perpendicular to the bar complex range in length from <37 meters (<120 feet) to about 148 meters (485 feet)
- 2) Mud layers parallel to the bar complex range in length from <37 meters (<120 feet) to about 222 meters (728 feet)

Vertical Profiles and Interval Units for Correlation

A Type Conductivity Log (Well #1, Fig. 20) shows the standard vertical succession of sand and mud encountered in the 19 cores taken from the point bar. The lower 6-8' of the fill yields a characteristic 'choppy' conductivity response that is related to the basal layer (our **100 Interval**) deposited on top of the underlying Permian Hennessey Formation. The frequency distributions of grain size (Fig. 21) and sorting (Fig 22) for the basal layer are negatively skewed and bimodal. One mode is medium grained (0.25-0.5mm) and moderately sorted. The other mode is very coarse grained (0.5-1mm) and poor- to very poorly sorted. Some wells contain granule- (2-4mm) and pebble-size materials (>4mm).

Norman Landfill – Well #7

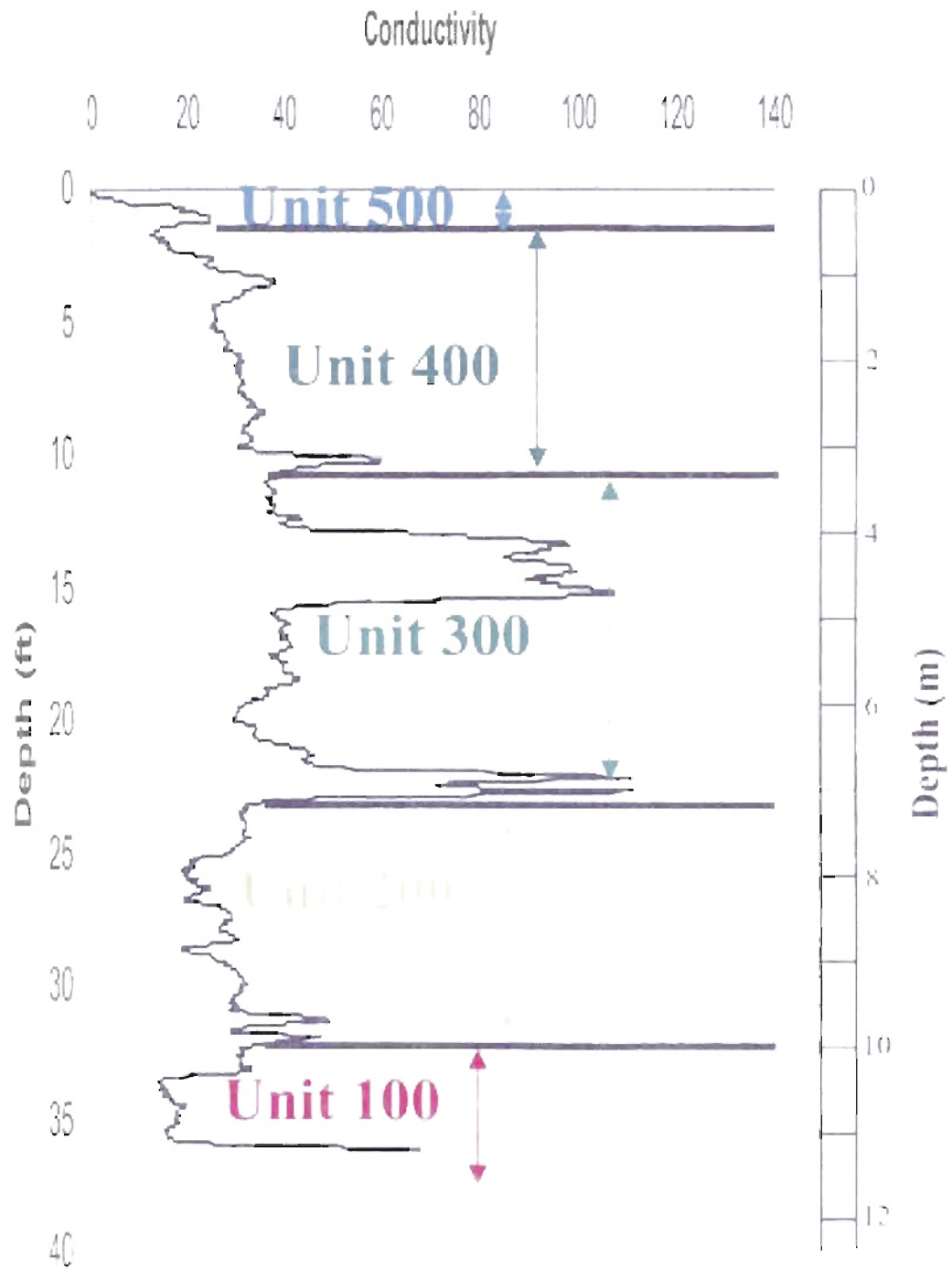


Fig. 20 - This is a type conductivity log from the Norman Landfill

Grain Size Sorting - NLF

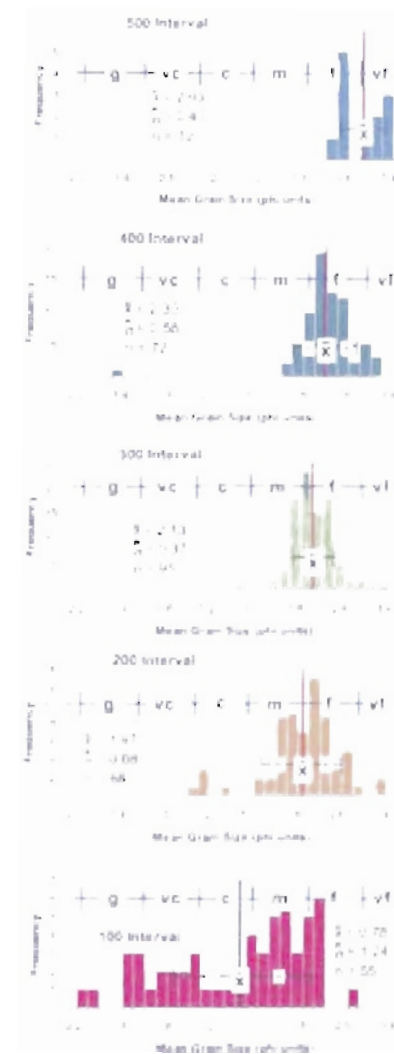
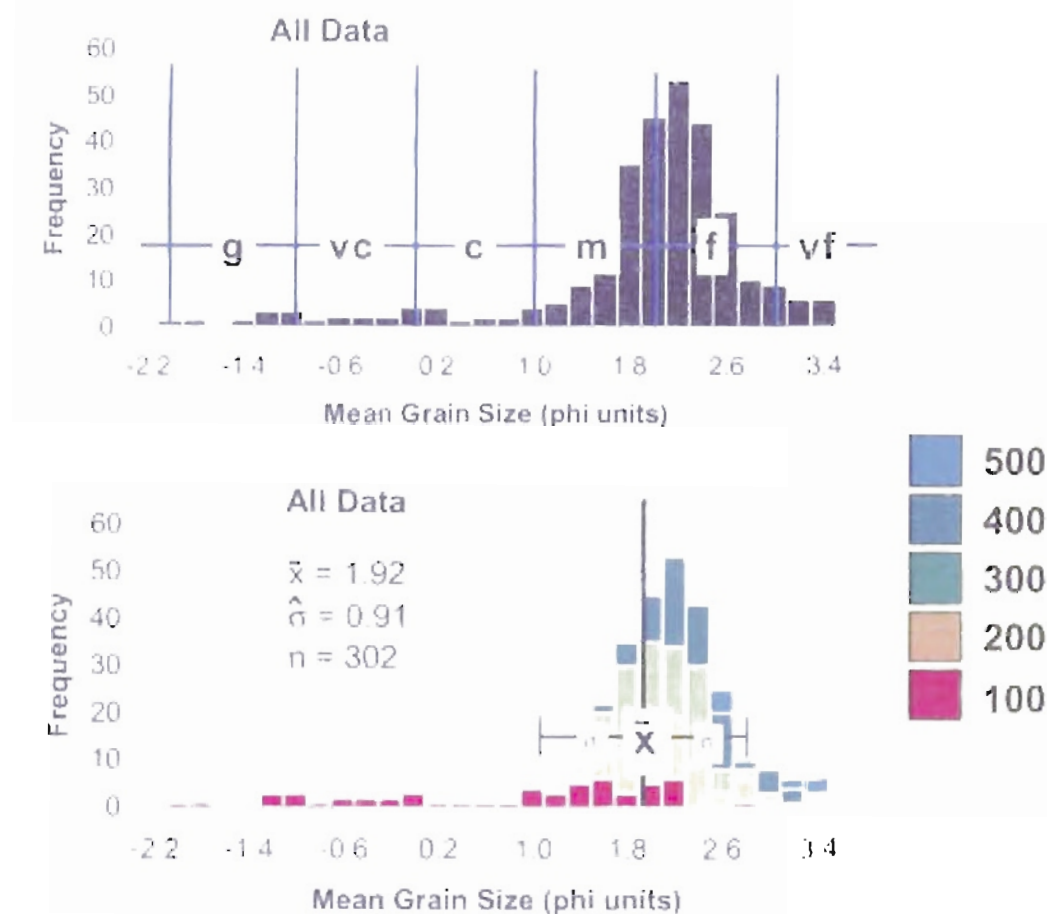
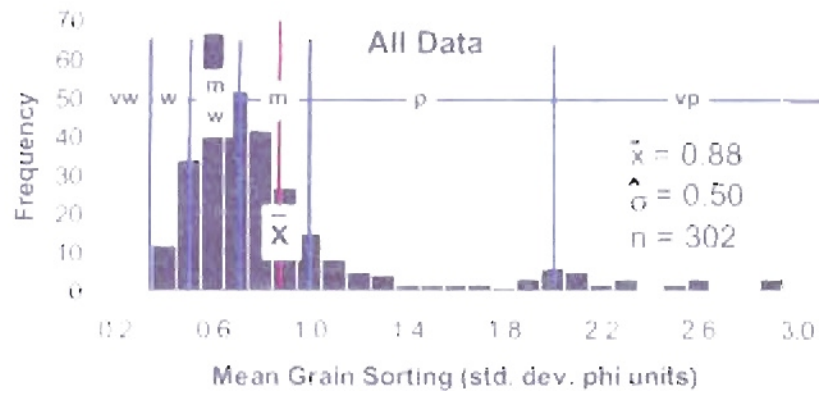
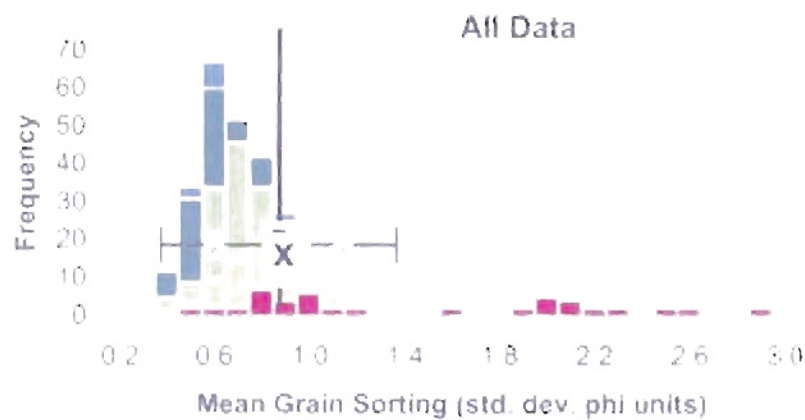


Fig. 21 Frequency distributions of mean grain size from sieve data. The intervals of unit designations (100, 200, etc.) used for correlation purposes are shown to the right.

Grain Size Sorting - NLF



at



- 500
- 400
- 300
- 200
- 100

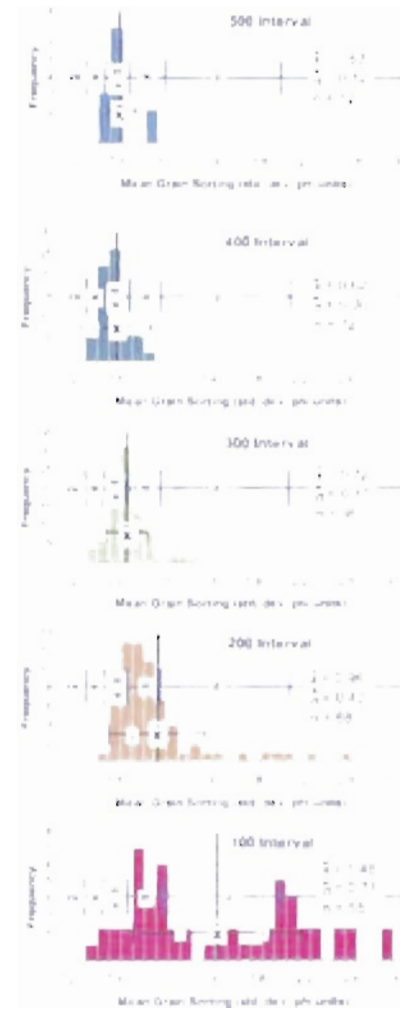


Fig. 22 Frequency distributions of mean grain sorting from sieve data. The intervals or unit designations (100, 200, etc.) used for correlation purposes are shown to the right.

There was no geographic significance seen in the bimodality. The bimodality may reflect inadequate sample size for such a heterogeneous population (n=55). The texture (grain size / sorting) of the basal layer is distinctly different from the texture of all the overlying layers on the basis of a Satterthwaite* t-test ($p < 0.0001$) performed in SAS, v. 8.01, 1999-2000 (Tables 2, 3). The null hypothesis (H_0) for this test assumes that the means for the two populations are equal (or not different). In this exercise, a significant difference was assumed to exist between populations means if $p < 0.1$.

A well developed but discontinuous mud layer (1-3' thick) was commonly present above the basal gravel. The overlying sand layer (**Interval 200**) is about 10' in thickness. This interval was fine to medium grained and moderately to moderately-well sorted. A few of the wells in this interval contain coarse grained, poorly sorted sand.

Another discontinuous interval of mud lenses (1-3' in thickness) lies above **Interval 200**. The **300 Interval** is fine to medium grained and moderately to moderately-well sorted. This interval was the thickest (about 15-20') and most heterogeneous of the layers with respect to the occurrence of mud layers and lenses. A t-test suggests that the **300 Interval** mean grain sorting is significantly different from the underlying **200 Interval** ($p < 0.0001$). The grain sizes between the two layers are slightly different ($p < 0.08$) (Tables 2, 3). Another 1-3' thick mud lenses occurs throughout the point bar at a depth interval between 5 and 10'.

The **400 Interval** is 8-9' in thickness and contains fine-grained, moderately-well to well sorted sand. The t-tests again indicated that the 400 Interval sand is finer grained ($p < 0.04$) and better sorted ($p < 0.01$) than the underlying **300 Interval**.

* Satterthwaite assumes unequal variances

Testing for Differences Between Layers in the NLF Point Bar

Table 2 - Grain Size (phi units)

	Variable	Method	Variances	DF	t Value	Pr > t
Interval						
500 vs. 400	Grain Size	Pooled	Equal	82	-3.63	0.0005*
		Satterthwaite	Unequal	19.7	-4.71	0.0001*
400 vs. 300	"	Pooled	Equal	165	-2.24	0.0264*
		Satterthwaite	Unequal	114	-2.12	0.0365*
300 vs. 200	"	Pooled	Equal	161	-1.91	0.0578*
		Satterthwaite	Unequal	96.2	-1.75	0.0836*
200 vs. 100	"	Pooled	Equal	121	-6.78	<0.0001*
		Satterthwaite	Unequal	79.5	-6.40	<0.0001*

* significant difference between population means

Testing for Differences Between Layers in the NLF Point Bar

Table 3 - Sorting (phi units standard deviation)

	Variable	Method	Variances	DF	t Value	Pr > t
Interval						
500 vs. 400	Sorting	Pooled	Equal	82	-0.11	0.9158ns
		Satterthwaite	Unequal	38.7	-0.19	0.8519ns
400 vs. 300	"	Pooled	Equal	165	2.68	0.0081*
		Satterthwaite	Unequal	107	2.50	0.0138*
300 vs. 200	"	Pooled	Equal	161	4.99	<0.0001*
		Satterthwaite	Unequal	83.9	4.44	<0.0001*
200 vs. 100	"	Pooled	Equal	121	4.89	<0.0001*
		Satterthwaite	Unequal	83.2	4.64	<0.0001*

* significant difference between population means

ns – not significant, means between two populations are the same

The **500 Interval** extends from the surface down to about 3'. This unit is fine to very-fine grained and moderately-well to well sorted. The **500 Interval** was significantly different from the underlying **400 Interval** with respect to grain size ($p < 0.0001$). Sorting does not vary between the **500** and **400 Intervals** ($p < 0.85$). The textural character of this upper layer is shaped by soil forming processes and aeolian sedimentation.

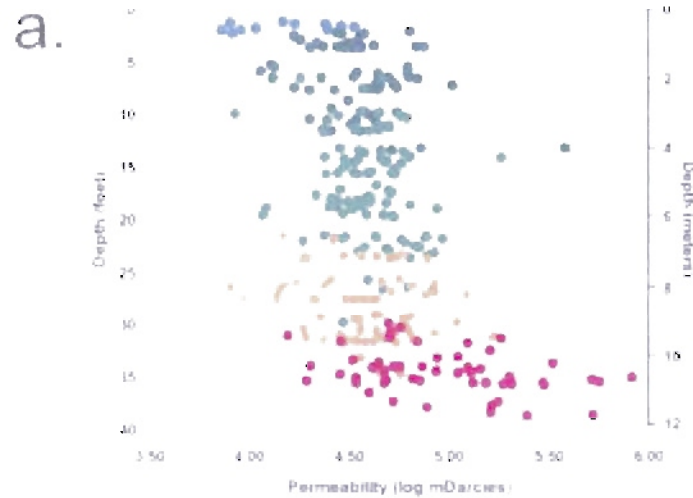
Calculated Permeabilities Relative to Stratigraphic Intervals

A SAS (v. 8.01) step-wise multivariate analysis of the grain size, sorting, and permeability data, taken from the experiments of Beard and Weyl (1973), was performed. The intent of this analysis was to estimate the relative importance of grain size and sorting in controlling the permeability of the grain packs used in their experiments. This analysis indicated that phi grain size explains 60% of the variation in permeability. This was followed in importance by grain sorting, which accounted for another 37% (60 + 37 = 97% total variation in permeability accounted for by these two variables). This analysis and inspection of the permeability equation (eq.4) suggests that the permeability of the point bar will increase directly with increasing grain size and vice versa. Likewise, better-sorted sands will have higher permeability, but this tendency can be offset quickly if the grain size grows small, resulting in lower permeability.

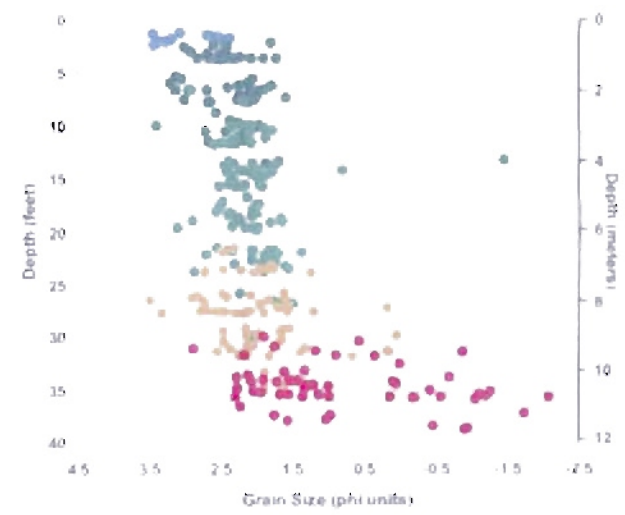
Accordingly, the vertical permeability profile for all the sieve data* (Fig. 23a) suggests that permeability varies more strongly with grain size than with sorting. Consequently, the permeability profile appears more similar in shape to the grain size

* calculated from an equation generated from data published by Beard and Weyl, 1973

Vertical Profiles in NLF Point Bar Deposits Canadian River, Oklahoma



b.



c.

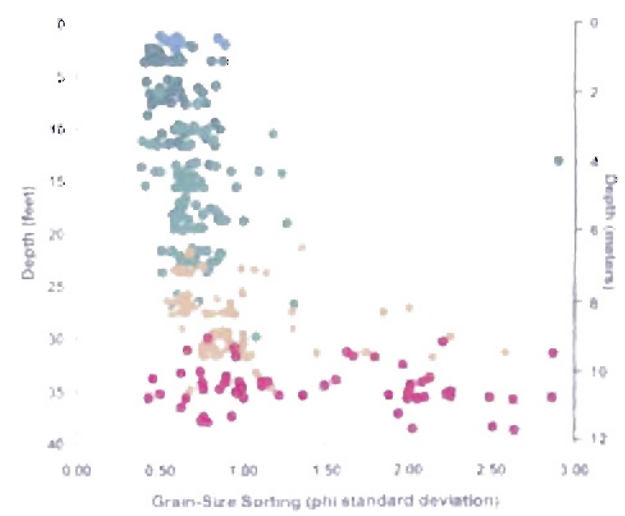
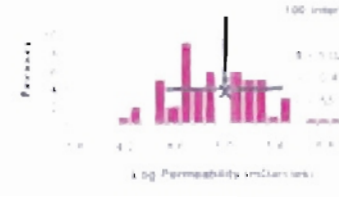
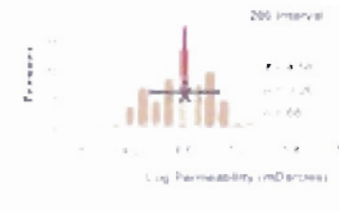
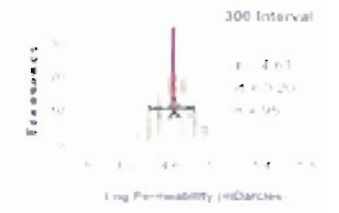
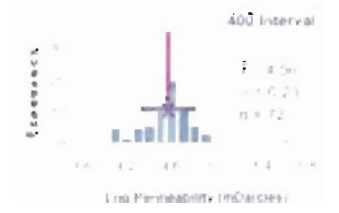
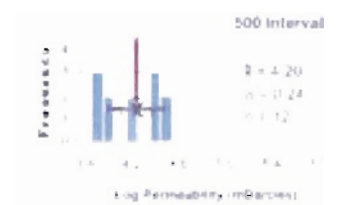
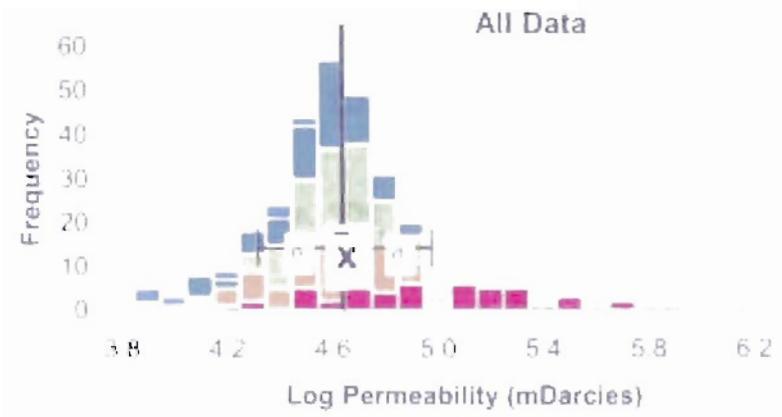
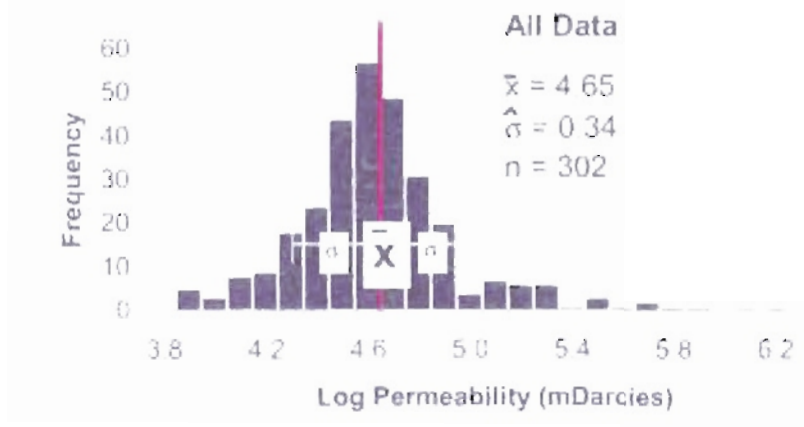


Fig. 23 Profiles of calculated permeability from measurements of grain size sorting in the Norman Landfill point bar subsurface intervals

profile (Fig. 23b) than to the sorting profile (Fig. 23c). The basal **100 Interval** (in red) exhibits the highest calculated permeabilities in the profile because of a population of large grains. This high permeability population has not been offset by the potential reduction in permeability because of poor sorting. Clearly, calculated permeabilities would be much higher if the coarsest grained sediments in the point bar of the Norman Landfill were better sorted. Likewise, the rapid fall in permeability in the **500 Interval** at the surface results from a strong shift in grain size to very fine-grained sand in these moderately-well sorted sands.

T-tests were performed on the permeability populations (Fig. 24) to determine if statistically significant permeability differences exist between the layers of the point bar. The basal **100 Interval** permeability is significantly different from the overlying **200 Interval** ($p < 0.0001$). The **200** and **300 Interval** permeabilities are not significantly different from one another ($p < 0.47$). Likewise, the **300** and **400 Intervals** are essentially the same with respect to permeability ($p < 0.19$). The mean permeability of the **500 Interval** population is significantly different from the underlying **400 Interval** ($p < 0.002$). These tests are summarized in Table 4.

Permeability - NLF



- 500
- 400
- 300
- 200
- 100

Fig. 24 Frequency distributions of mean permeability calculated from sieve data. The intervals or unit designations (100, 200, etc.) used for correlation purposes are shown to the right.

Testing for Differences Between Layers in the NLF Point Bar

Table 4 – Permeability (log units, mDarcies)

	Variable	Method	Variances	DF	t Value	Pr > t
Interval						
500 vs. 400	Log Perm	Pooled	Equal	82	4.98	<0.0001*
		Satterthwaite	Unequal	14.6	4.85	0.0002*
400 vs. 300	"	Pooled	Equal	165	1.35	0.1775ns
		Satterthwaite	Unequal	140	1.33	0.1867ns
300 vs. 200	"	Pooled	Equal	161	-0.75	0.4537ns
		Satterthwaite	Unequal	122	-0.72	0.4715ns
200 vs. 100	"	Pooled	Equal	121	6.68	<0.0001*
		Satterthwaite	Unequal	81.2	6.32	<0.0001*

* significant difference between population means

ns – not significant, means between two populations are the same

Permeability and Fining Upward Profile of Fluvial Sediments

Vertical profiles of the sieve data (Fig. 23) indicate that the 'classic fining-upward' profile for fluvial systems is punctuated at both the channel base and at the top by rapid changes in grain size and / or sorting (at least for the Canadian River). The **100 Interval** displays a very rapid yet progressive grain size decrease and improvement in size sorting from the channel base to about 8' up from the base. Likewise, the grain size of the upper few feet (**500 Interval**) of the point bar is much finer grained. As mentioned above, this rapid shift to finer grain size is due primarily to aeolian reworking of the floodplain sediments.

Excluding these deepest and shallowest intervals, the grain-size sorting improves progressively from 30' to a depth of about 3'. Grain size does not change very much through the base of the **200 Interval** to the top of the **400 Interval** (Fig. 23). Visual inspection of the grain size trends in the thick **300 Interval** shows no vertical variation in grain size. The statistically significant differences in grain size noted earlier for the **200 to 400 Intervals** (upward fining) appears to not be translated to an upward decrease in permeability. This finding appears compatible with the following observations: (1) the vertical grain size differences are quite subtle and (2) there is a concomitant improvement (statistically significant) in grain sorting. The improved grain sorting has resulted in higher porosity that compensates for the progressively decreasing grain size upward.

The work of Christenson et al. (1998) used slug tests and calculations of hydraulic conductivity to conclude that the highest permeability in the alluvium adjacent to the NLF is located at the base of the sediment package. The vertical permeability profile in Fig. 23a is similar in appearance to the data of Christenson et al. (1998) (Fig. 25a).

Hydraulic Conductivity

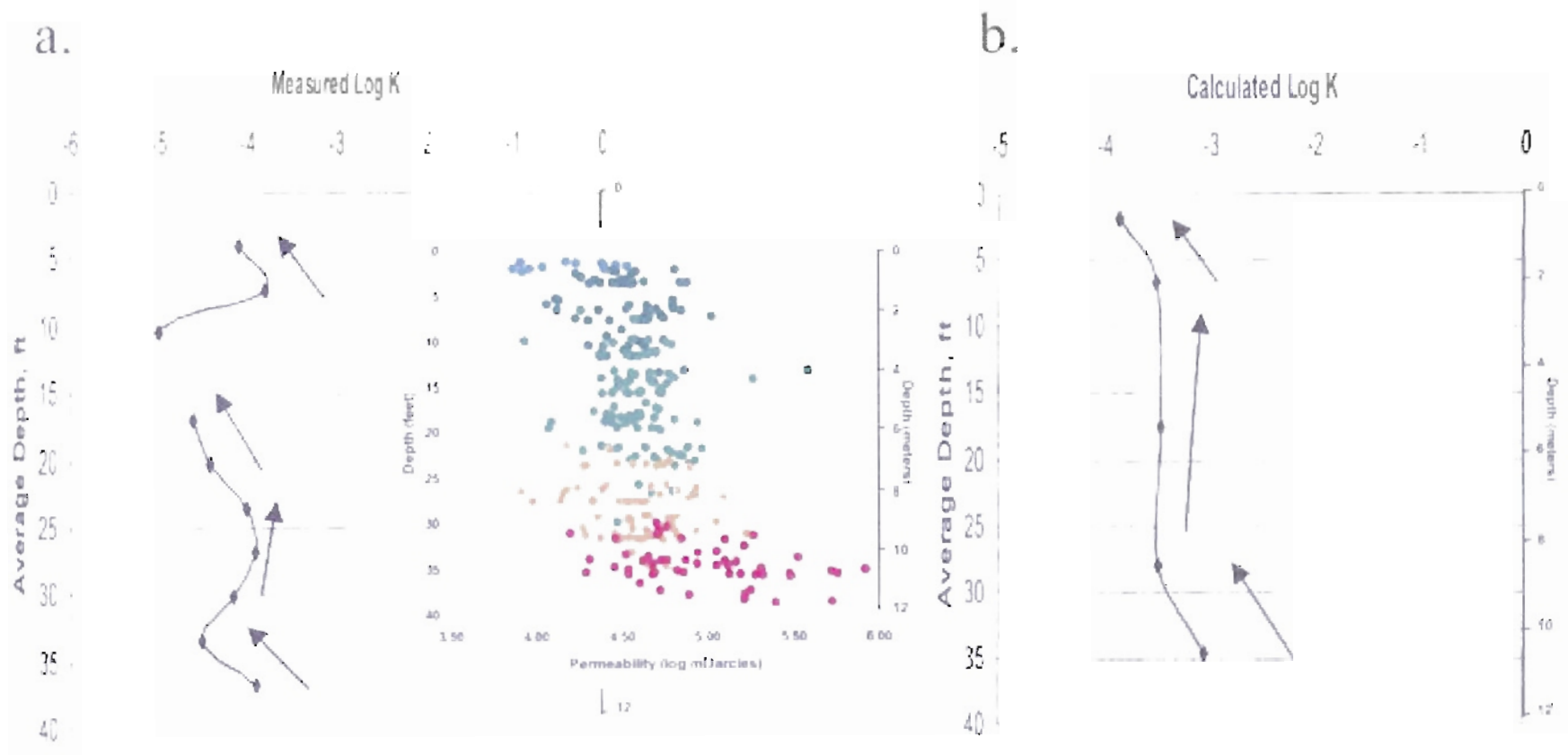


Fig. 25 Calculated hydraulic conductivity (right, this study) compared to measured hydraulic conductivity (left) reported by Scholl and Christenson (1998) at Norman Landfill well 37SL1. The hydraulic conductivity units are in m^2/s . The color inset shows the vertical profile of permeability that is color coded by the interval layers.

Conversion of the NLF permeabilities calculated from sieve data to hydraulic conductivity values (Fig. 25b) yielded a profile that is also similar in appearance to the Christenson et al. (1998) data. The present study concurs with the findings of the Christenson et al. (1998) and finds significant evidence for a preferred permeability pathway at the base of the alluvial fill. The sand intervals above the base (with exception of the 500 Interval near the surface), however, all have comparable permeability. The calculated hydraulic conductivity resulted in a range from $1.4\text{E-}04$ m/s to $9.22\text{E-}04$ m/s. The higher hydraulic conductivity was seen in the basal segment of the alluvium. It is estimated that the plume is moving at a rate of at least 48 meters per year in the basal unit. This estimate was calculated using a gradient of .0006 which is characteristic between the floodplain and the slough. The gradient becomes steeper, however, as you approach the slough so the rate of plume movement may increase. This rate of movement also decreases shallower in the section as hydraulic conductivity of the sediments declines (Fig. 26).

Texture and permeability profiles for Wells #1 and 15 are provided in Figs. 27 and 28, respectively. In some of the wells, the correspondence between grain sizes, sorting, and conductivity is quite striking (Fig. 27, 28). The correspondence suggests that lower conductivity sand intervals are finer grained and better sorted than higher conductivity sand intervals. This relationship is not understood. The data would suggest that deeper, coarser grained and more poorly sorted sand intervals contain more disseminated silt and clay than the shallow sand intervals. No evidence for this was seen in the cores.

Norman Landfill

Calculated Rate of Plume Movement

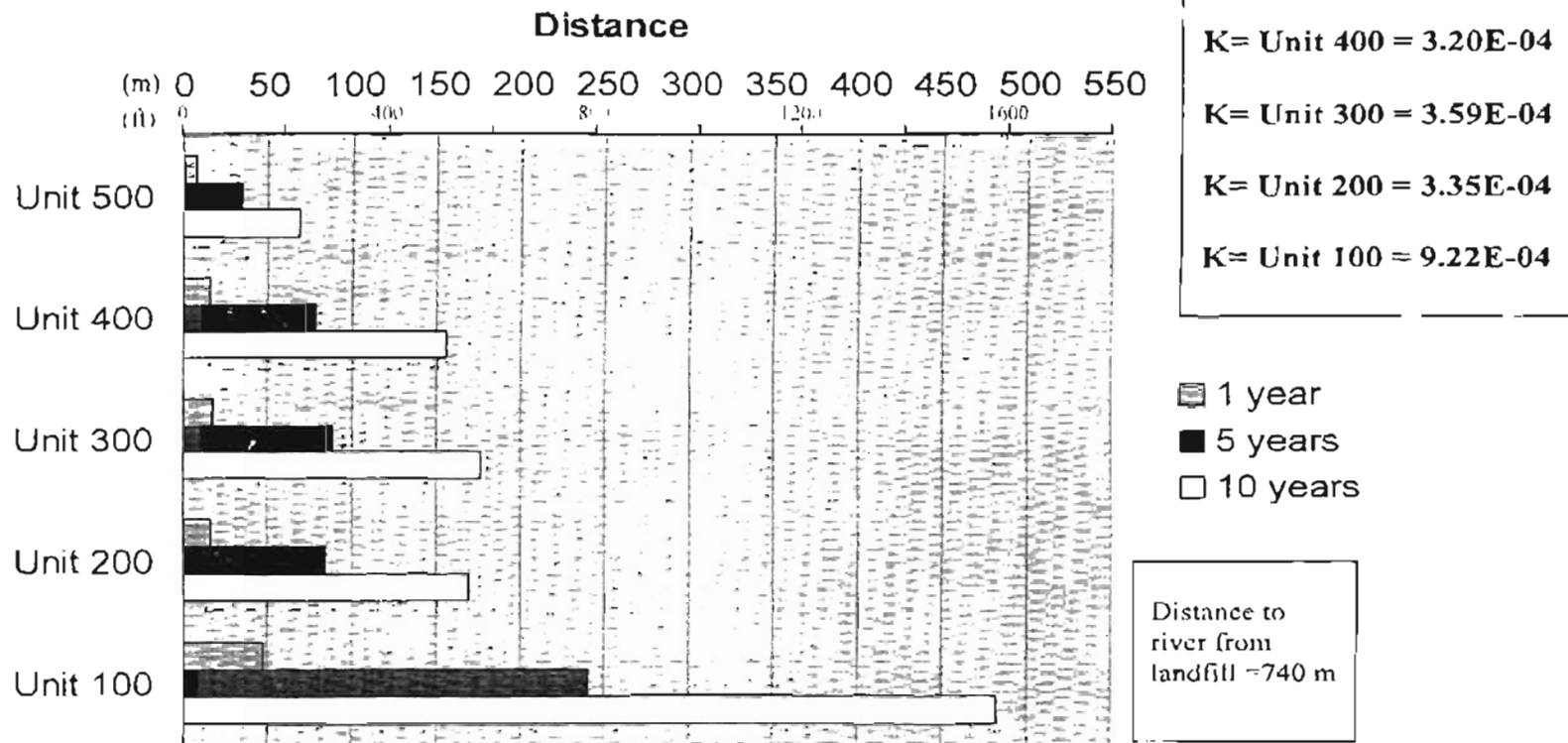


Fig. 26 – Rate of plume movement based upon calculated hydraulic conductivity of each of the sand intervals. The velocity of the plume was calculated using the equation $V = (K * I) / \text{effective porosity}$. The effective porosity for each unit was calculated from the mean grain size / sorting data obtained from the cores. A gradient (I) of 0.006 was used for the calculation. This gradient is characteristic of the floodplain between the slough and the river. The gradient becomes steeper near the slough and landfill.

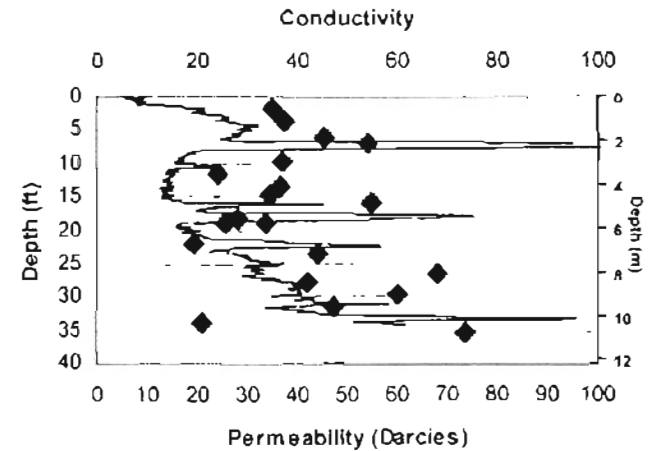
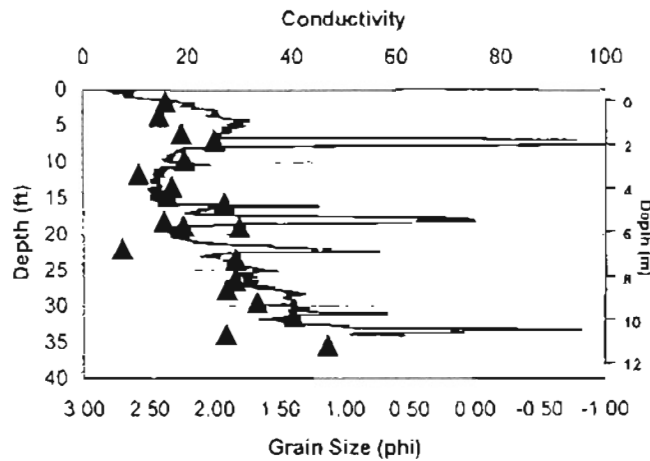
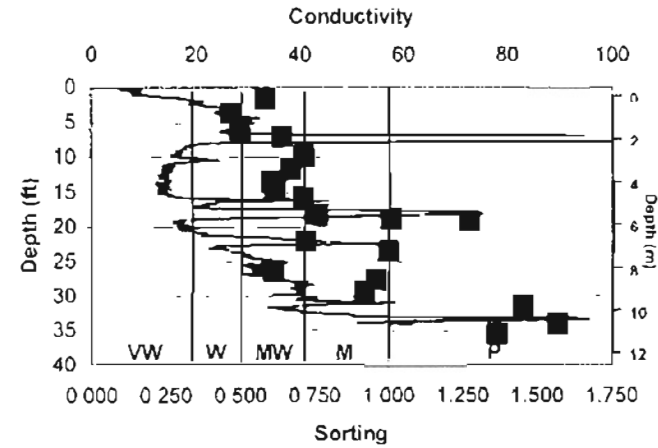
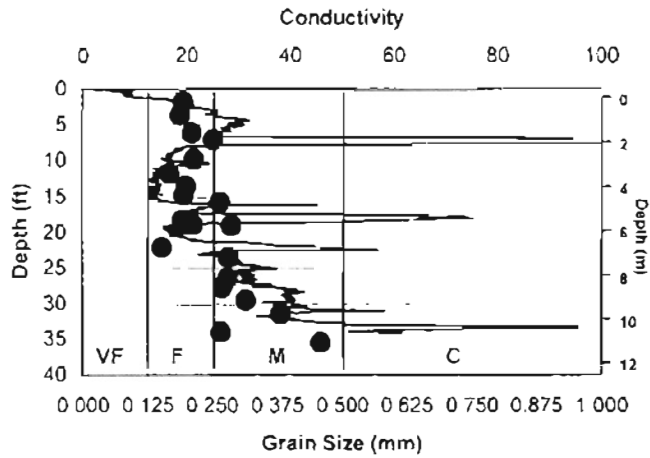


Fig. 27 – Vertical profiles of grain size, sorting and calculated permeability in Norman Landfill well #1. Note the correspondence between conductivity and the sediment grain size and sorting.

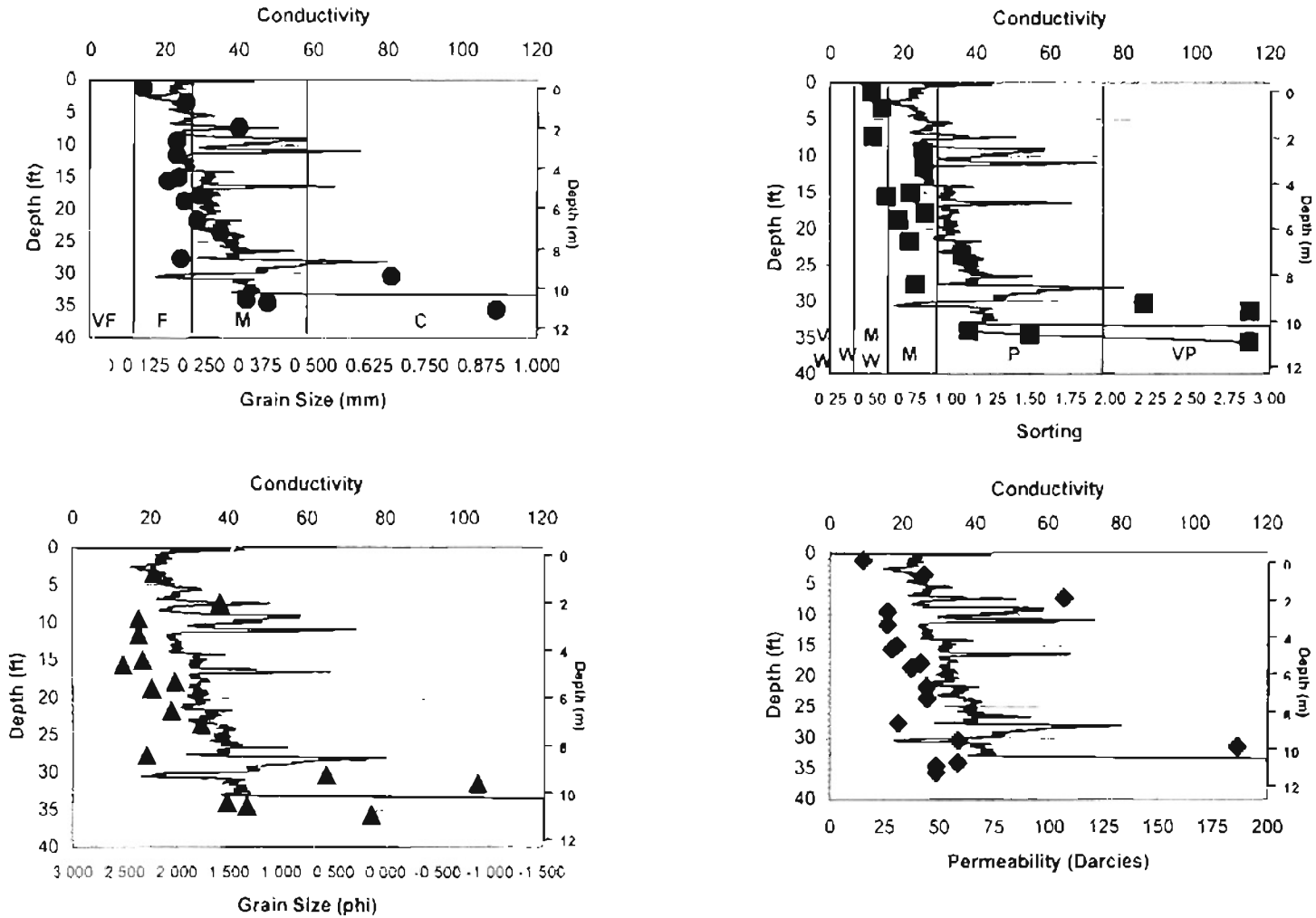


Fig. 28 – Vertical profiles of grain size, sorting and calculated permeability in Norman Landfill well #15. Note the correspondence between Geoprobe conductivity and the sediment grain size and sorting. Permeability also tracks the conductivity.

Block Diagrams

Six block diagrams were created of the floodplain alluvium. They provide a three-dimensional (3-D) perspective of the geometry and thickness of the five distinct sand intervals in the point bar. Three of the block diagrams view the study area from the southwest corner (Fig. 29), and three view it from the southeast corner (Fig. 30). The southwest and southeast views are illustrated with 25%, 50%, and 75% of the model cutaway. These diagrams provide a 3-D view of the gross stratigraphy of the floodplain. As determined by the cross-sections it is essentially horizontal (layer-cake) and similar to the flat floodplain topography seen today.

Two block diagrams of the conductivity data were also created. These diagrams provide visuals of changes in conductivity throughout the floodplain. One is viewing the site from the southeast corner (Fig 31), and the other is viewing the site from the southwest corner (Fig. 32). In Figure 31 the higher conductivity values near the slough are apparent between 1055 and 1075 feet. These higher conductivity zones, near Wells #23 and #28, are between the slough and the landfill. Thick, dense clay layers were found in these cores about 1070 feet, which is 15 feet below the surface.

Conductivity slices were also created for each of the five sediment intervals (Figs. 33-37). The slices provide visualization of conductivity changes with depth. By comparing each of the slices it is seen that not much differentiation exists in conductivity in the west side of the study area. The highest conductivity zones are limited to the area adjacent to the landfill. In the east side of the study area very high conductivity occurs in the upper part of the 300 unit (Fig 35). This high conductivity zone is associated with the thick, dense clay as seen in cores from wells 23 and 28. The conductivity in this zone

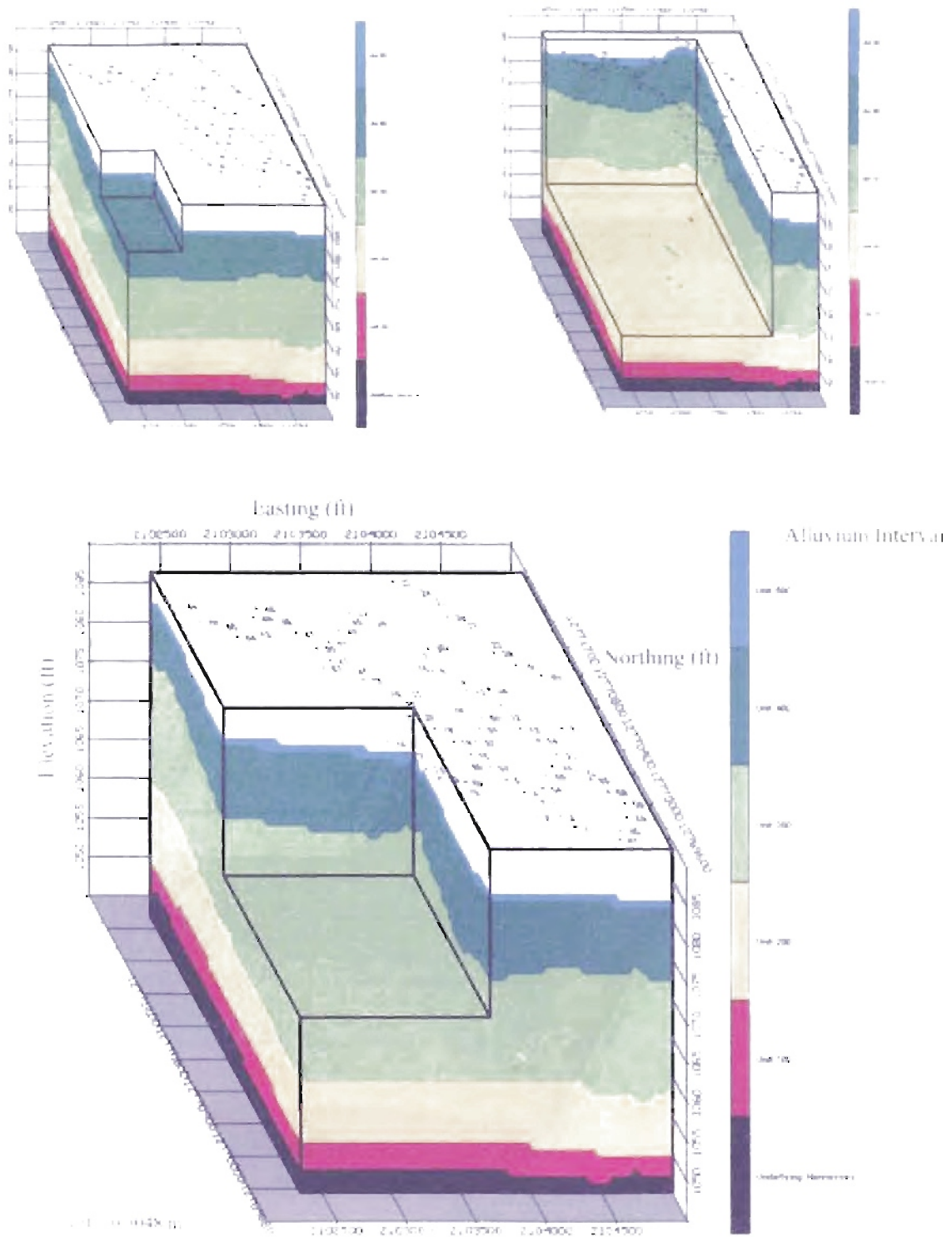


Fig. 29 - Block diagrams of the alluvium intervals. View is from southwest corner of study area. Easting and Northing are based on UTM-Zone 14 in feet. Mean sea level elevation is in feet. (Rockworks converted Easting and Northing coordinates to feet)

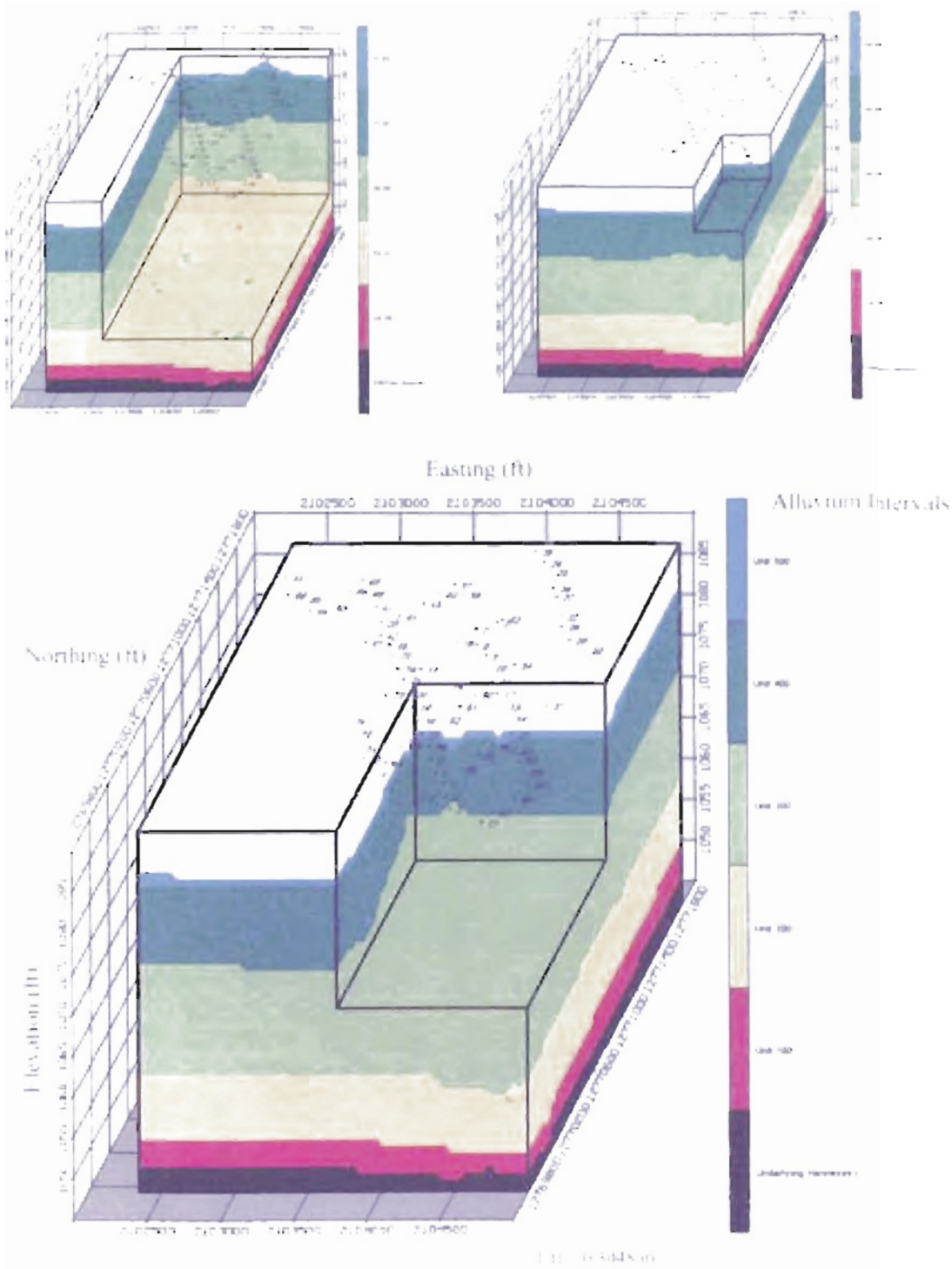


Fig. 30 - Block diagrams of the alluvium intervals. View is from southeast corner of study area. Easting and Northing are based on UTM-Zone 14 in feet. Mean sea level elevation is in feet. (Rockworks converted Easting and Northing coordinates to feet.)

View from Southeast

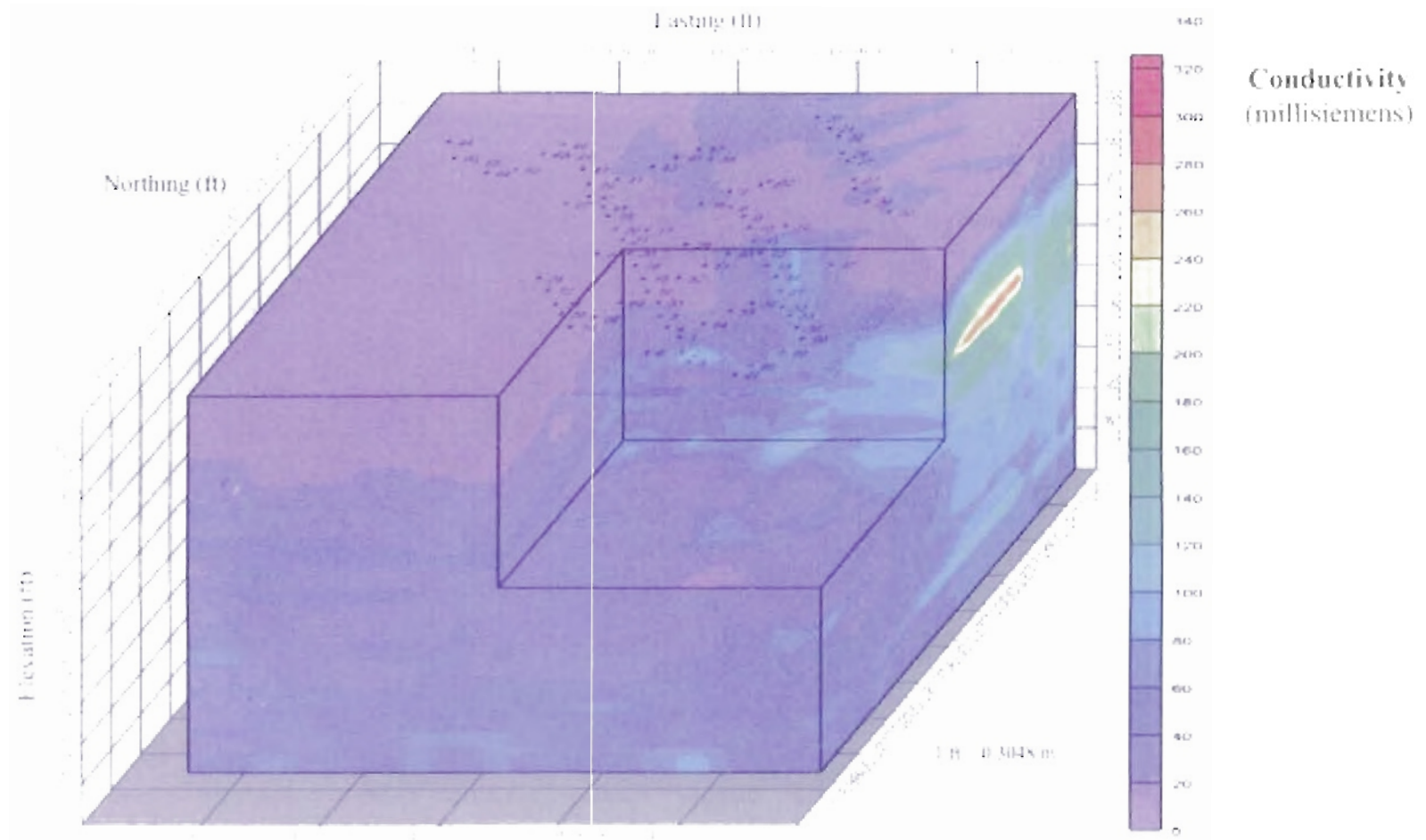
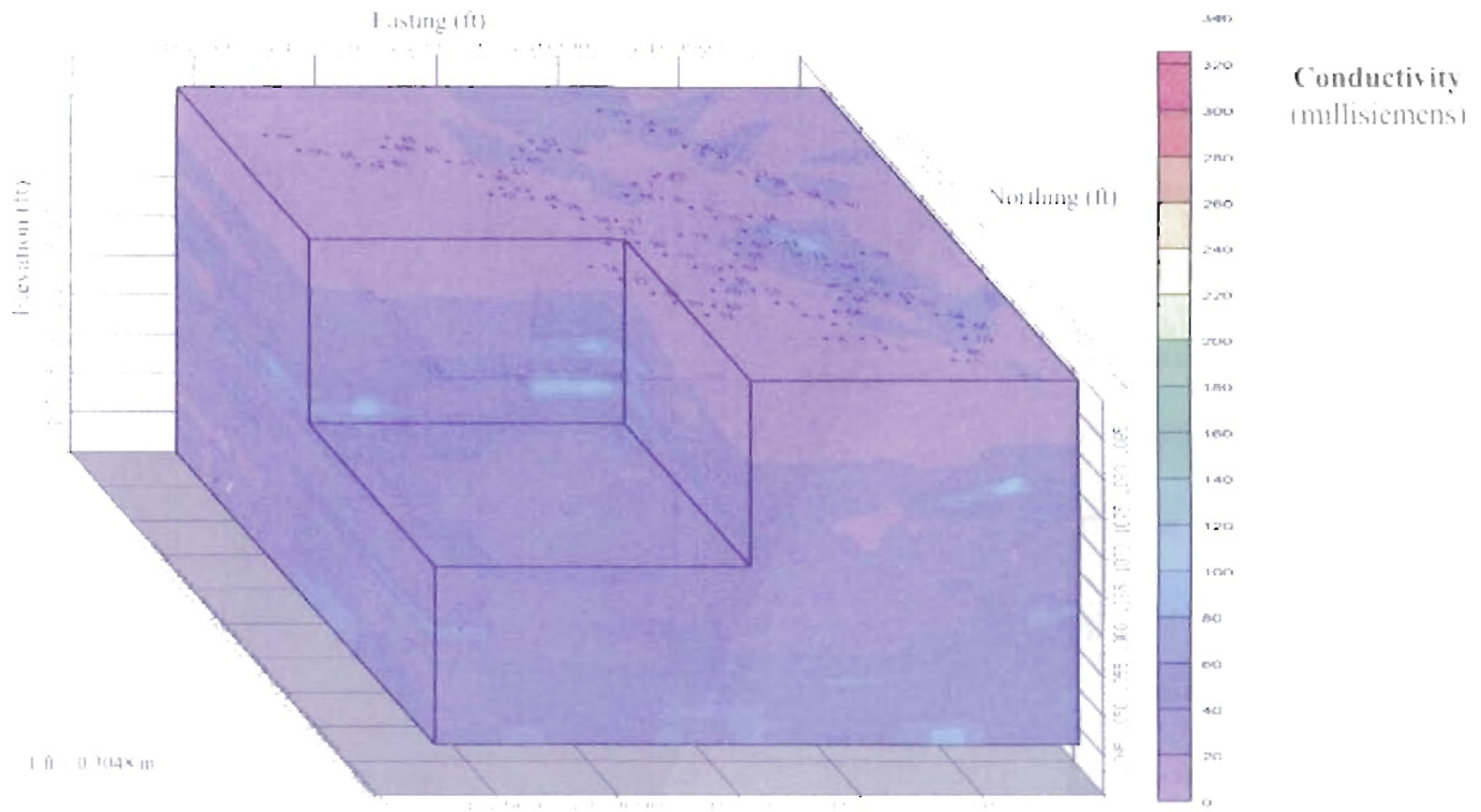


Fig. 31- Block diagram of conductivity values. View is from southeast corner of the study area. Easting and Northing are based on UTM Zone 14 in feet. Elevation above mean sea level is in feet. (Rockworks converted Easting and Northing coordinates to feet.)

View from Southwest



68

Fig. 32- Block diagram of conductivity values. View is from southwest corner of the study area. Easting and Northing are based on UTM Zone 14 in feet. Elevation above mean sea level is in feet. (Rockworks converted Easting and Northing coordinates to feet)

Unit 100

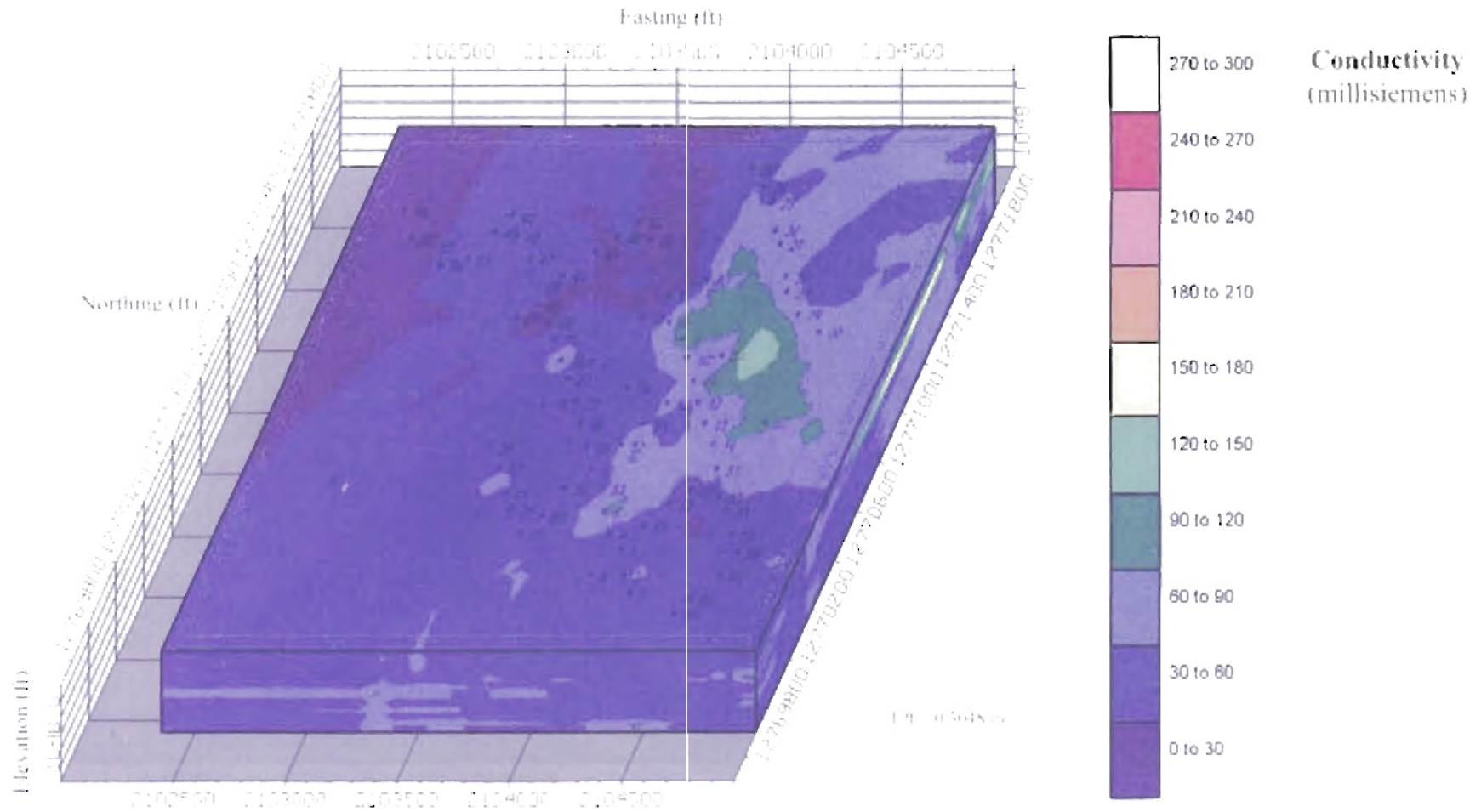


Fig. 33- Conductivity map of the 100 Unit slice. View is from southeast corner of the study area. Easting and Northing are based on UTM Zone 14 in feet. Elevation above mean sea level is in feet. (Rockworks converted Easting and Northing coordinates to feet.)

Unit 200

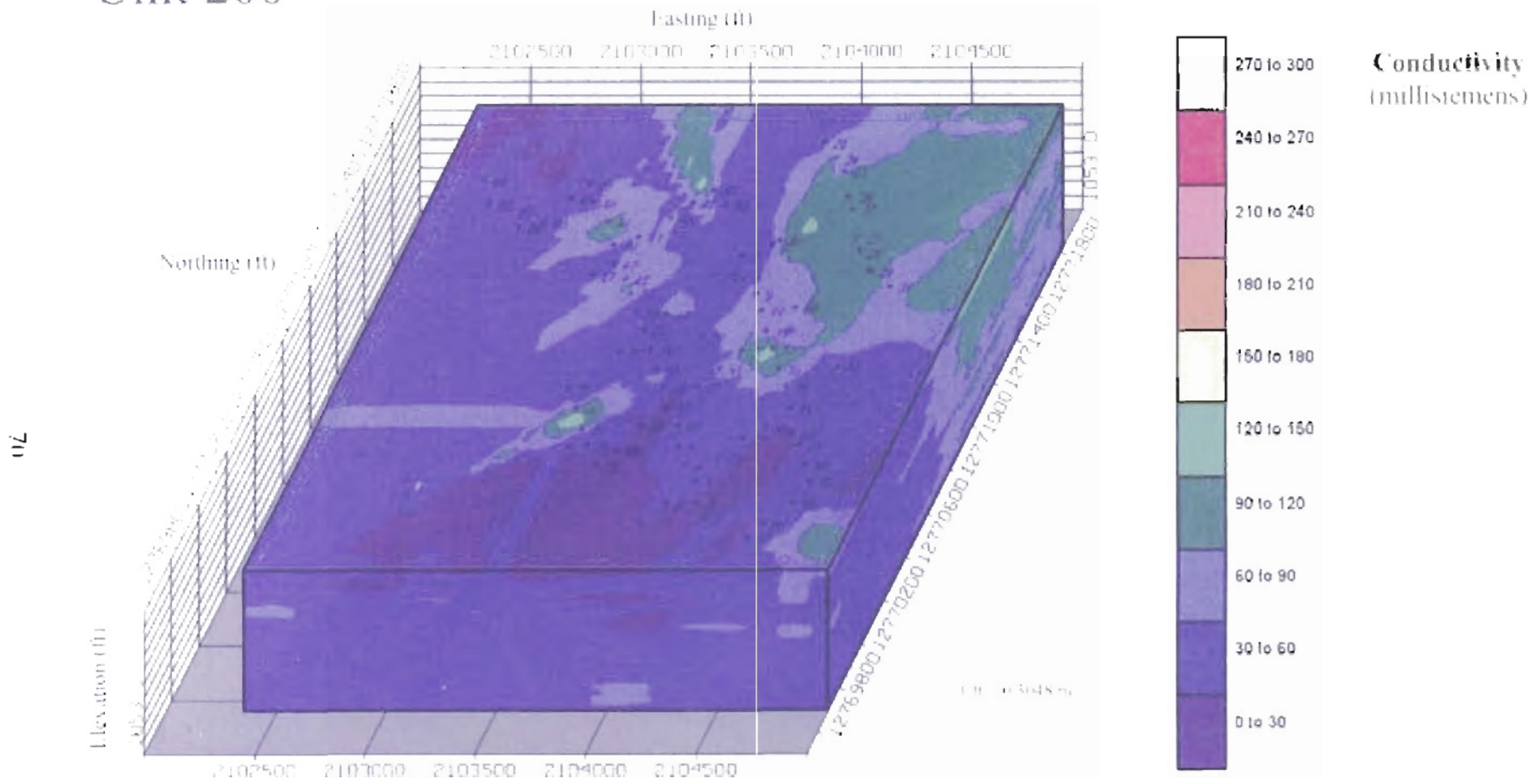


Fig. 34- Conductivity map of the 200 Unit slice. Easting and Northing are based on UTM Zone 14 in feet. Elevation above mean sea level is in feet. (Rockworks converted Easting and Northing coordinates to feet.)

Unit 300

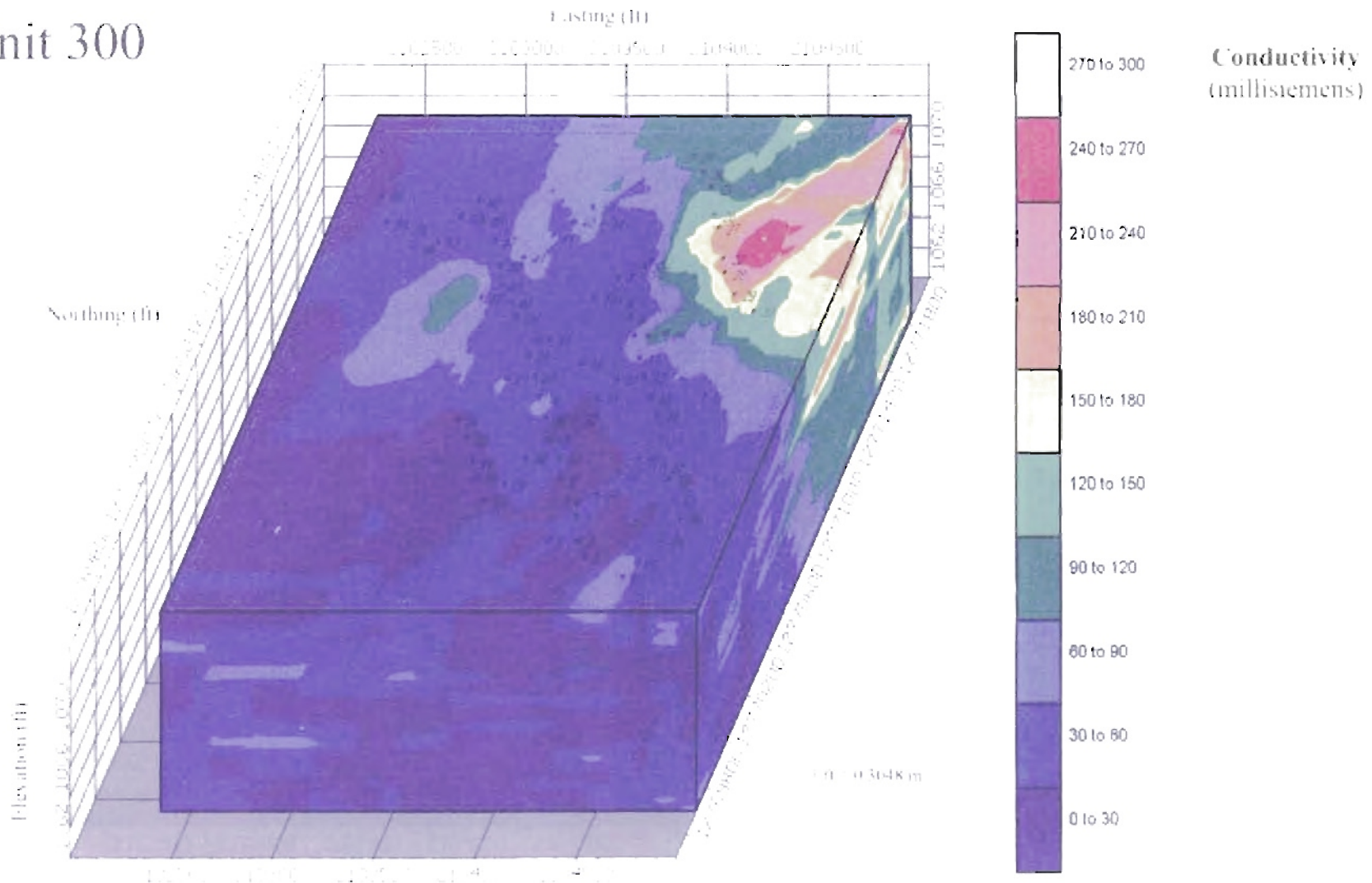


Fig. 35 - Conductivity map of the 300 Unit slice (Easting and Northing are based on UTM Zone 14 in feet. Elevation above mean sea level is in feet. (Rockworks converted Easting and Northing coordinates to feet.)

Unit 400

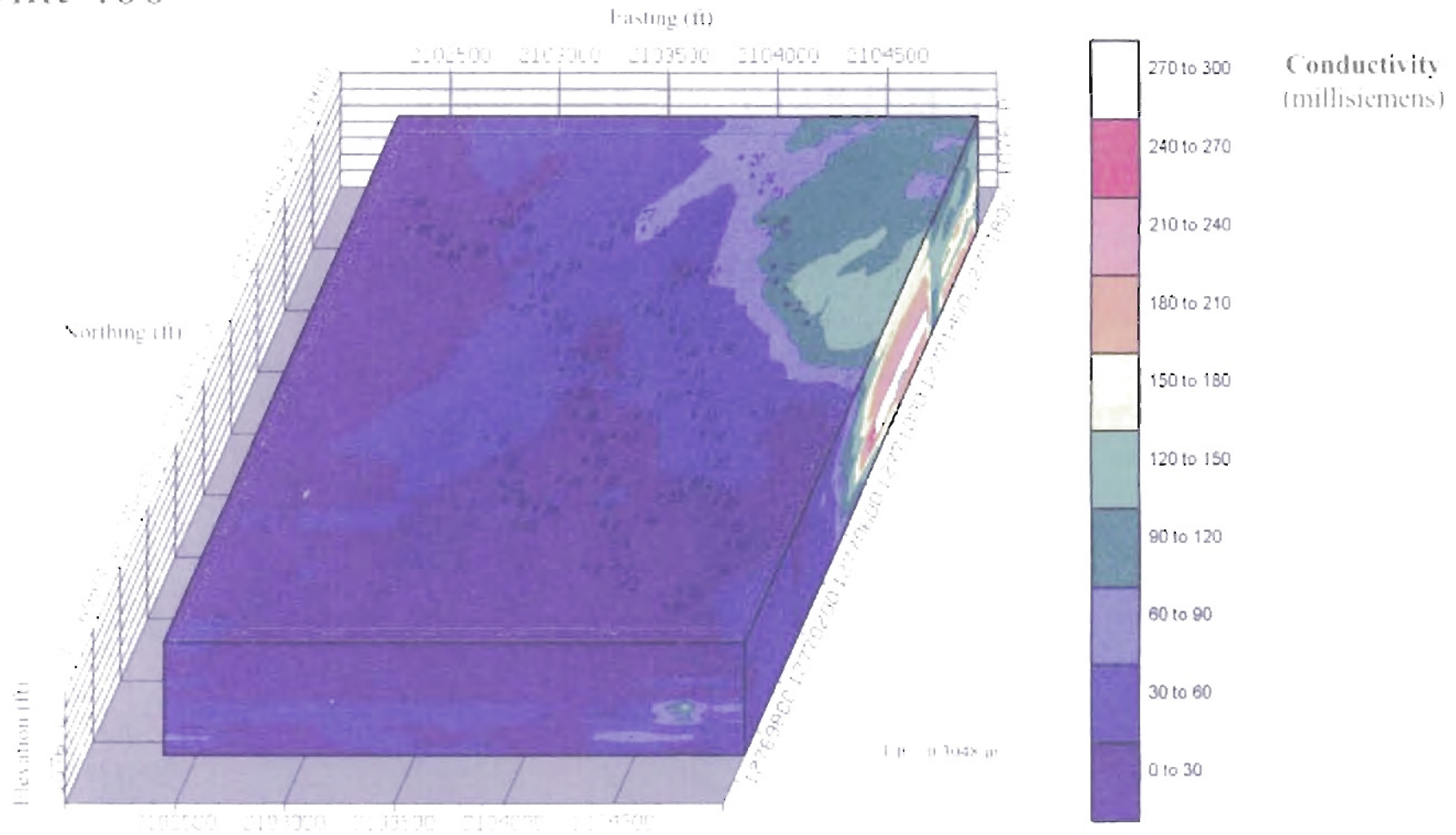


Fig. 36- Conductivity map of the 400 Unit slice. (Easting and Northing are based on UTM Zone 14 in feet. Elevation above mean sea level is in feet. (Rockworks converted Easting and Northing coordinates to feet.)

Unit 500

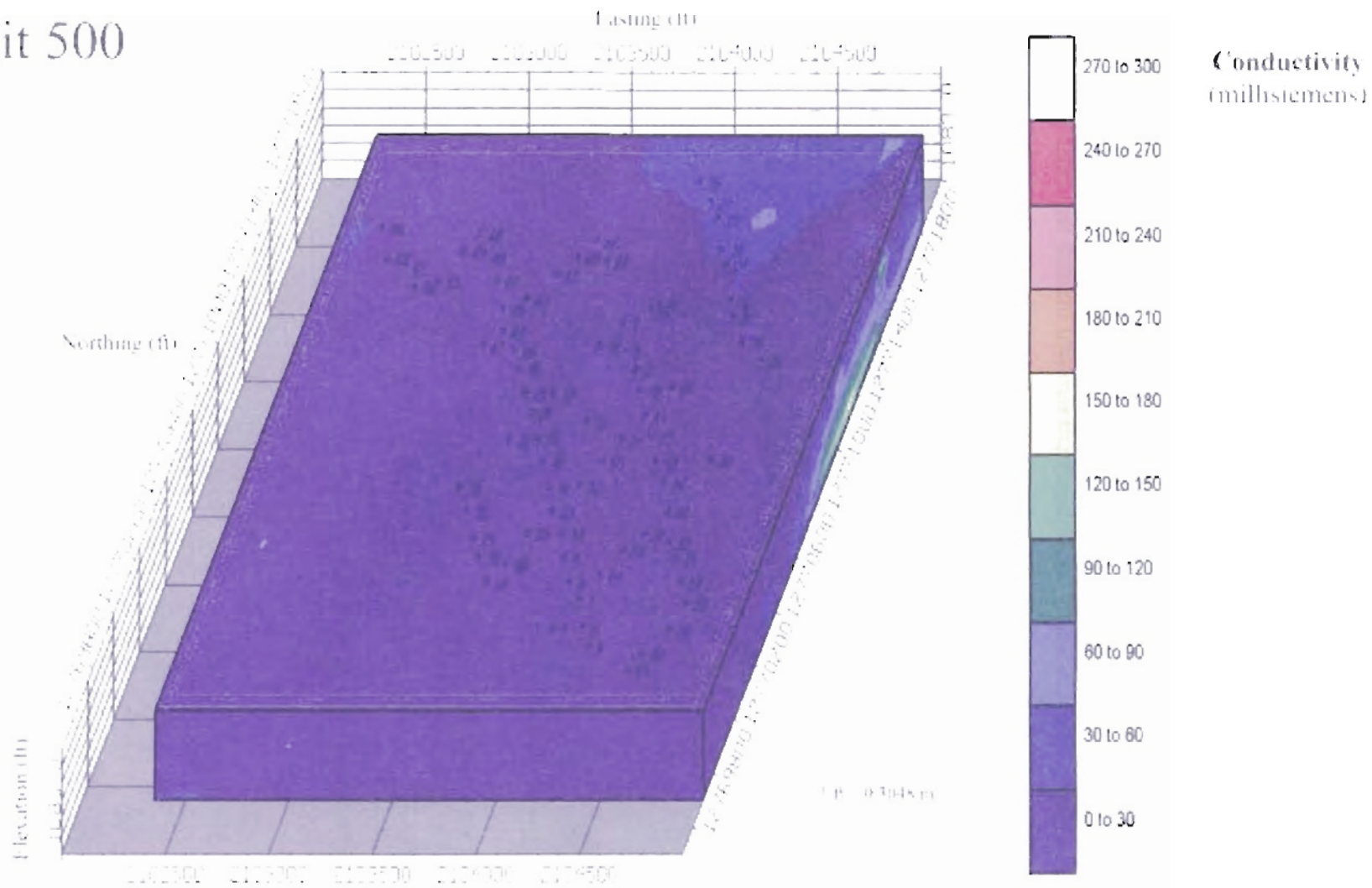


Fig. 37- Conductivity map of the 500 Unit slice. Easting and Northing are based on UTM Zone 14 in feet. Elevation above mean sea level is in feet. (Rockworks converted Easting and Northing coordinates to feet.)

remains high near the landfill and decreases as you move further west. Conductivity near the landfill is higher than expected for clay rich sediment, and may suggest interaction of the clay with the leachate.

The high conductivity zone seen adjacent to the landfill appears to extend vertically through units 400, 300, 200 and 100. The conductivity values decline as you move away from the landfill towards the floodplain. These elevated conductivity values could result from the increase in number of muds in the east side of the study site, or it could be possible that the higher conductivity in the east is a reflection of leachate contamination. Not enough information exists at this point to distinguish between what may be the plume or may be clays.

CHAPTER V

CONCLUSIONS

Principle findings of the study are as follows:

- 1) On the basis of conductivity patterns, sediment texture, and vertical succession, five distinct layers exist beneath the floodplain. Of these, the basal layer is the most significant in the transport of the plume. Earlier studies, based on specific conductance of the groundwater, have determined that the plume is already in this layer.
- 2) The flow pathways are bounded by mud layers that are discontinuous. The mud layers act as impermeable units locally and can direct movement of the leachate. These mud layers are found in similar stratigraphic positions and were likely formed during periods of time when the surface was exposed. Some layers do appear to be more extensive throughout the area. The dimensions of these larger mud layers are:
 - a) Mud layers perpendicular to the bar complex range in length from <37 meters (<120 feet) to about 148 meters (485 feet)
 - b) Mud layers parallel to the bar complex range in length from <37 meters (<120 feet) to about 222 meters (728 feet)

- 3) The number and thickness of mud layers increases toward the slough (adjacent to the landfill).
- 4) The maximum permeability pathway (as defined by grain size / sorting) occurs in the basal segment of the valley fill. This interval encompasses the lower 1.8 to 2.4 meters (6 to 8 feet) of the alluvium and has an average permeability of 105 Darcies.
 - a) The sediment overlying the basal unit has a permeability of 38 Darcies. This encompasses units 200, 300, and 400 for a total thickness of about 8.6 meters (28 feet).
 - b) The sediments in the upper 0.6 meters (2 feet) of the alluvium have a permeability of 16 Darcies. These sediments are mainly aeolian.
- 5) Block models of the different sand units provide a 3-D view of the geometry and thickness of the five distinct sand intervals in the point bar. The models suggest the highest conductivity occurs in the lower part of the 400 unit and the upper part of the 300 unit.
- 6) Conversion of permeability data to hydraulic conductivity results in a range from $1.4\text{E-}04$ m/s to $9.22\text{E-}04$ m/s. The higher hydraulic conductivity is seen in the basal segment of the alluvium. This data compared very favorably to hydraulic conductivity measurements taken by Scholl and Christenson (1998).
- 7) It was estimated that the plume is moving at a rate of at least 48 meters (157 feet) per year in the basal unit. This estimate was calculated using a gradient of .0006 which is characteristic of the area between the floodplain and the slough. The gradient becomes steeper, however, as you approach the slough. so the rate of

plume movement may increase. This rate of movement also decreases shallower in the section as hydraulic conductivity of the sediments declines.

- 8) Block models were also created of the conductivity data. These models show higher conductivities near the landfill and slough. This supports the findings that the number and thickness of muds increases as the slough is approached. A thick, dense clay layer is located about 4 meters (13 feet) below the surface between the landfill and the slough (wells 23 and 28). This clay is highly conductive as compared with the rest of the landfill alluvium and does not appear in cores away from the slough.
- 9) On balance, much higher conductivities are found in the areas near the slough and landfill because of the number of clays in the area. However, the base conductivity level for clean sands in this area is much higher than seen in most of the floodplain sands. Therefore, it is possible these higher conductivities are indication of direct detection of the leachate plume with the Geoprobe conductivity tool.
- 10) The pebbles and gravels in the high permeability zones are not derived from the bedrock in the vicinity of Norman, Oklahoma.

Recommendations

The purpose of this project was to gain an understanding of the permeability pathways in the Canadian River alluvium. With over 50,000 inactive municipal solid waste landfills existing in the United States, the Norman Landfill site was established as a test site to develop methodology for evaluating similar environments. Based on this

work, future studies should consider the following recommendations that attempt to define landfill plumes.

- 1) A sampling grid should be designed that provides adequate and representative coverage of the surrounding floodplain. A higher concentration of cores should be collected from areas where the leachate is believed to be present. In this study it was difficult to determine whether the higher conductivities seen in the conductivity logs around the slough indicated the presence of leachate or if the conductivities simply reflected clays. Without an intensive sampling of cores within the contaminated area it may be difficult to determine whether or not the higher conductivity values are associated with leachate or with clays.
- 2) The depth of the valley fill is another consideration. The location of the leachate within the fill and the thickness of the alluvium are factors that determine how easily the leachate plume could be dissected by the river. If the valley fill is not thick, the river could easily incise the alluvium and release leachate into the river. If the valley fill is very deep, and the leachate is traveling along the base of the fill, the river may not be able to dissect the plume regardless of the magnitude of the discharge event.
- 3) The type of river system is also important. A channel that is more active, such as a braided or meandering channel, may be of more concern than a straight channel because the more active systems have a higher potential for eroding laterally into the landfill or the leachate plume. The main channel of the Canadian River has been located at the base of the Norman Landfill approximately 15 percent of the years between 1937-1997 (Marston, et al., 2001).

- 4) The permeability pathways in the floodplain alluvium can be strongly influenced by the sediment provenance. The gravel in the basal unit of the Canadian River alluvium was not derived from local bedrock but from northeastern New Mexico. The basal gravel unit is the main permeability pathway in the alluvium. The texture of the basal gravel is inherited from durable sediments that were probably deposited after formation of the incised valley. Consequently, when evaluating permeability pathways at new landfill locations, consideration should be given to the potential role of texture from upstream sediment sources. If the basal sediment fill is derived from a provenance that is finer grained, the preferred permeability pathway may not necessarily be located at the base of the channel.

REFERENCES

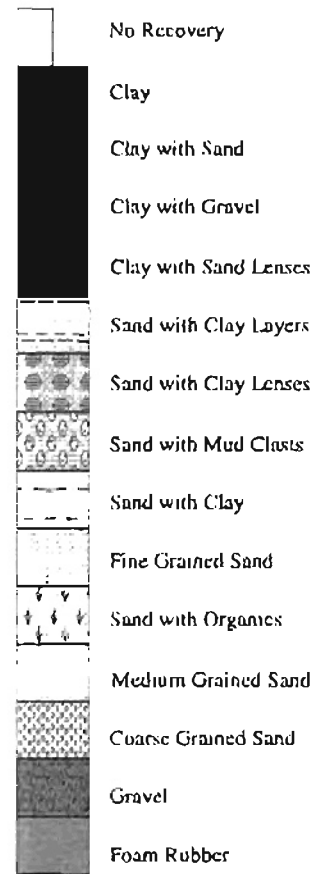
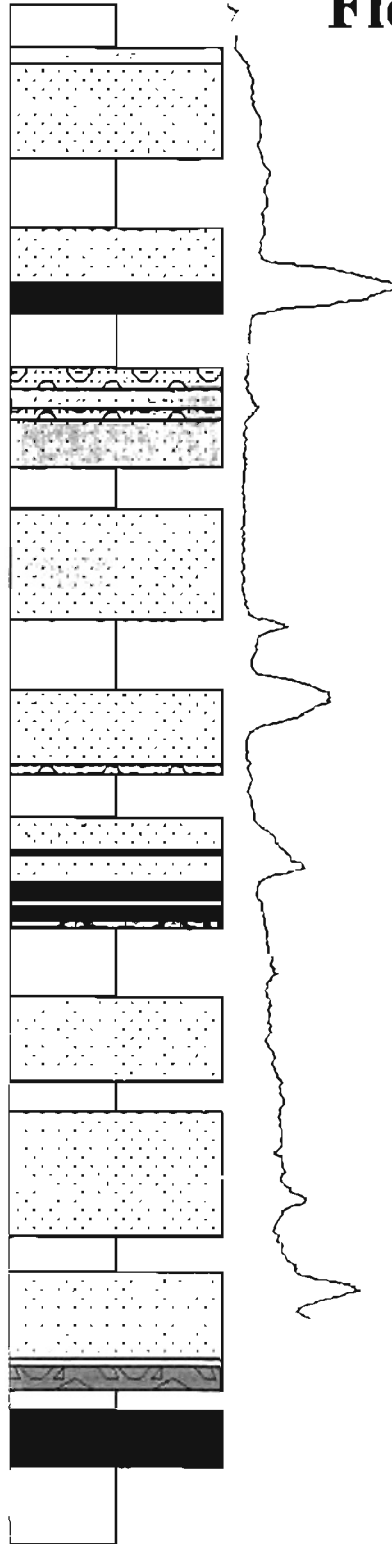
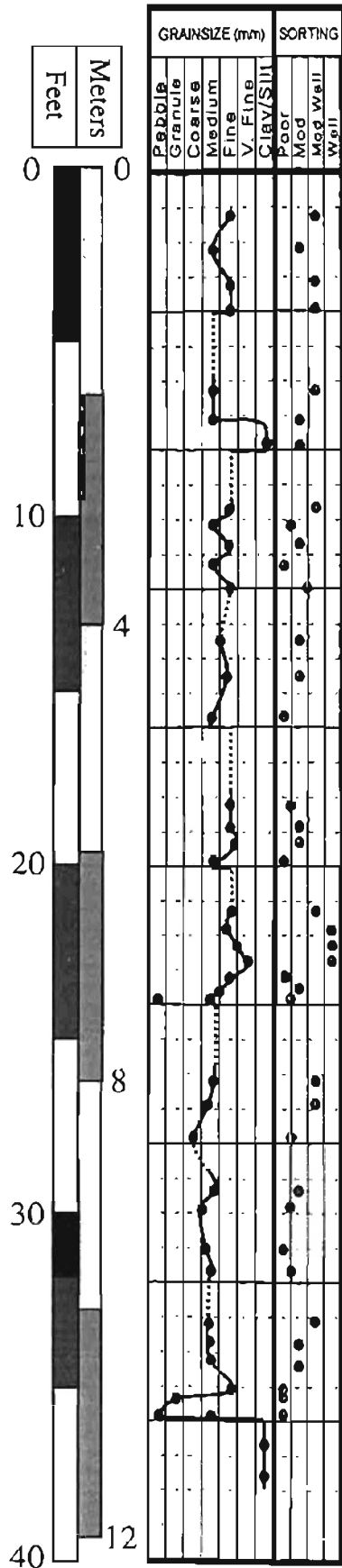
- Beard, D. C. and P. K. Weyl, 1973, Influence of texture on porosity and permeability of Unconsolidated Sand: AAPG Bulletin, v. 57, no. 2, p. 349-369.
- Boggs, Sam Jr., 1995, Principles of Sedimentology and Stratigraphy: Prentice Hall, New Jersey, p. 250.
- Butler, J. J. Jr., Healey J. M., and Zheng, L., 1999, Hydrostratigraphic Characterization of Unconsolidated Alluvial Deposits with Direct-Push Sensor Technology, Kansas Geological Survey Open File Report #99-40.
- Curtis, Jennifer and Whitney, John W., 2000, Geomorphology and flood hazards at a toxic landfill on the Canadian River floodplain, central Oklahoma. Preliminary draft of a USGS report.
- Folk, Robert L., 1980, Petrology of Sedimentary Rocks (Second Edition): Hemphill Publishing Company, Austin, Texas, p. 42 – 43, 184.
- Geoprobe Systems. www.geoprobesystems.com
- Hermance, J. R., 1999, A Mathematical Primer on Groundwater Flow: Prentice Hall, New Jersey, p. 10.
- Klefstad, G. E., 1973, Limitations of the Electrical Resistivity Method for Detecting Landfill Leachate in Alluvial Deposits, Master's Thesis, Iowa State University.
- Krumbein, W. C., 1936, The use of quartile measurements in describing and comparing Sediments: American Journal of Science, v. 232, p. 98 – 111.
- Krumbein, W. C. and Monk, G. D., 1942, Permeability as a function of the size Parameters of unconsolidated sand. Petroleum Technology, 5, 1-11.
- Lee, G. F. and Jones-Lee, A., 1995, "Overview of Landfill Post Closure Issues." Presented at American Society of Civil Engineers session "Landfill Closures – Environmental Protection and Land Recovery," New York, NY, October Issue.
- Lucius, J.E. and Bisdorf, R.J., 1995, Results of Geophysical Investigation Near Norman, Oklahoma, Municipal Landfill, 1995: U.S. Geological Survey Open-File Report 95-825, 125 p.
- Marston, R. A., Paxton, S. T., Collins, K. C., and Pickup, B. E., April 2001, Geomorphology and Sedimentology of the Canadian River Alluvium Adjacent to the Norman Landfill, Norman, Oklahoma. Final report submitted to the Environmental Institute/Oklahoma Water Resources Research Institute.

Scholl, M. A. and Christenson, Scott, 1998, Spatial Variation in Hydraulic Conductivity Determined by Slug Tests in the Canadian River Alluvium Near the Norman Landfill, Norman, Oklahoma, USGS, Water Resources Investigations Report 97-4292, p. 1-28.

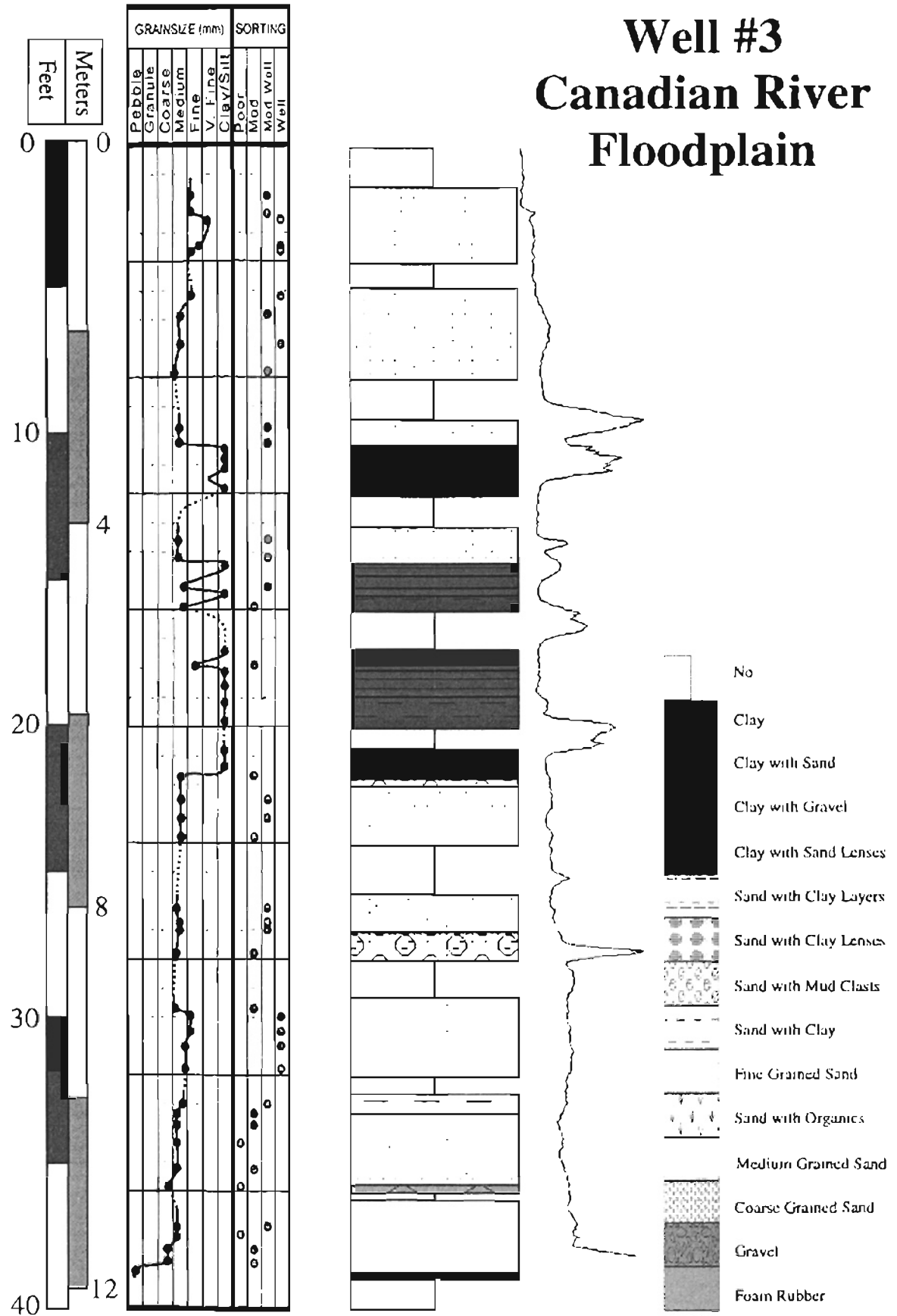
Trask, P. D., 1930, Mechanical analysis of sediments by centrifuge: *Economic Geology*, v. 25, p. 581-599.

APPENDIX A
CORE DESCRIPTIONS

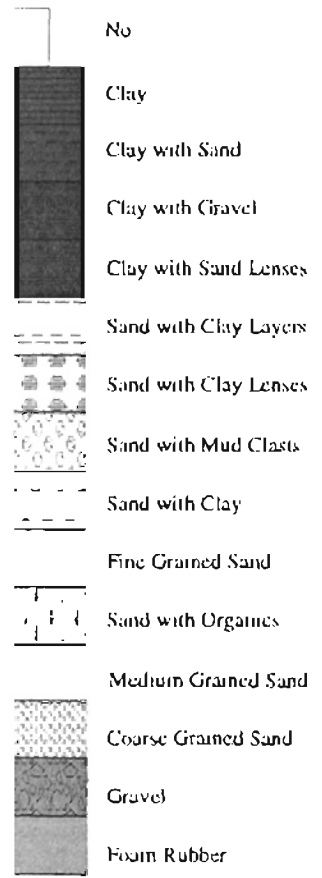
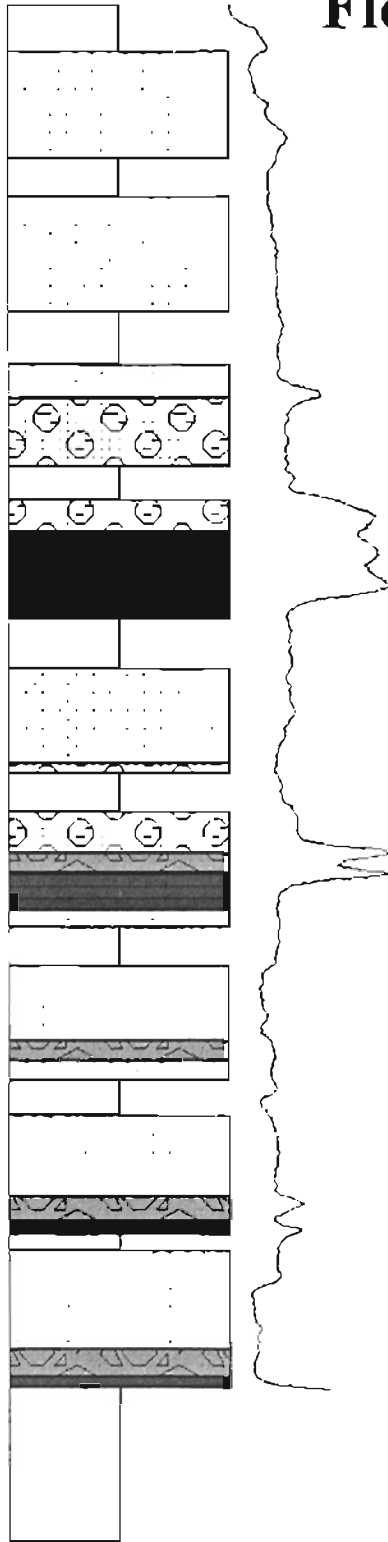
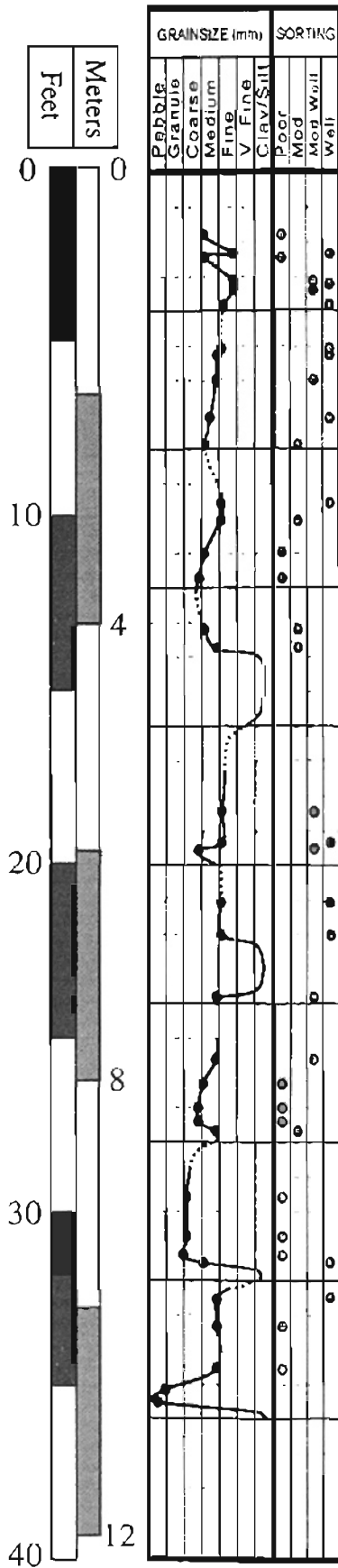
Well #1 Canadian River Floodplain



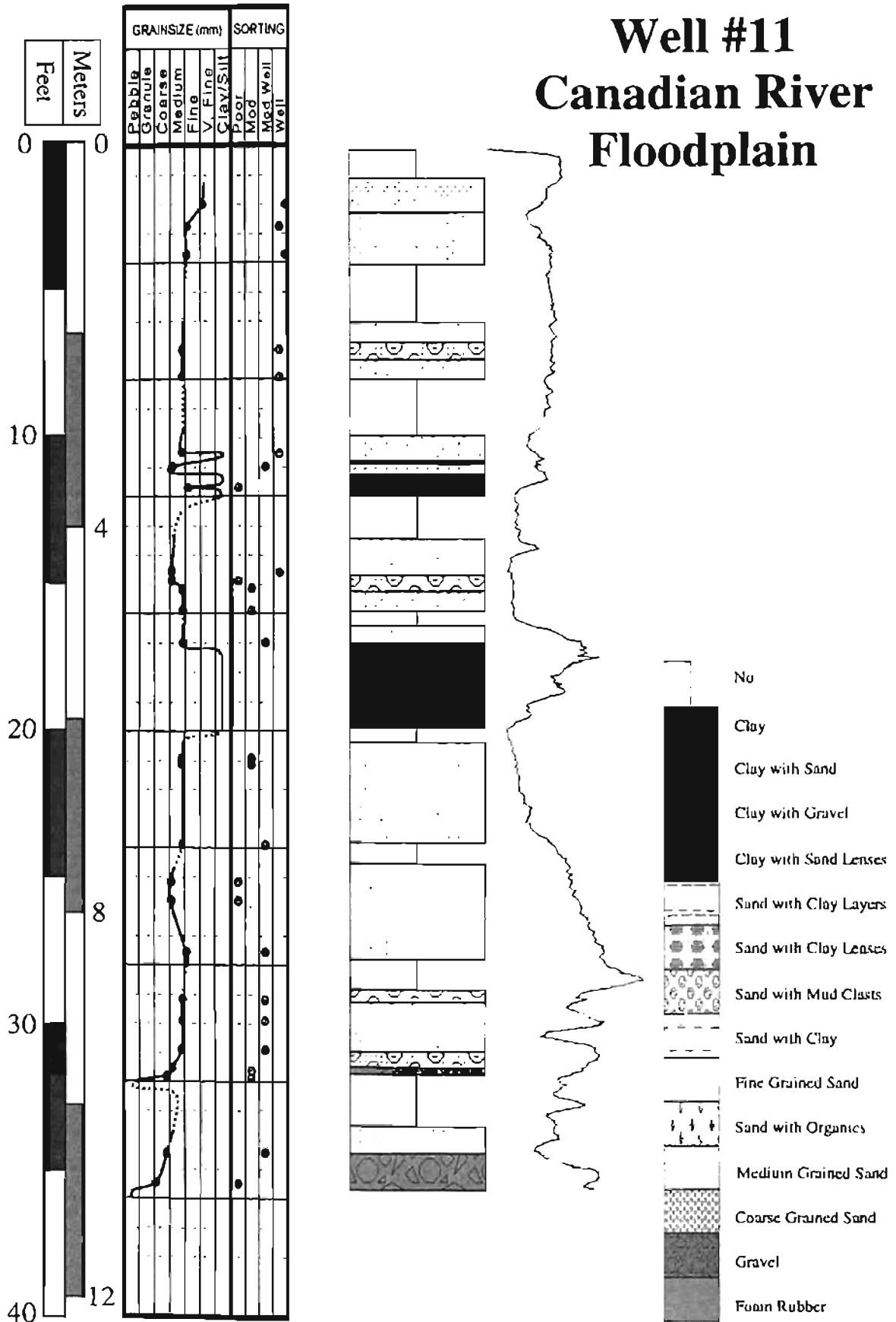
Well #3 Canadian River Floodplain



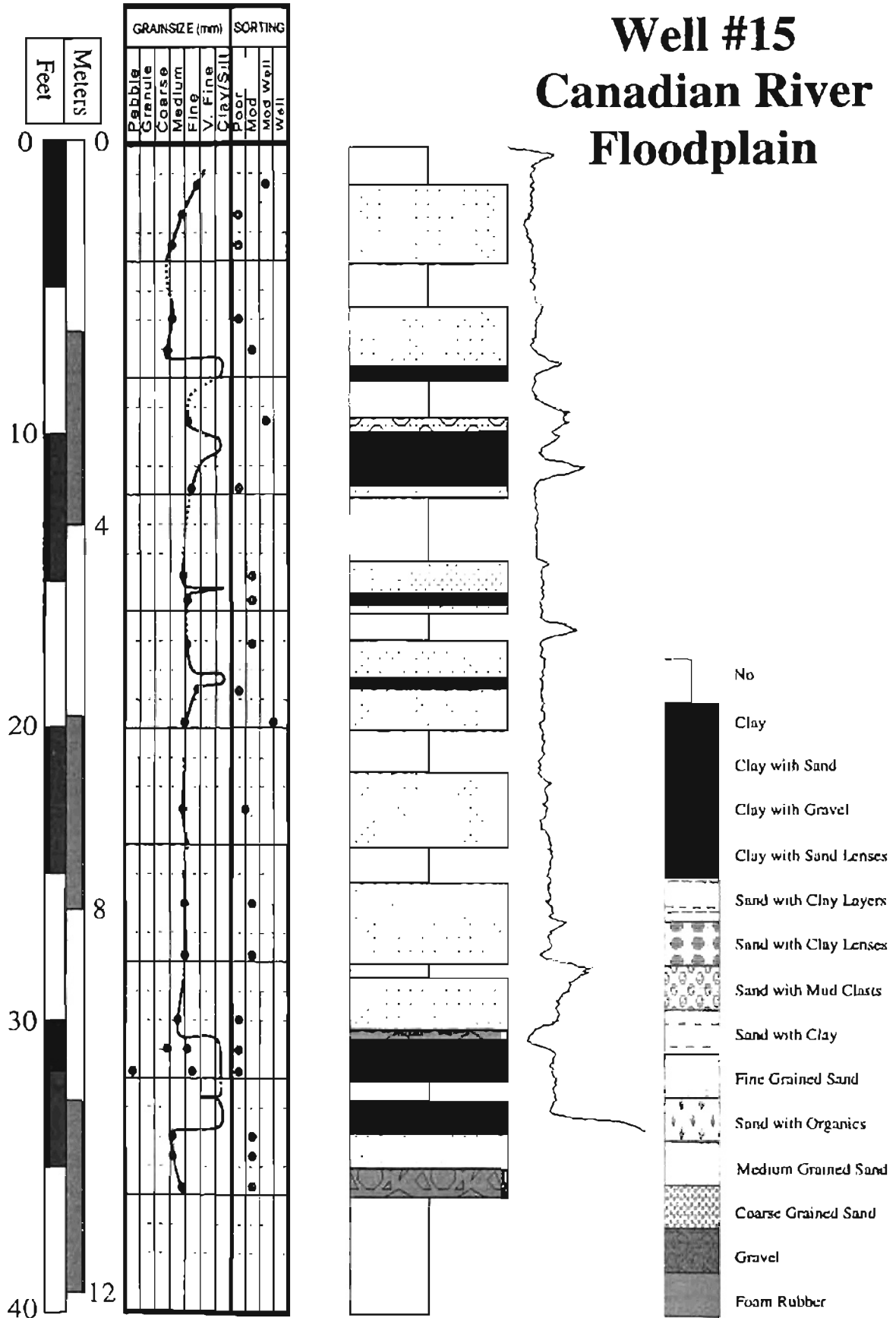
Well #7 Canadian River Floodplain



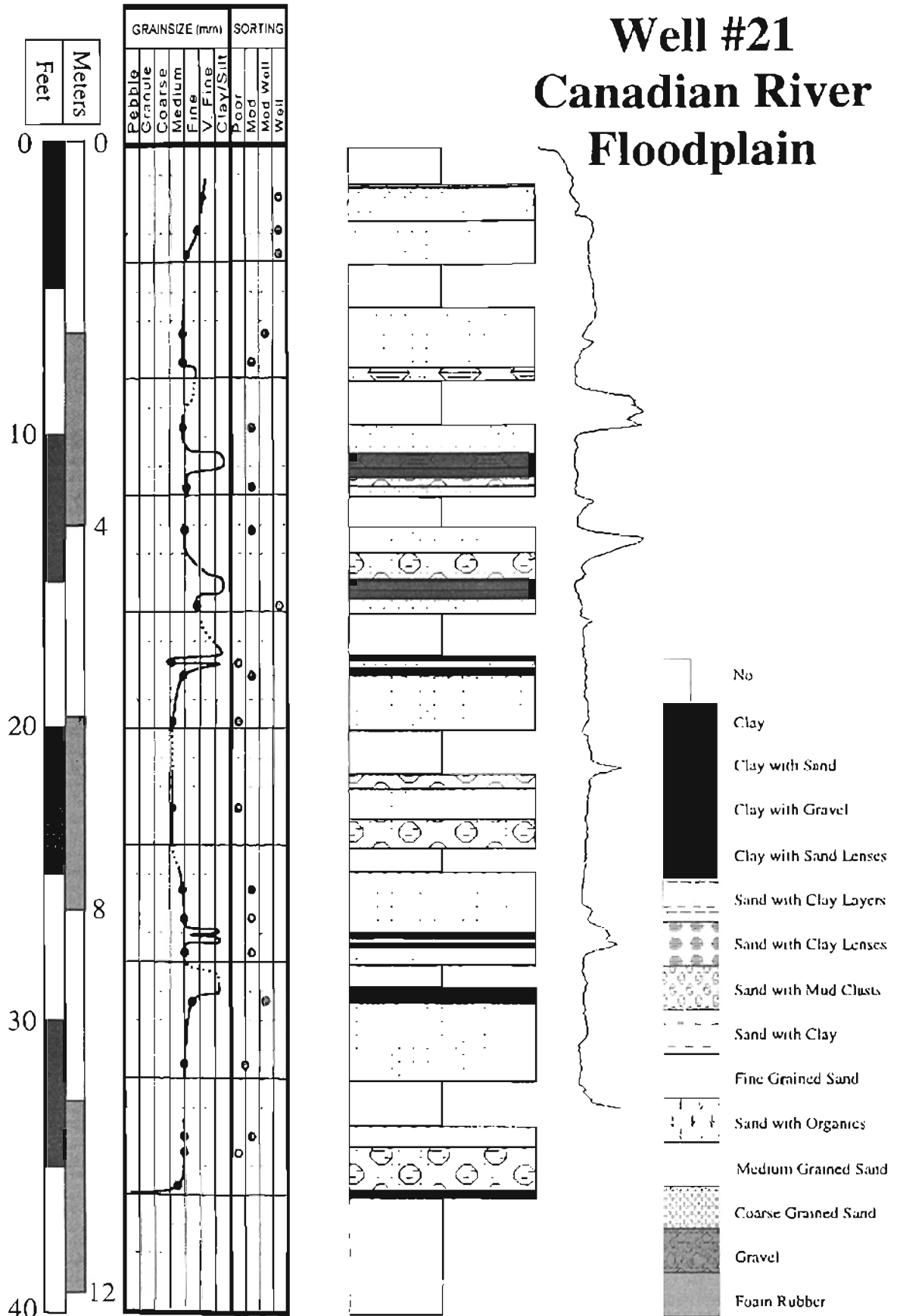
Well #11 Canadian River Floodplain



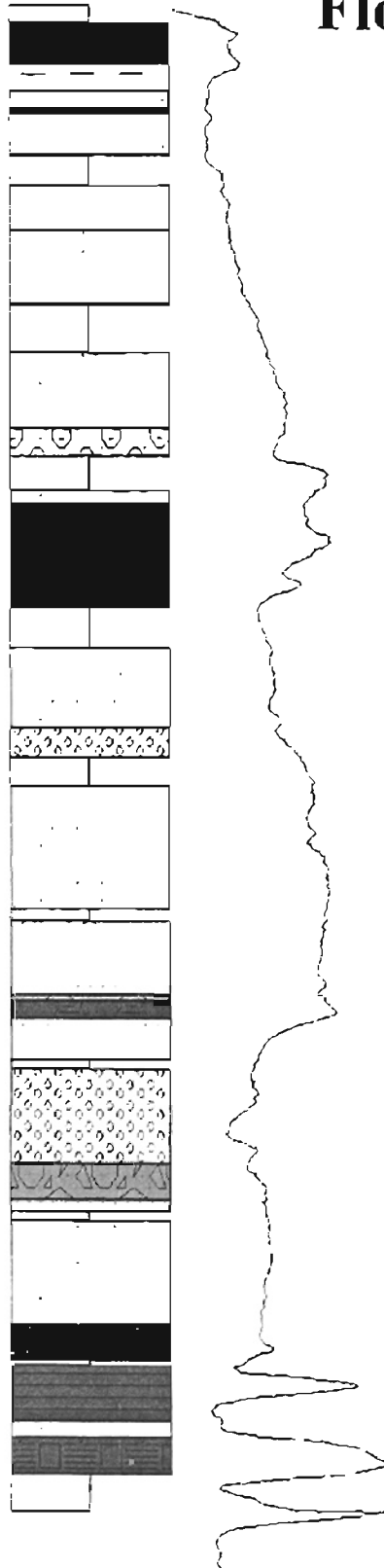
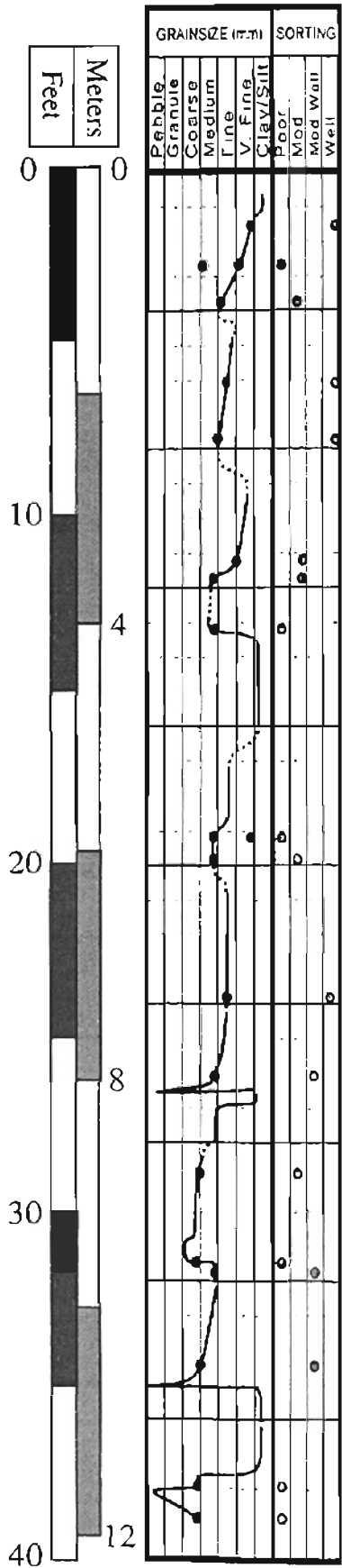
Well #15 Canadian River Floodplain



Well #21 Canadian River Floodplain

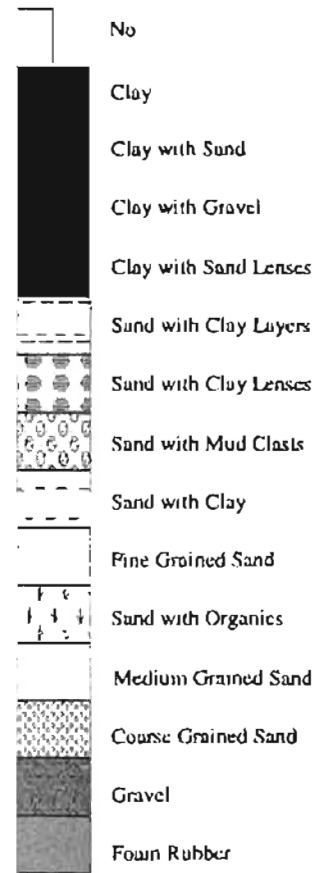
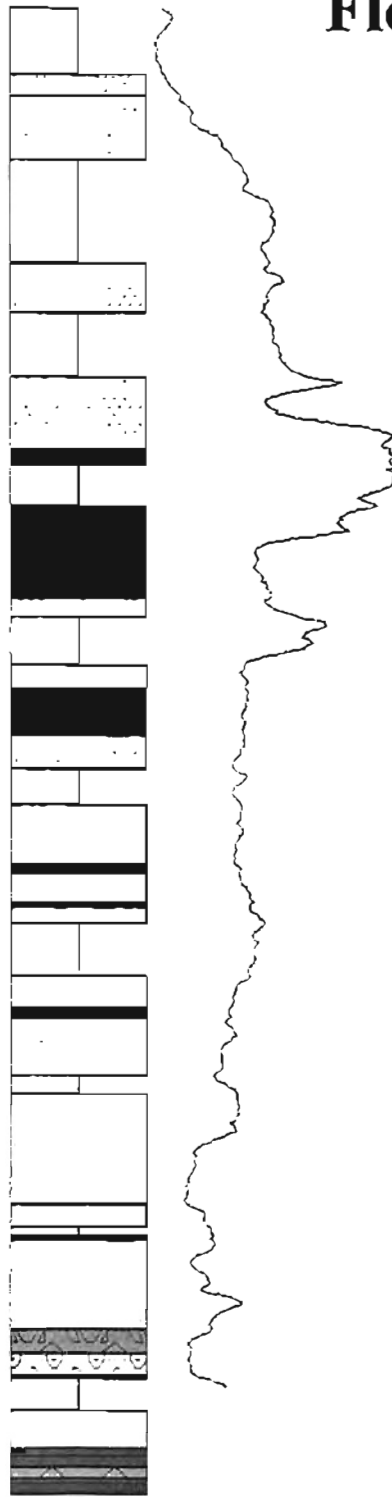
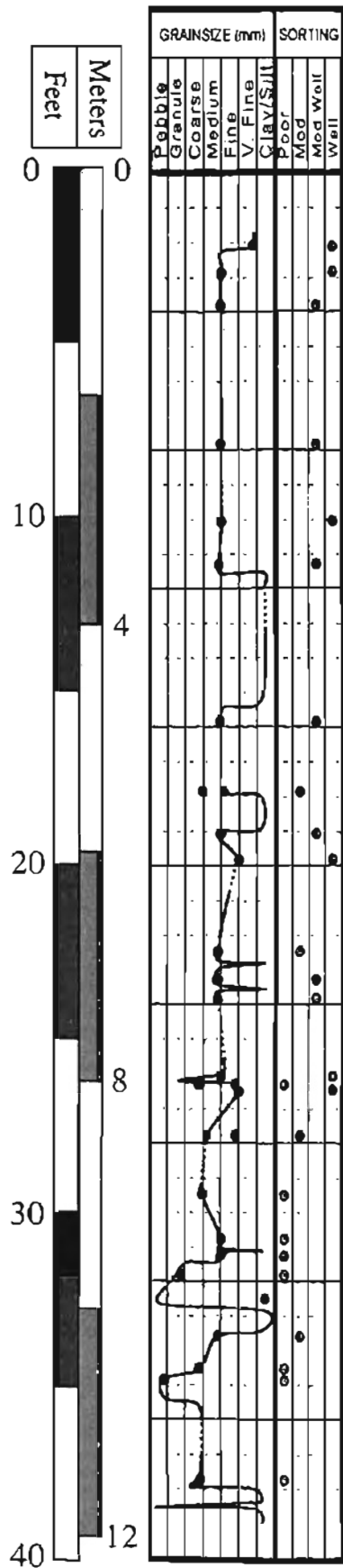


Well #23 Canadian River Floodplain

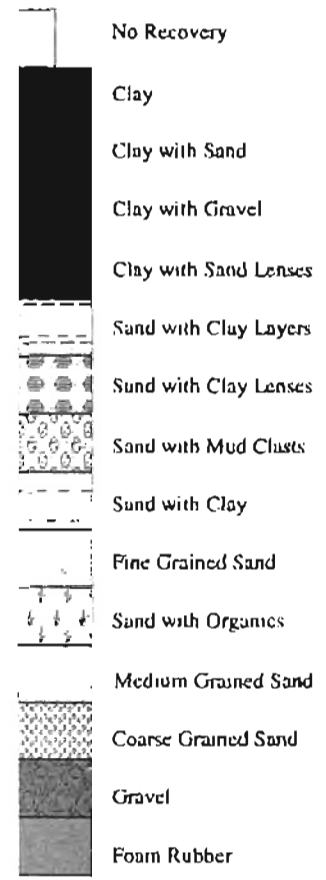
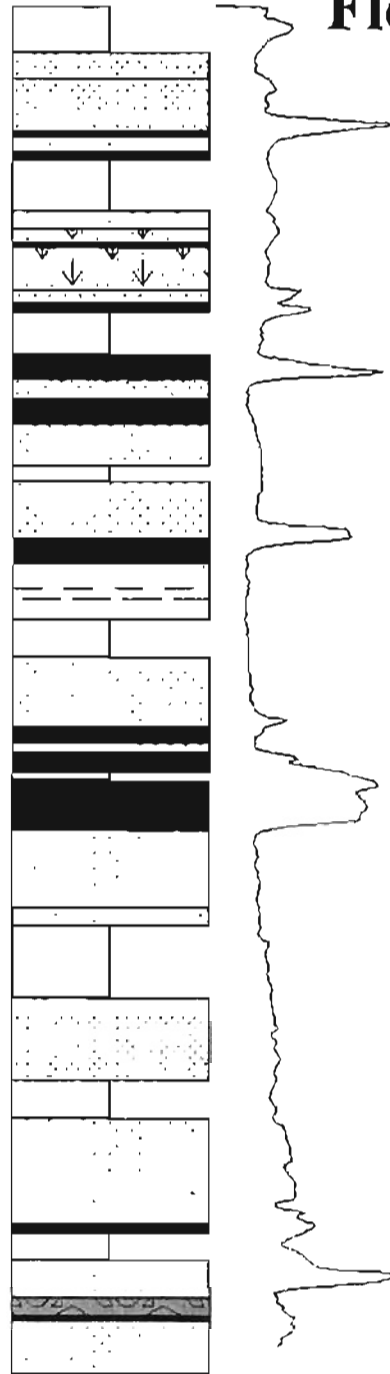
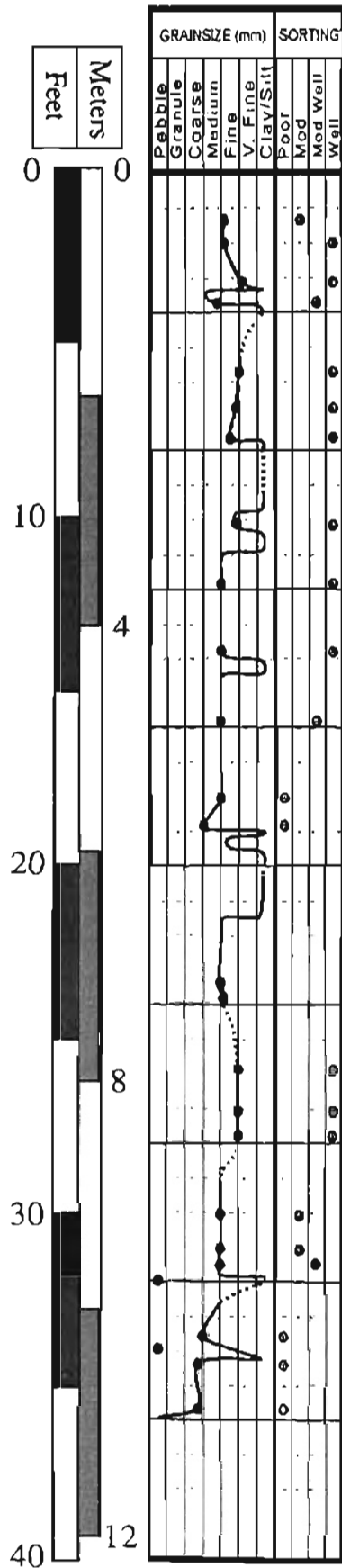


- No
- Clay
- Clay with Sand
- Clay with Gravel
- Clay with Sand Lenses
- Sand with Clay Layers
- Sand with Clay Lenses
- Sand with Mud Clasts
- Sand with Clay
- Fine Grained Sand
- Sand with Organics
- Medium Grained Sand
- Coarse Grained Sand
- Gravel
- Foam Rubber

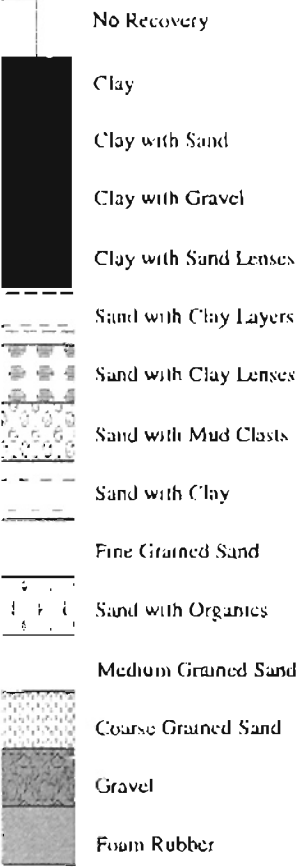
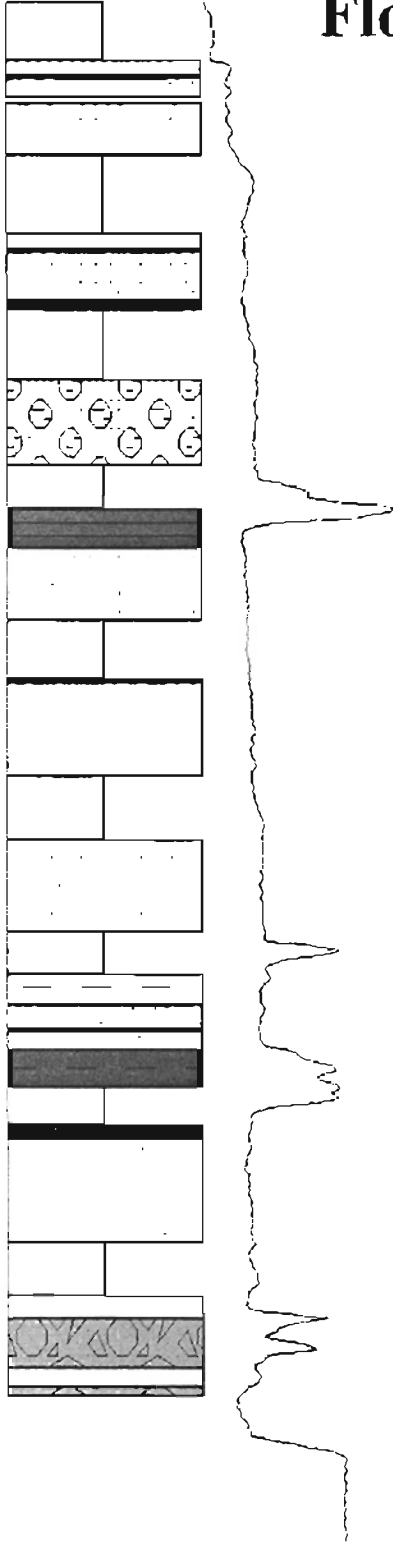
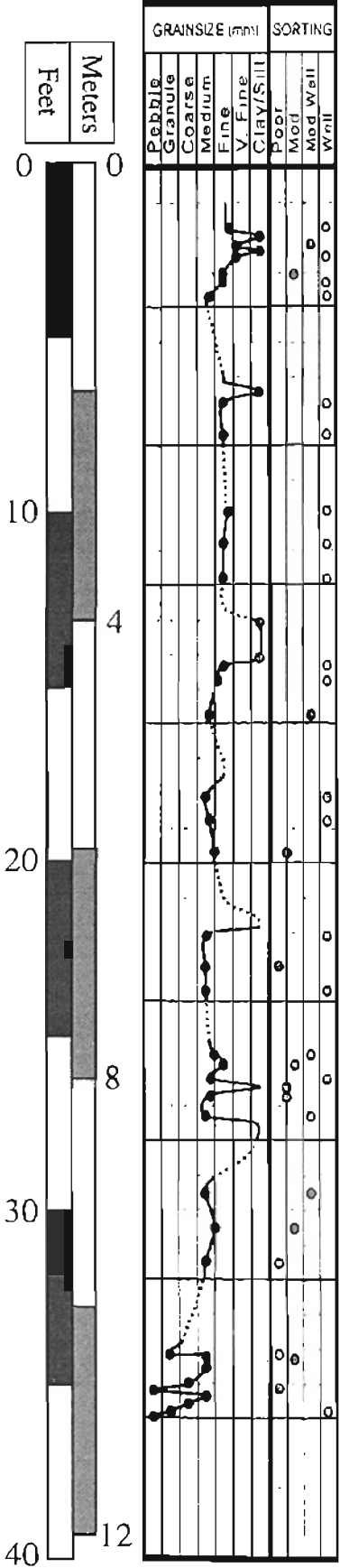
Well #28 Canadian River Floodplain



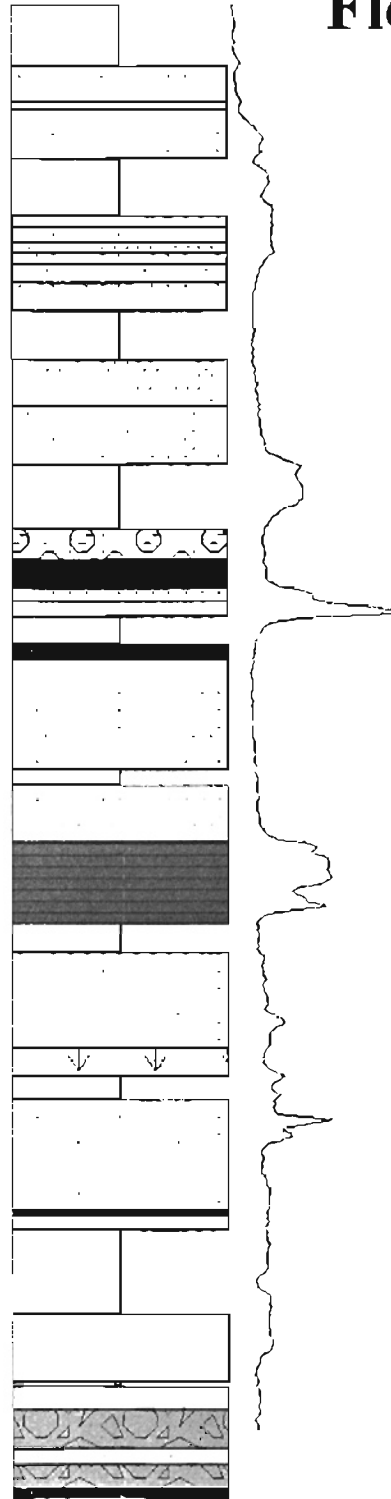
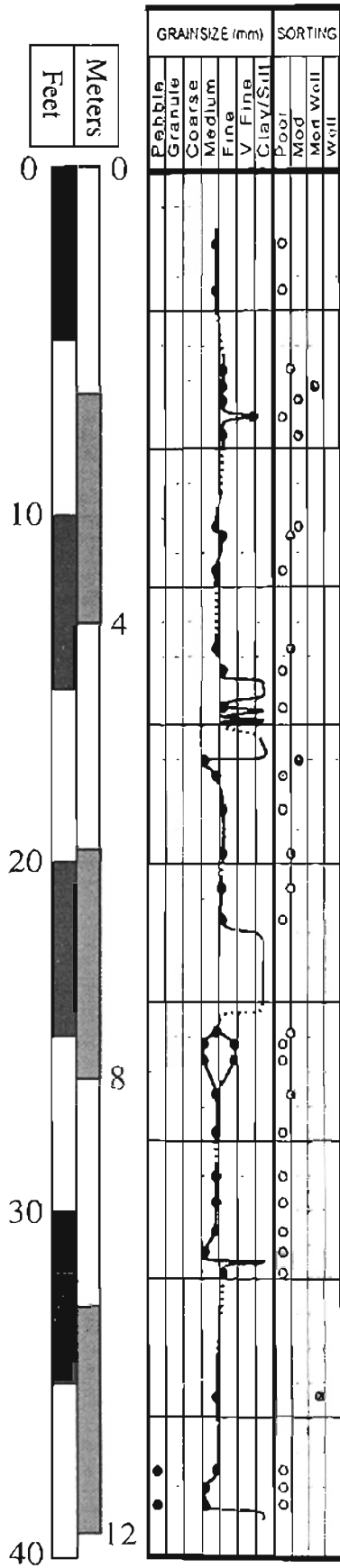
Well #31 Canadian River Floodplain



Well #42 Canadian River Floodplain

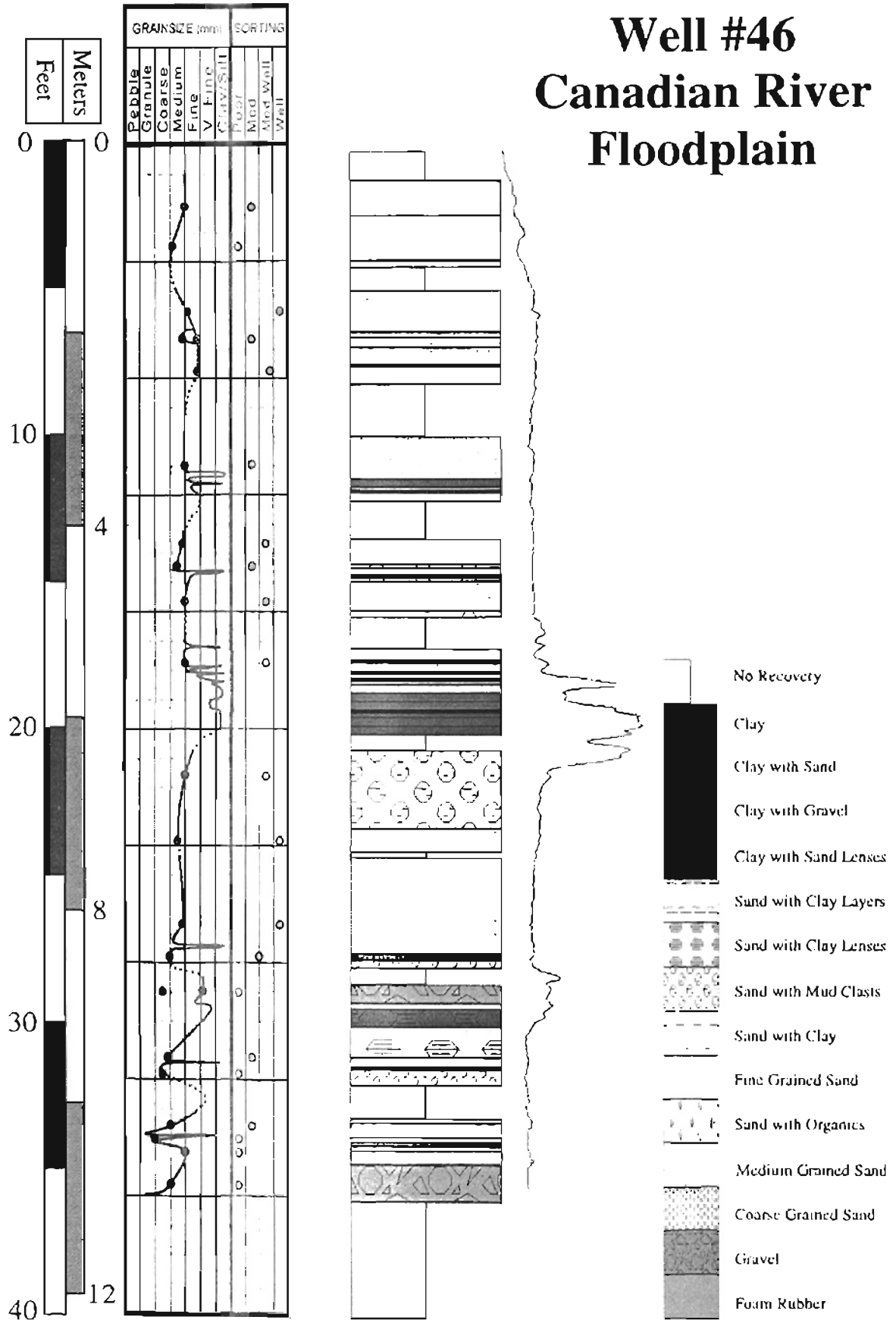


Well #44 Canadian River Floodplain

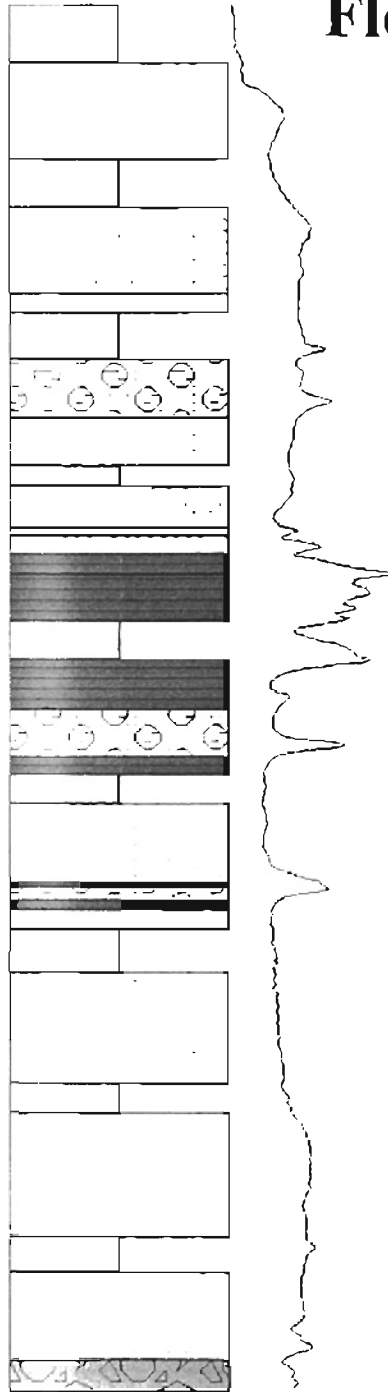
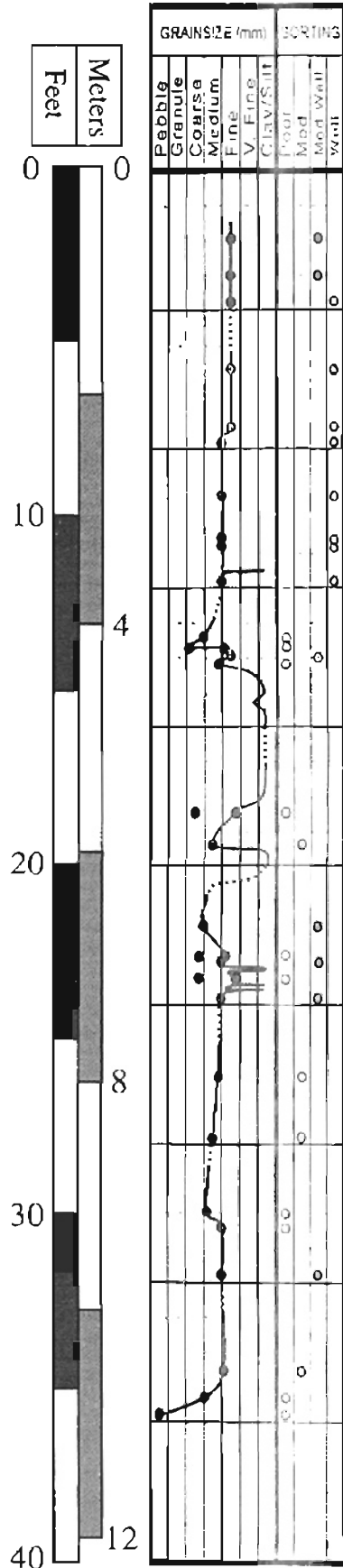


- No Recovery
- Clay
- Clay with Sand
- Clay with Gravel
- Clay with Sand Lenses
- Sand with Clay Layers
- Sand with Clay Lenses
- Sand with Mud Clasts
- Sand with Clay
- Fine Grained Sand
- Sand with Organics
- Medium Grained Sand
- Coarse Grained Sand
- Gravel
- Foam Rubber

Well #46 Canadian River Floodplain

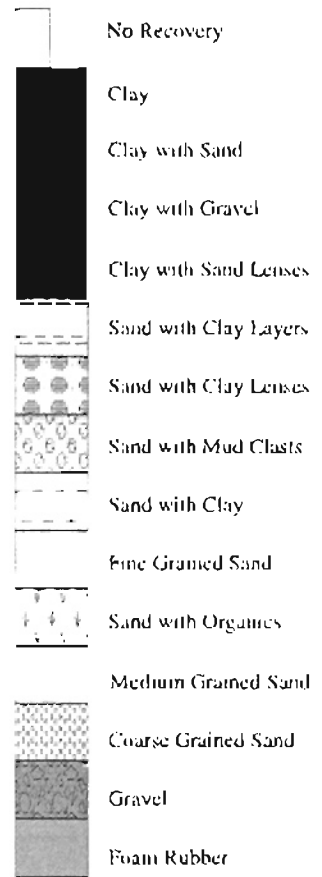
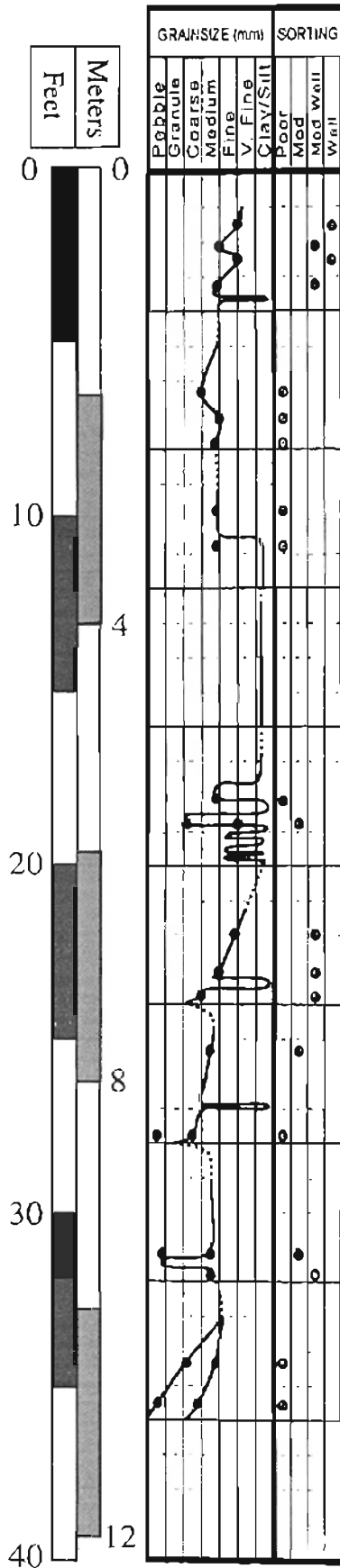


Well #56 Canadian River Floodplain

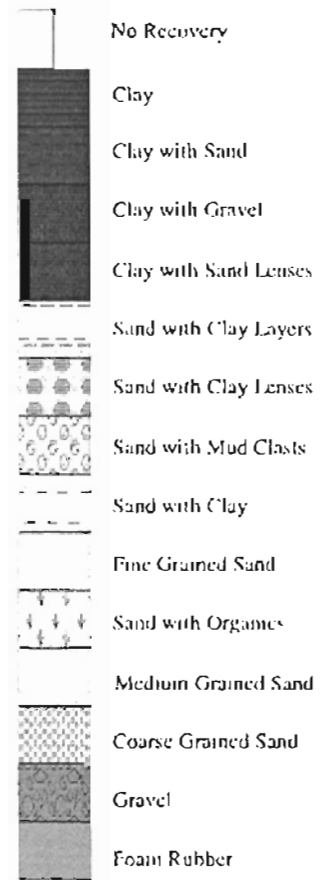
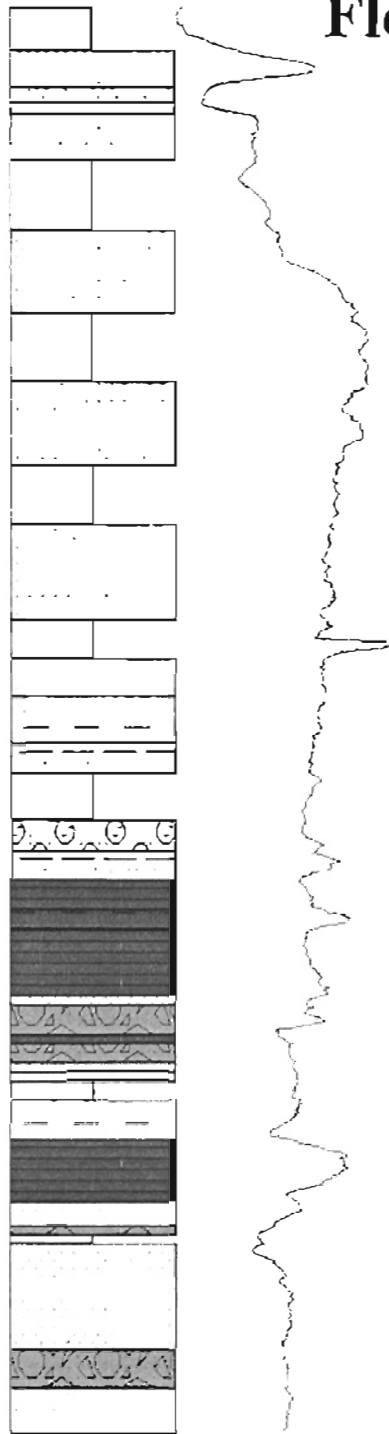
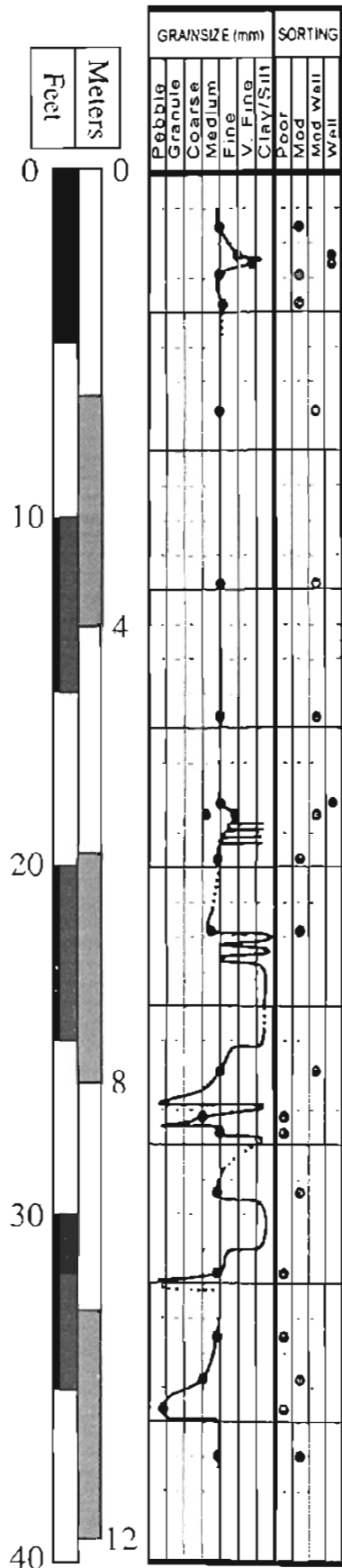


- No Recovery
- Clay
- Clay with Sand
- Clay with Gravel
- Clay with Sand Lenses
- Sand with Clay Layers
- Sand with Clay Lenses
- Sand with Mud Clasts
- Sand with Clay
- Fine Grained Sand
- Sand with Organics
- Medium Grained Sand
- Coarse Grained Sand
- Gravel
- Foam Rubber

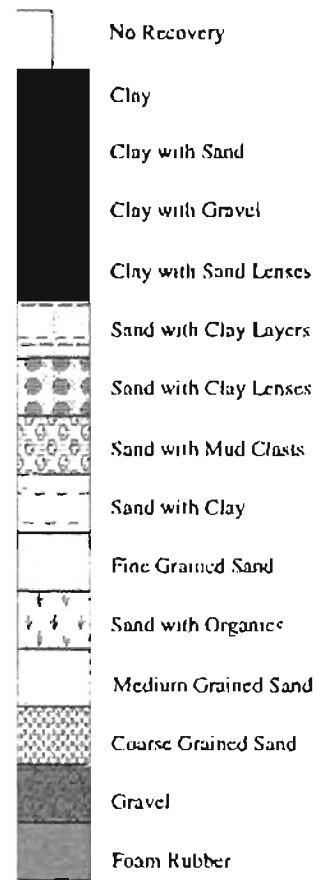
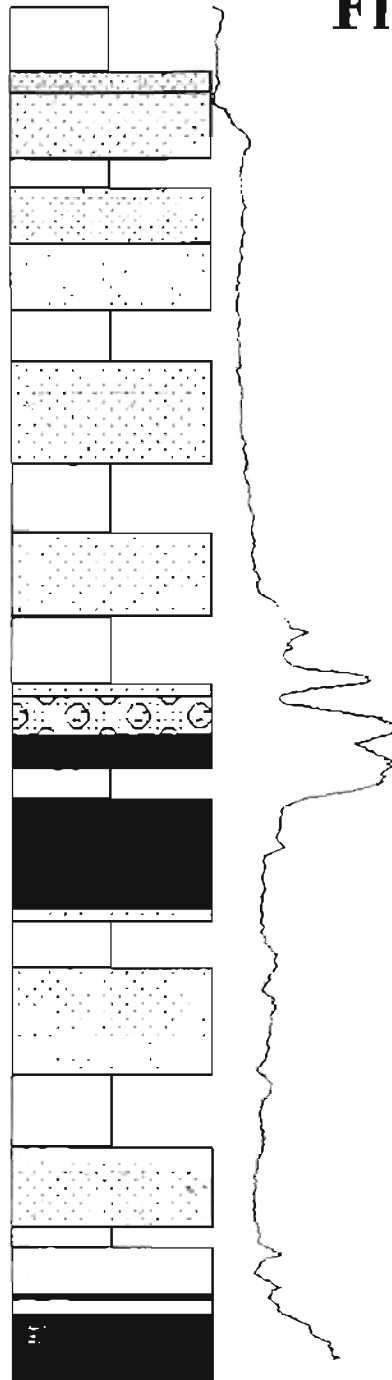
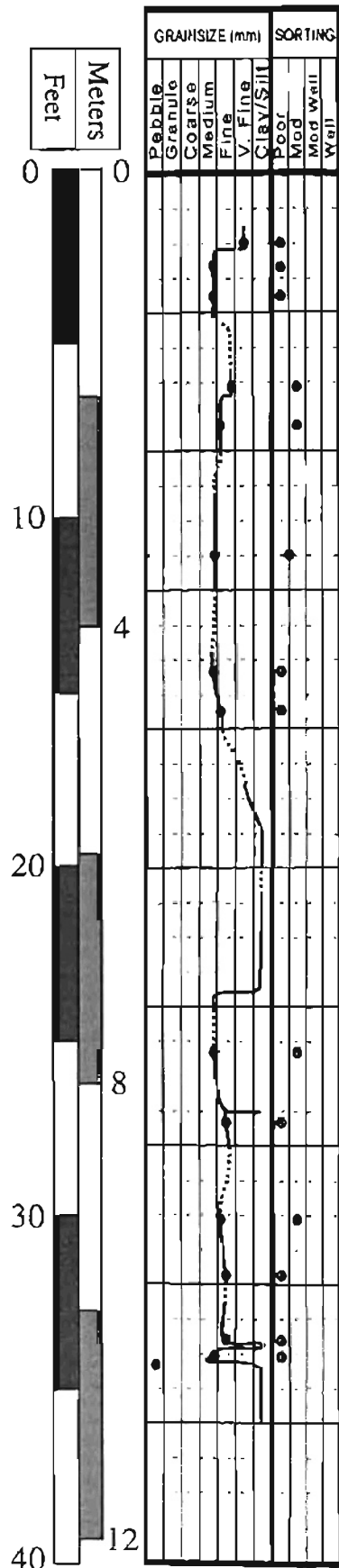
Well #57 Canadian River Floodplain



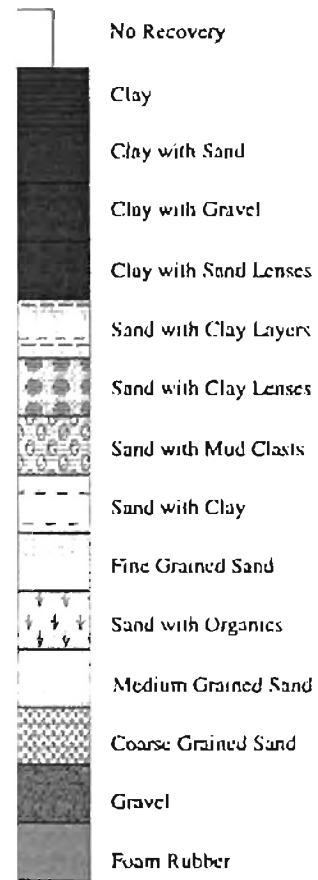
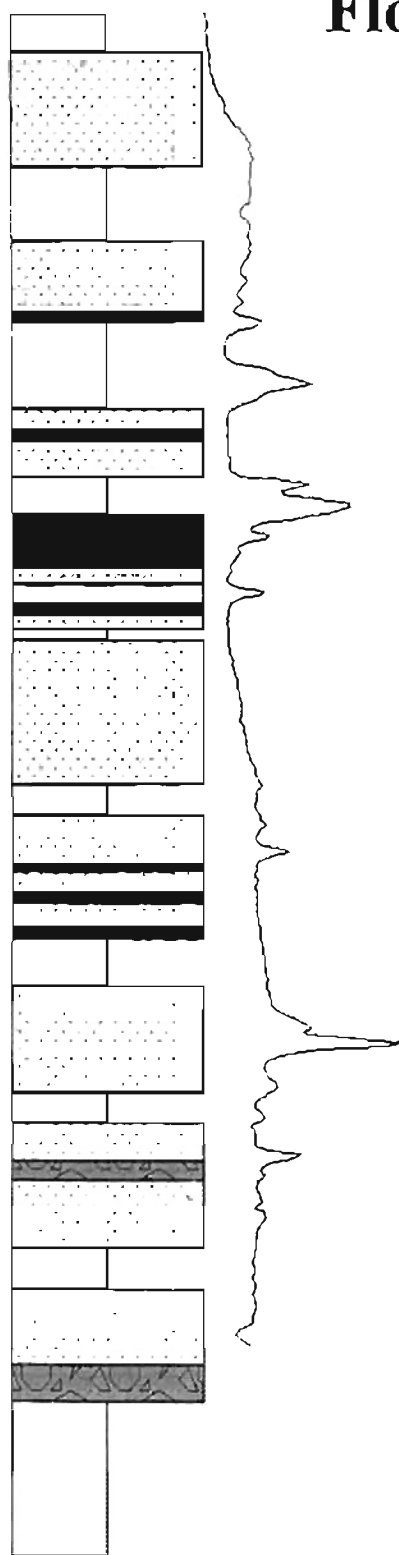
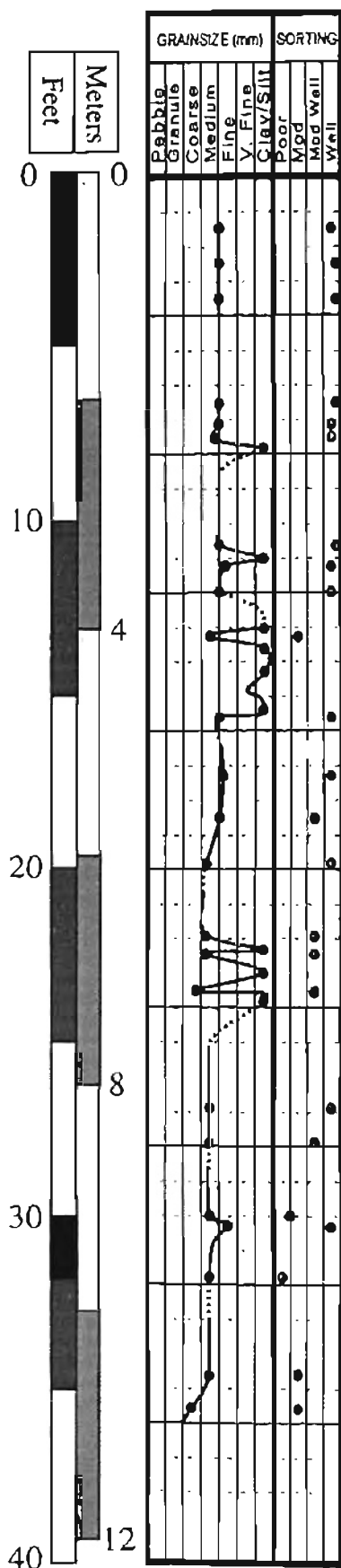
Well #62 Canadian River Floodplain



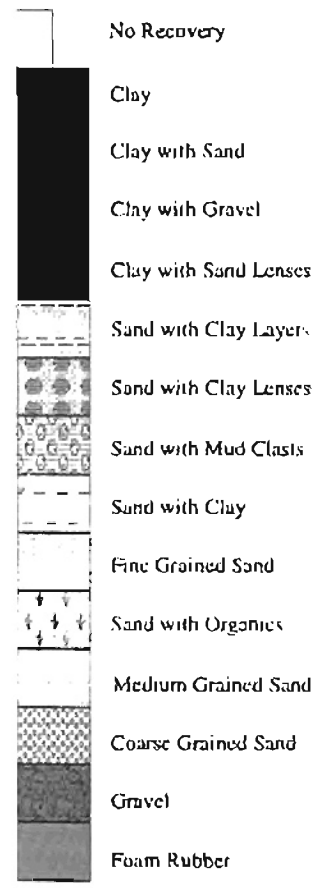
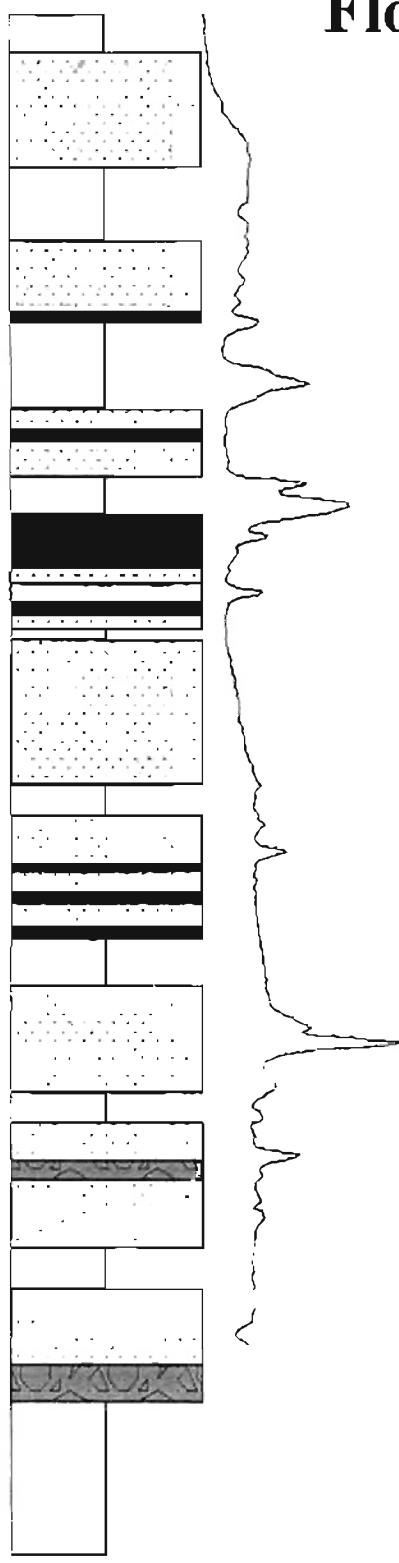
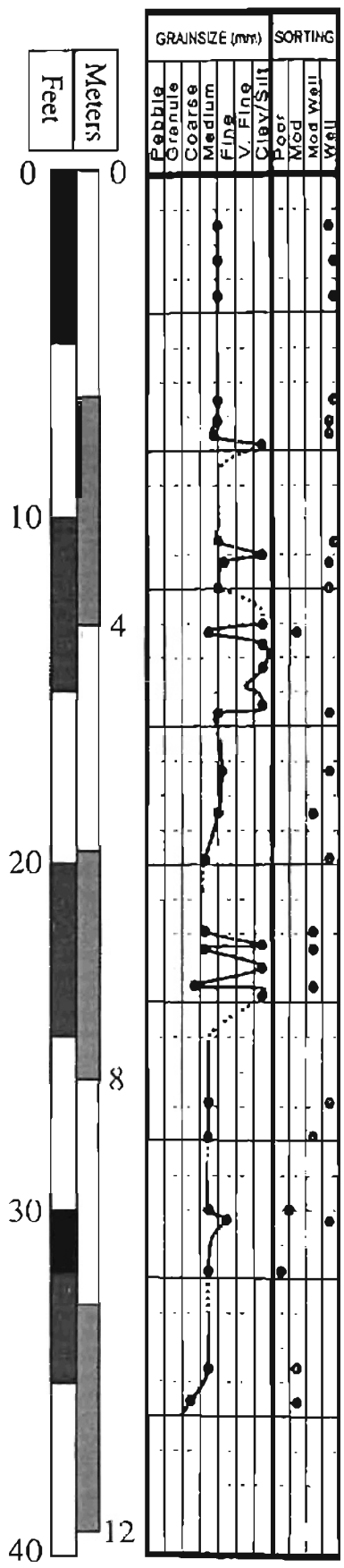
Well #64 Canadian River Floodplain



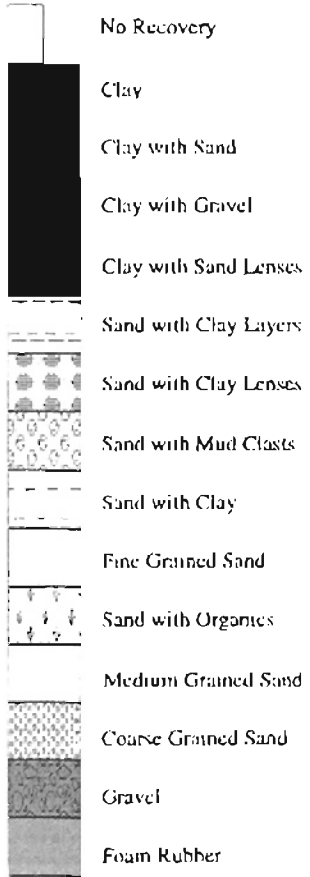
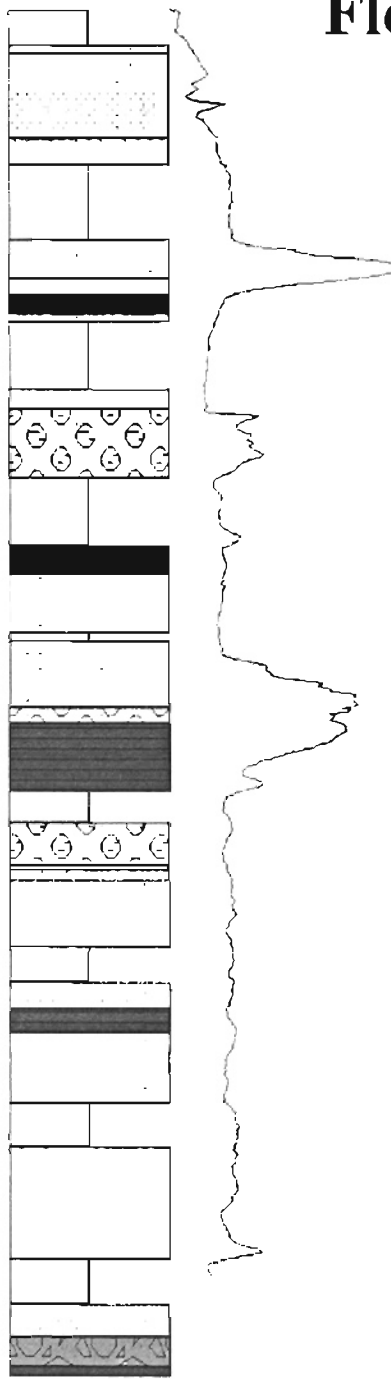
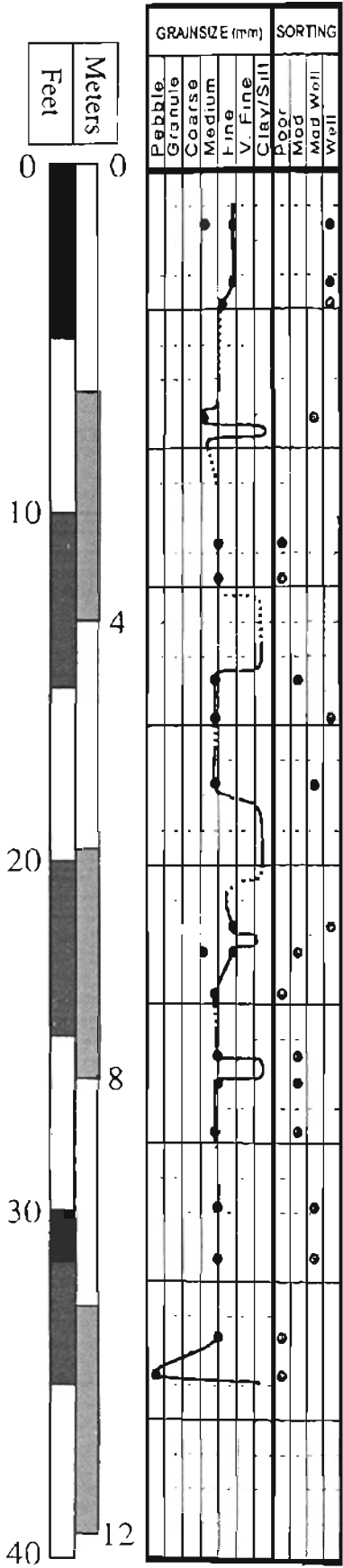
Well #74 Canadian River Floodplain



Well #74 Canadian River Floodplain



Well #78 Canadian River Floodplain

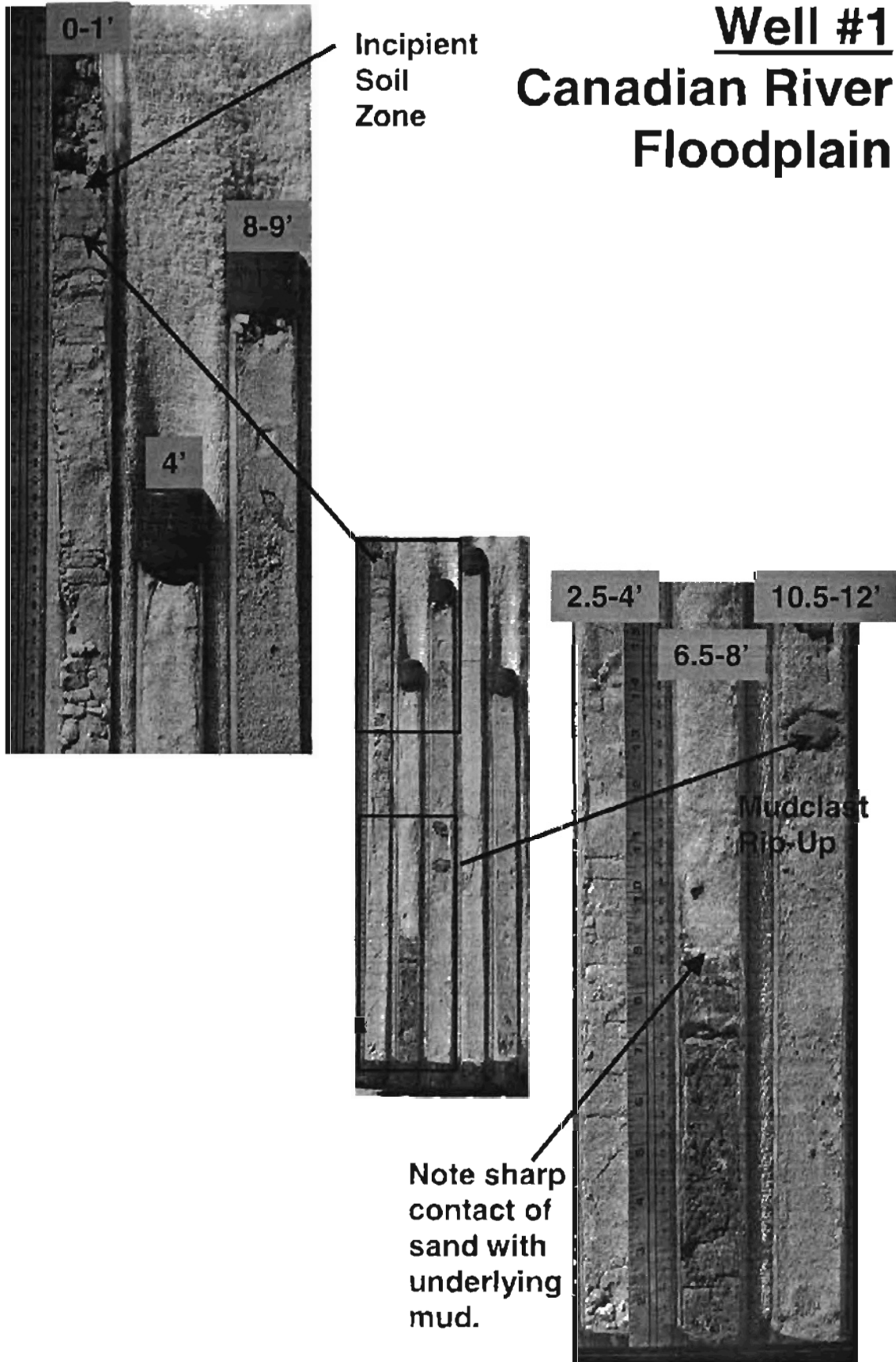


APPENDIX B
CORE PHOTOS

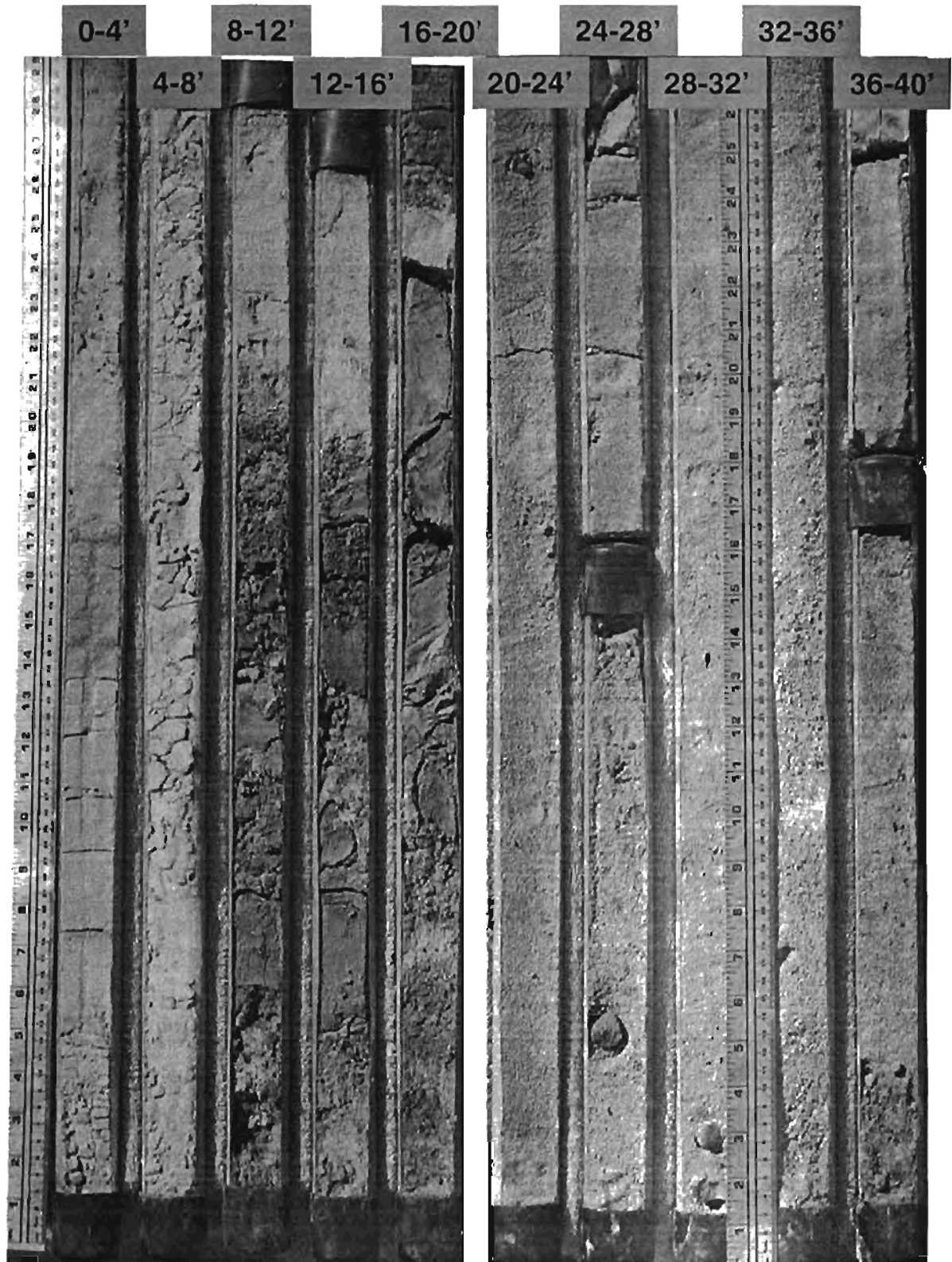
Well #1 – Canadian River Floodplain



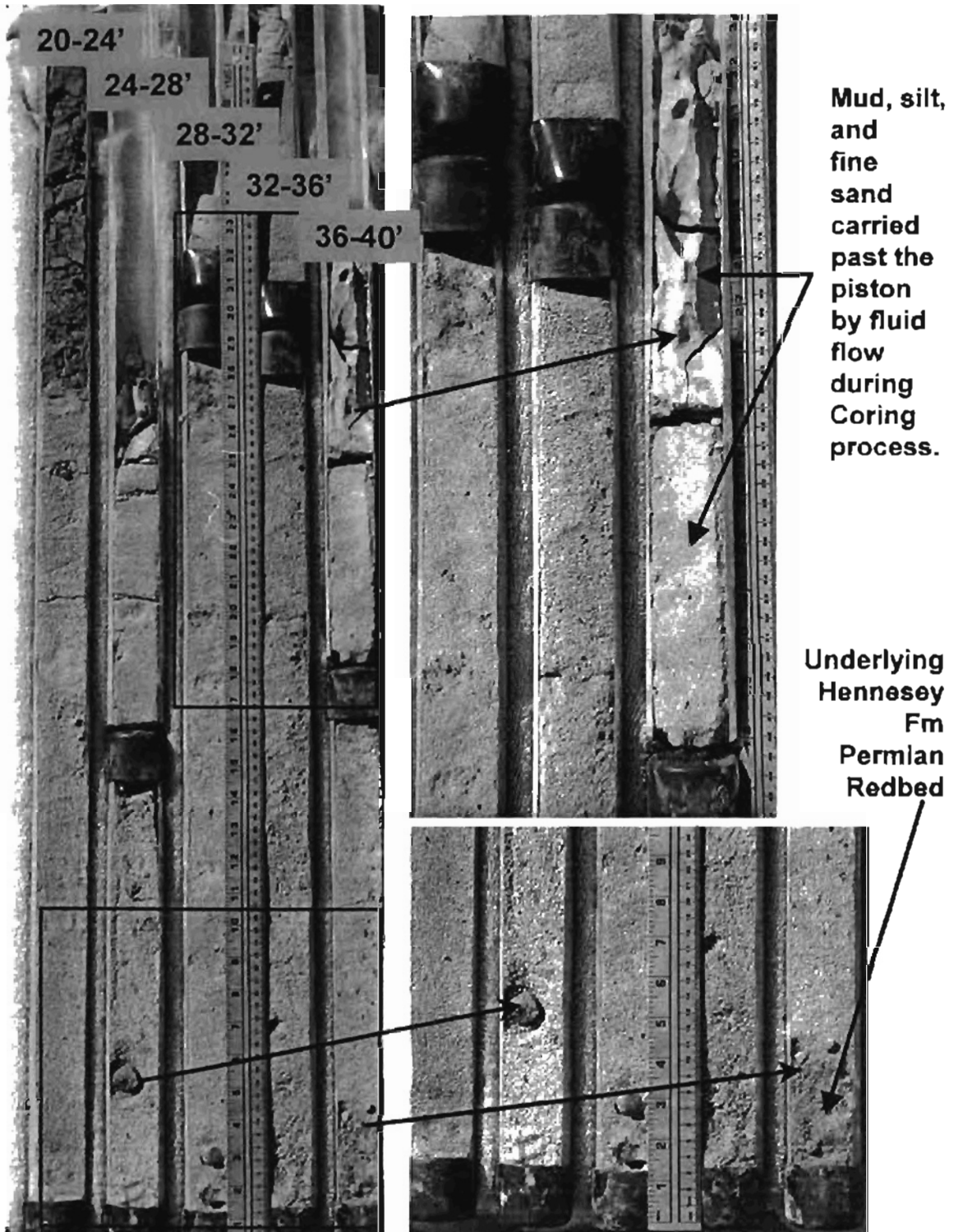
Well #1 Canadian River Floodplain



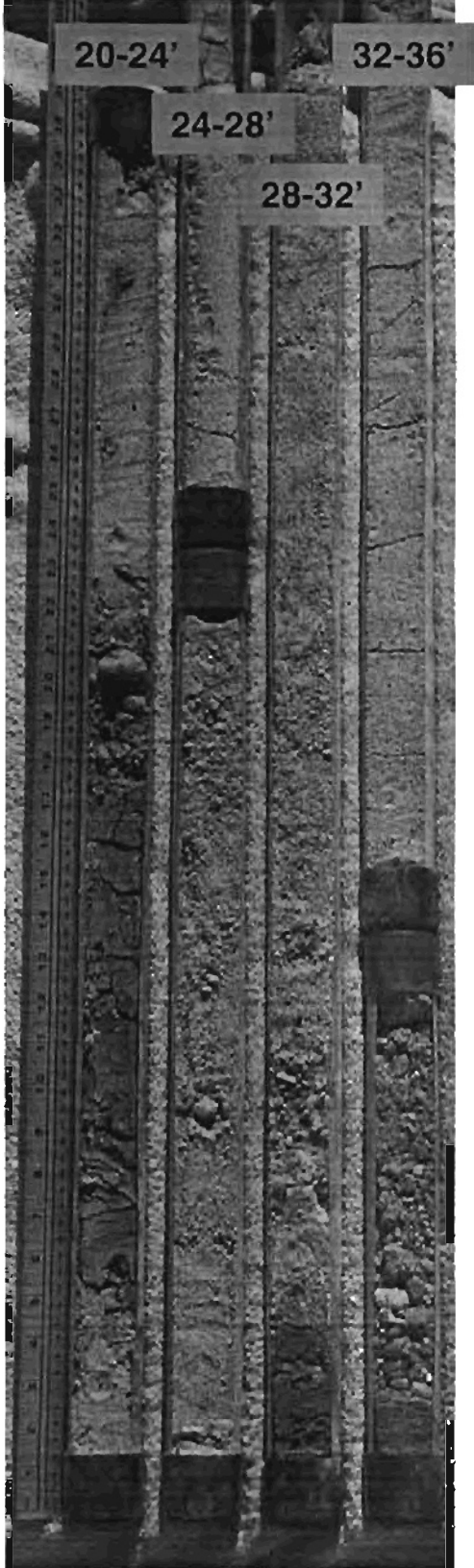
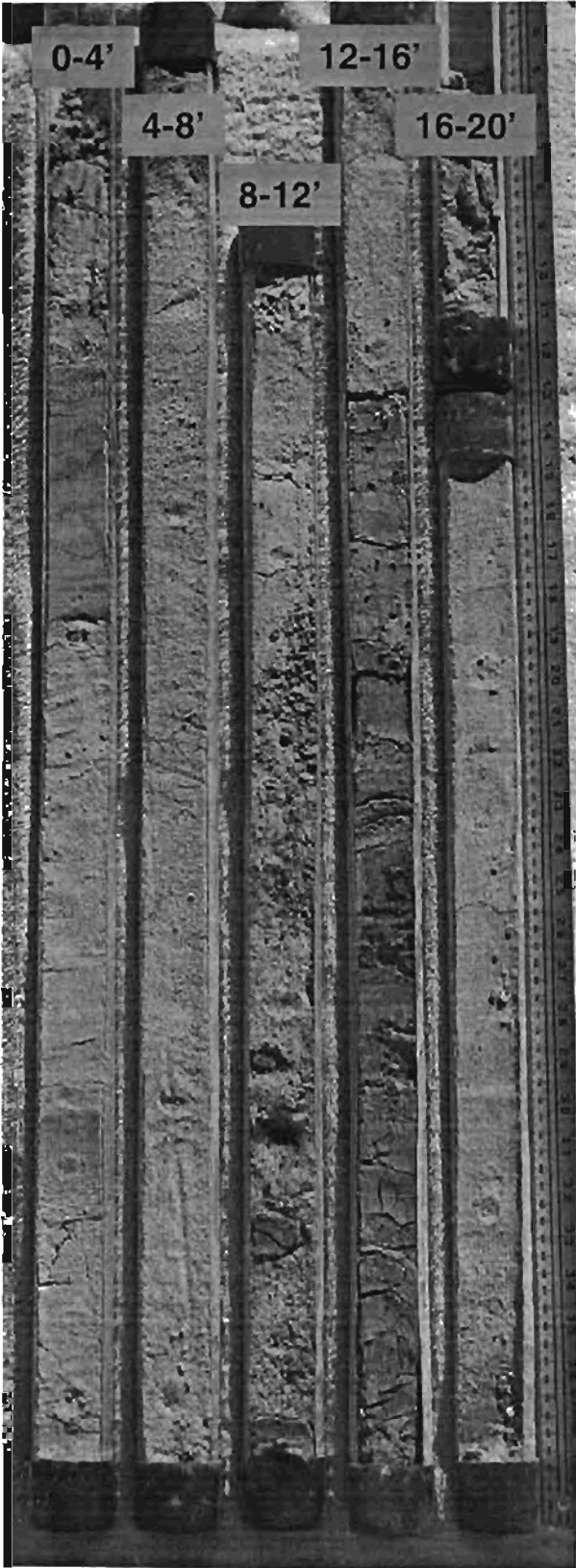
Well #3 – Canadian River Floodplain



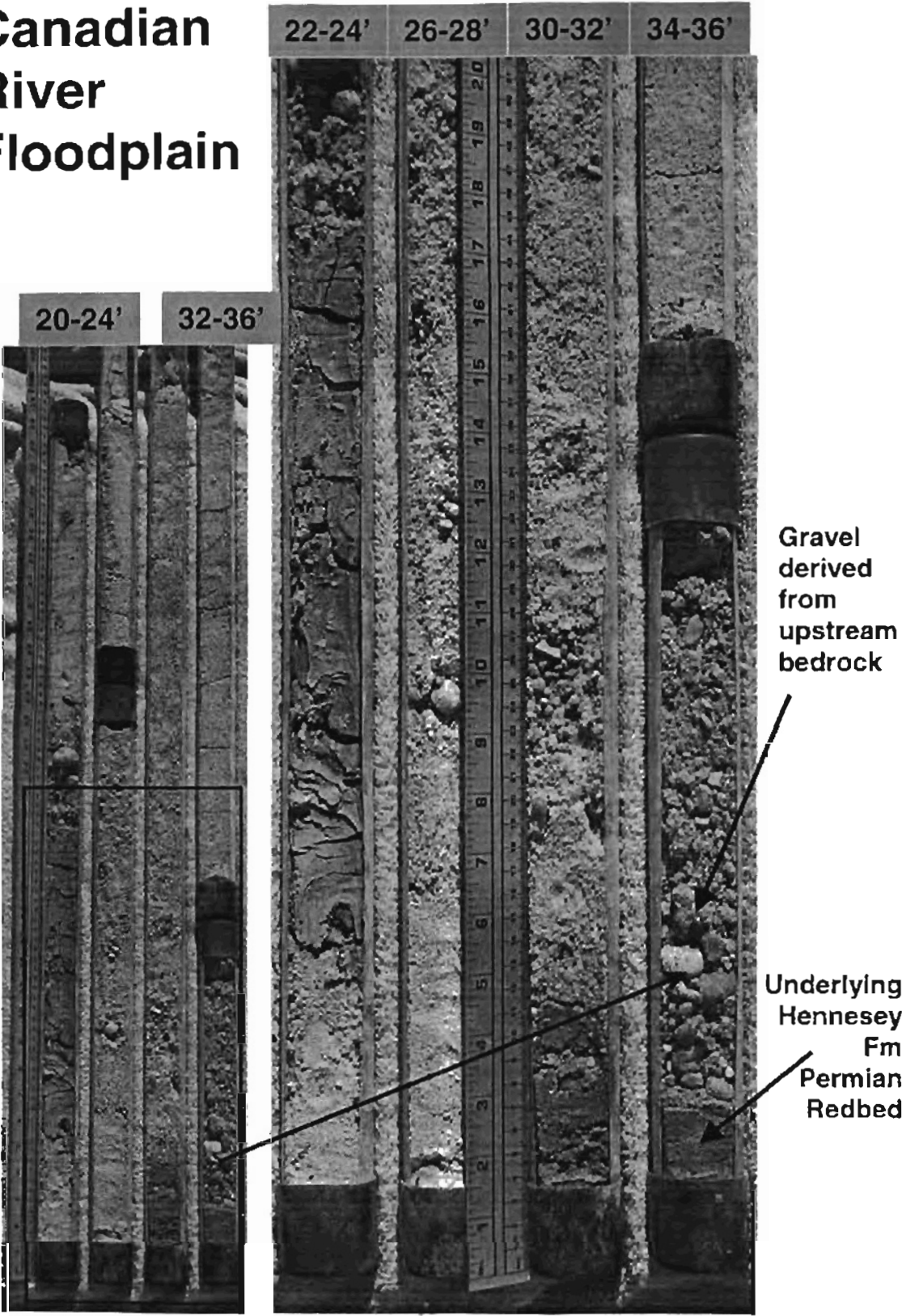
Well #3 – Canadian River Floodplain



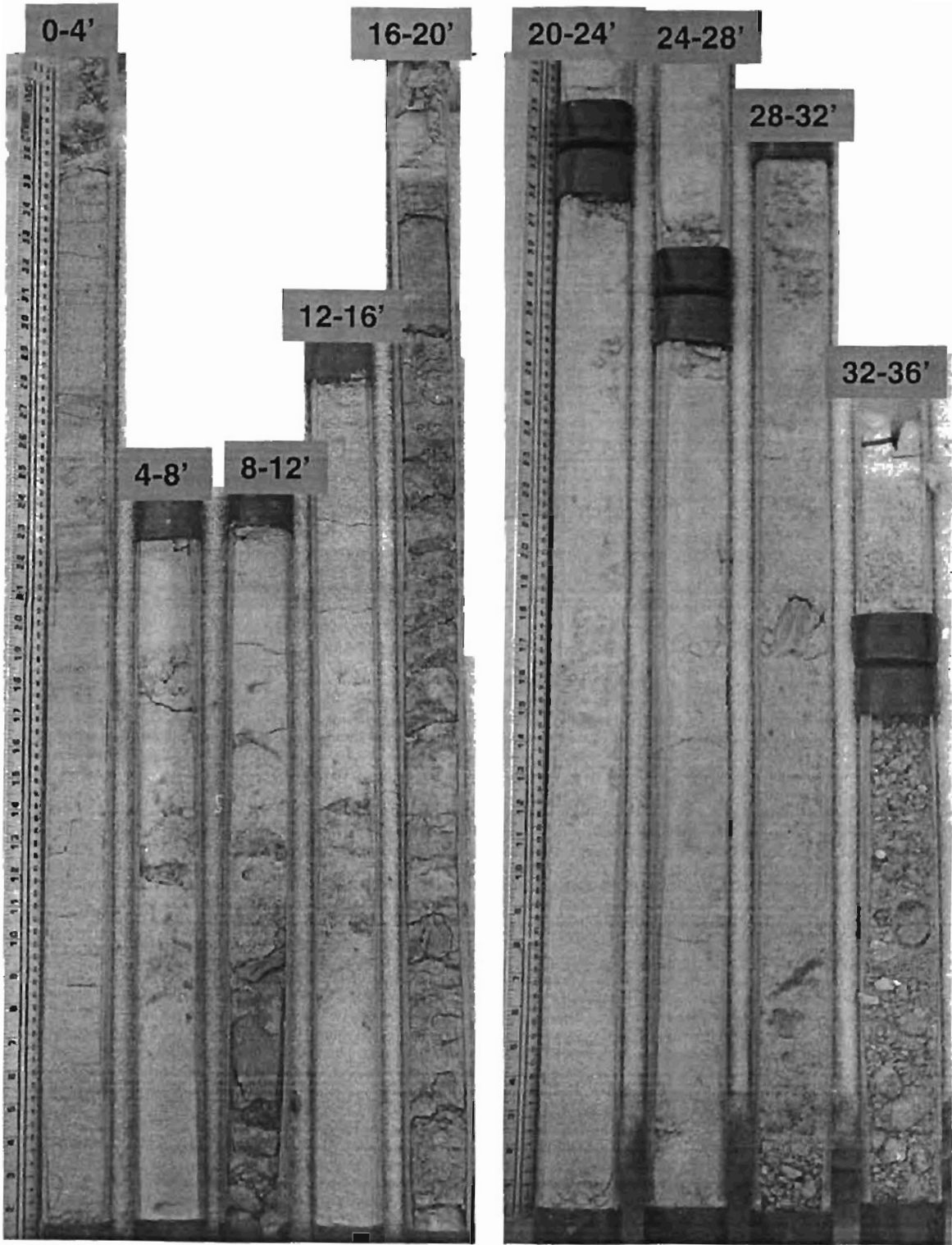
Well #7 – Canadian River Floodplain



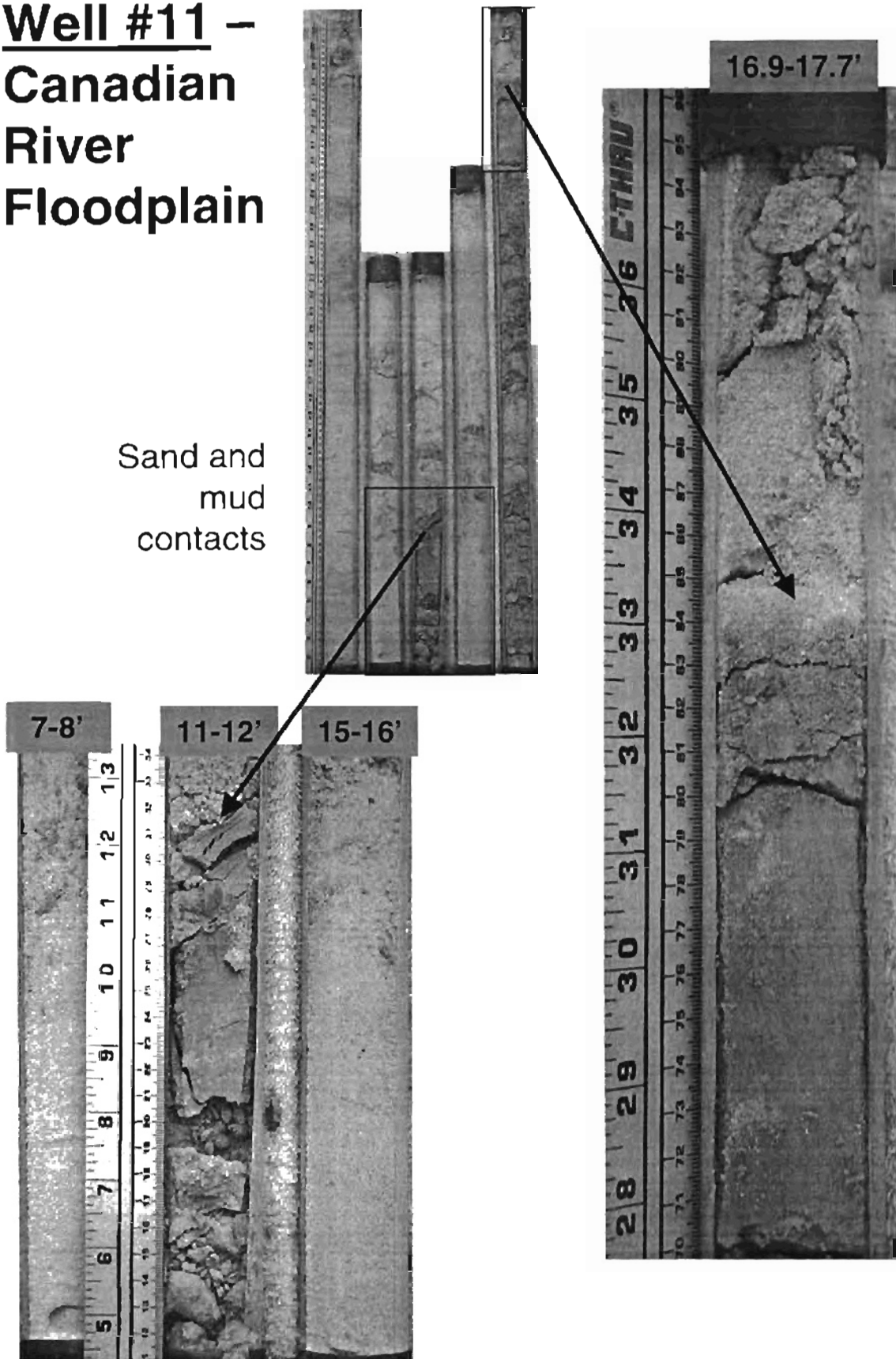
Well #7
Canadian
River
Floodplain



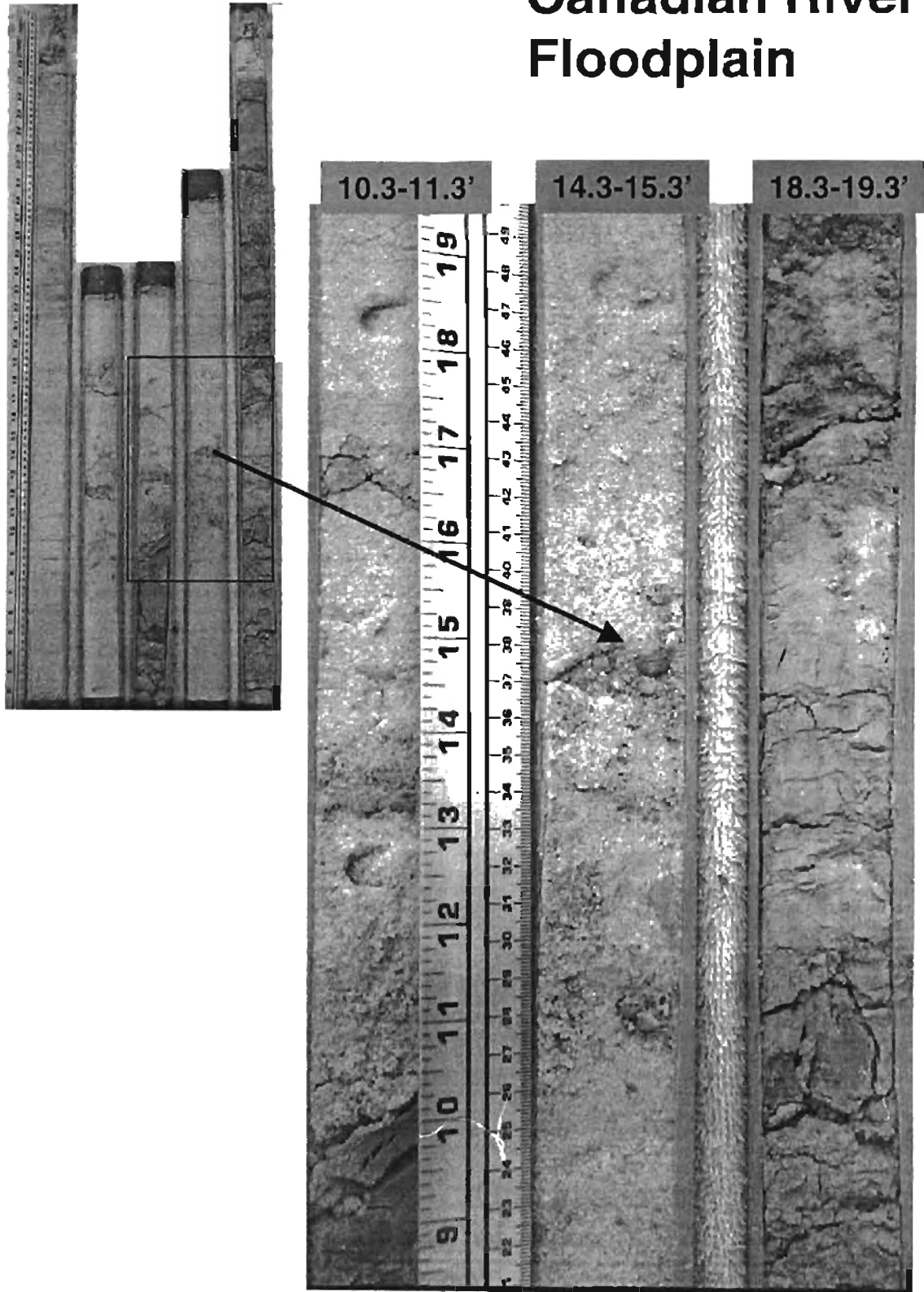
Well #11 – Canadian River Floodplain



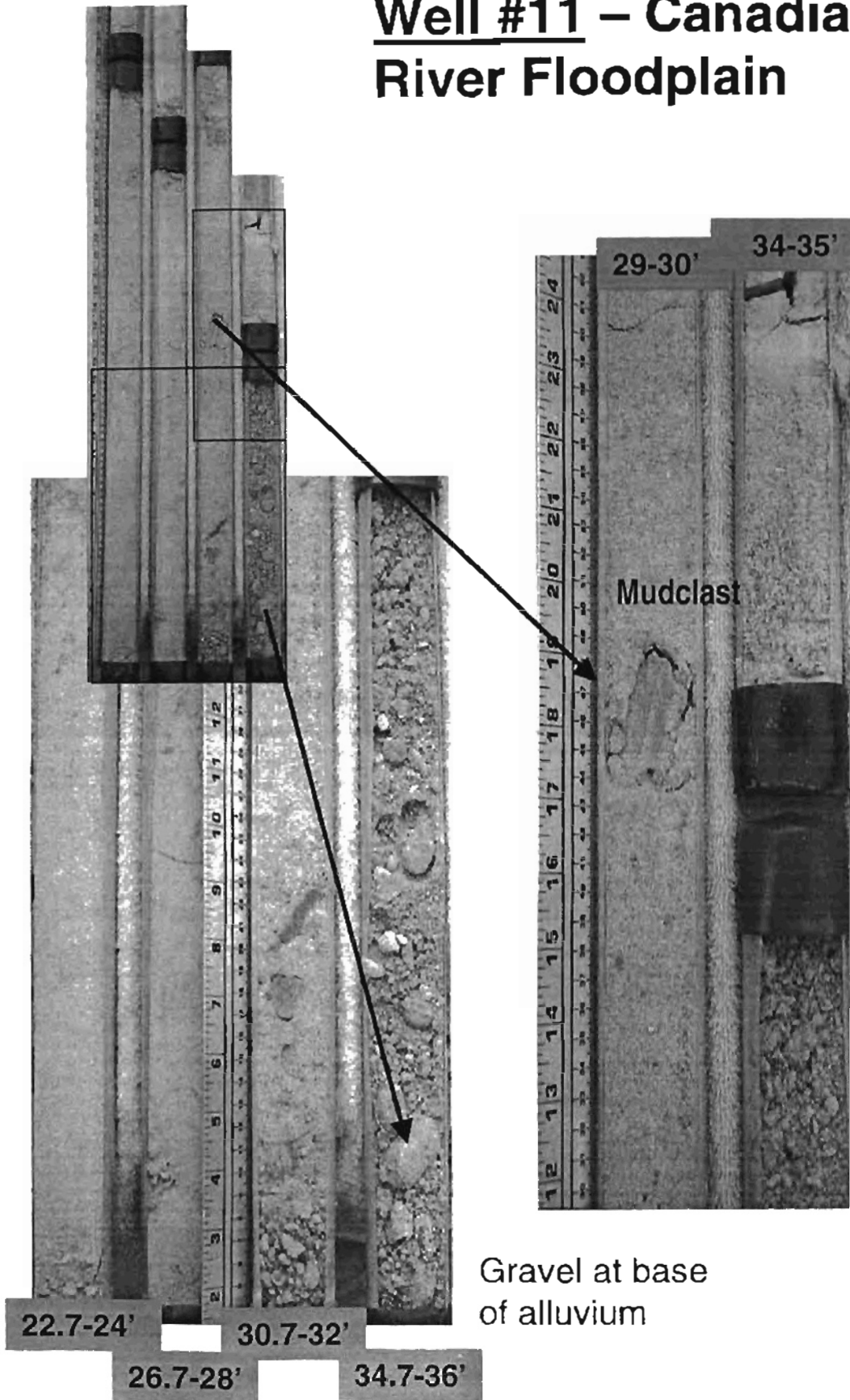
Well #11 – Canadian River Floodplain



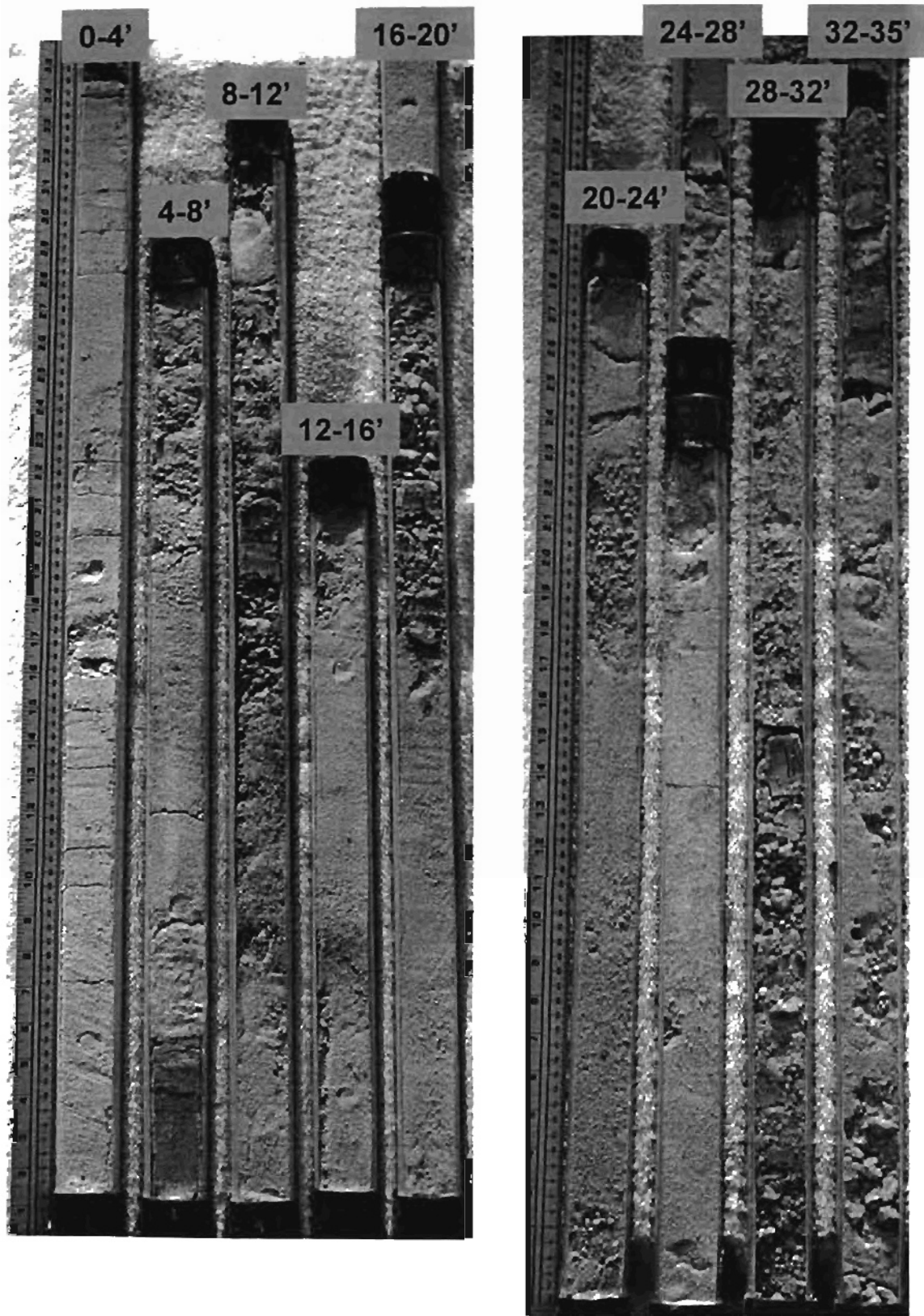
Well #11 – Canadian River Floodplain

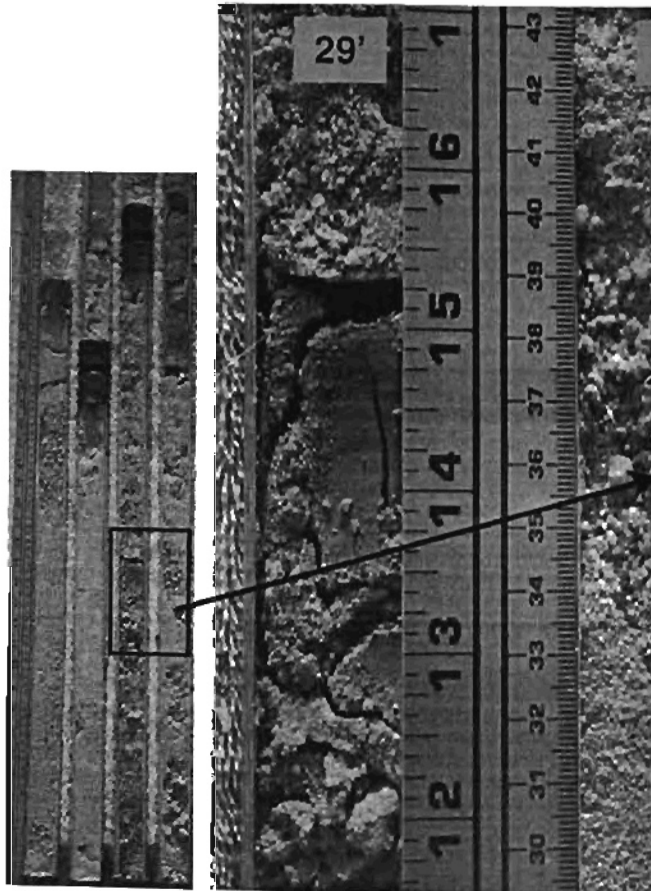


Well #11 – Canadian River Floodplain

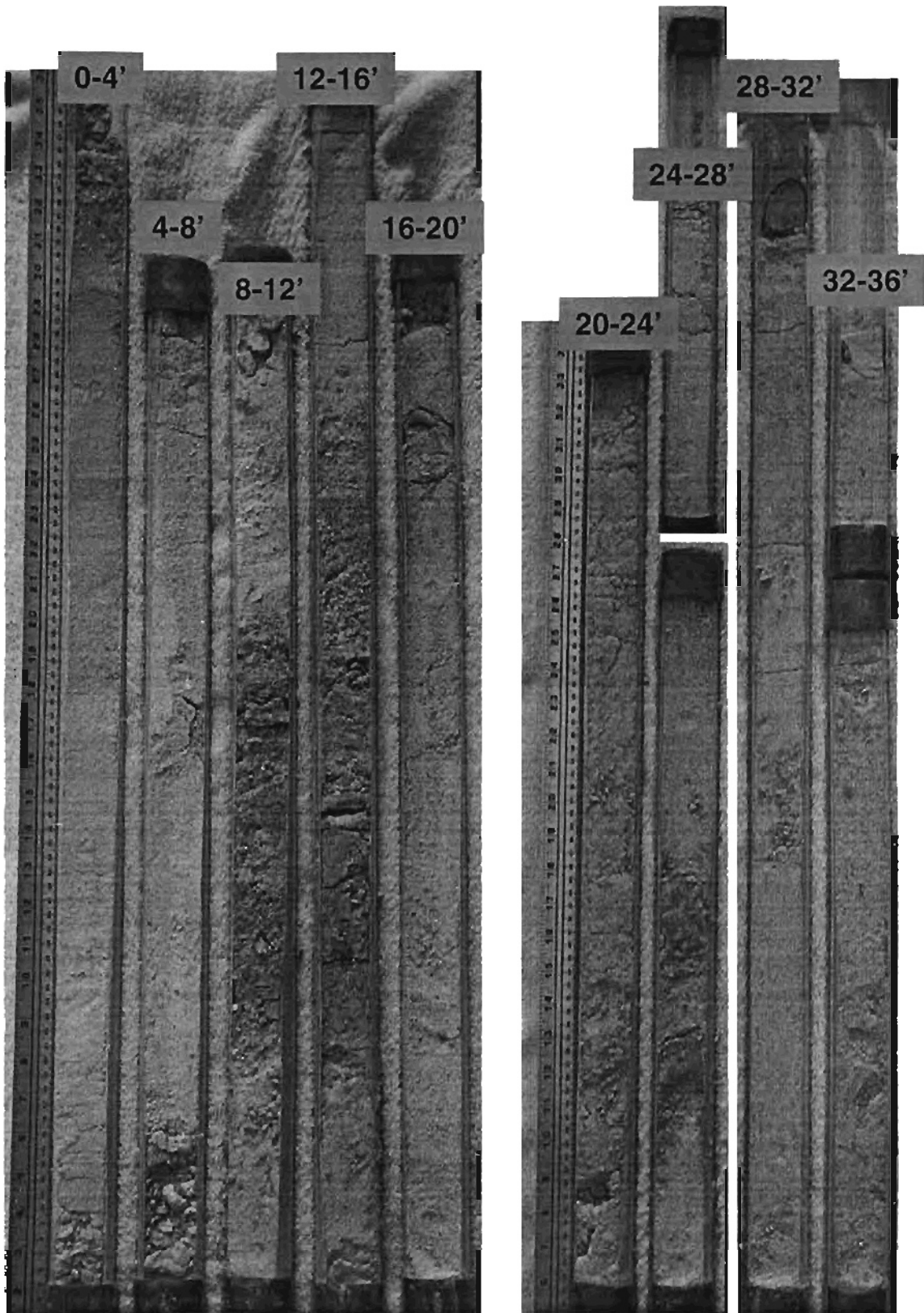


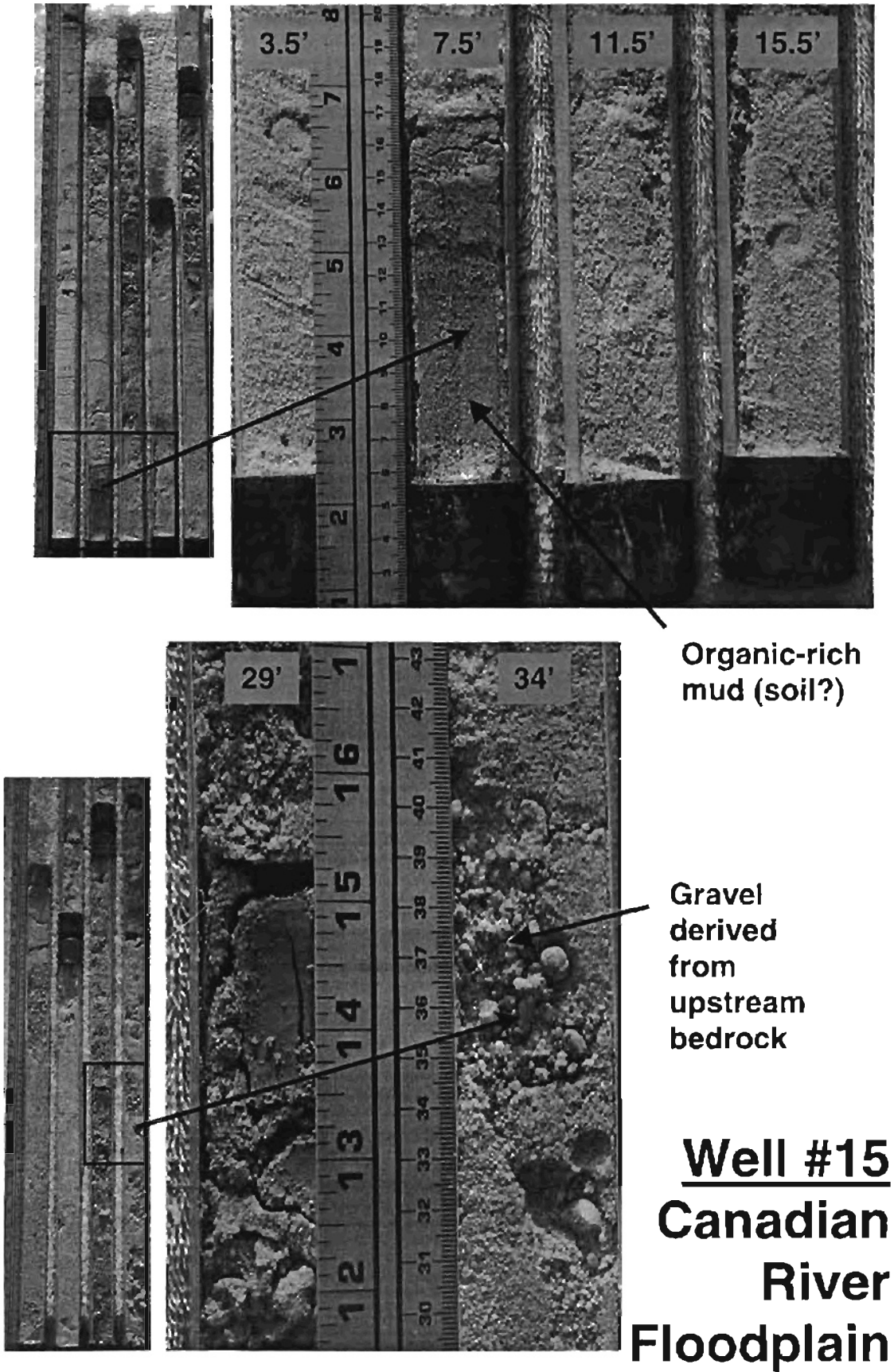
Well #15 – Canadian River Floodplain



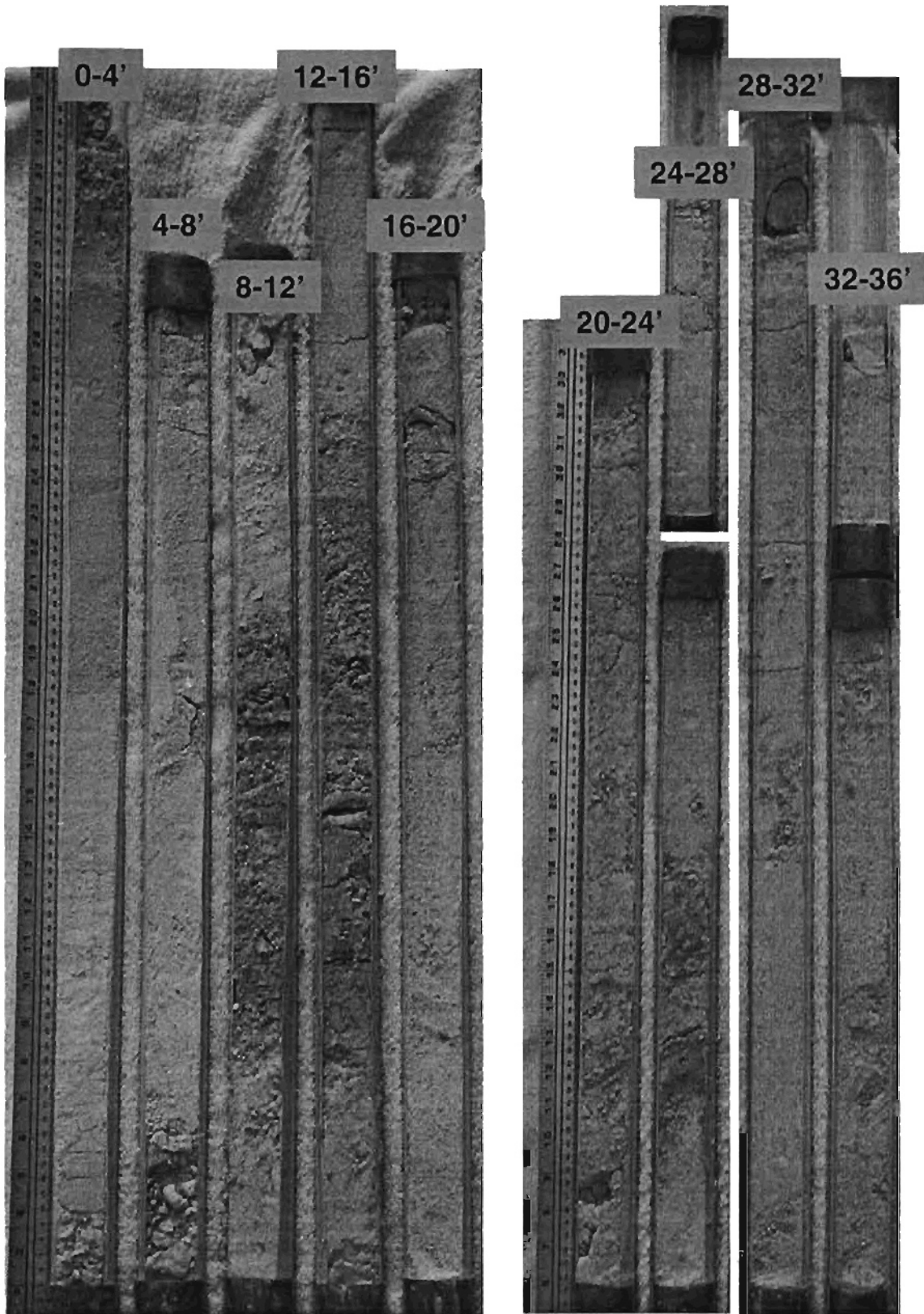


Well #21 – Canadian River Floodplain

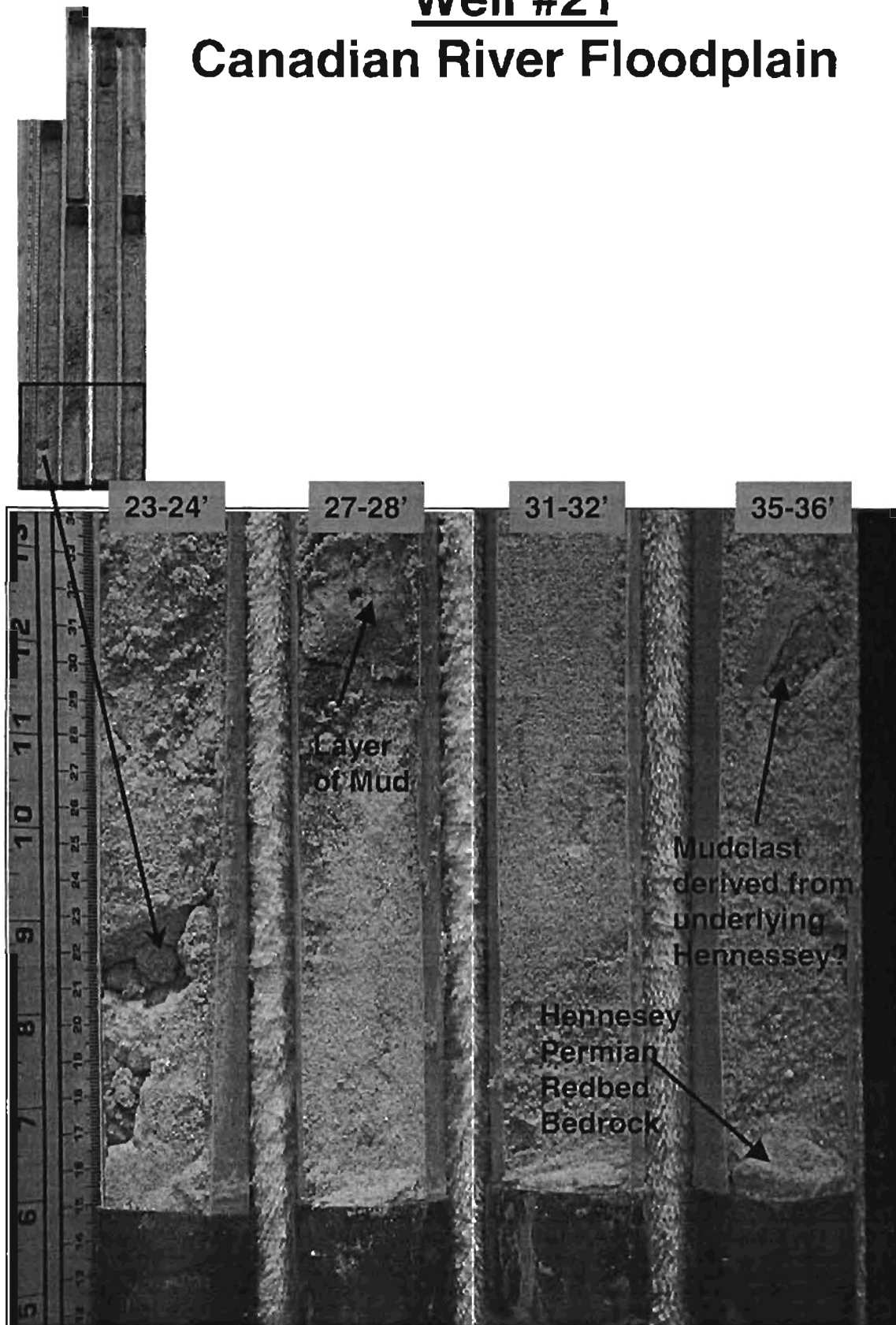




Well #21 – Canadian River Floodplain



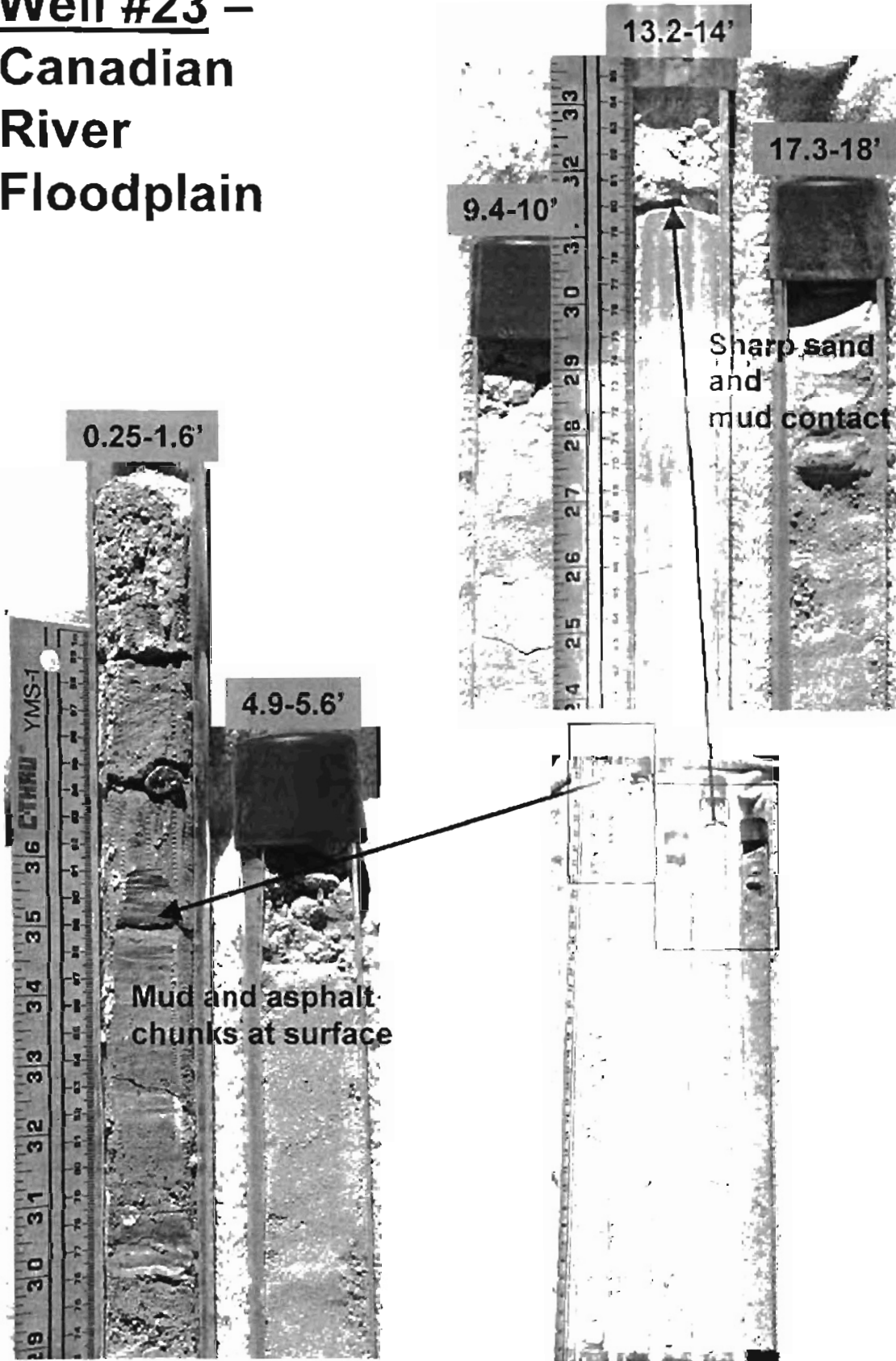
Well #21 Canadian River Floodplain



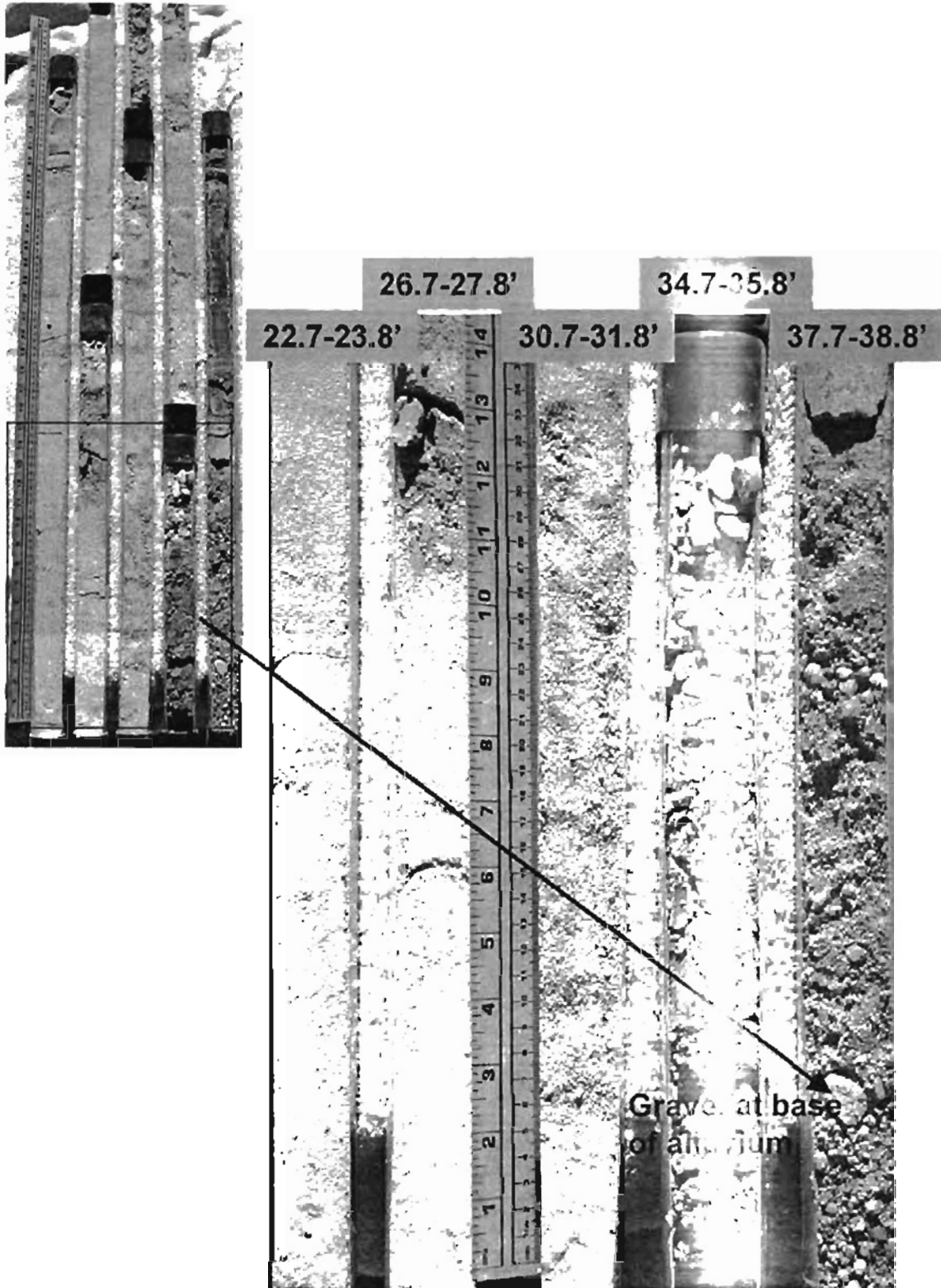
Well #23 – Canadian River Floodplain



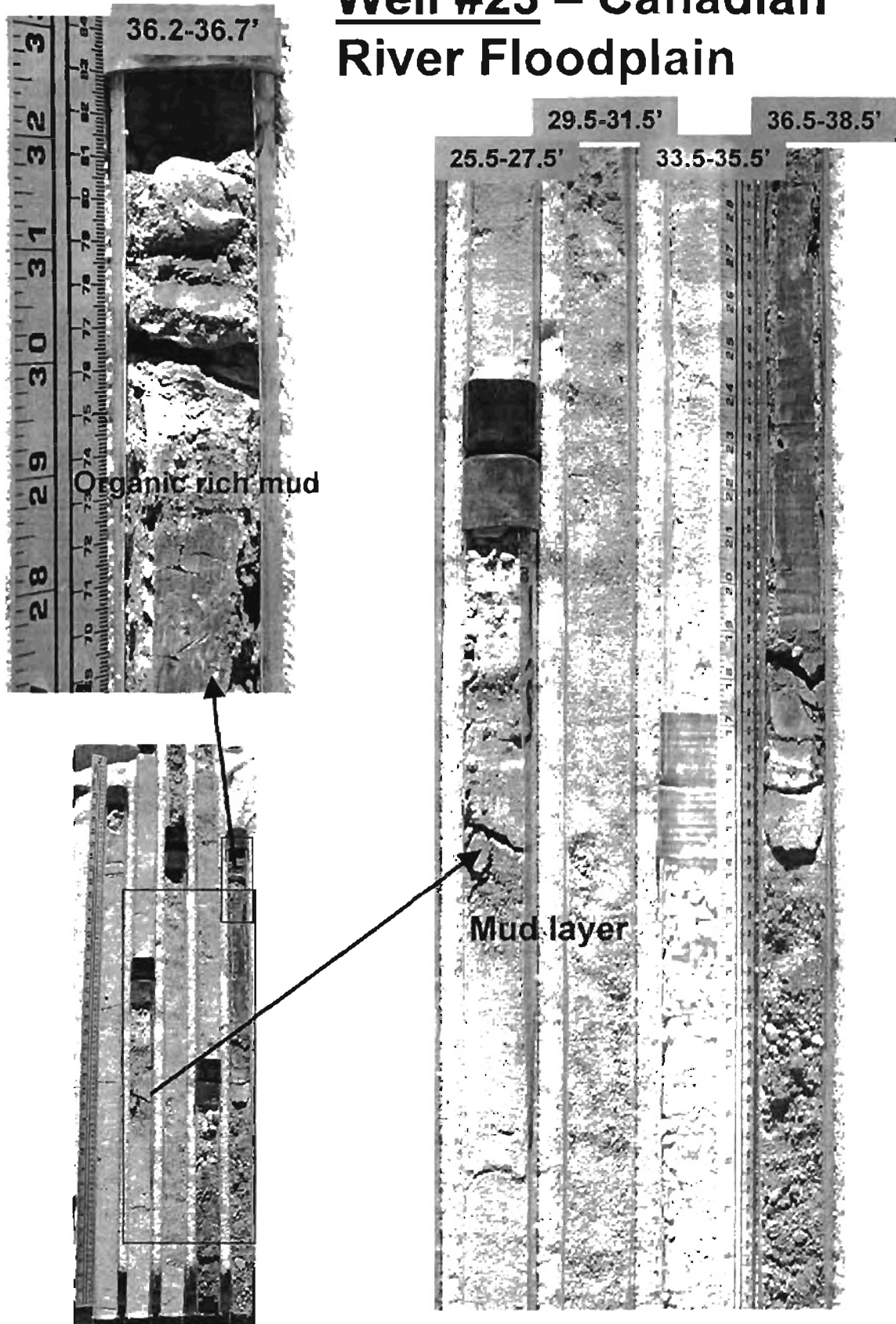
Well #23 – Canadian River Floodplain



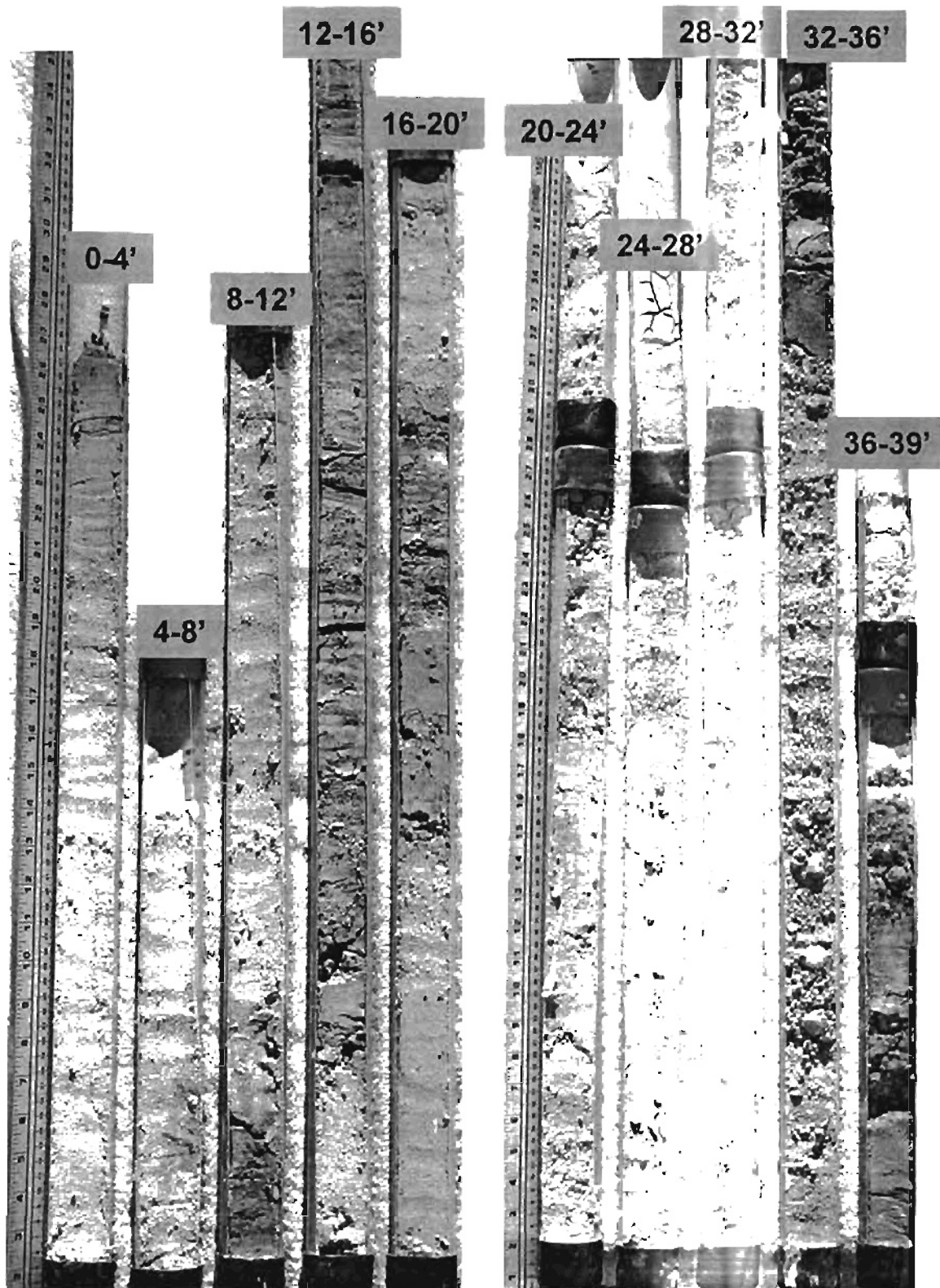
Well #23 – Canadian River Floodplain



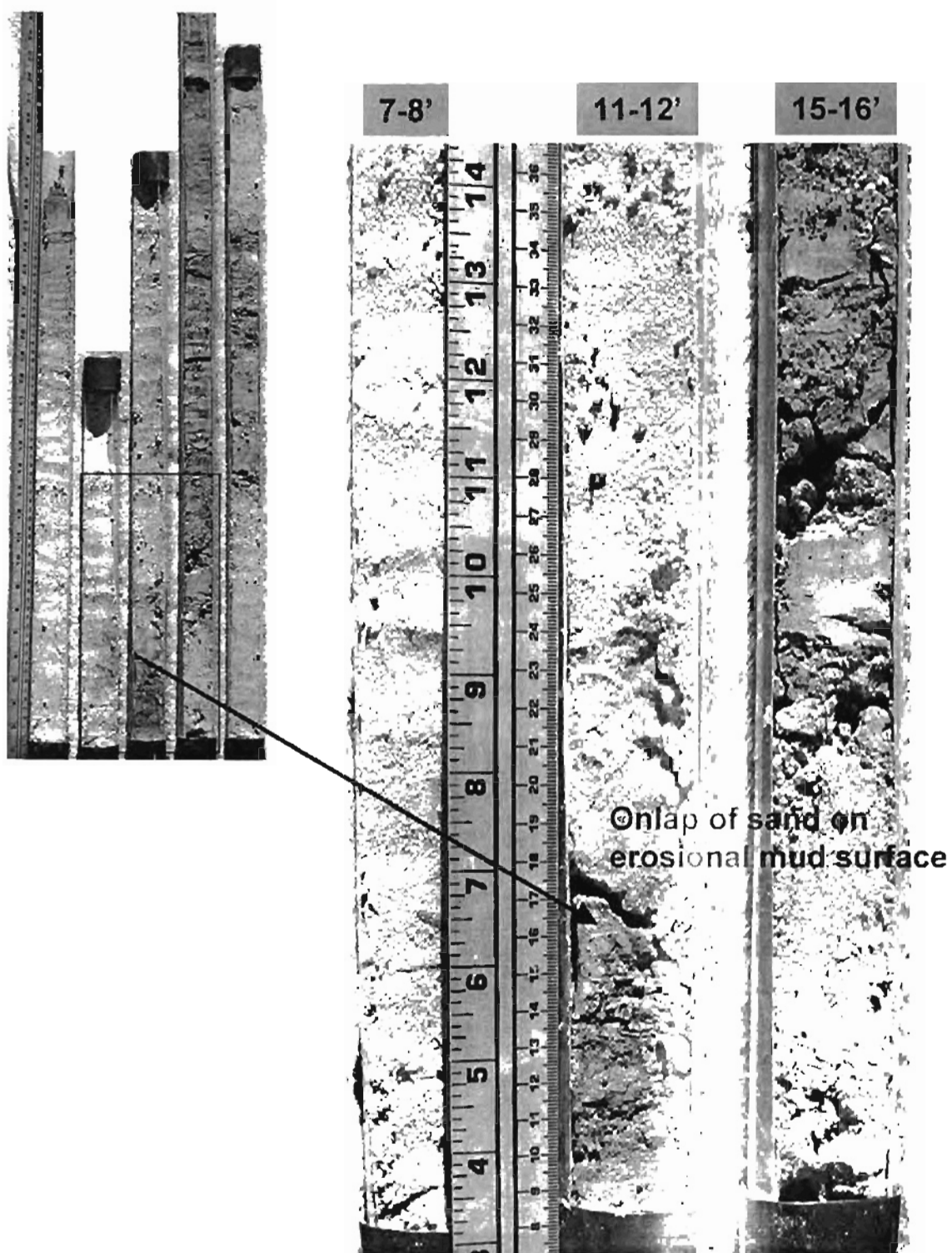
Well #23 – Canadian River Floodplain



Well #28 – Canadian River Floodplain



Well #28 – Canadian River Floodplain

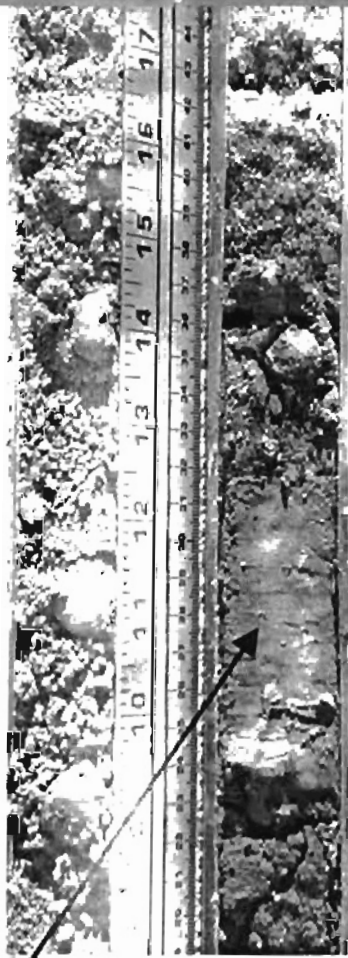


Well #28 – Canadian River Floodplain

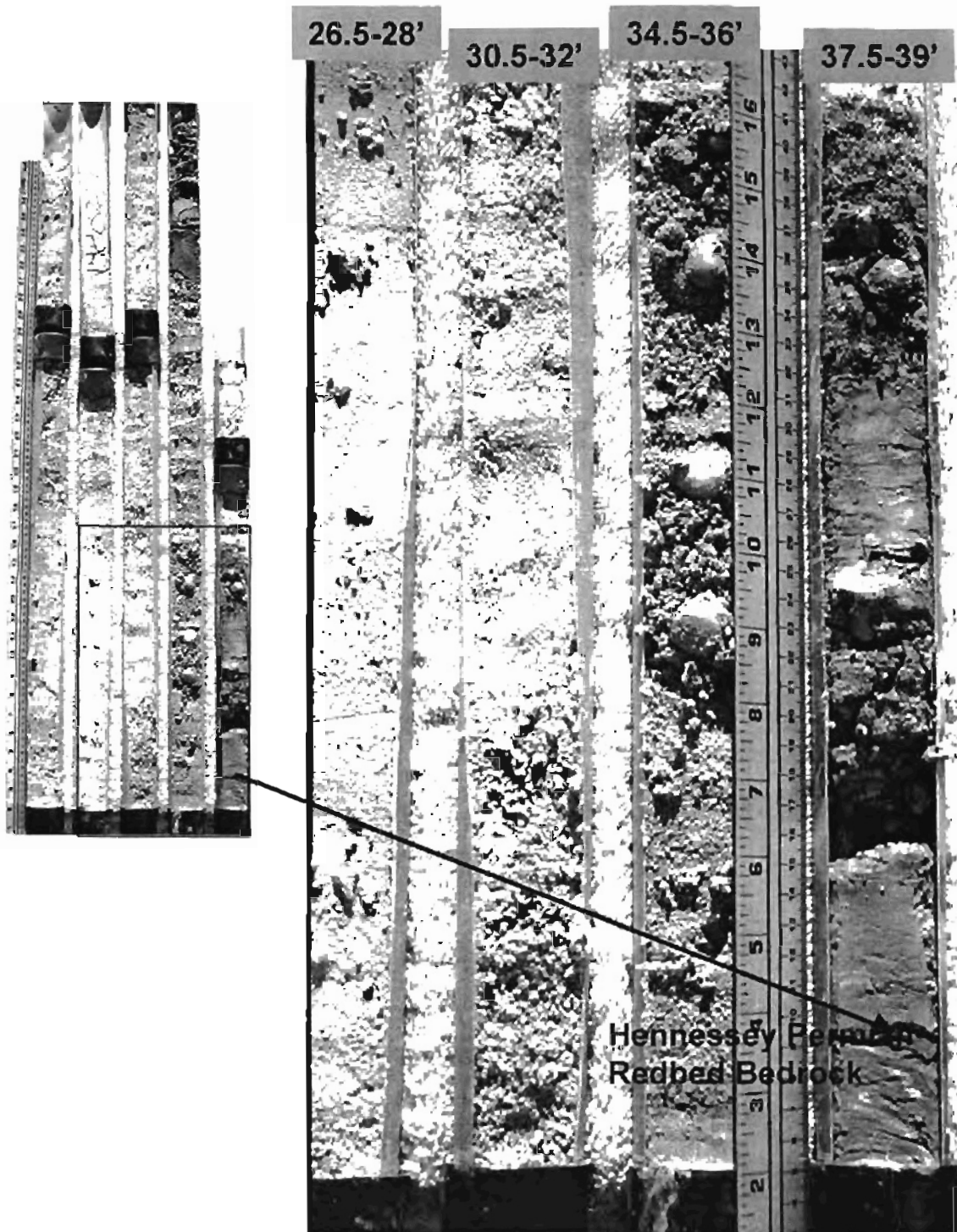
28.5-29.8' 32.5-33.8'



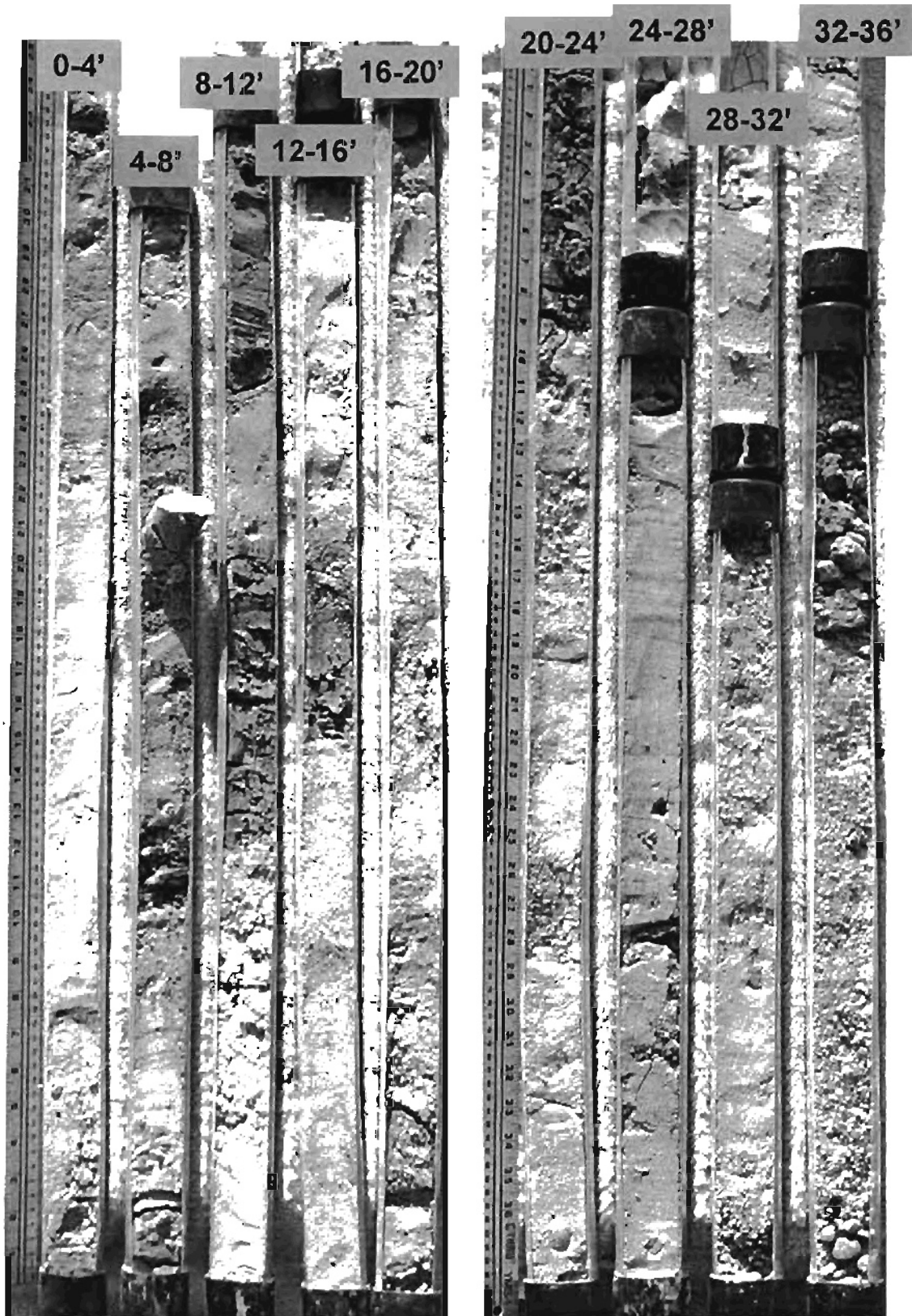
34.5-35.6' 37.5-38.6'



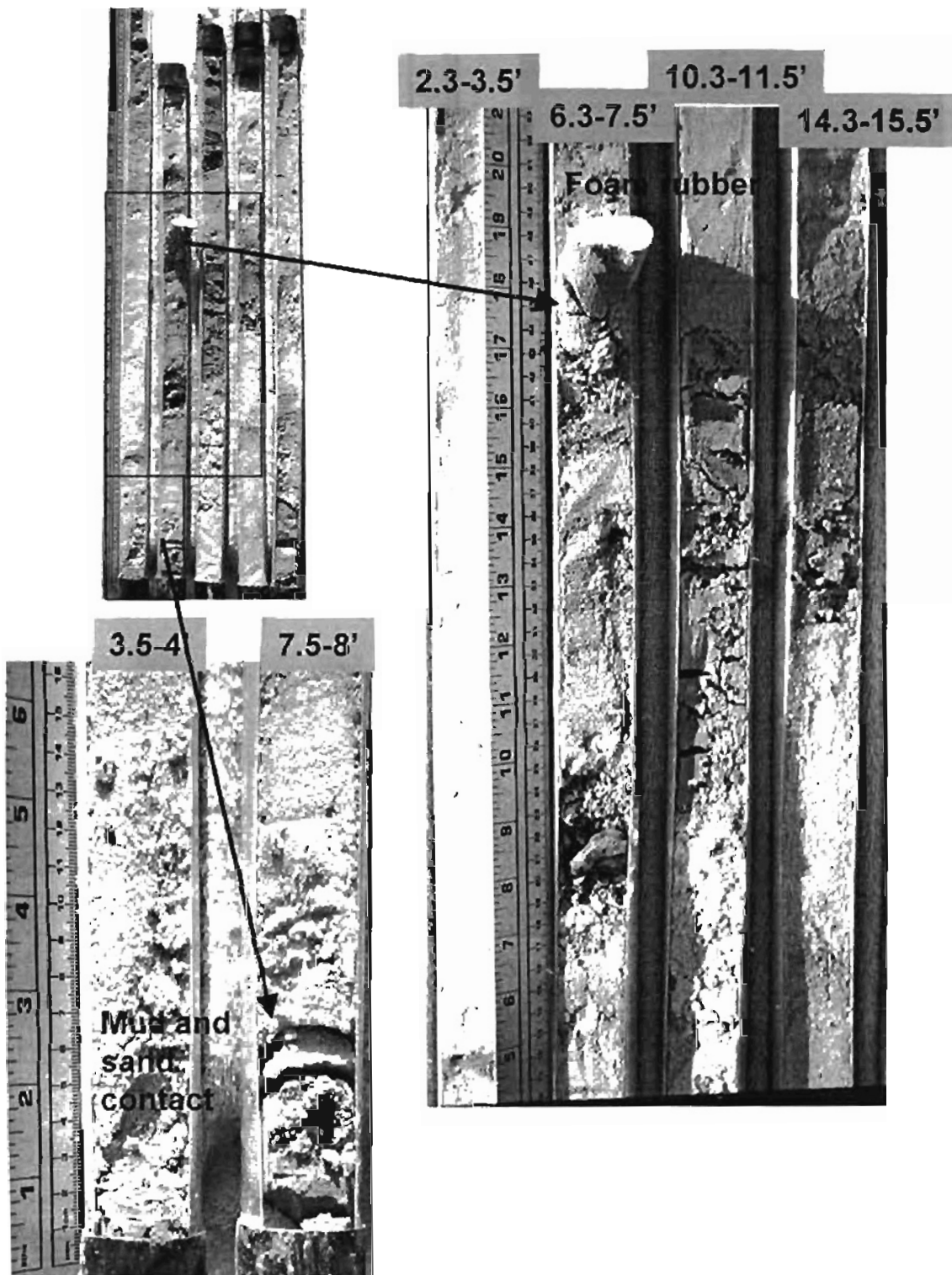
Well #28 – Canadian River Floodplain



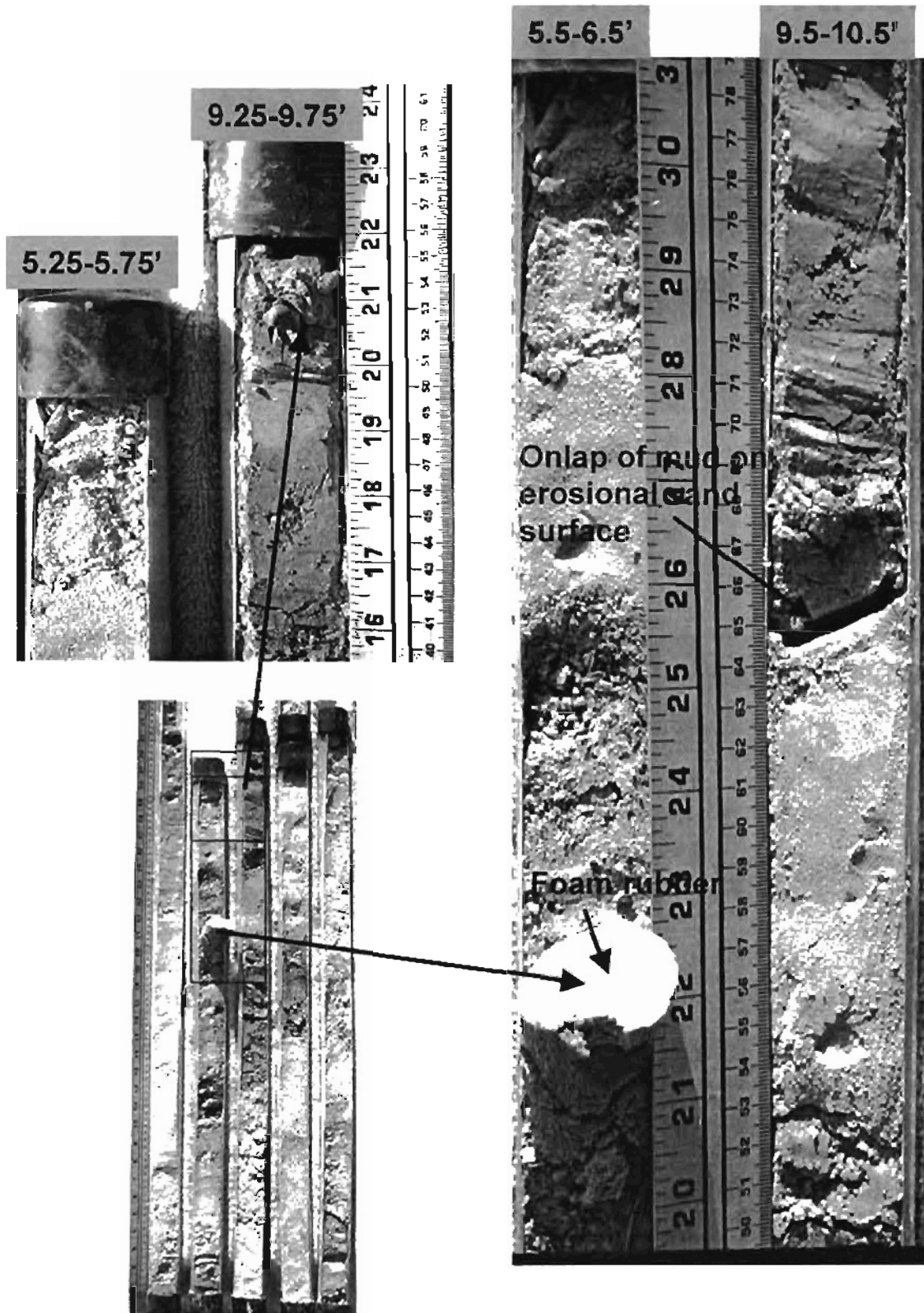
Well #31 – Canadian River Floodplain



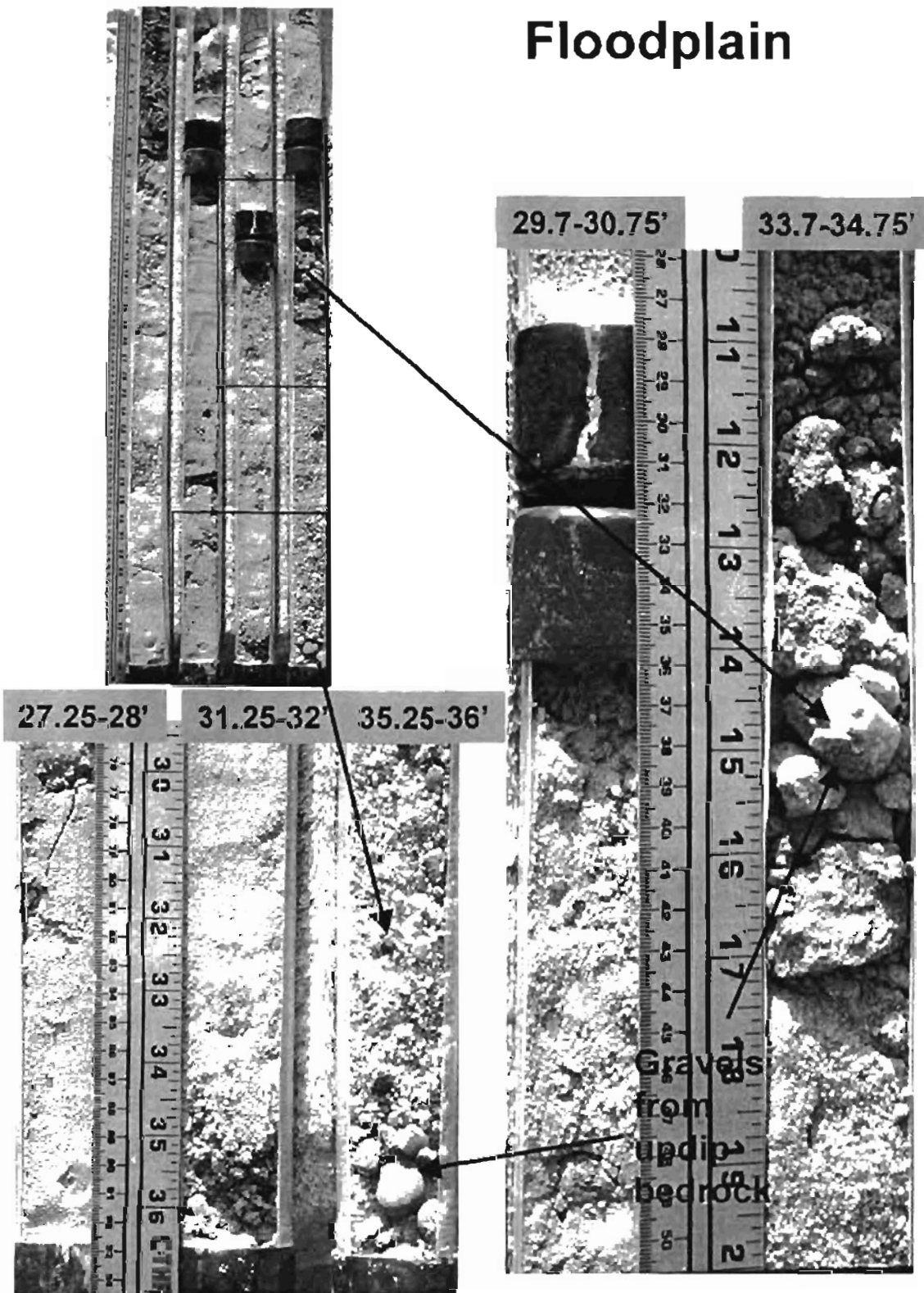
Well #31 – Canadian River Floodplain



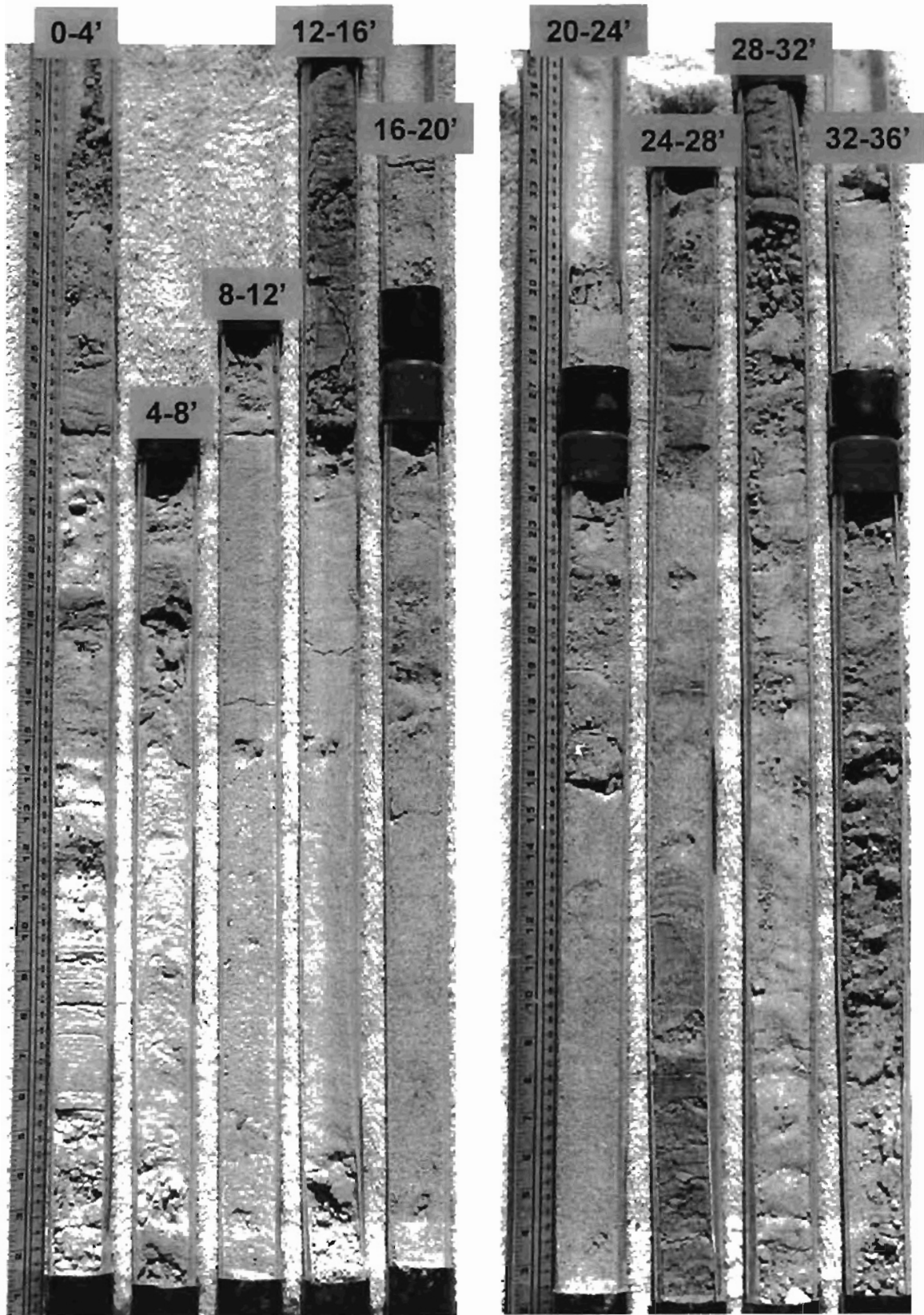
Well #31 – Canadian River Floodplain

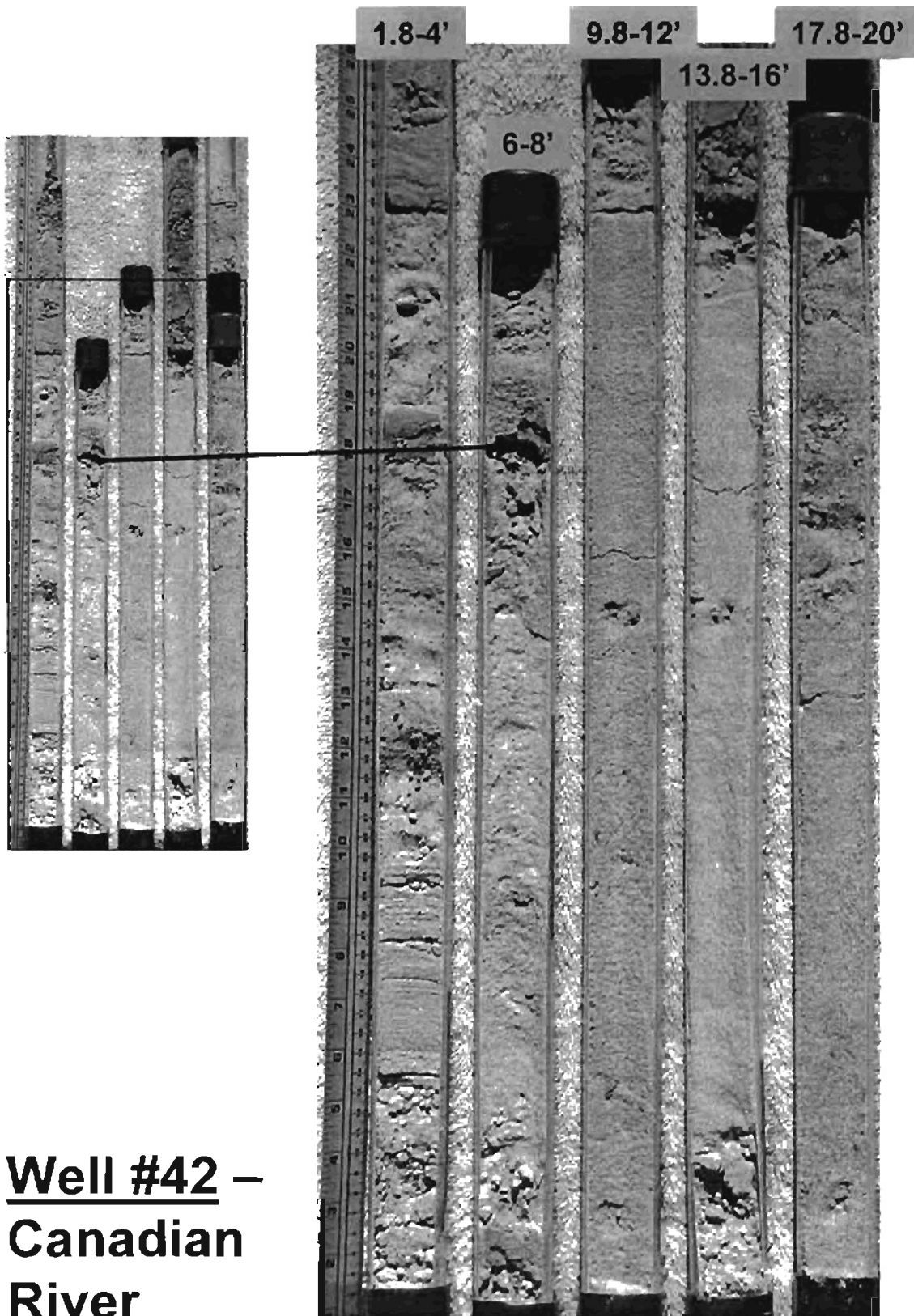


Well #31 – Canadian River Floodplain



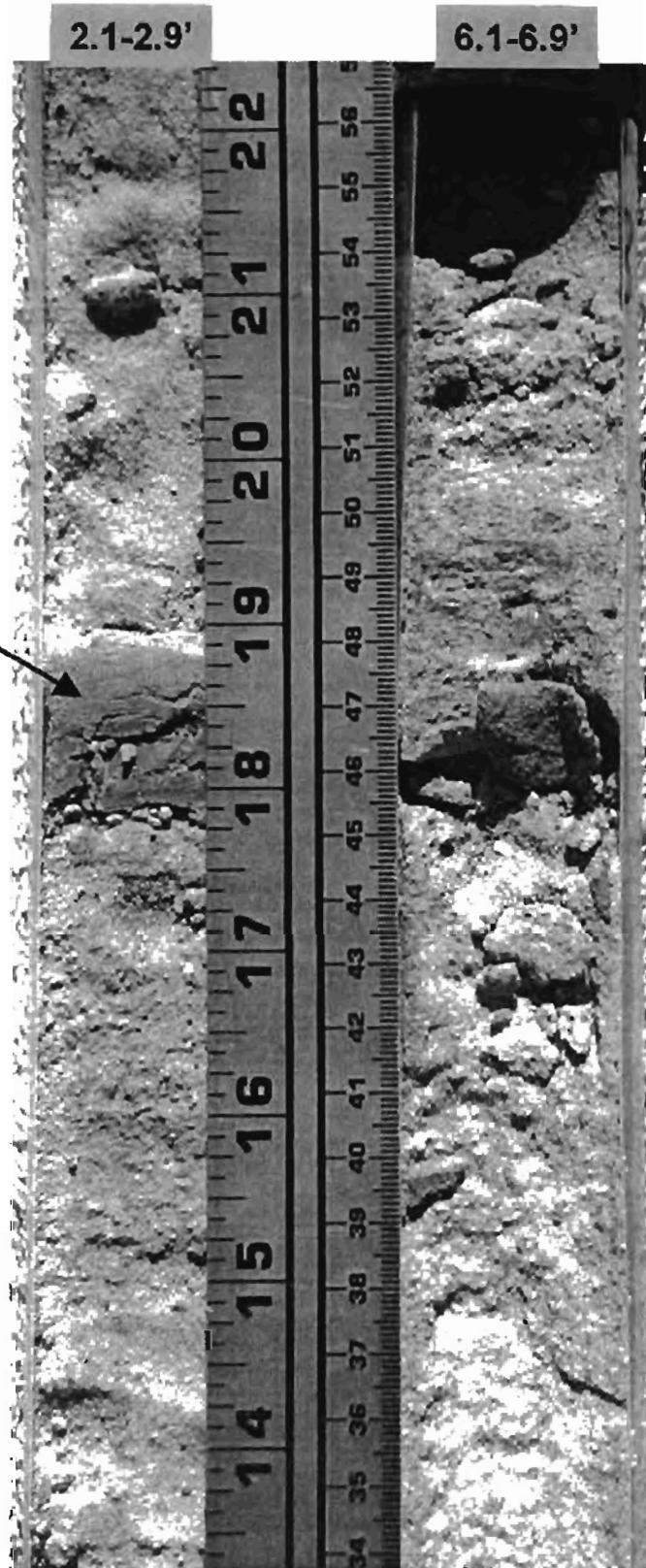
Well #42 – Canadian River Floodplain



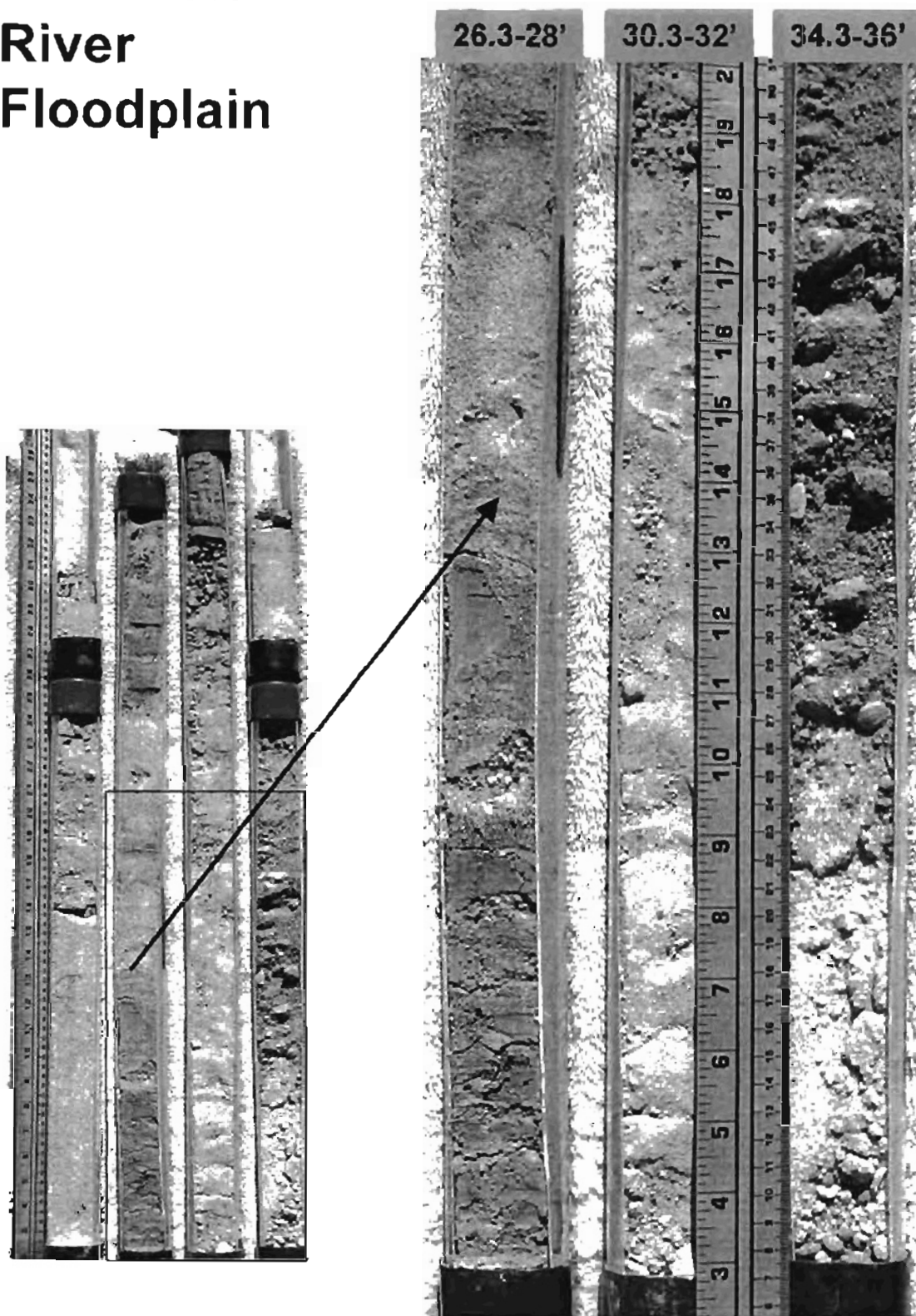


**Well #42 –
Canadian
River
Floodplain**

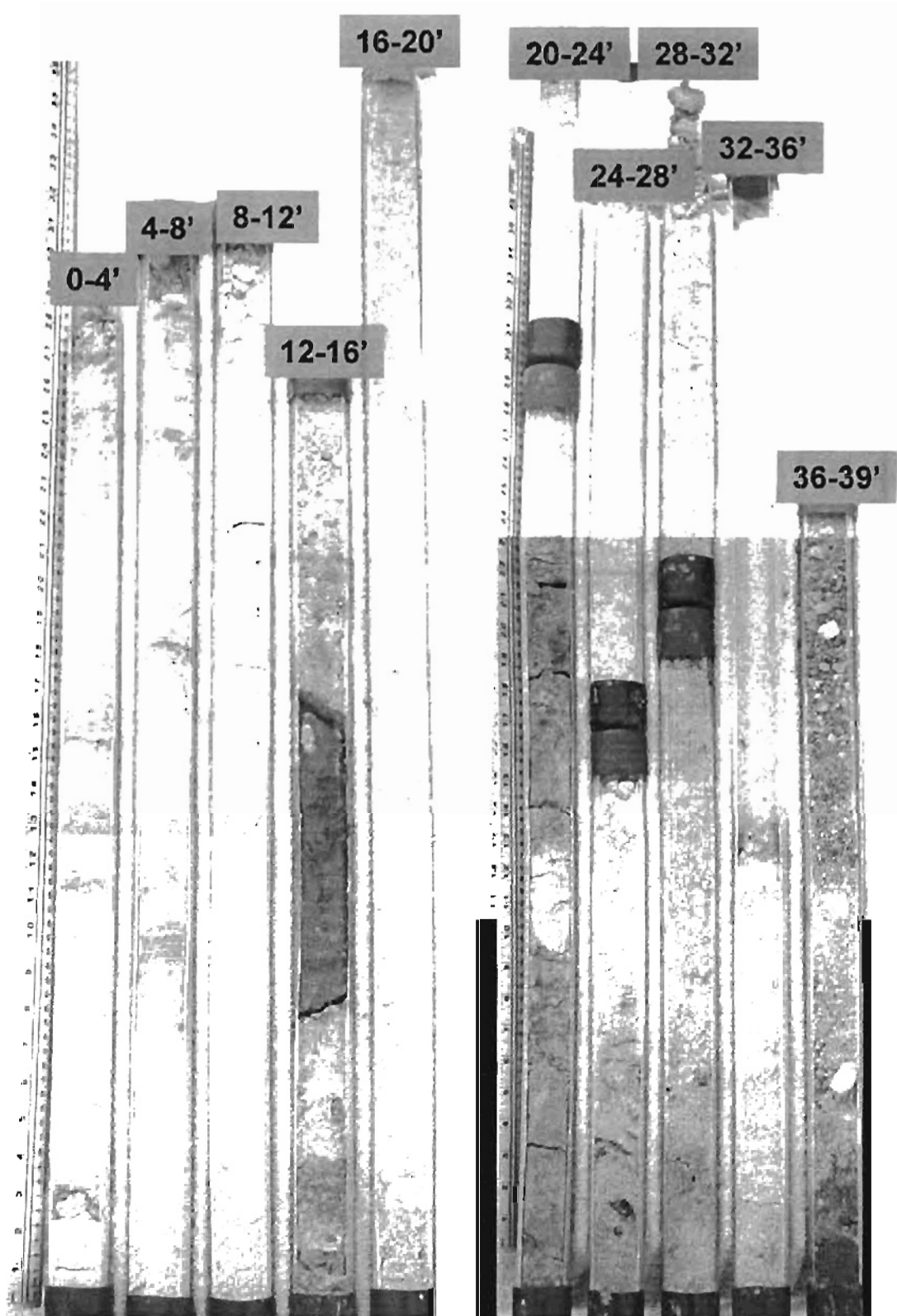
**Well #42 –
Canadian
River
Floodplain**



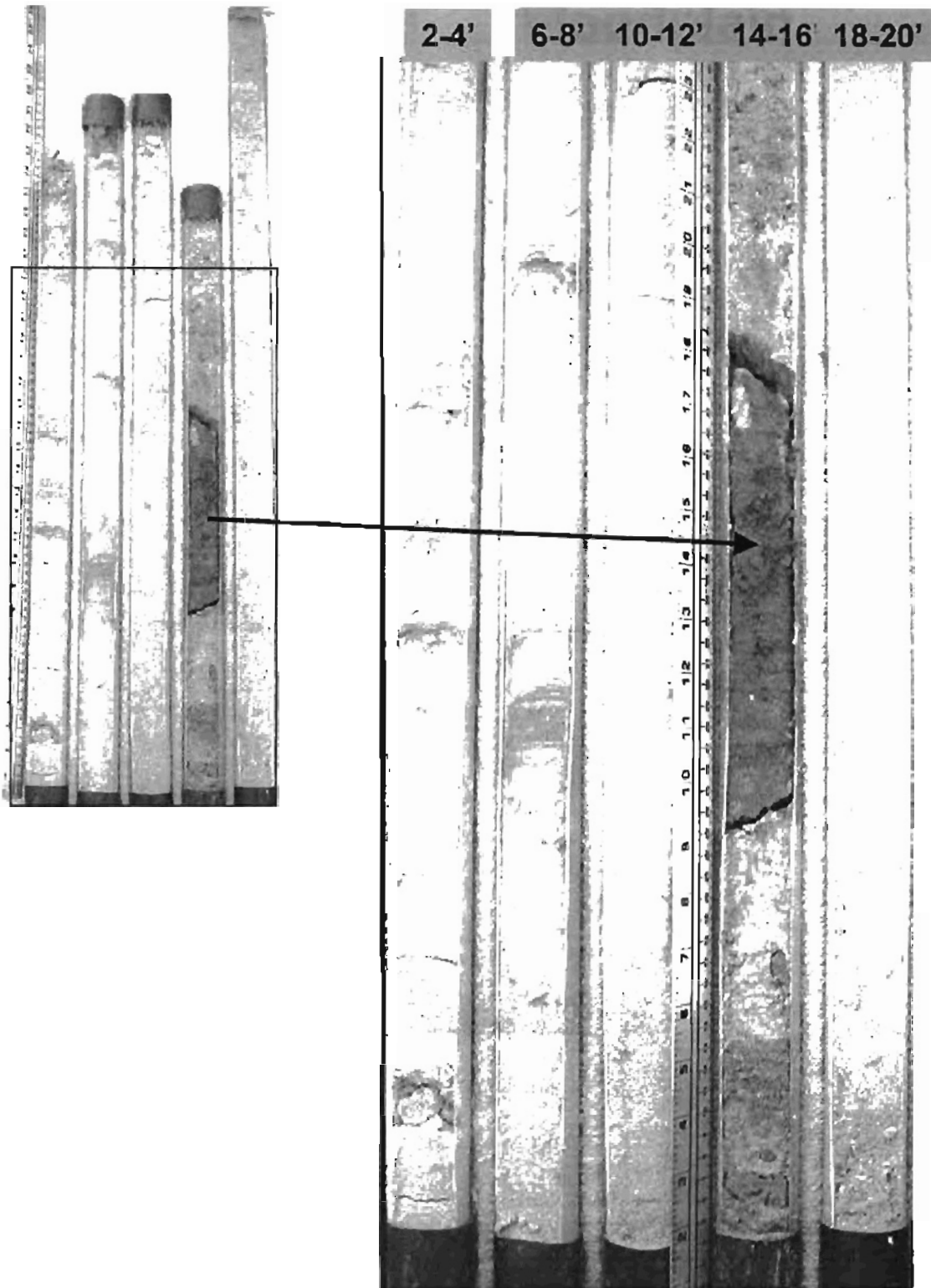
Well #42 – Canadian River Floodplain



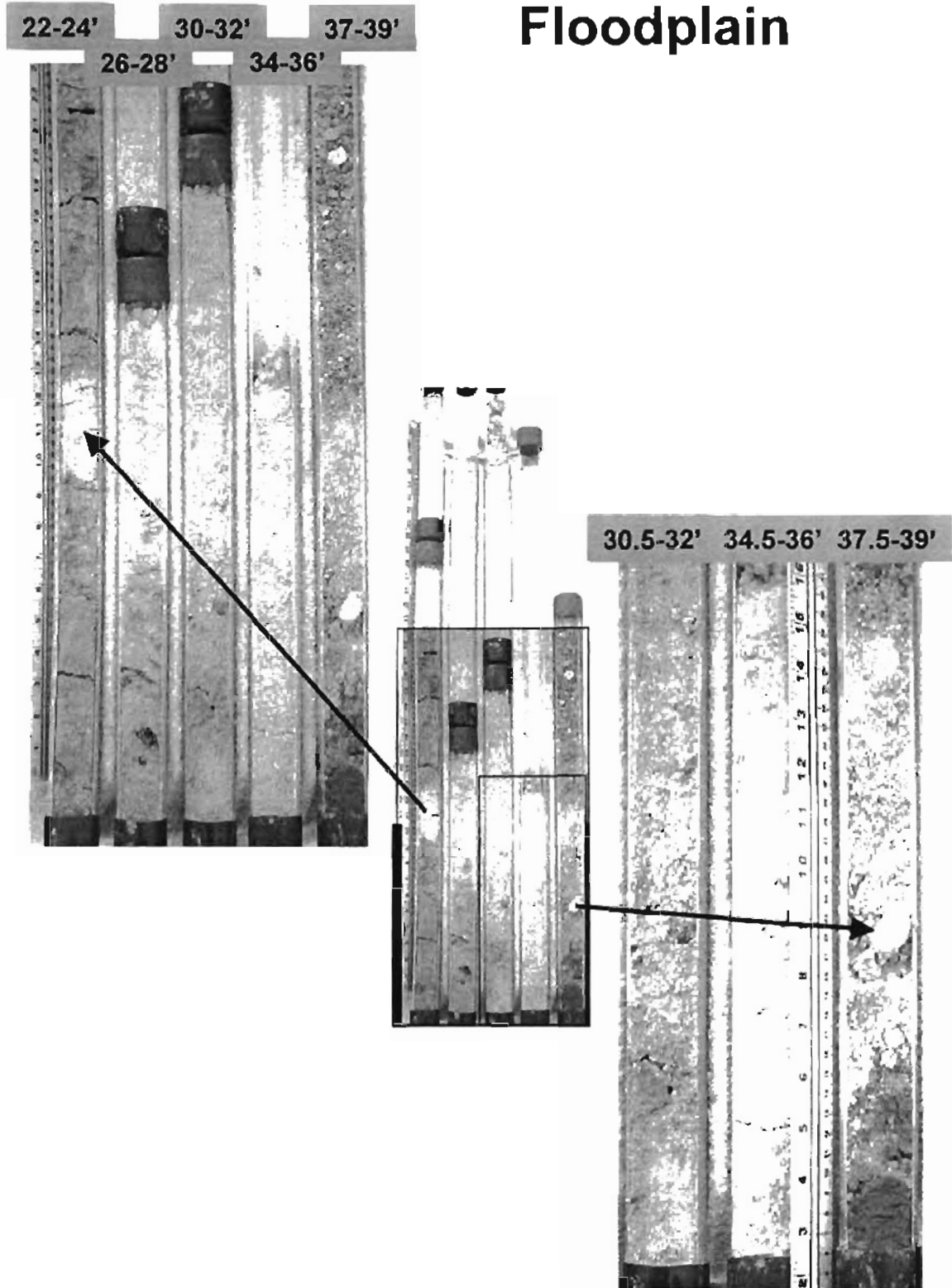
Well #44 – Canadian River Floodplain



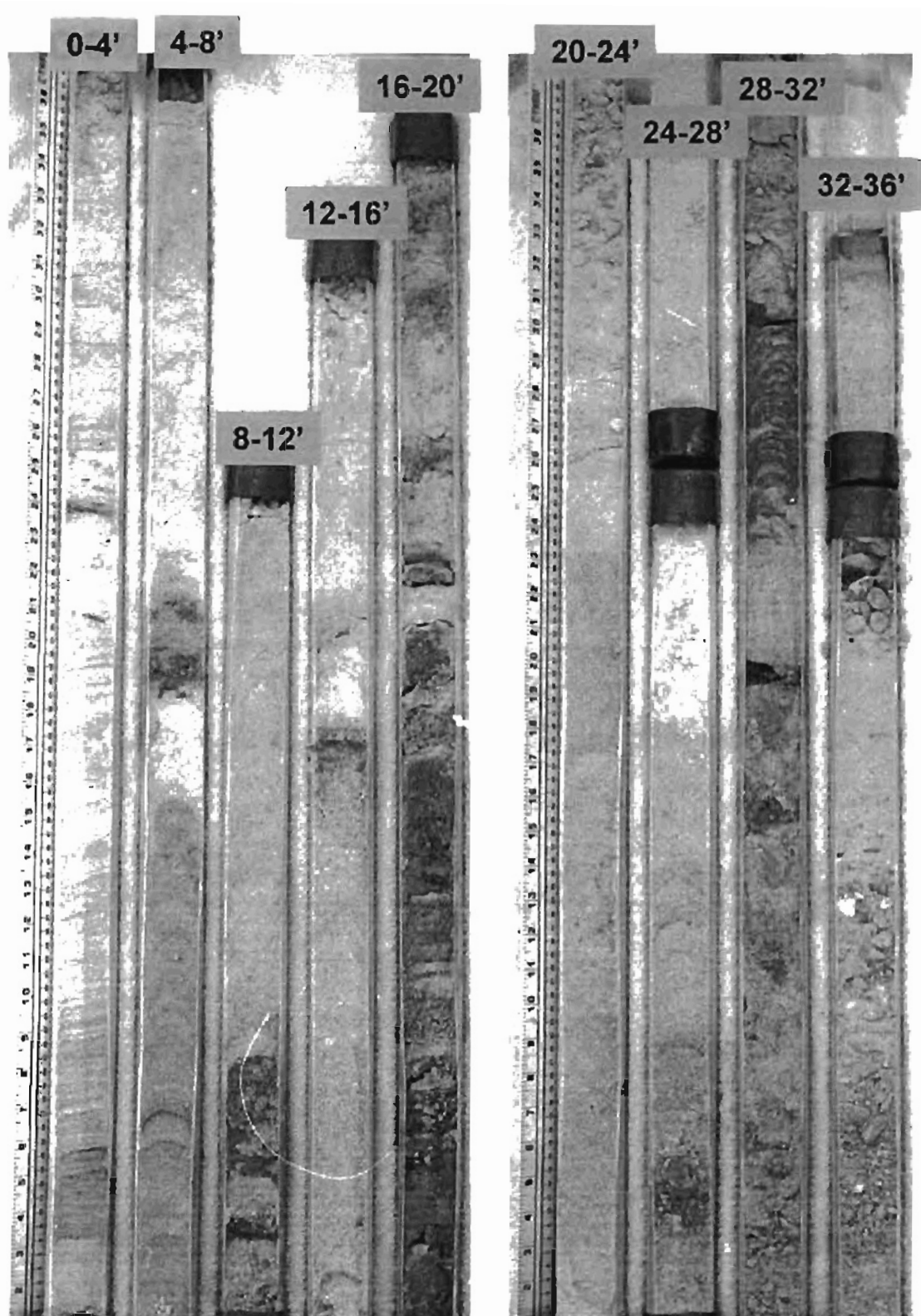
Well #44 – Canadian River Floodplain



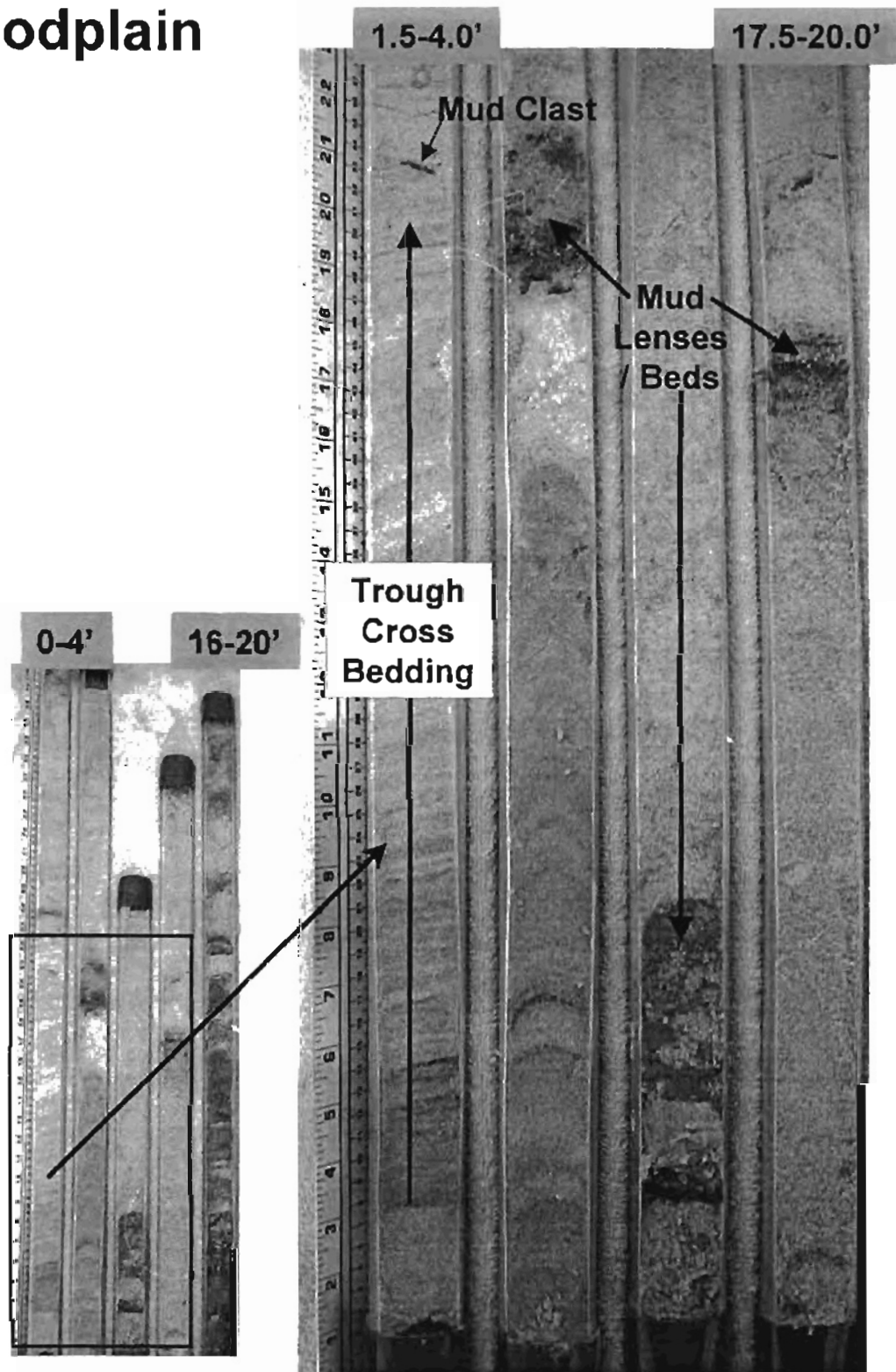
Well #44 – Canadian River Floodplain



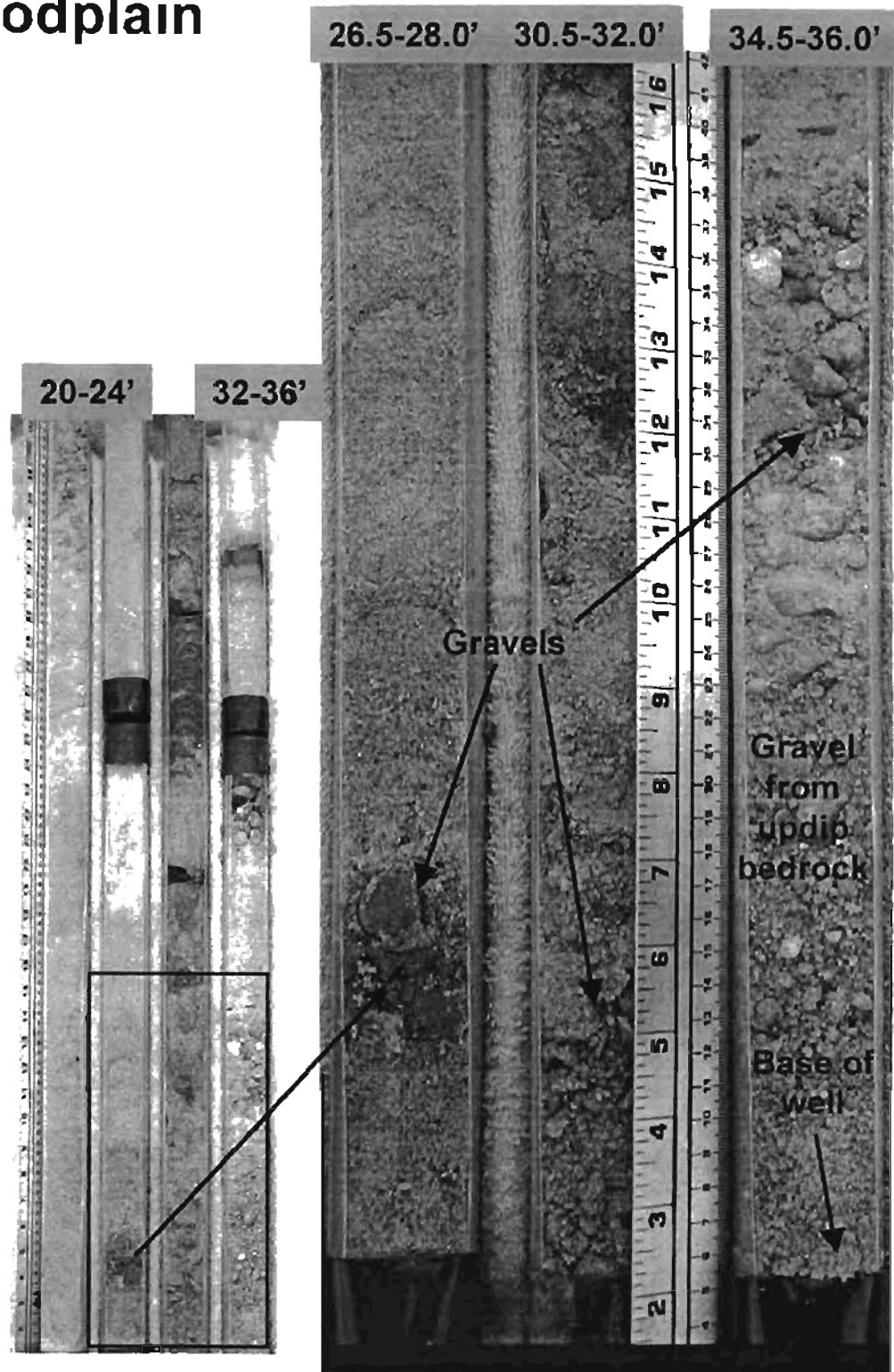
Well #46 – Canadian River Floodplain



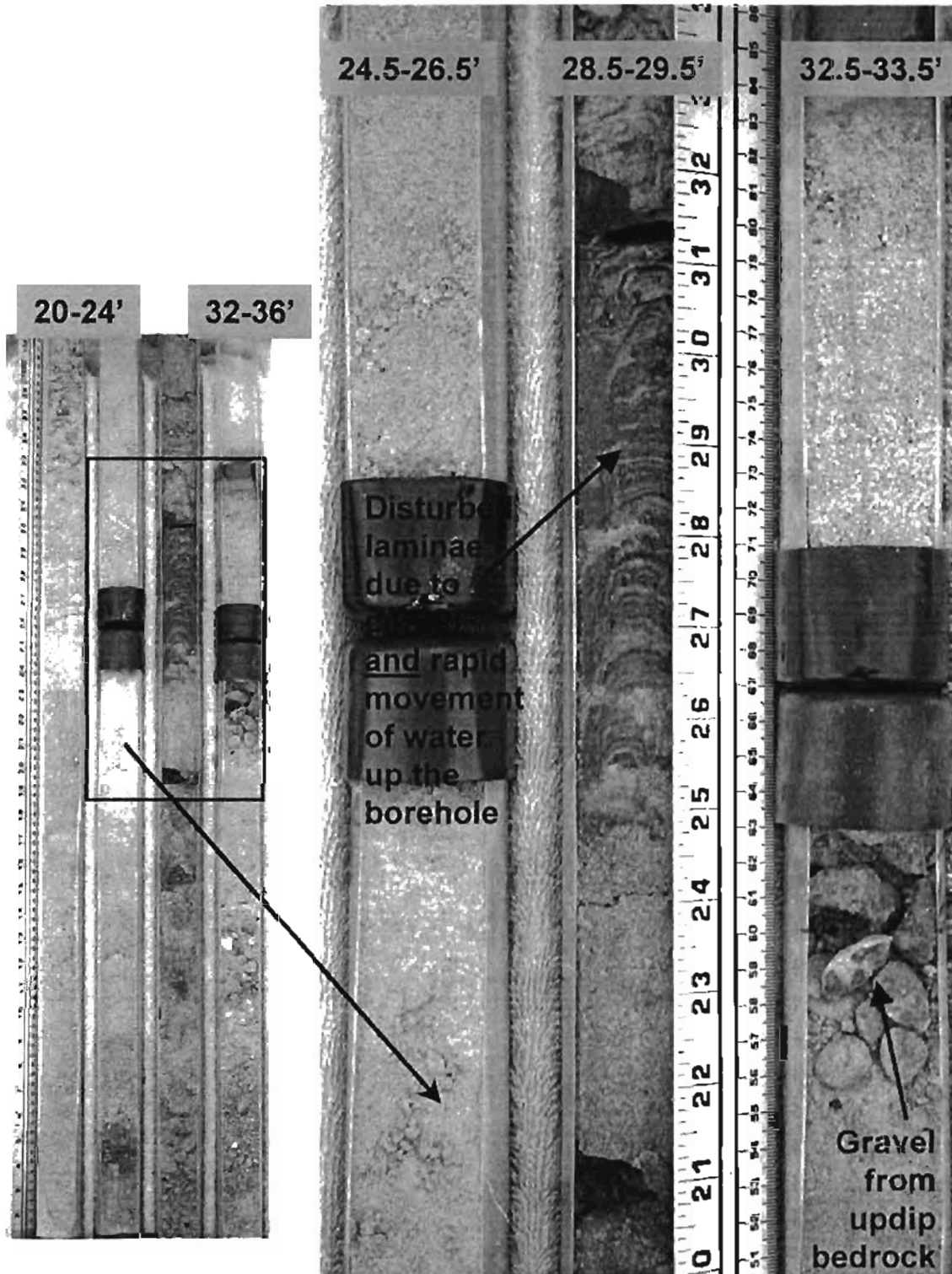
Well #46 Canadian River Floodplain



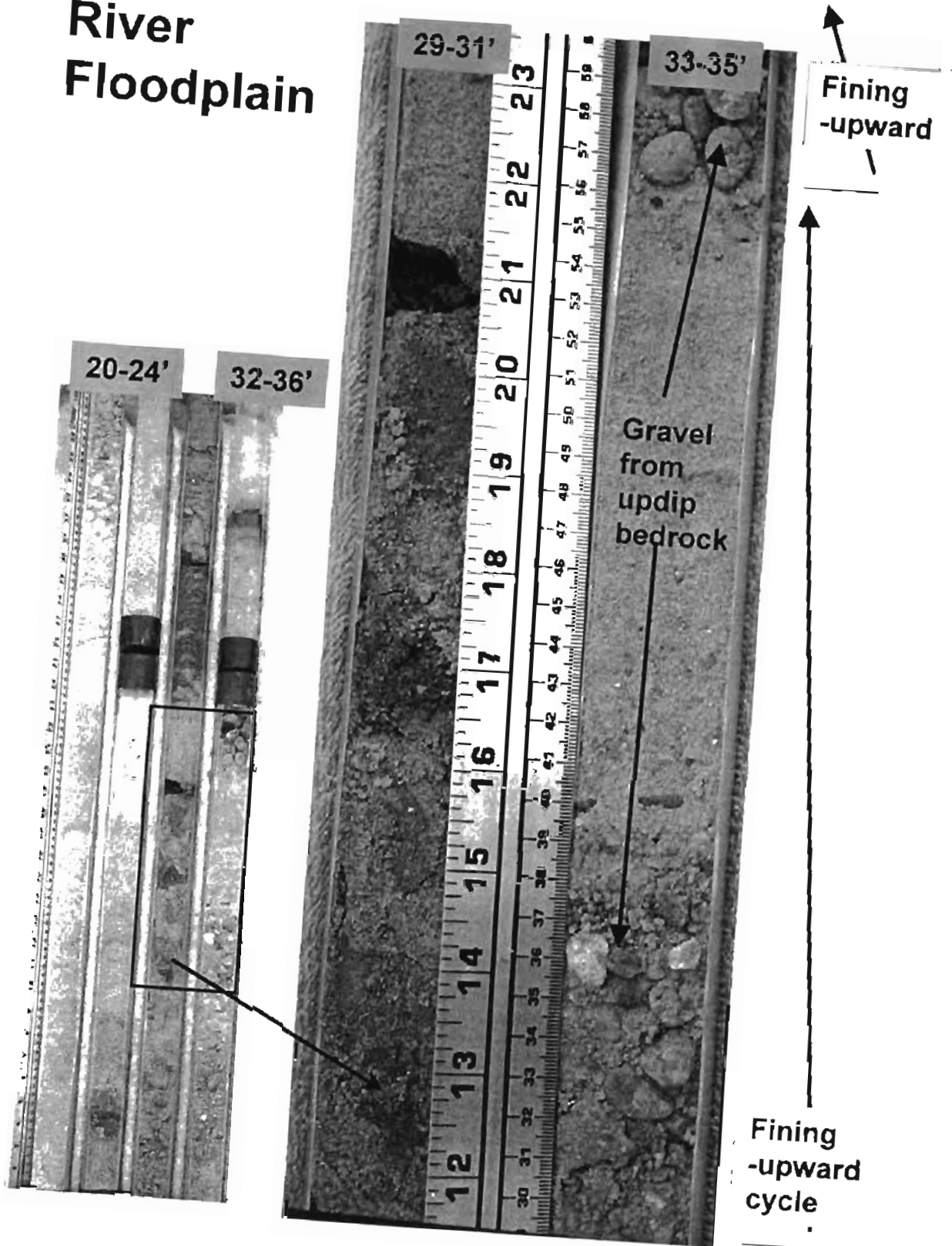
Well #46 Canadian River Floodplain



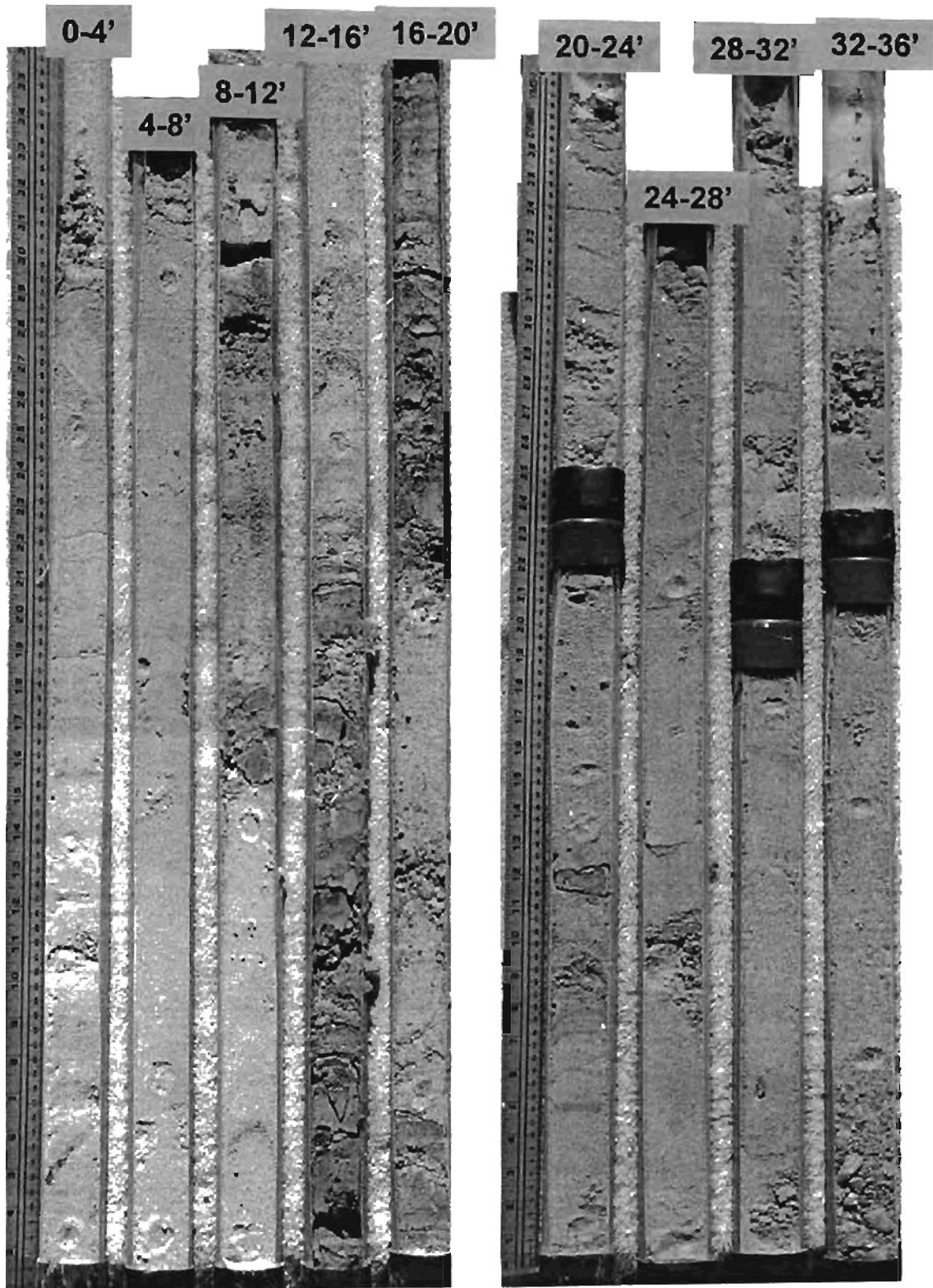
Well #46 Canadian River Floodplain



Well #46
Canadian
River
Floodplain



Well #56 – Canadian River Floodplain



Well #56 – Canadian River Floodplain

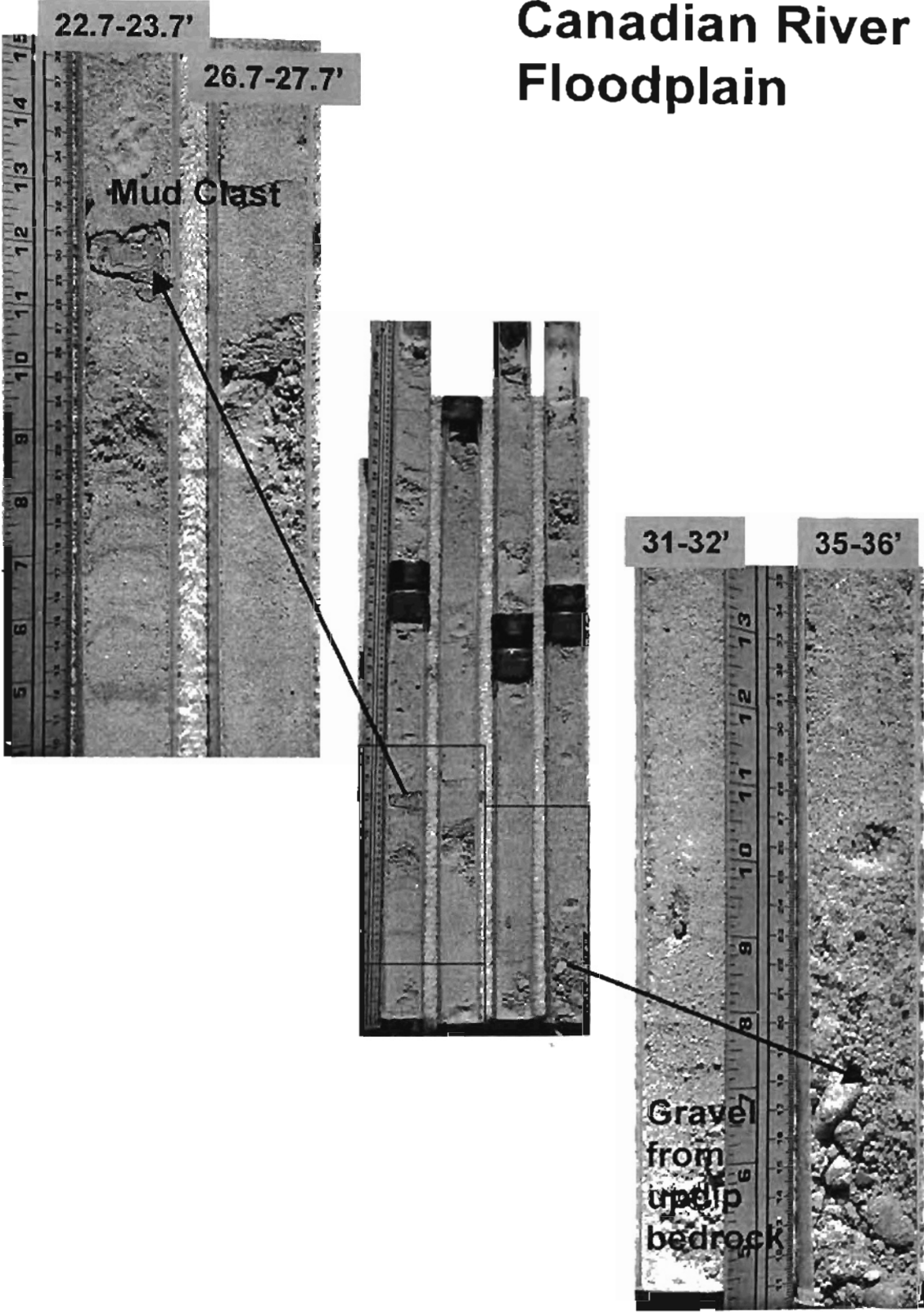


14.5-16'

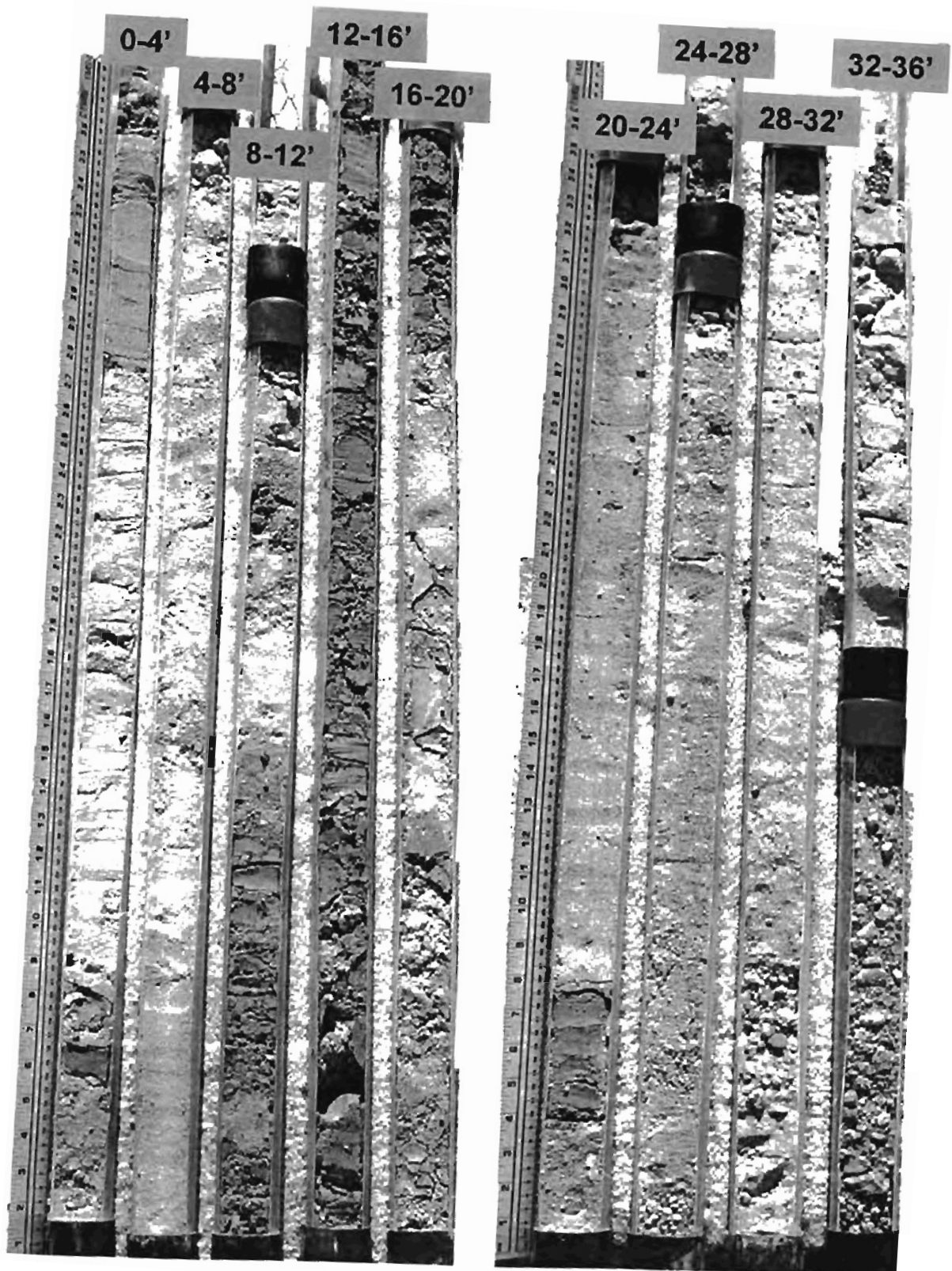
18.5-20'



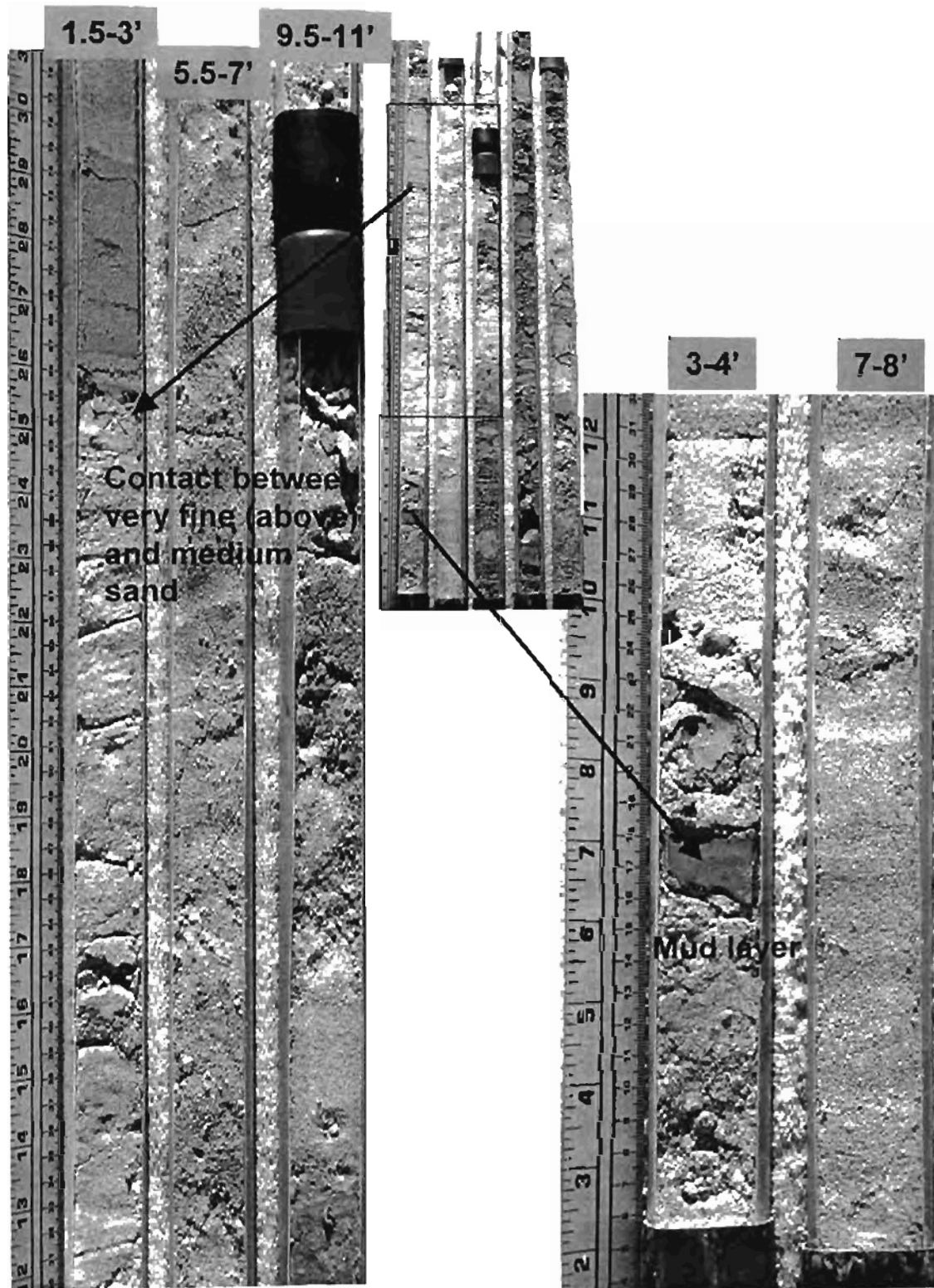
Well #56 – Canadian River Floodplain



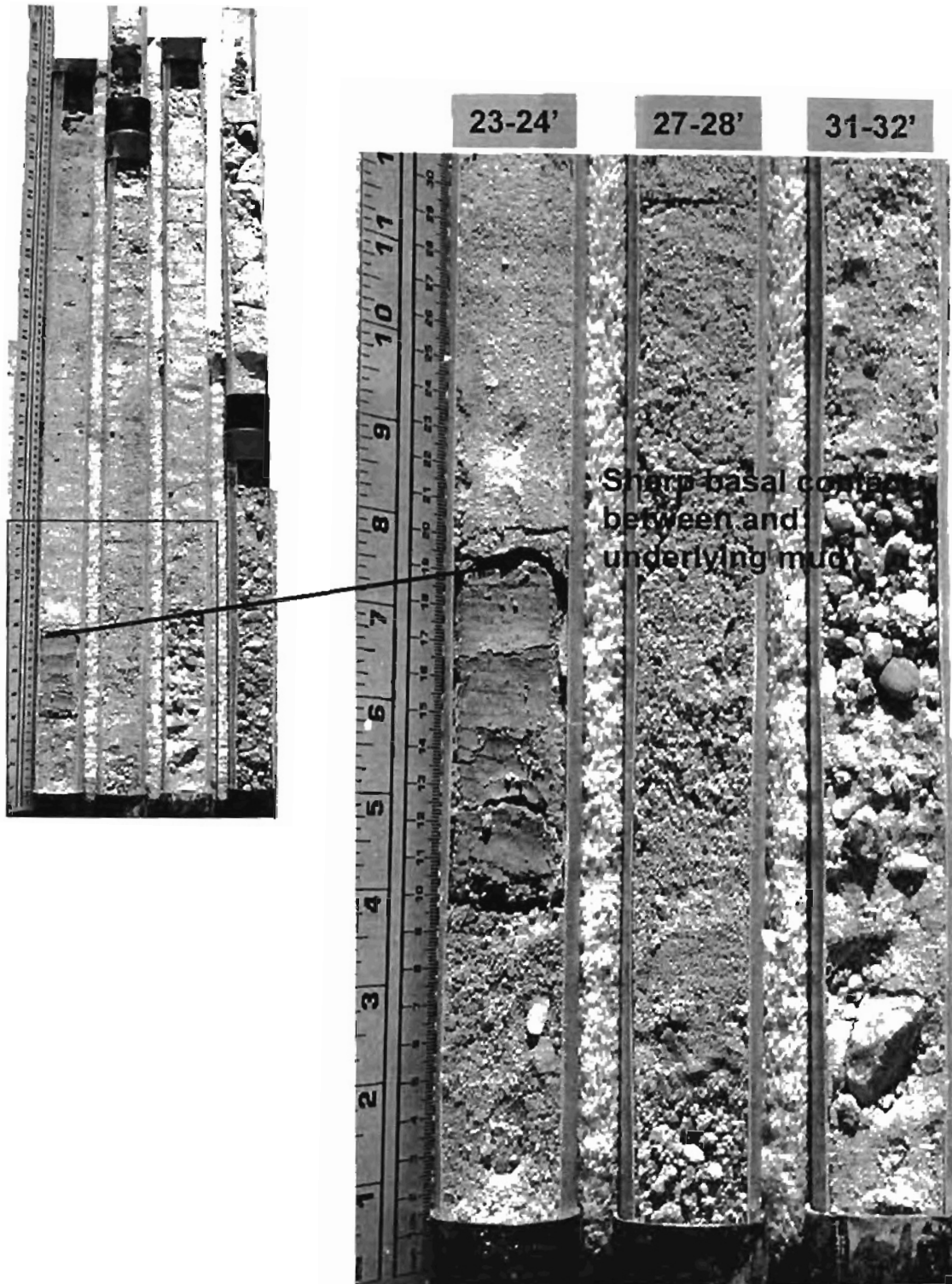
Well #57 – Canadian River Floodplain



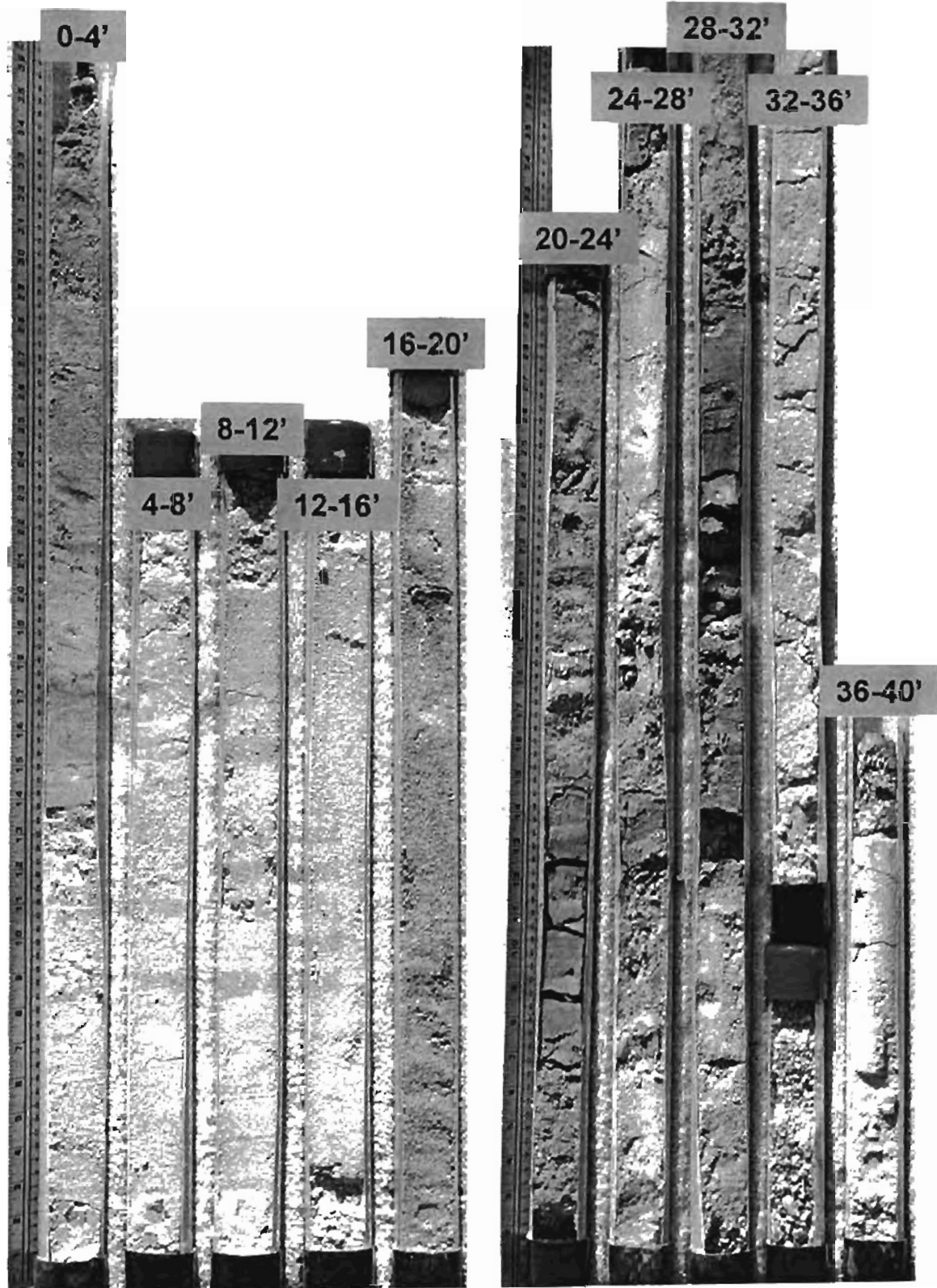
Well #57 – Canadian River Floodplain



Well #57 – Canadian River Floodplain



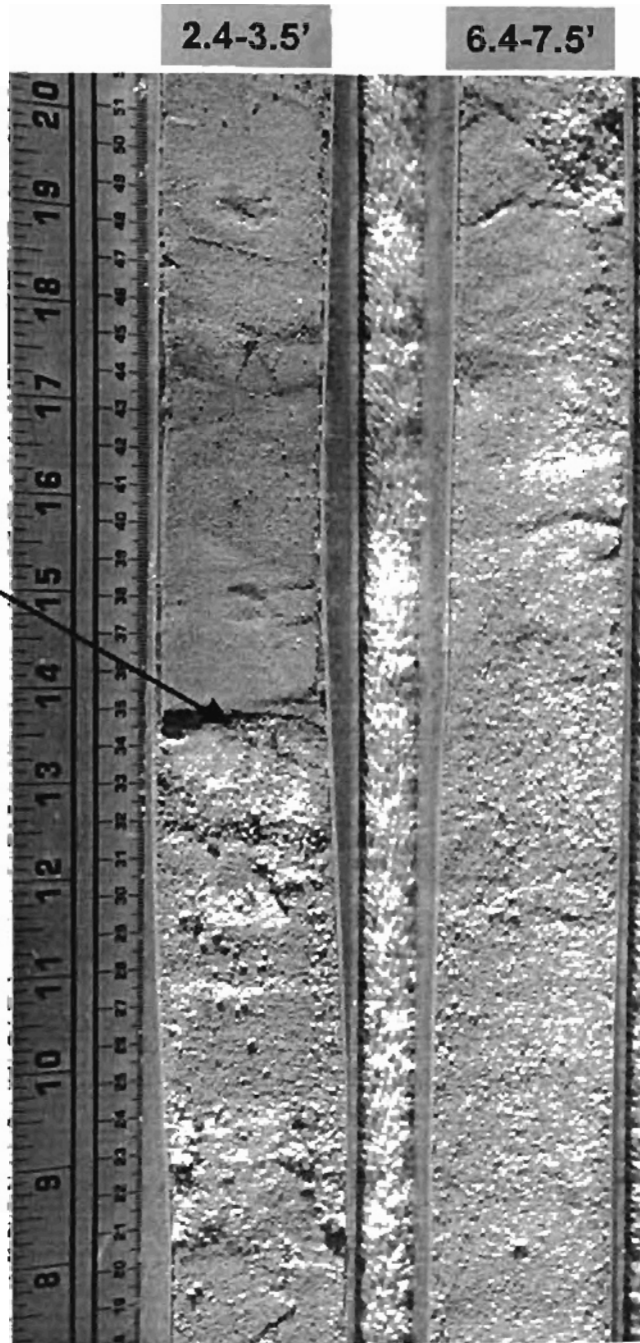
Well #62 – Canadian River Floodplain



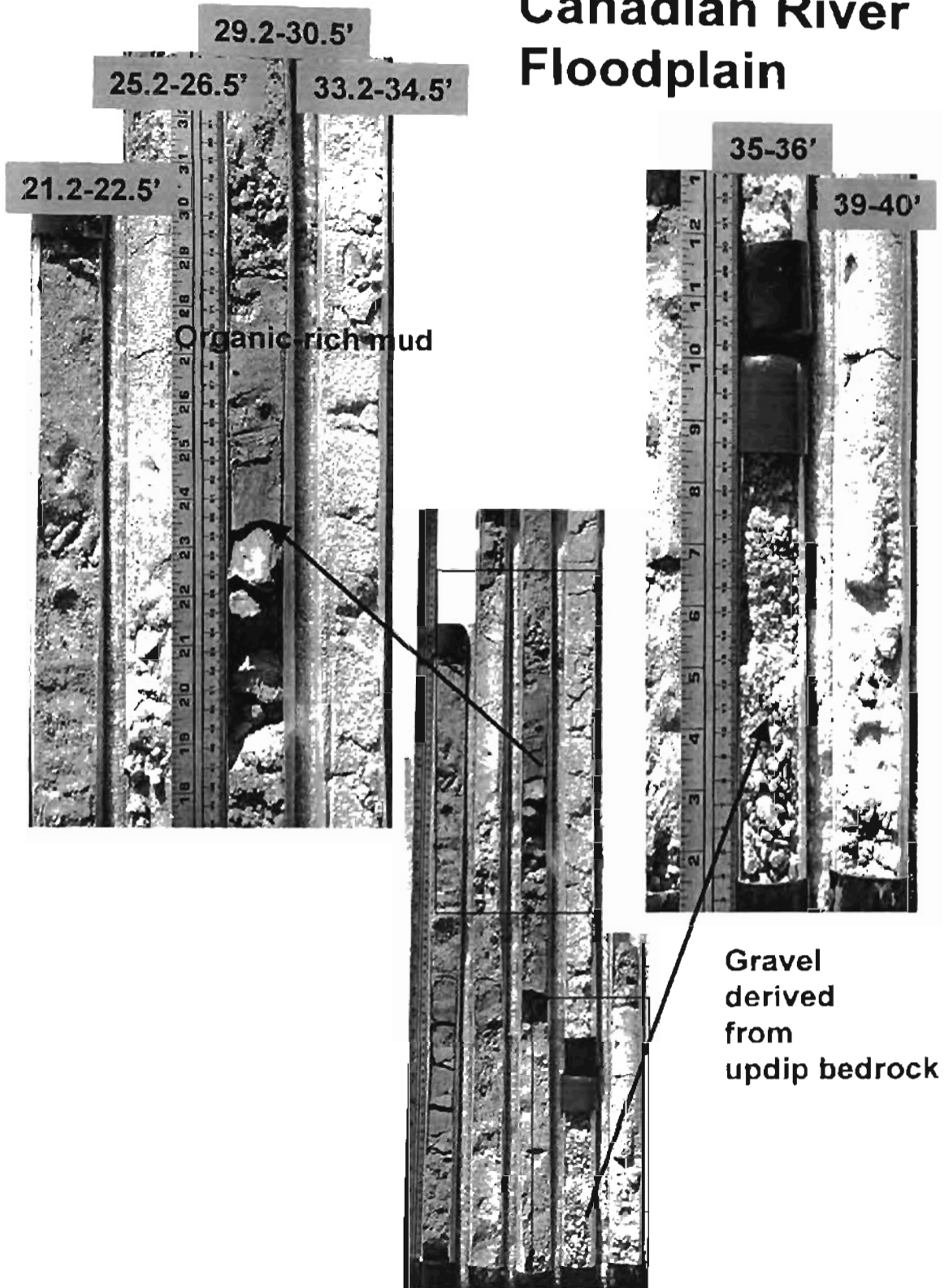
Well #62 – Canadian River Floodplain



Sharp contact
between
very-fine sand (above)
and
medium sand



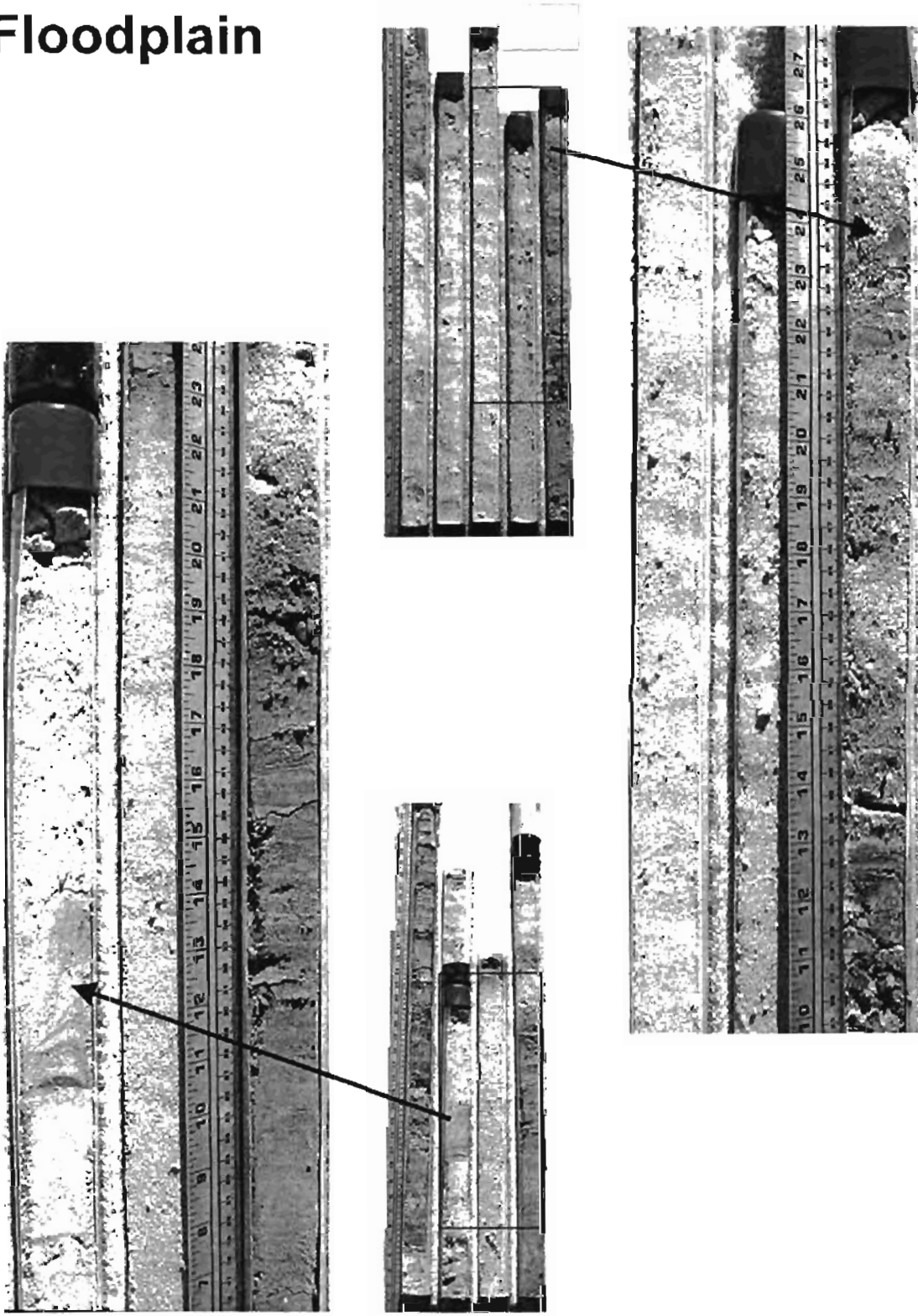
Well #62 – Canadian River Floodplain



Well #64 – Canadian River Floodplain



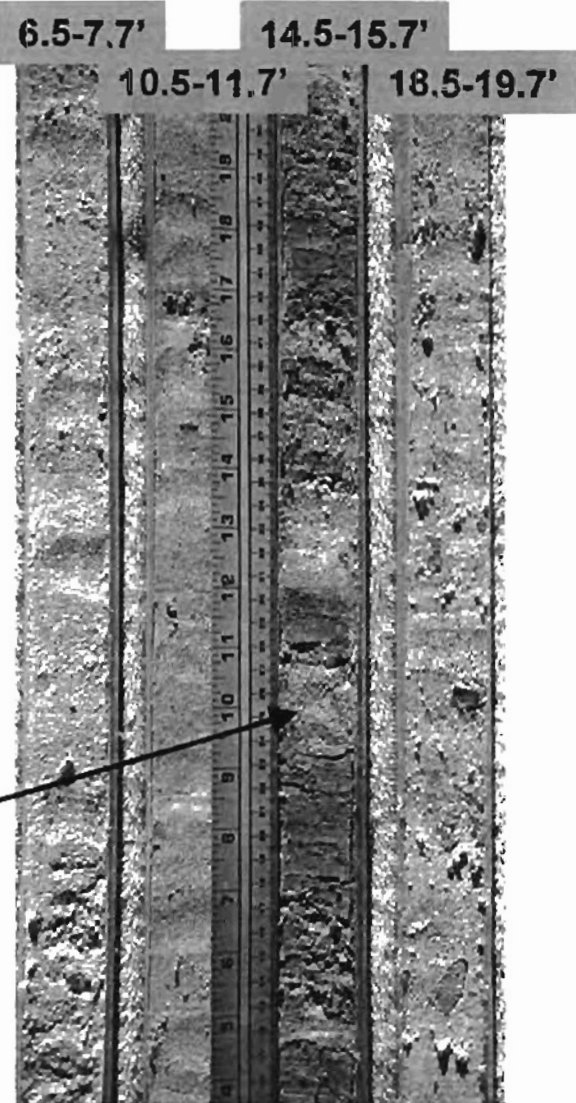
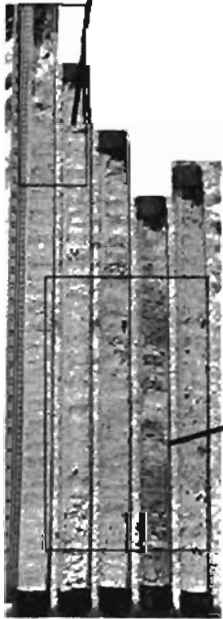
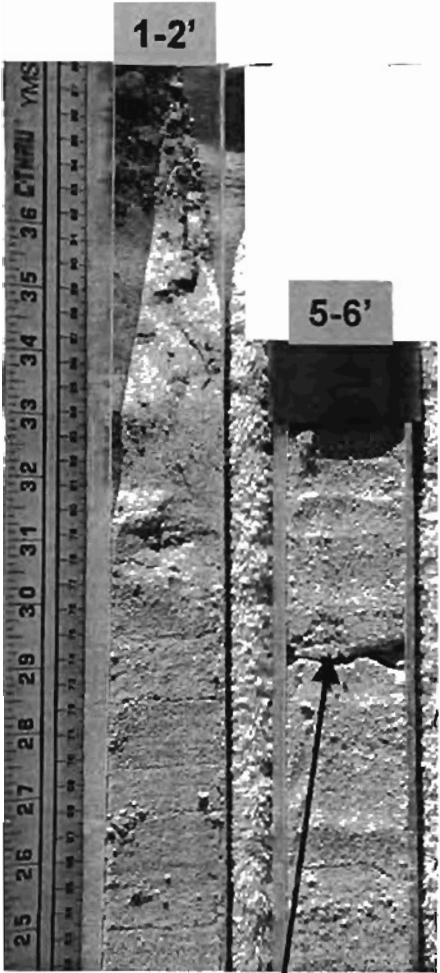
Well #64 –
Canadian River
Floodplain



Well #73 – Canadian River Floodplain

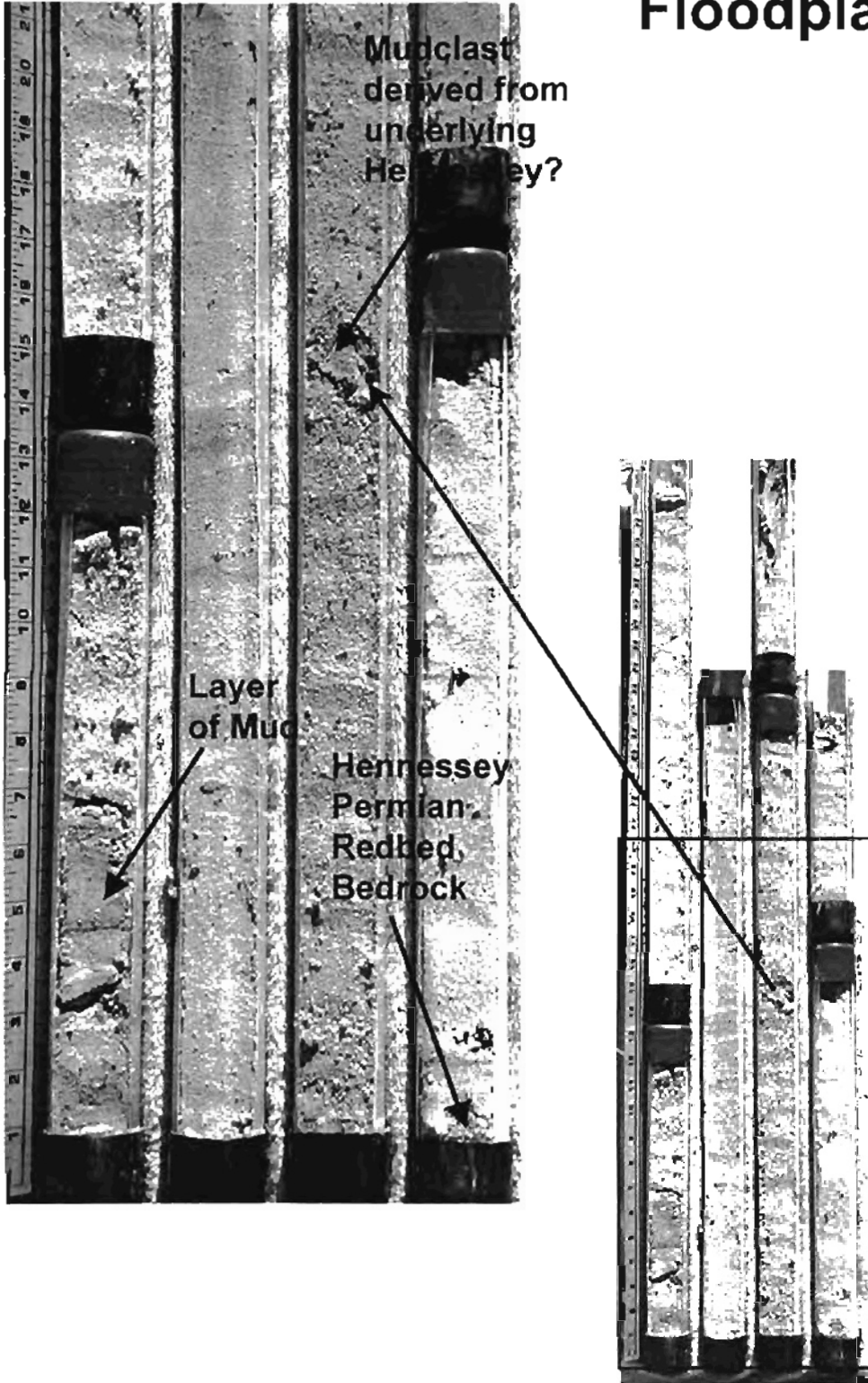


Well #73 Canadian River Floodplain

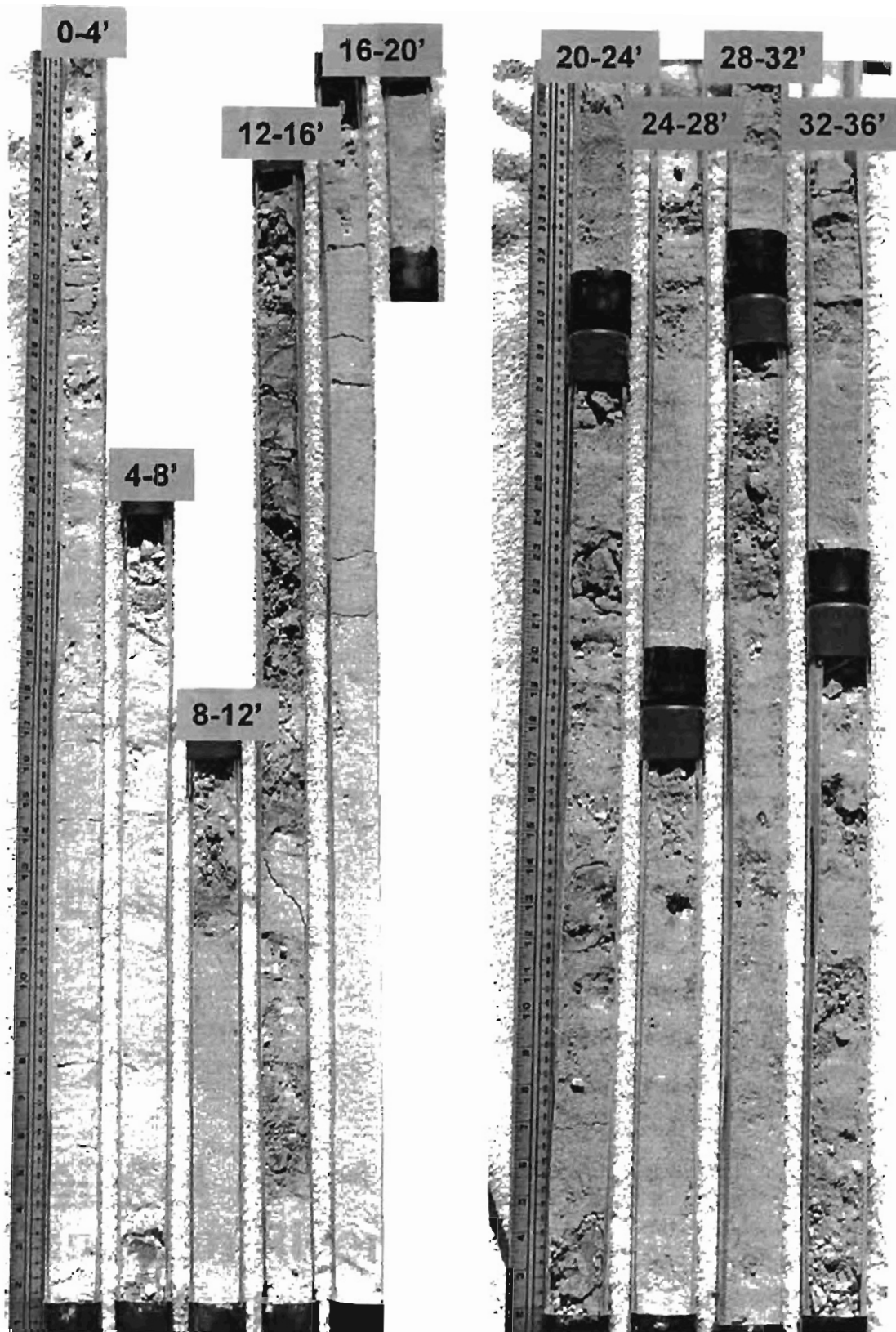


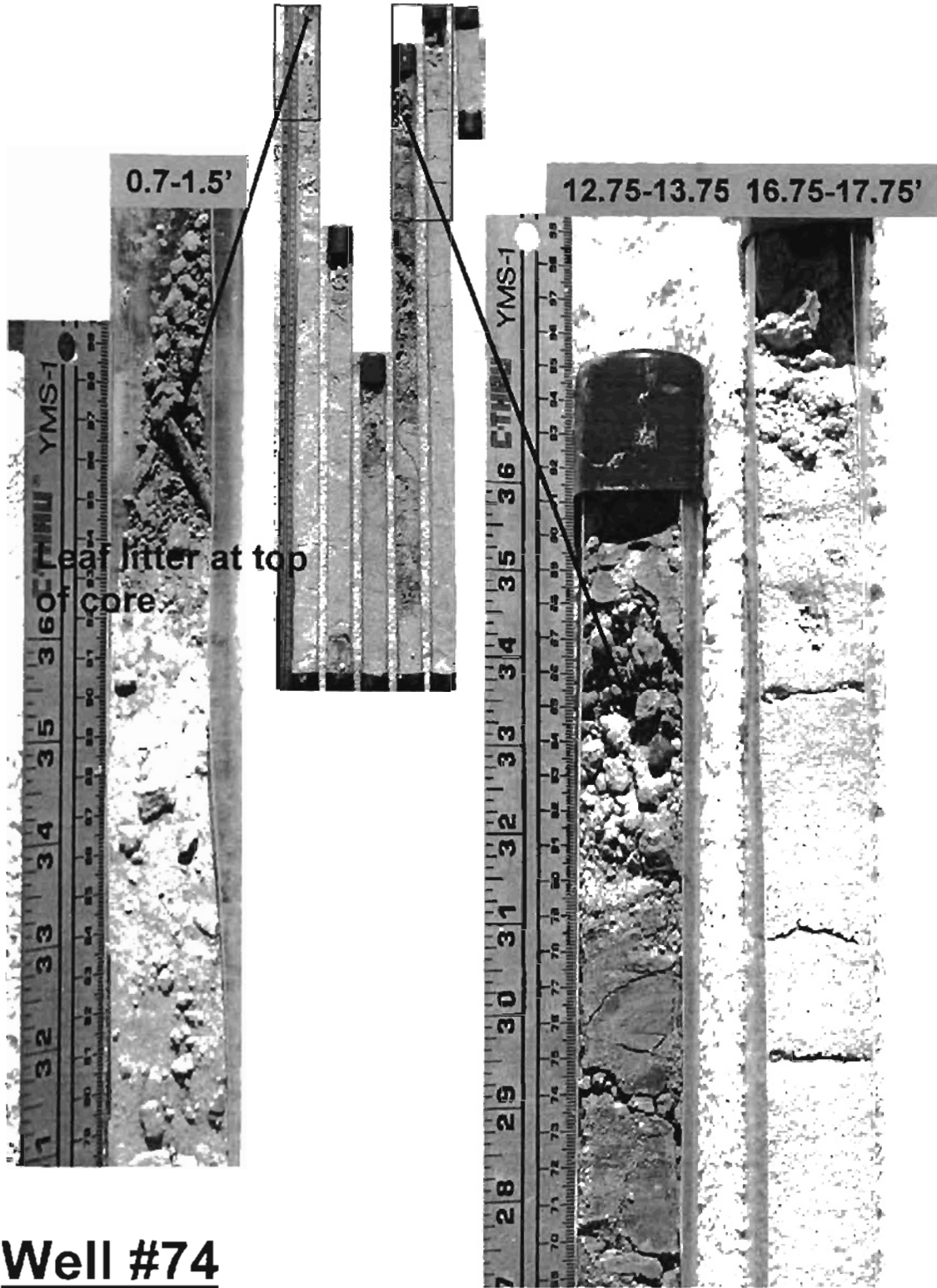
Well #73 Canadian River Floodplain

22-24' 26-28' 30-32' 34-36'



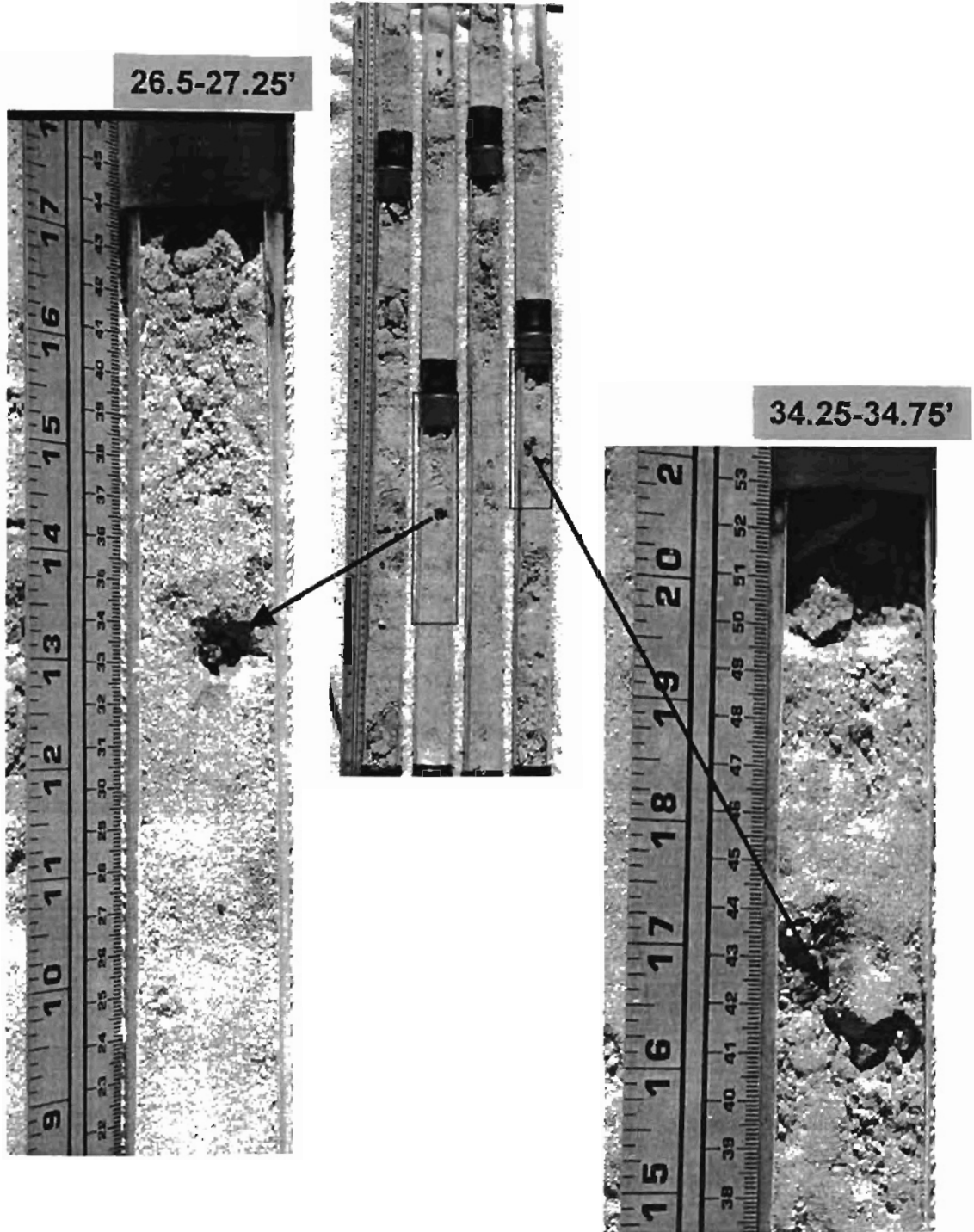
Well #74 – Canadian River Floodplain



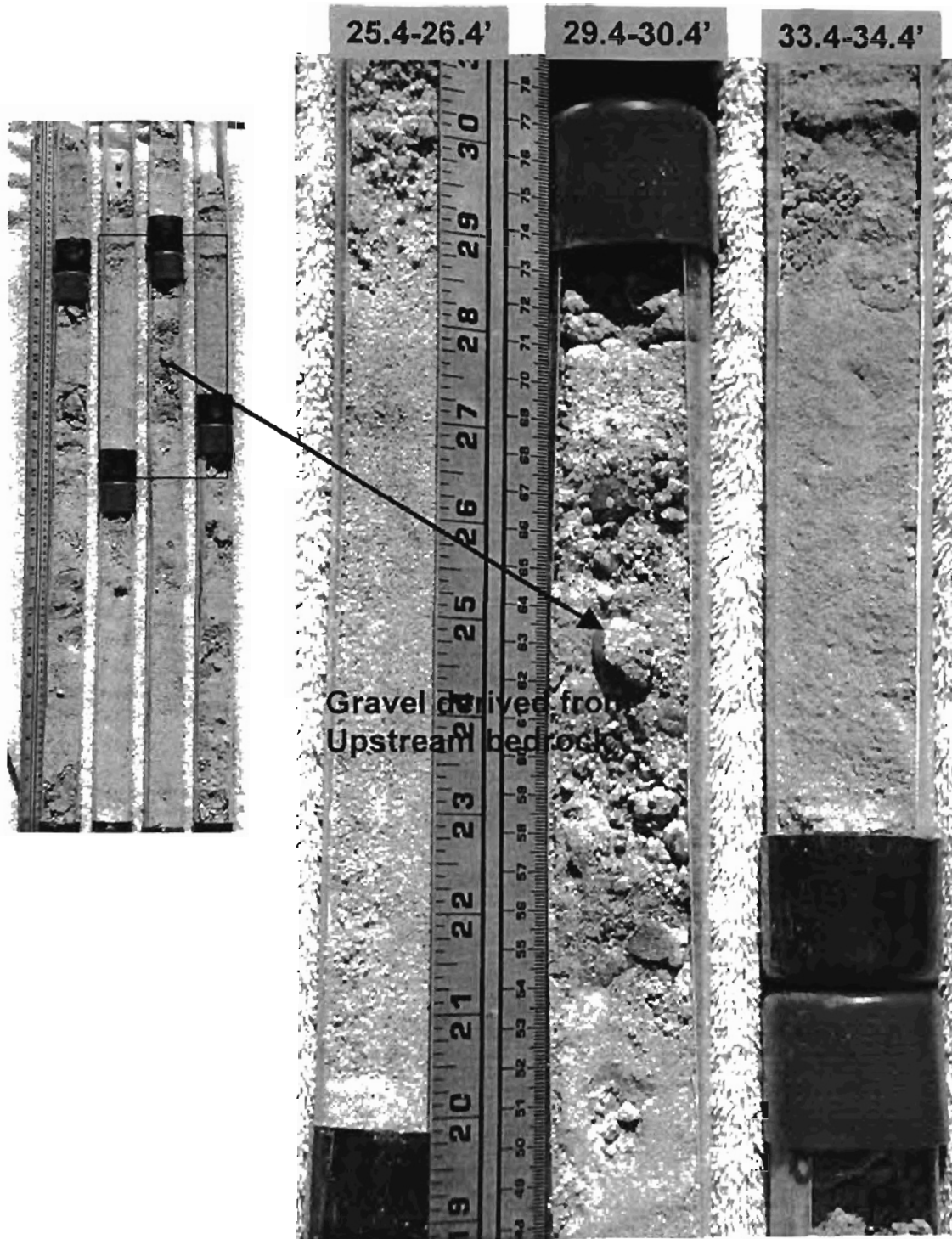


Well #74
**Canadian River
Floodplain**

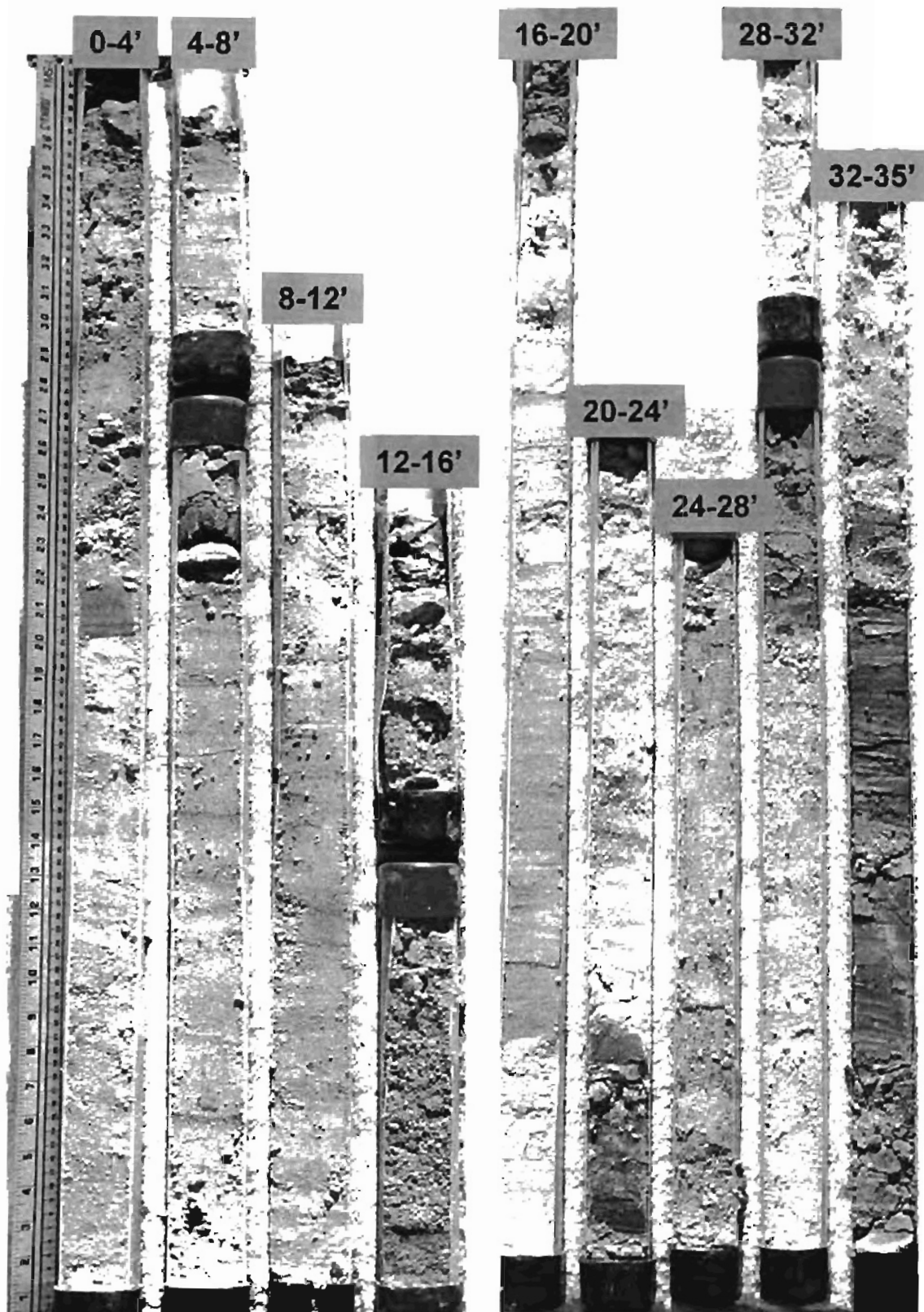
Well #74 Canadian River Floodplain



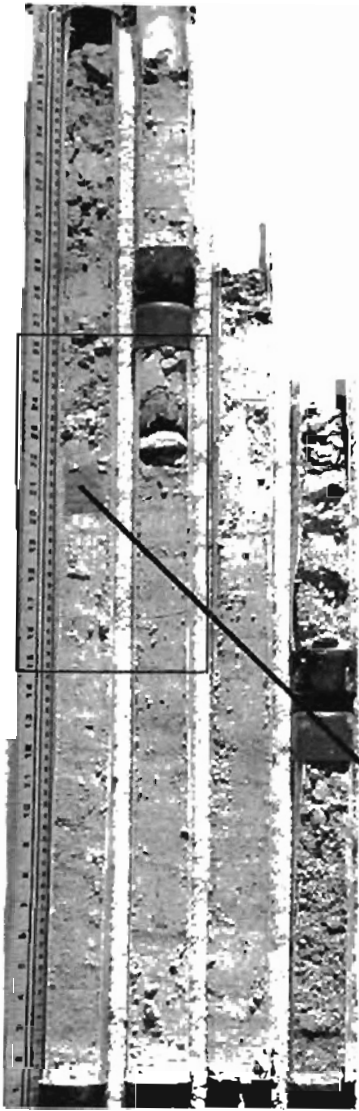
Well #74 Canadian River Floodplain



Well #78 – Canadian River Floodplain

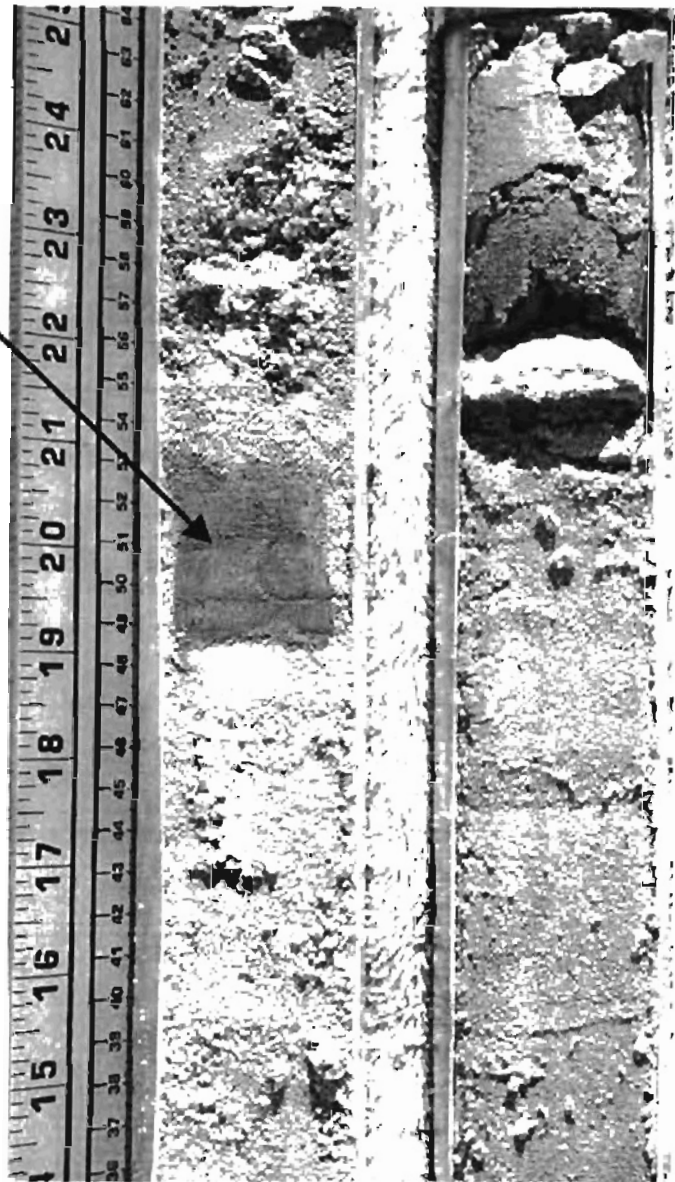


Well #78 Canadian River Floodplain

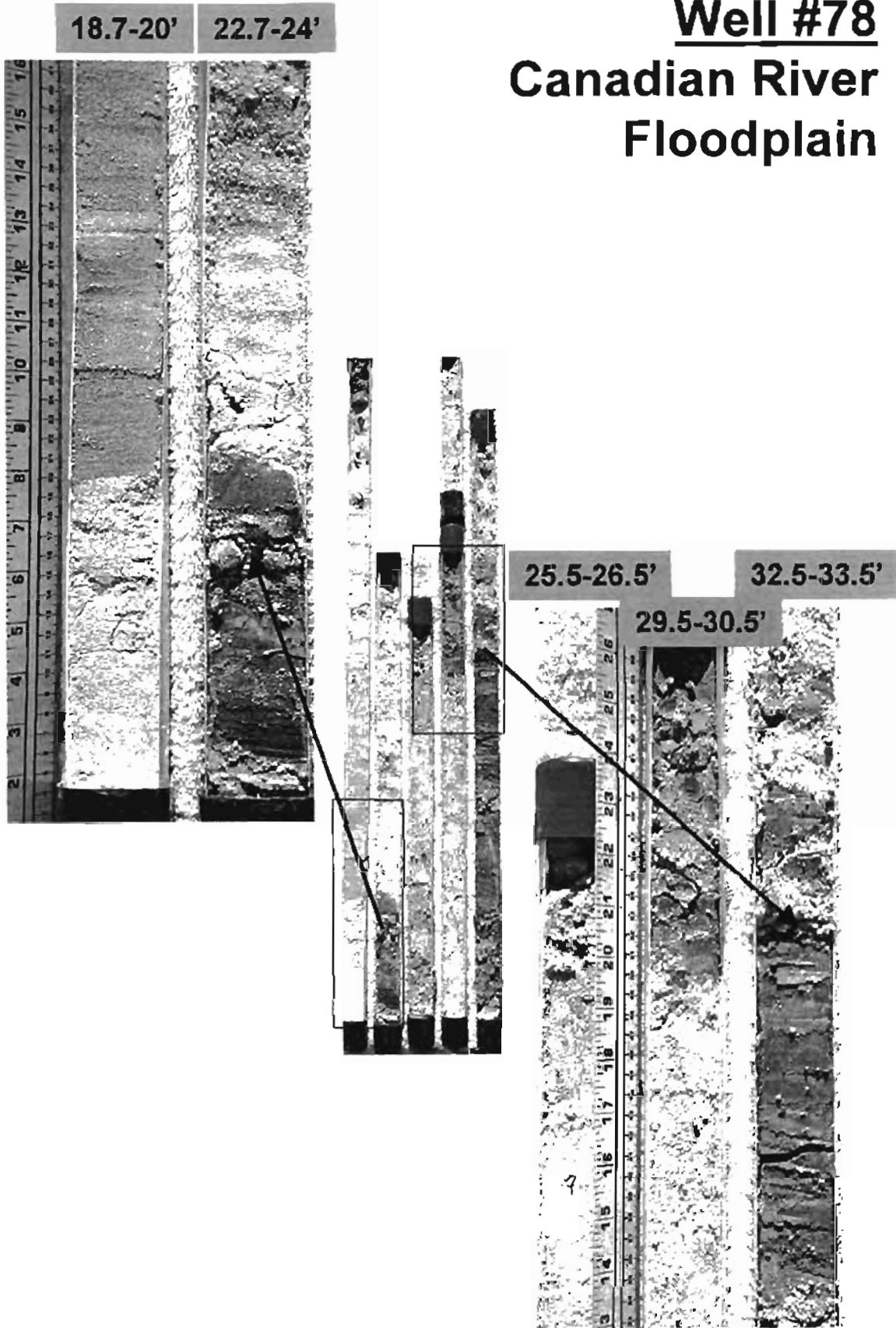


2-3'

6-7'

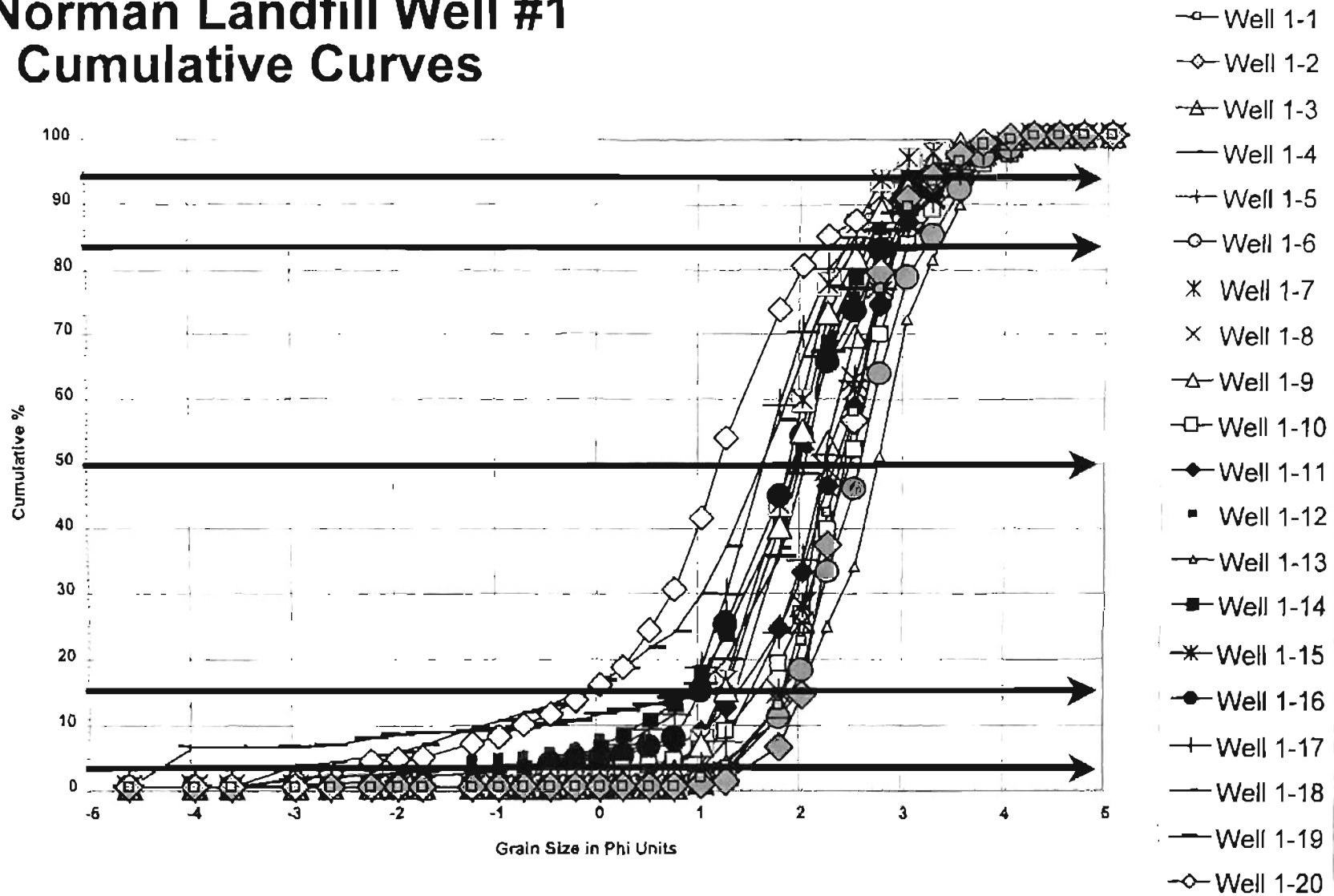


Well #78 Canadian River Floodplain



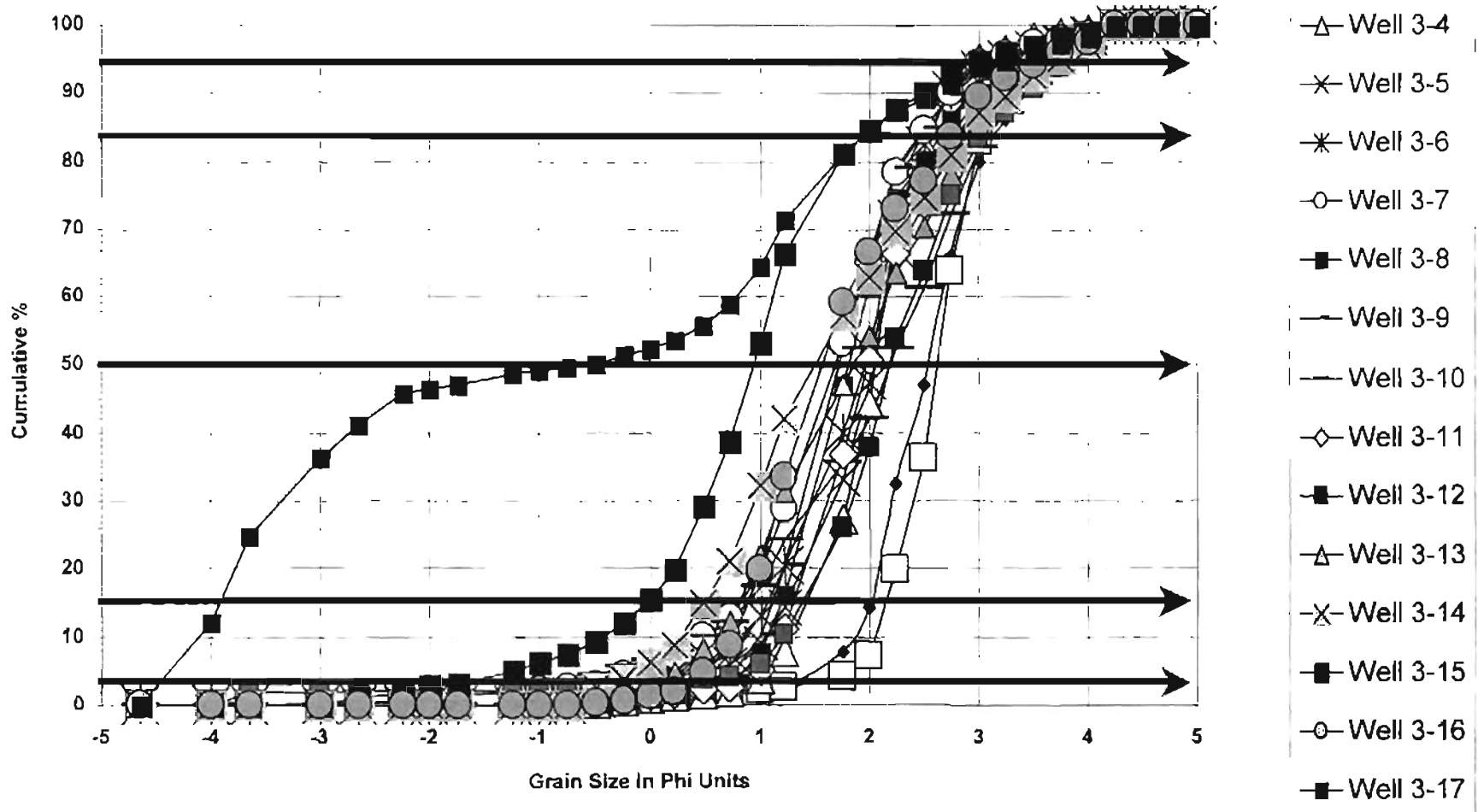
APPENDIX C
CUMULATIVE GRAIN SIZE CURVES

Norman Landfill Well #1 Cumulative Curves

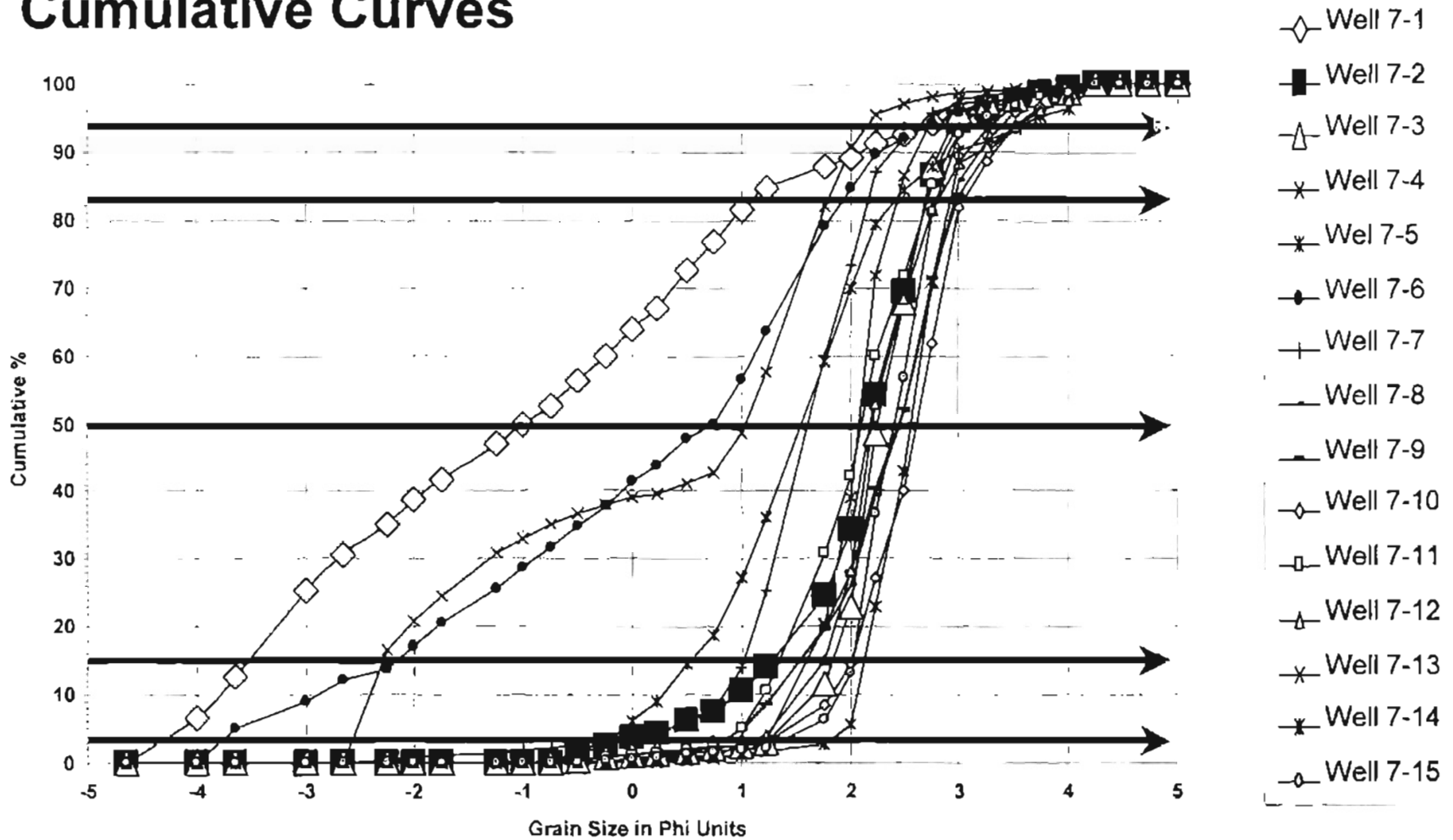


Norman Landfill Well #3 Cumulative Curves

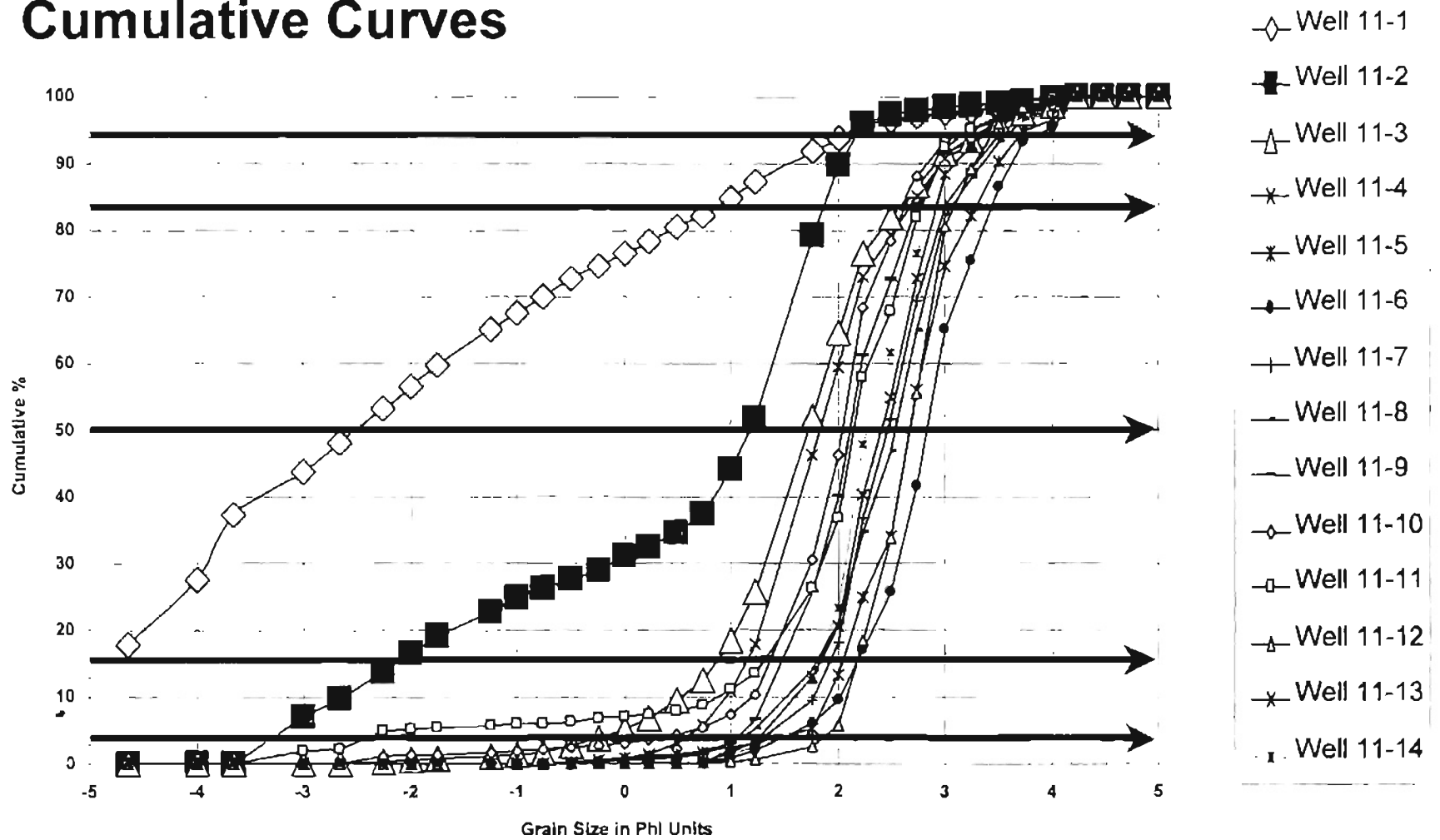
1991



Norman Landfill Well #7 Cumulative Curves

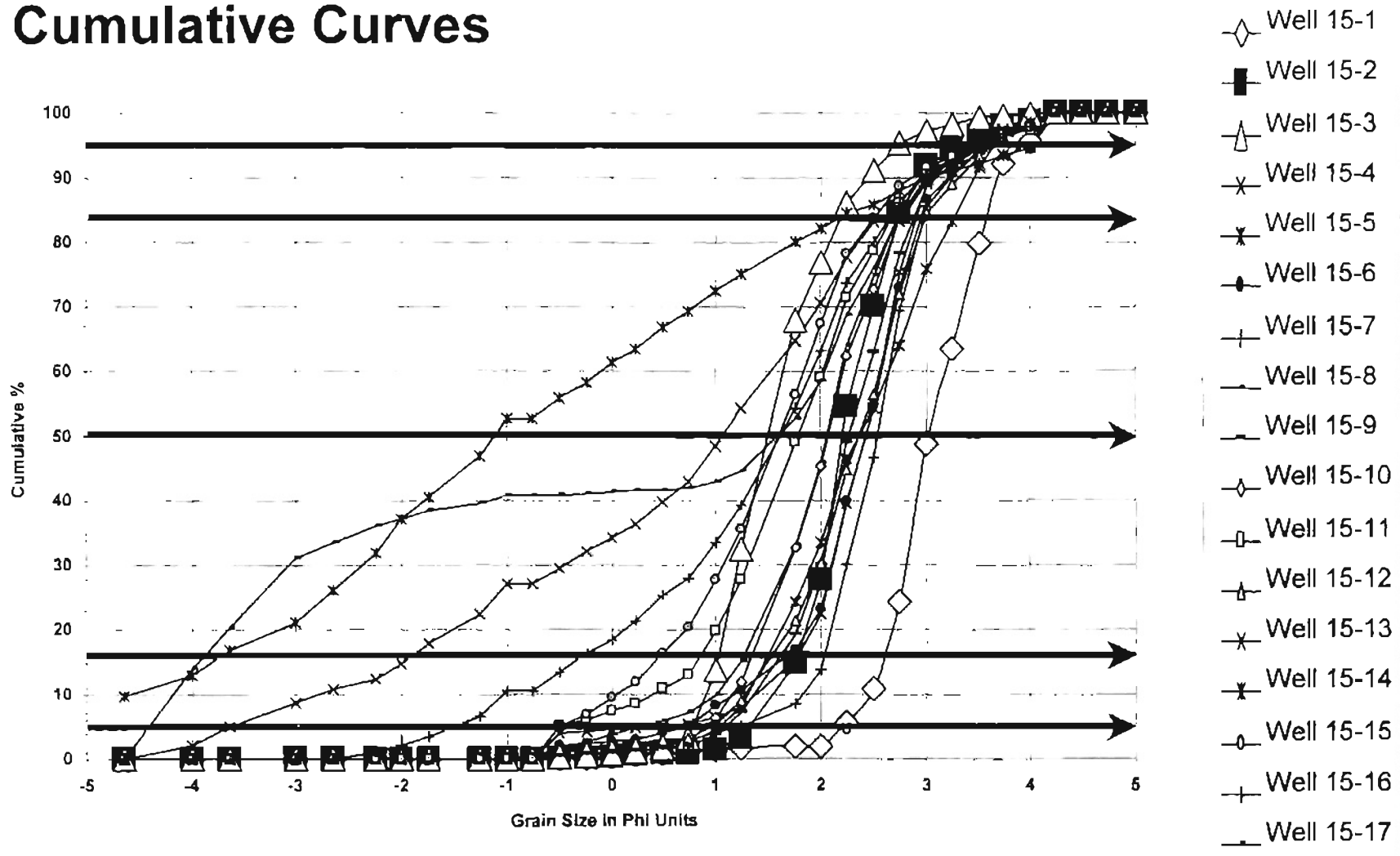


Norman Landfill Well #11 Cumulative Curves

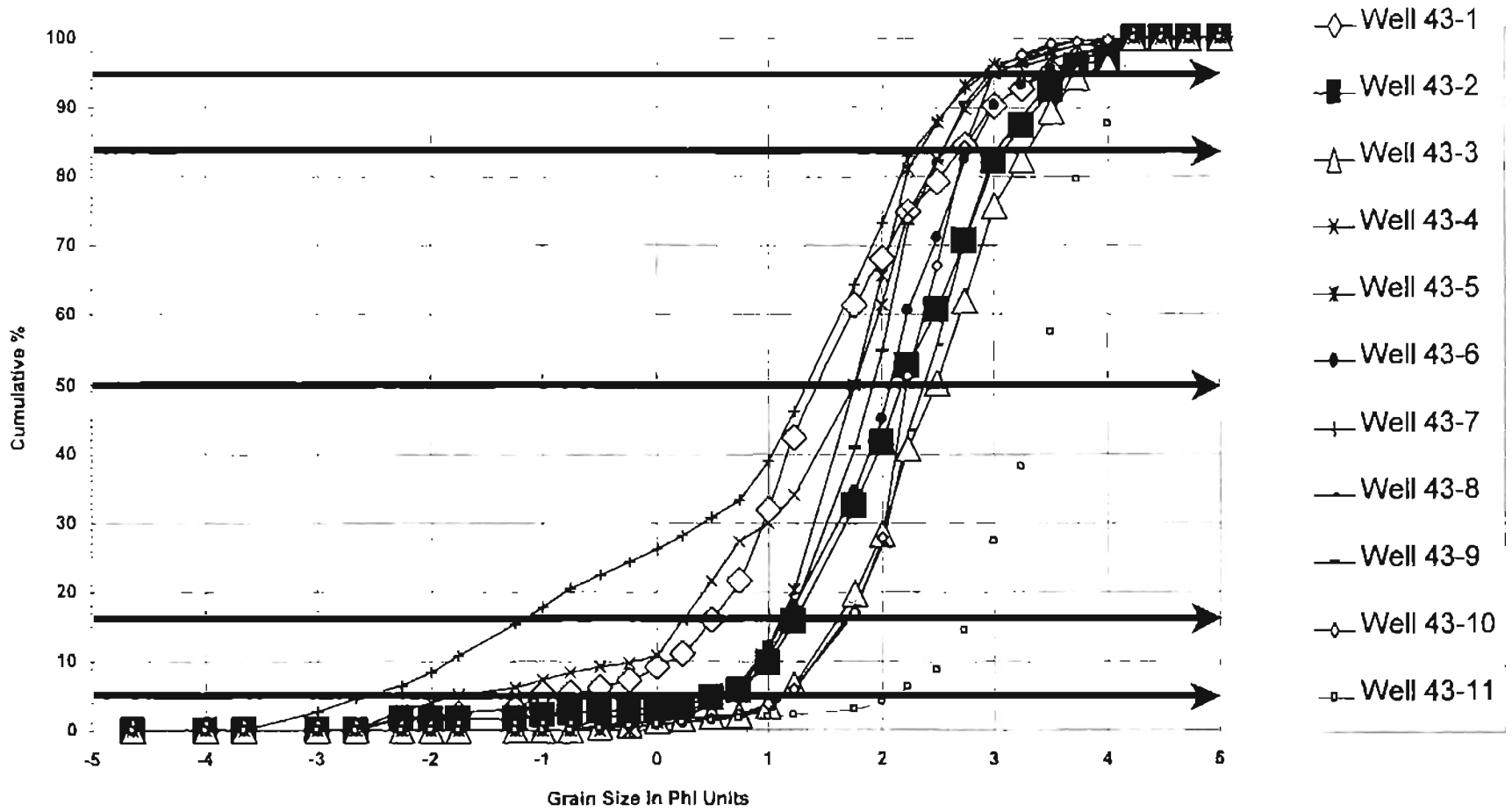


Norman Landfill Well #15 Cumulative Curves

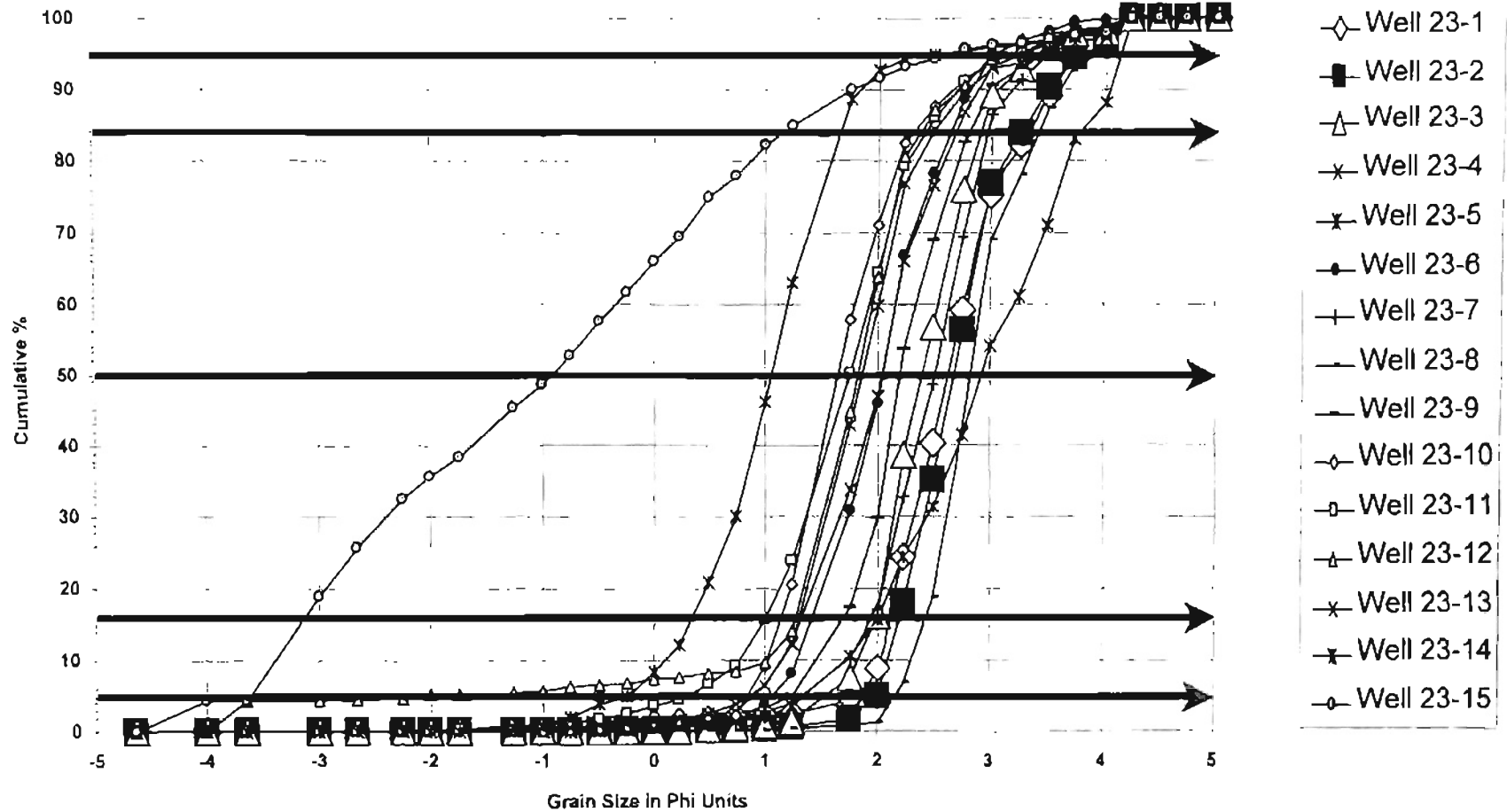
169



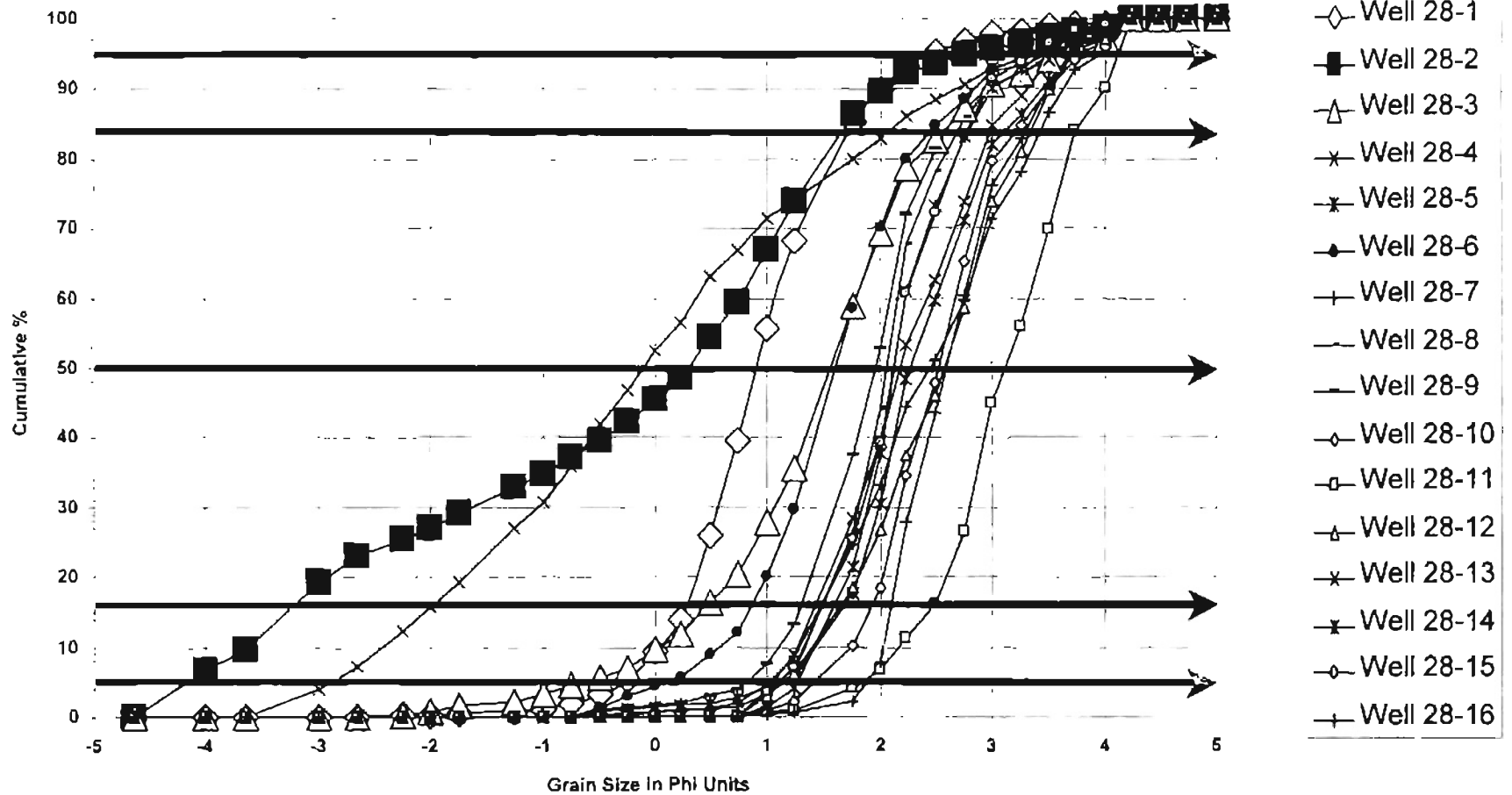
Norman Landfill Well #21 Cumulative Curves



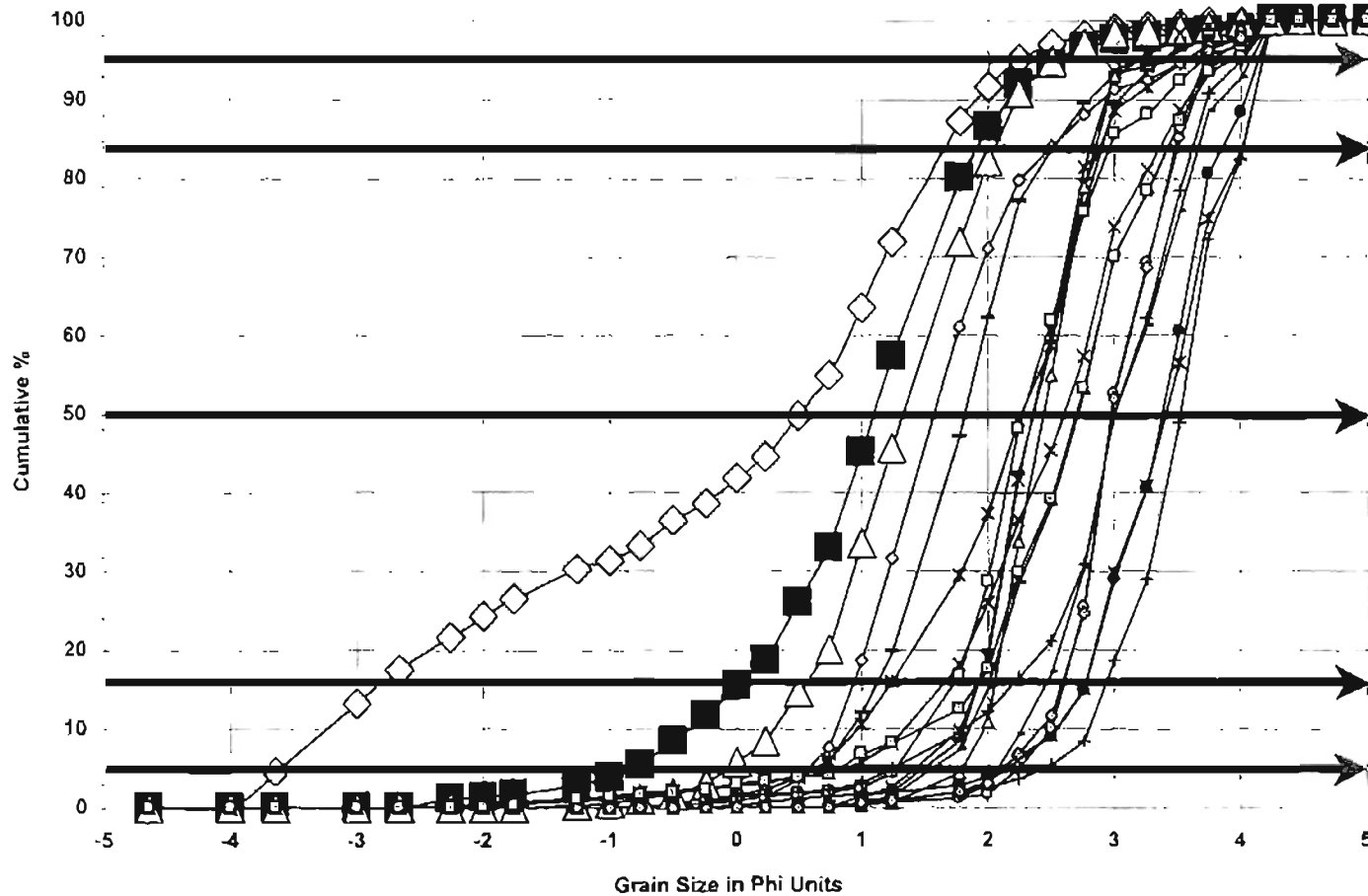
Norman Landfill Well #23 Cumulative Curves



Norman Landfill Well #28 Cumulative Curves

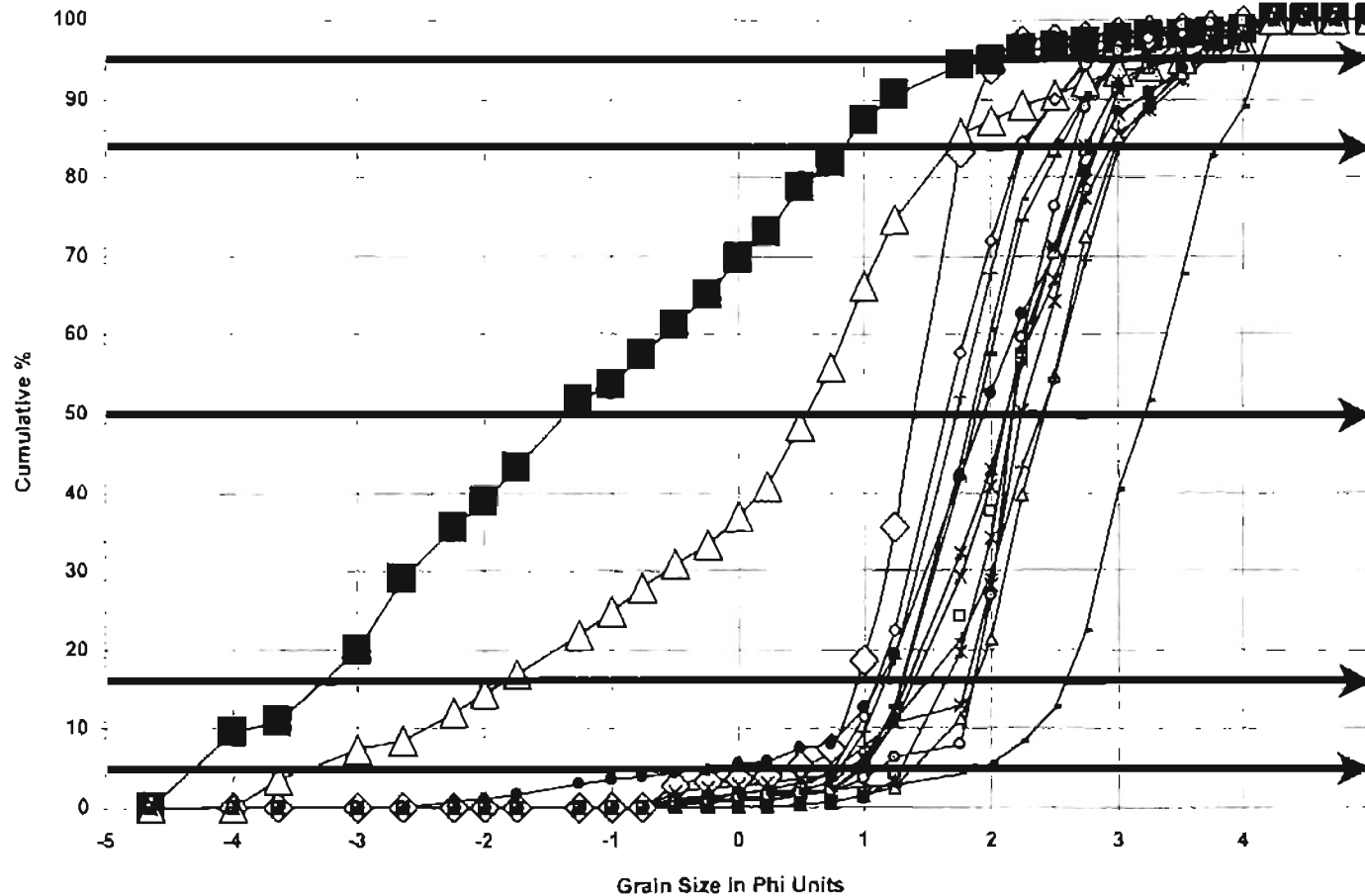


Norman Landfill Well #31 Cumulative Curves



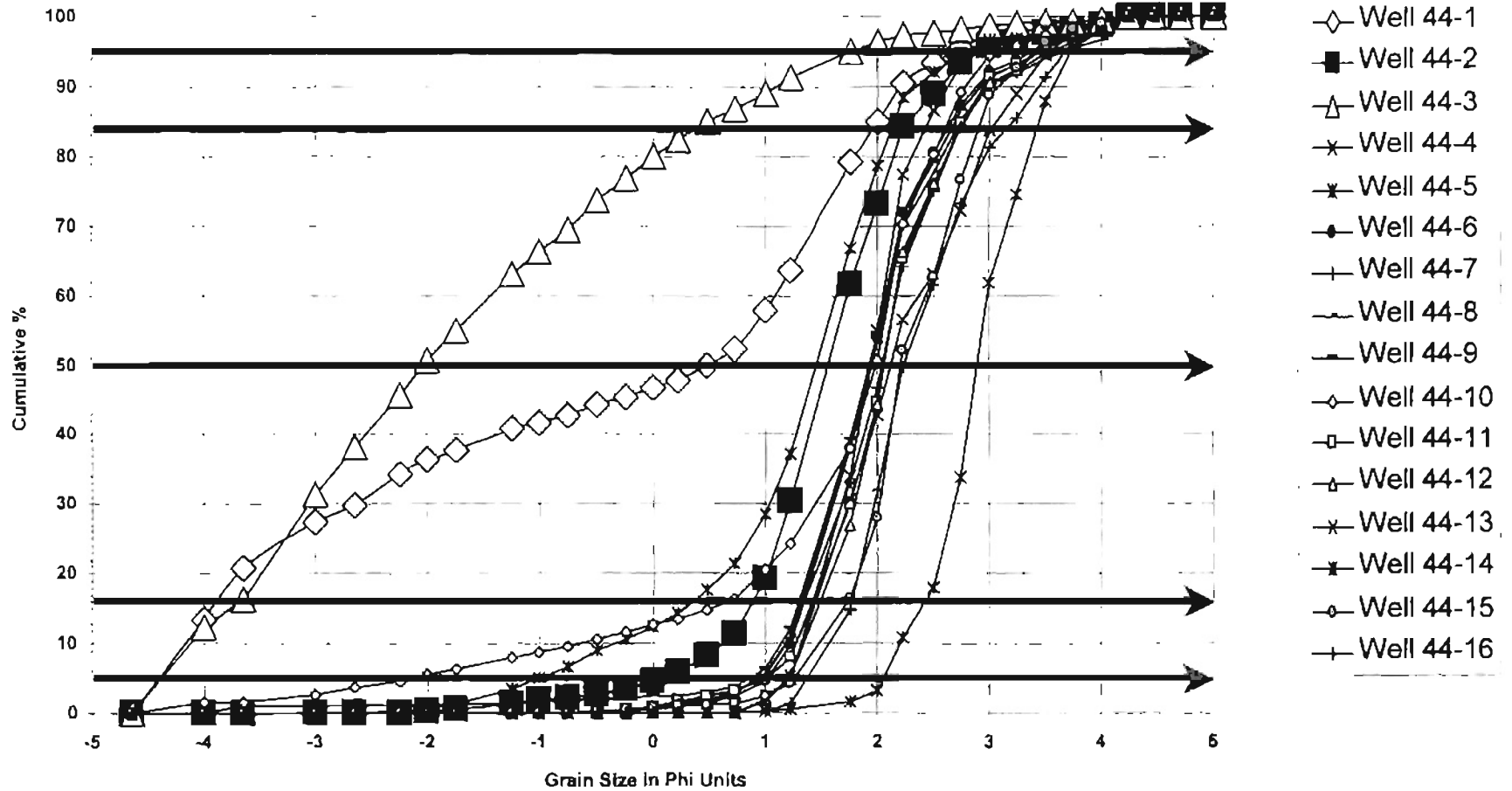
- ◇ Well 31-1
- Well 31-2
- △ Well 31-3
- × Well 31-4
- ✕ Well 31-5
- Well 31-6
- + Well 31-7
- Well 31-8
- Well 31-9
- ◇ Well 31-10
- Well 31-11
- △ Well 31-12
- × Well 31-13
- ✕ Well 31-14
- ◇ Well 31-15
- + Well 31-16
- Well 31-17
- Well 31-18
- ◇ Well 31-19
- Well 31-20

Norman Landfill Well #42 Cumulative Curves

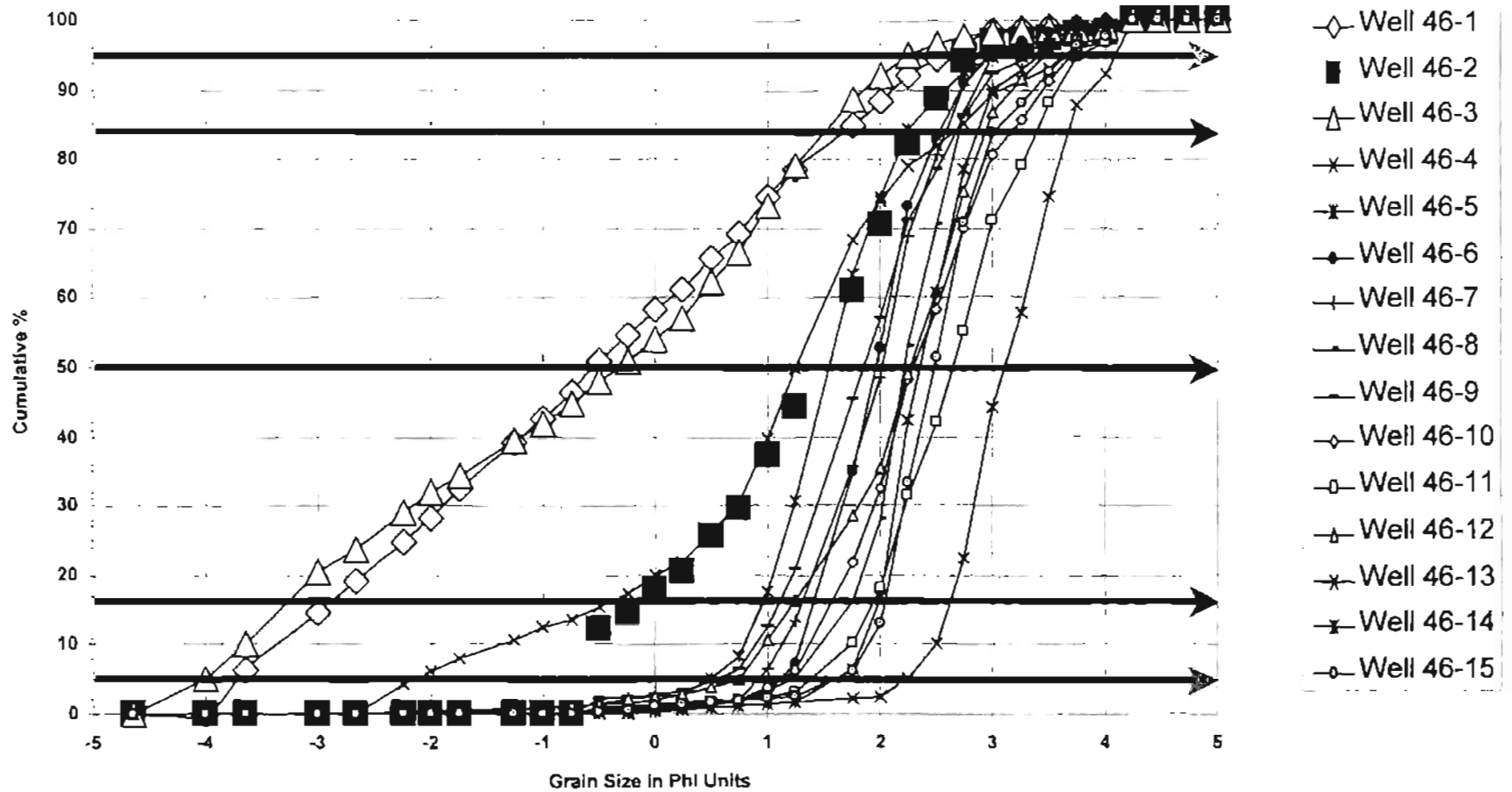


- ◇ Well 42-1
- Well 42-2
- △ Well 42-3
- × Well 42-4
- ✱ Well 42-5
- Well 42-6
- + Well 42-7"
- Well 42-8
- Well 42-9
- ◇ Well 42-10
- Well 42-11
- △ Well 42-12
- × Well 42-13
- ✱ Well 42-14
- Well 42-15
- + Well 42-16
- Well 42-17

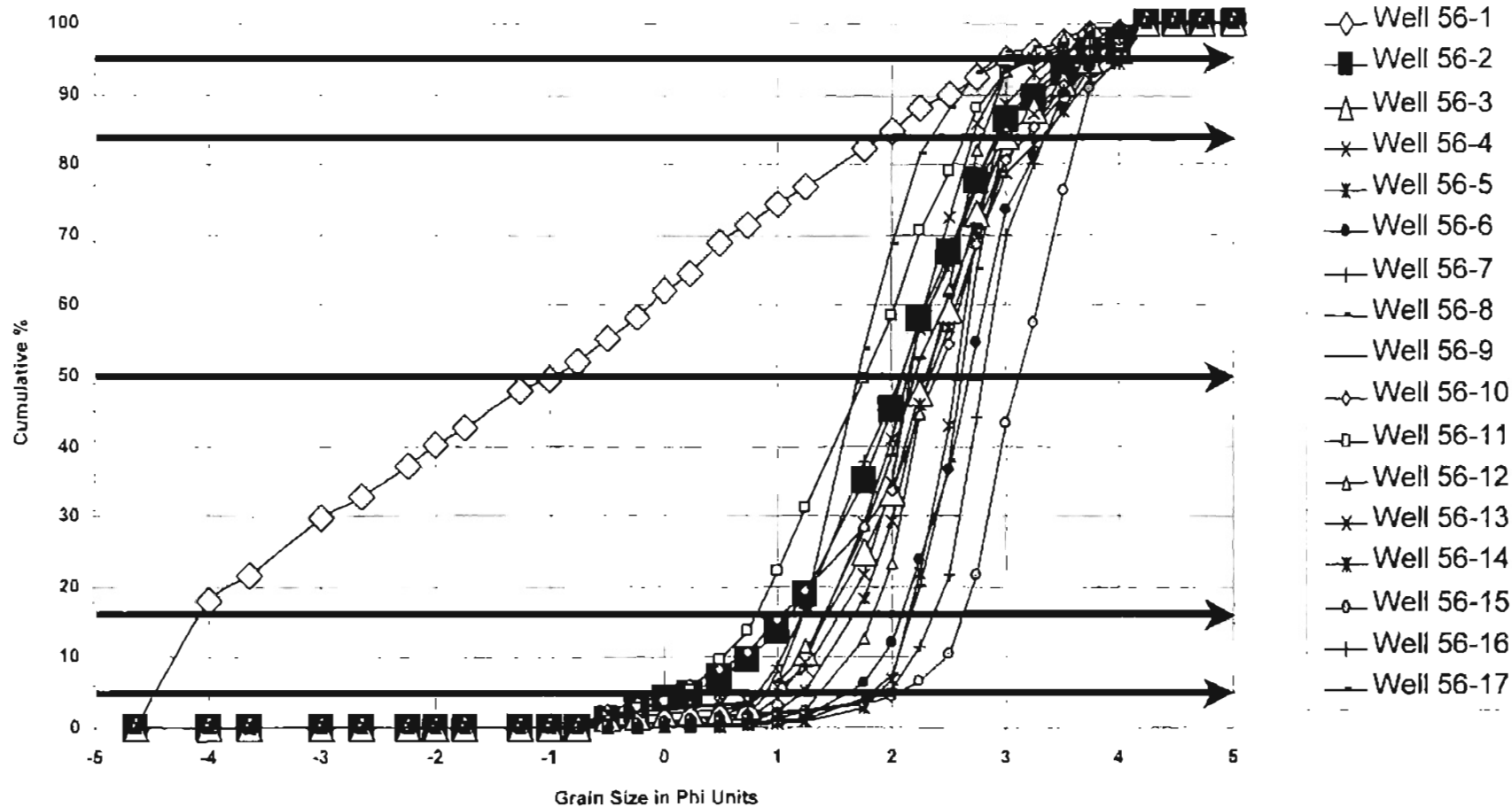
Norman Landfill Well #44 Cumulative Curves



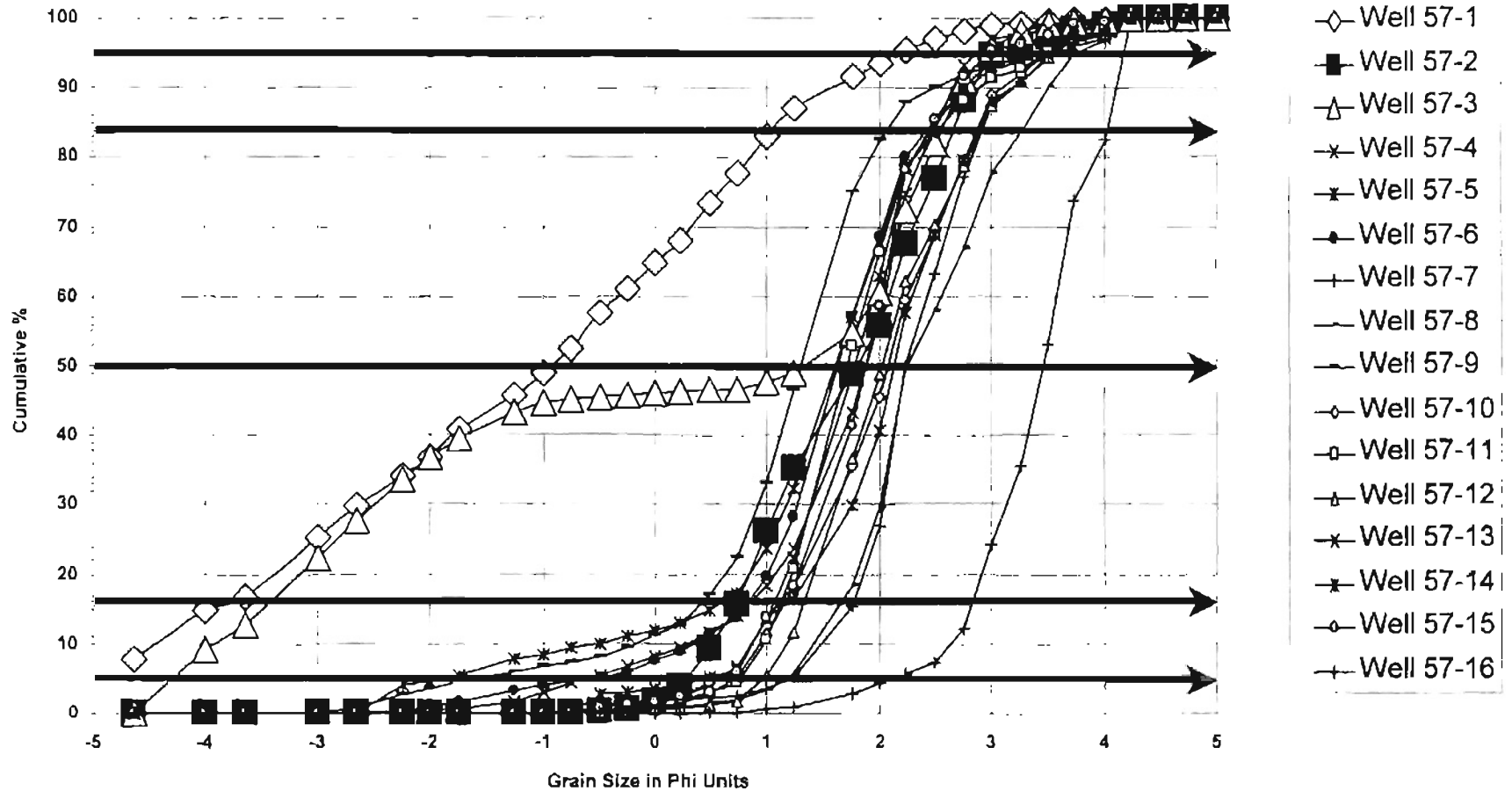
Norman Landfill Well #46 Cumulative Curves



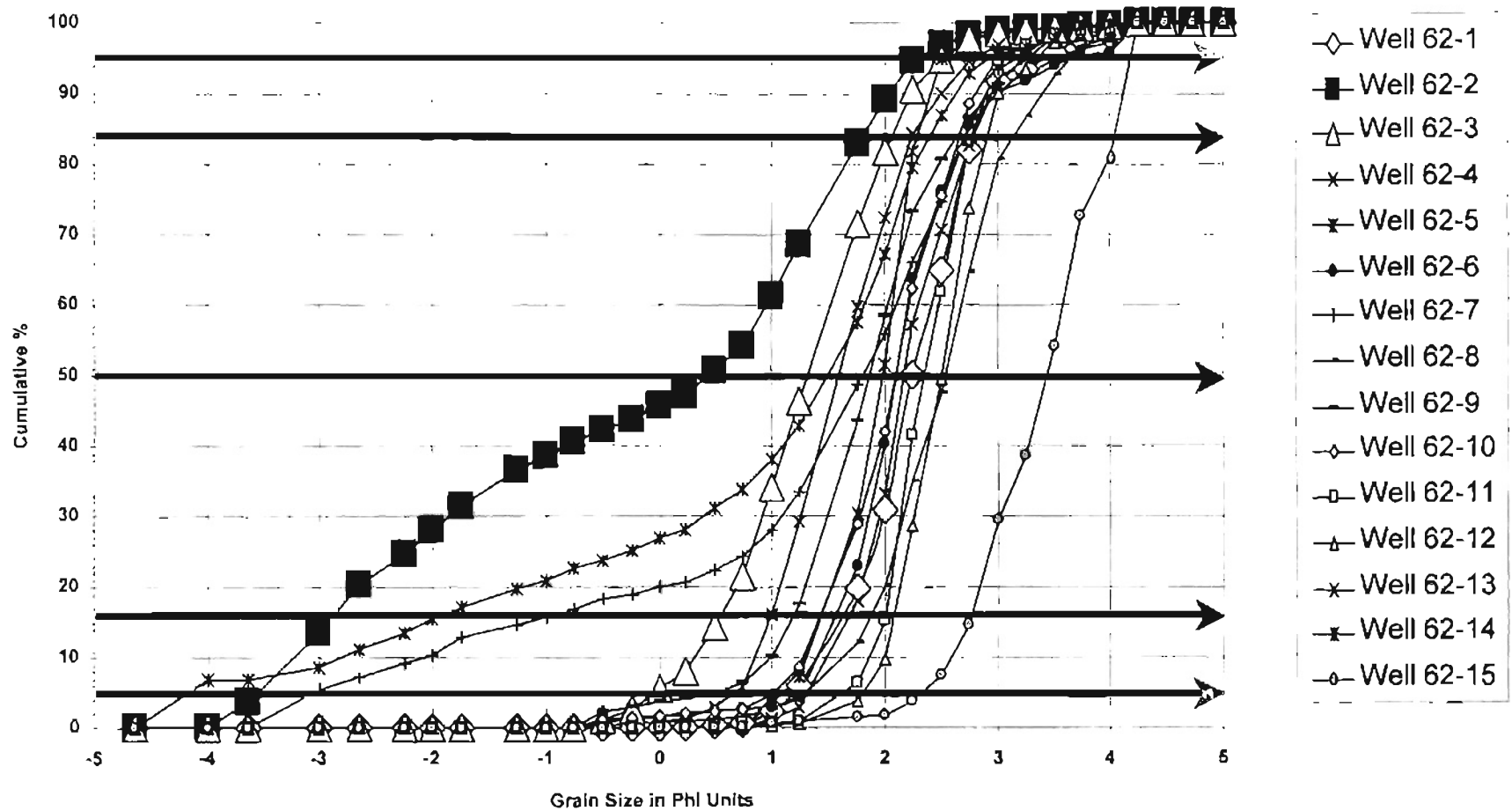
Norman Landfill Well #56 Cumulative Curves



Norman Landfill Well #57 Cumulative Curves

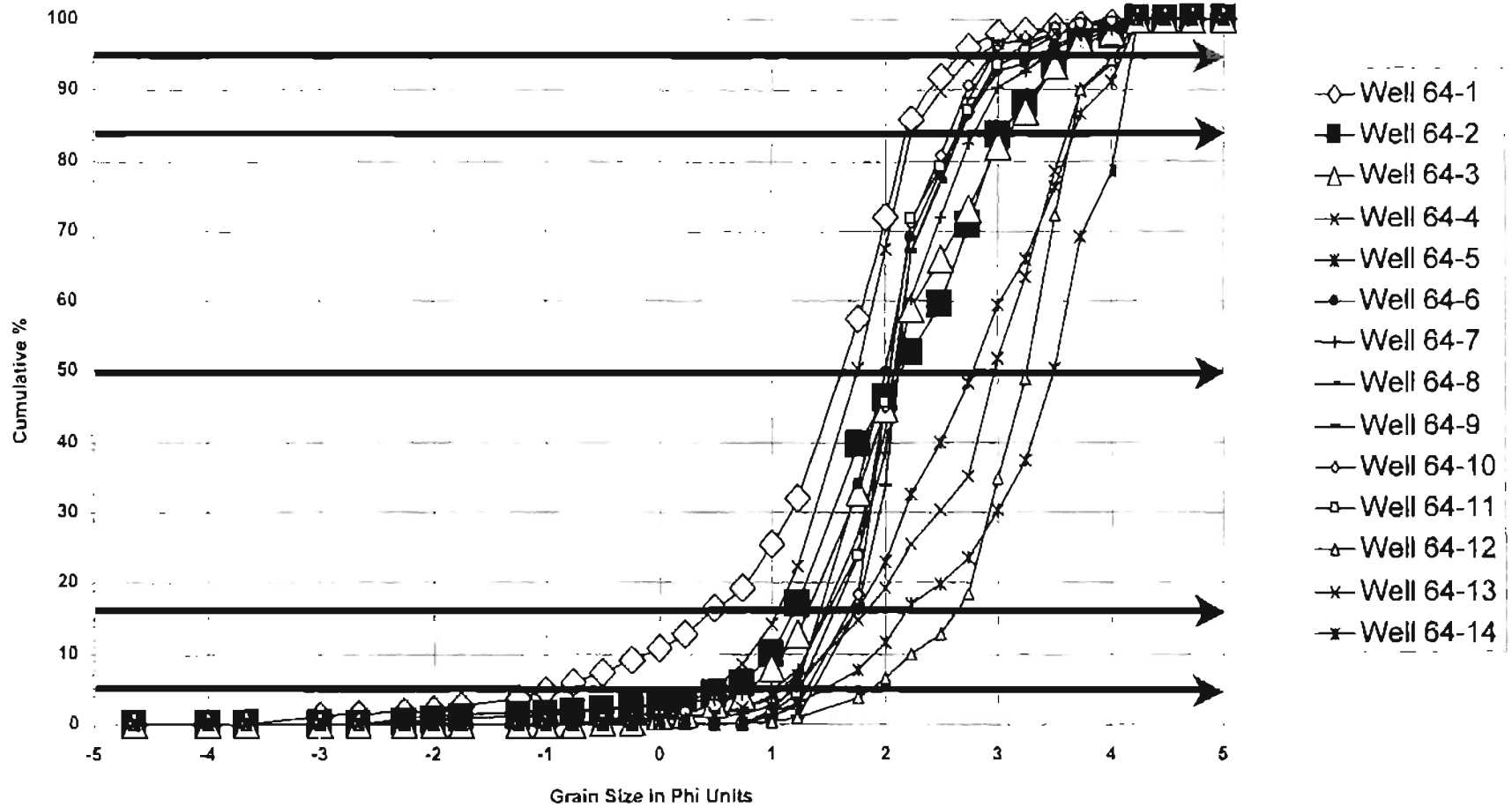


Norman Landfill Well #62 Cumulative Curves

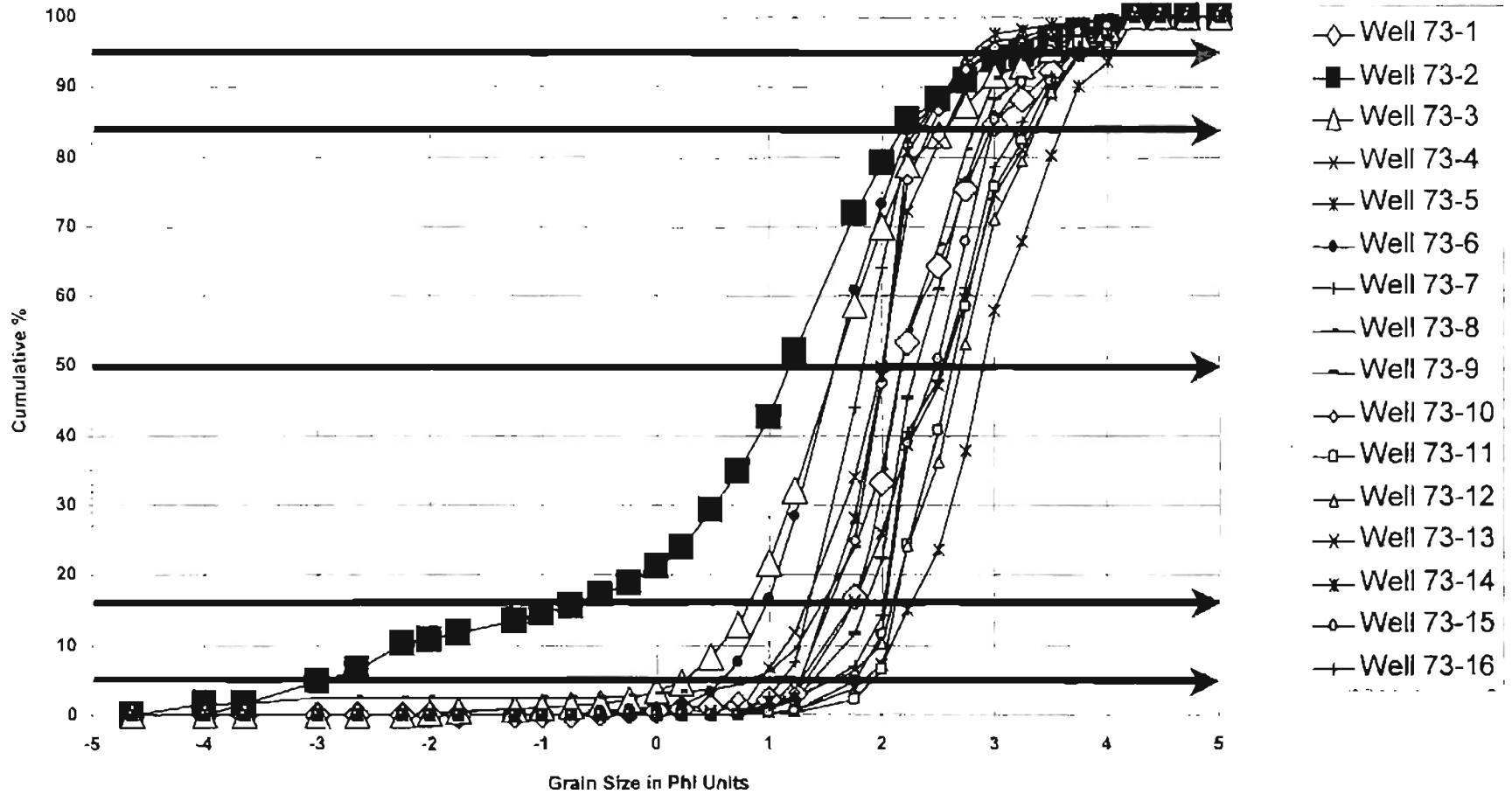


Norman Landfill Well #64 Cumulative Curves

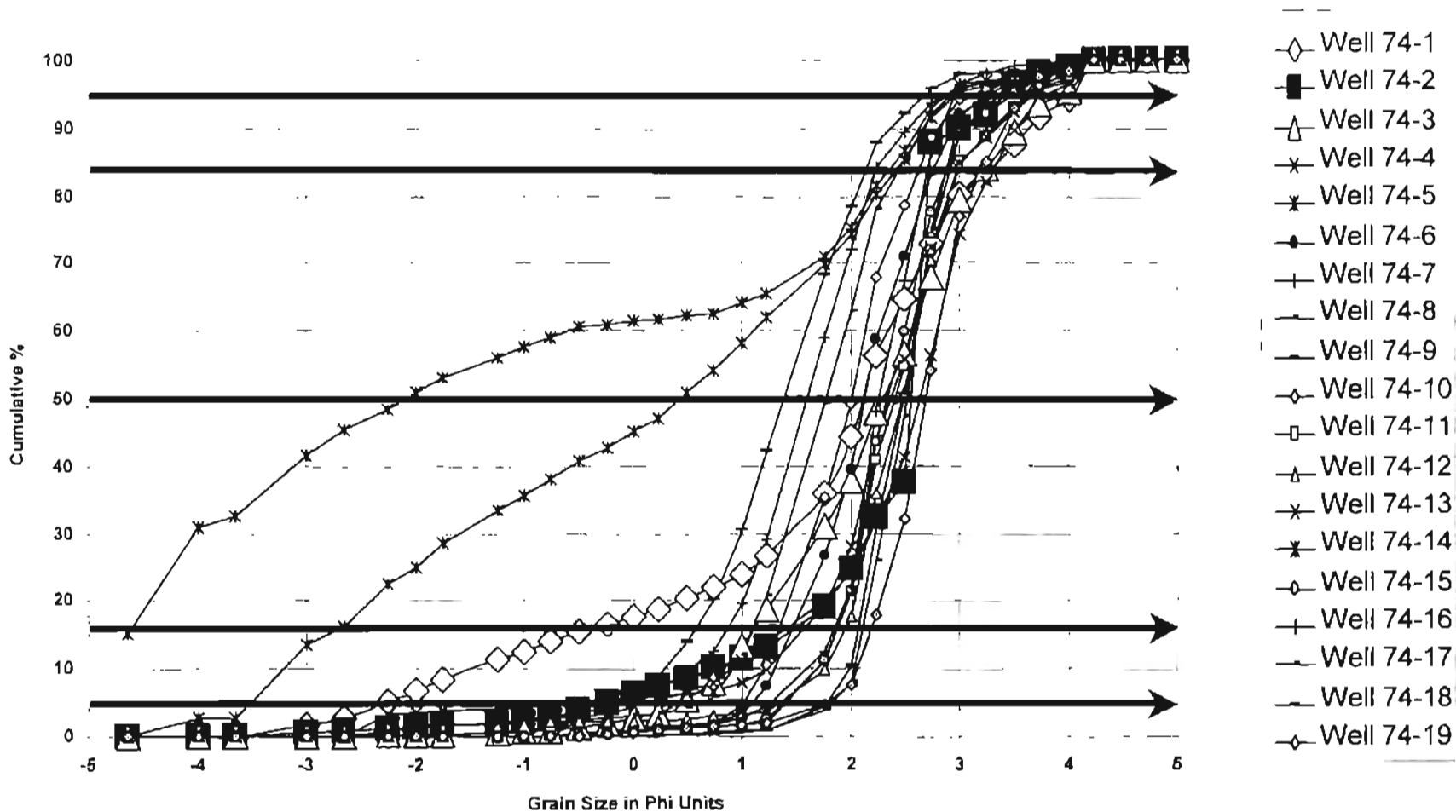
081



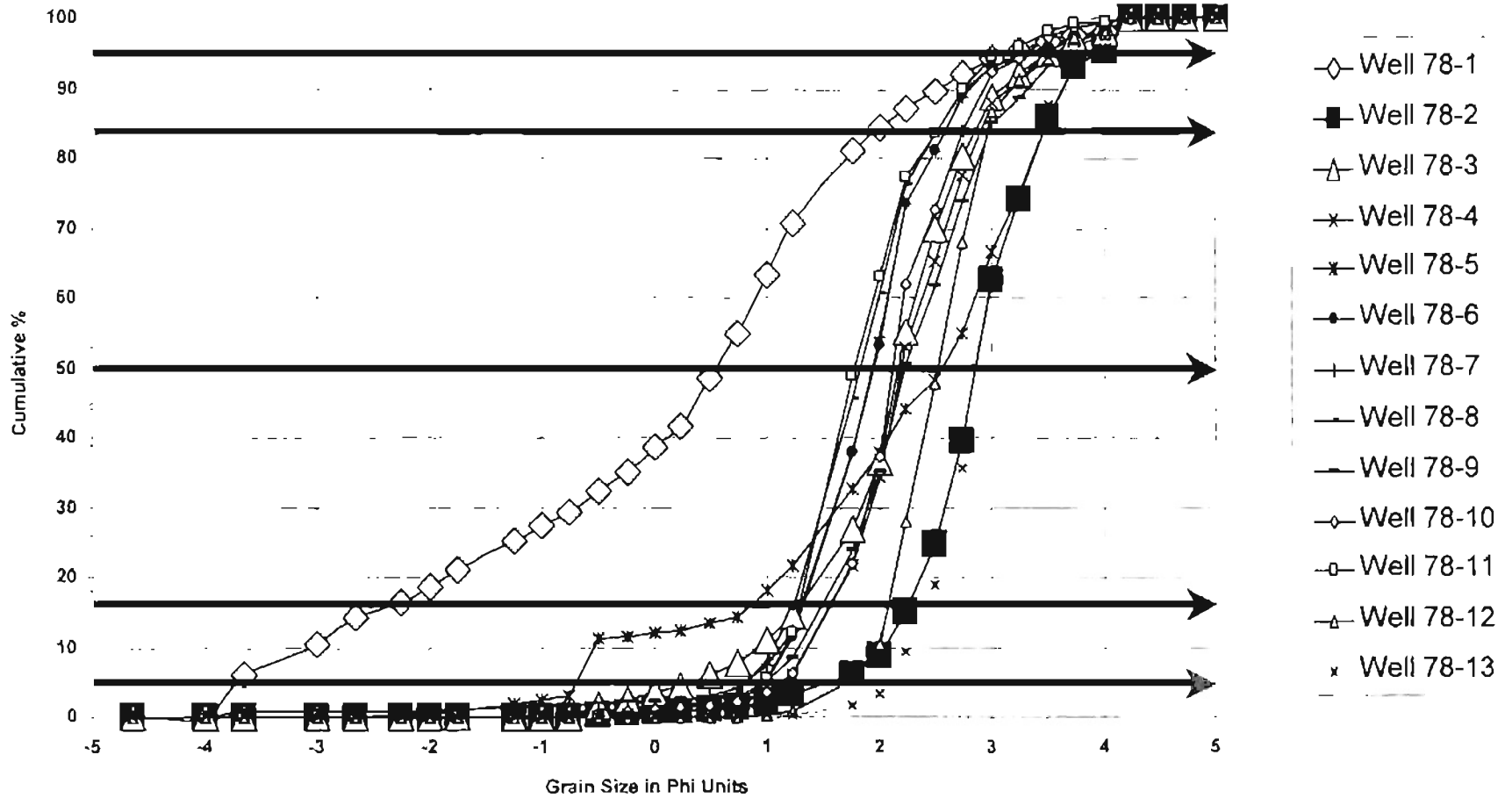
Norman Landfill Well #73 Cumulative Curves



Norman Landfill Well #74 Cumulative Curves

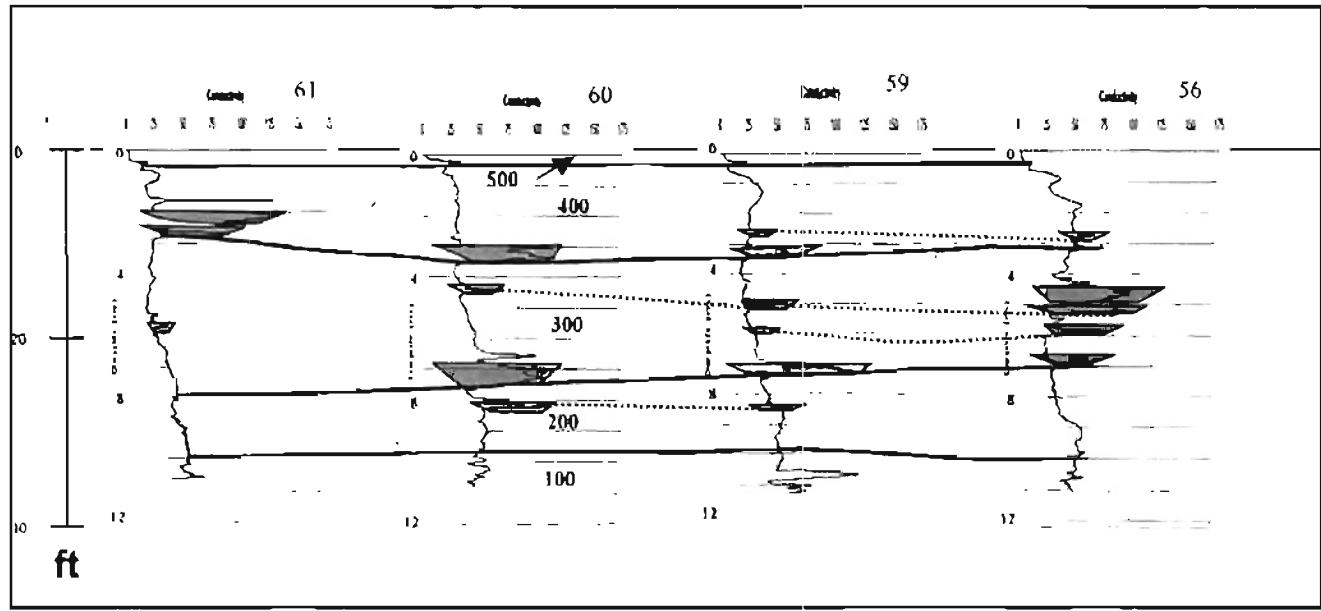
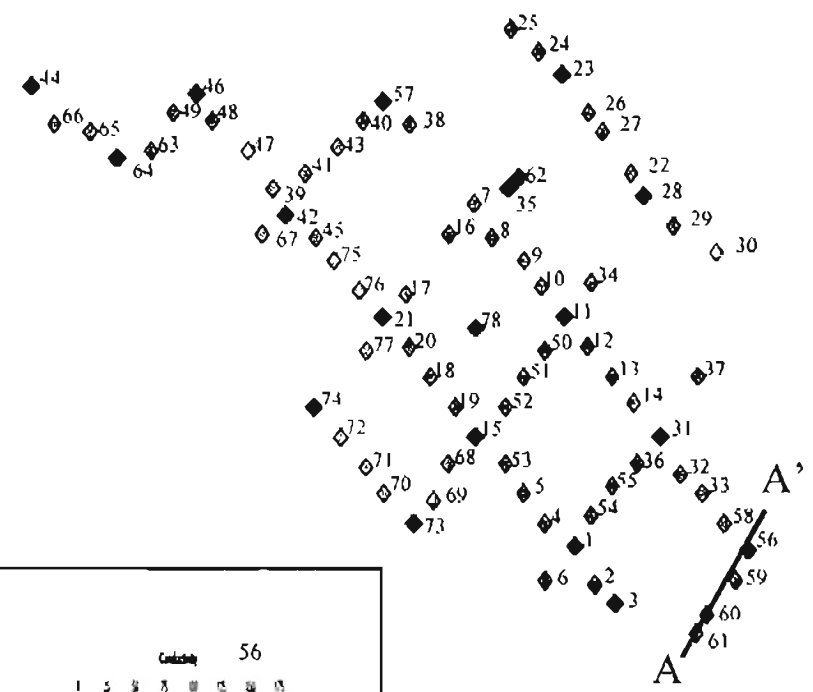


Norman Landfill Well #78 Cumulative Curves

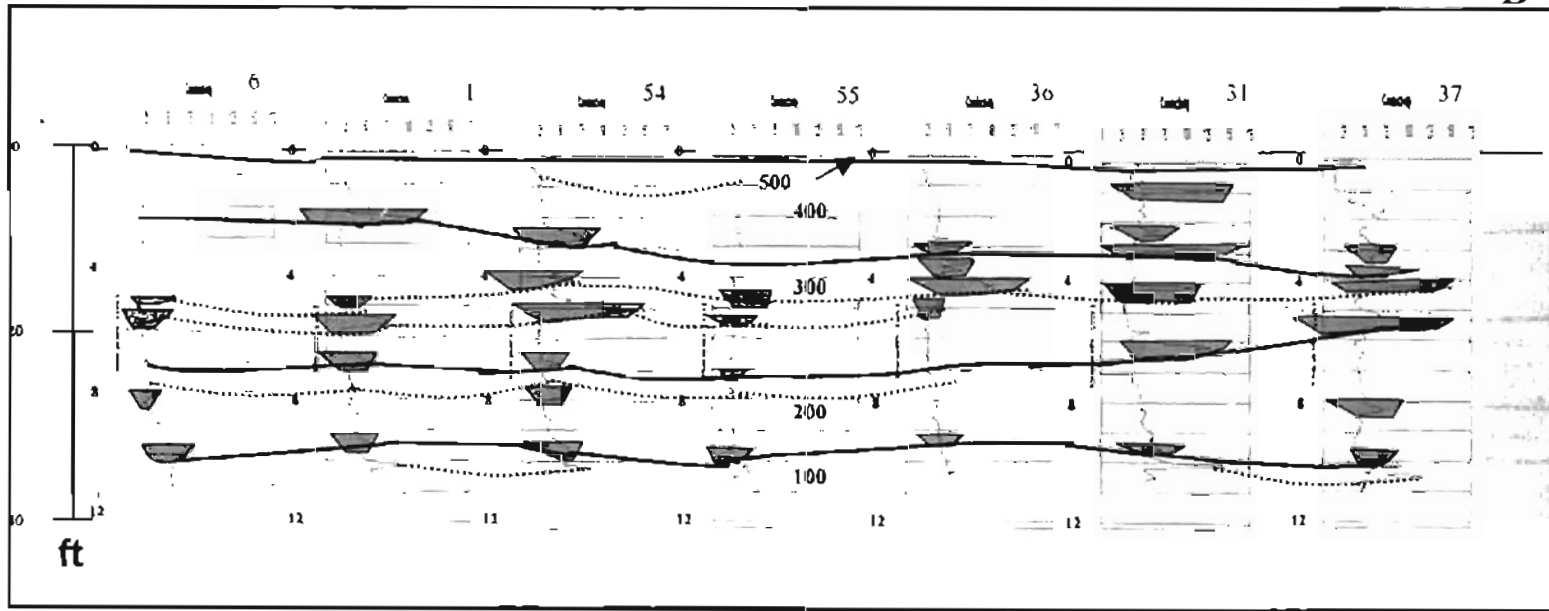
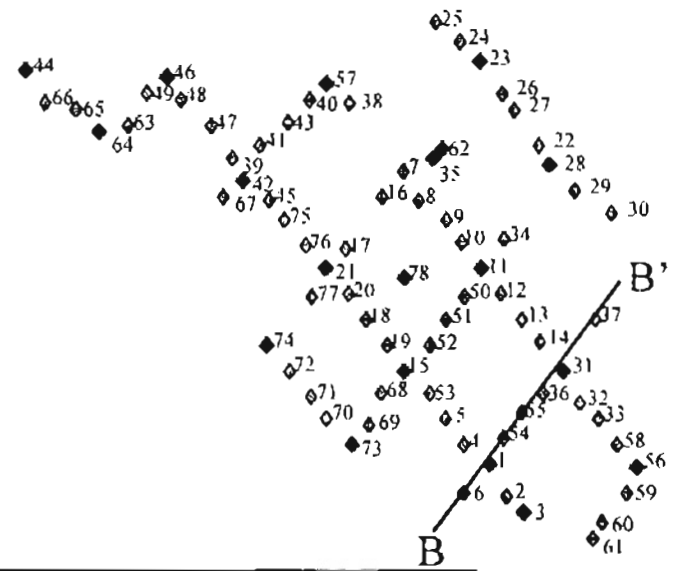


APPENDIX D
CROSS SECTIONS

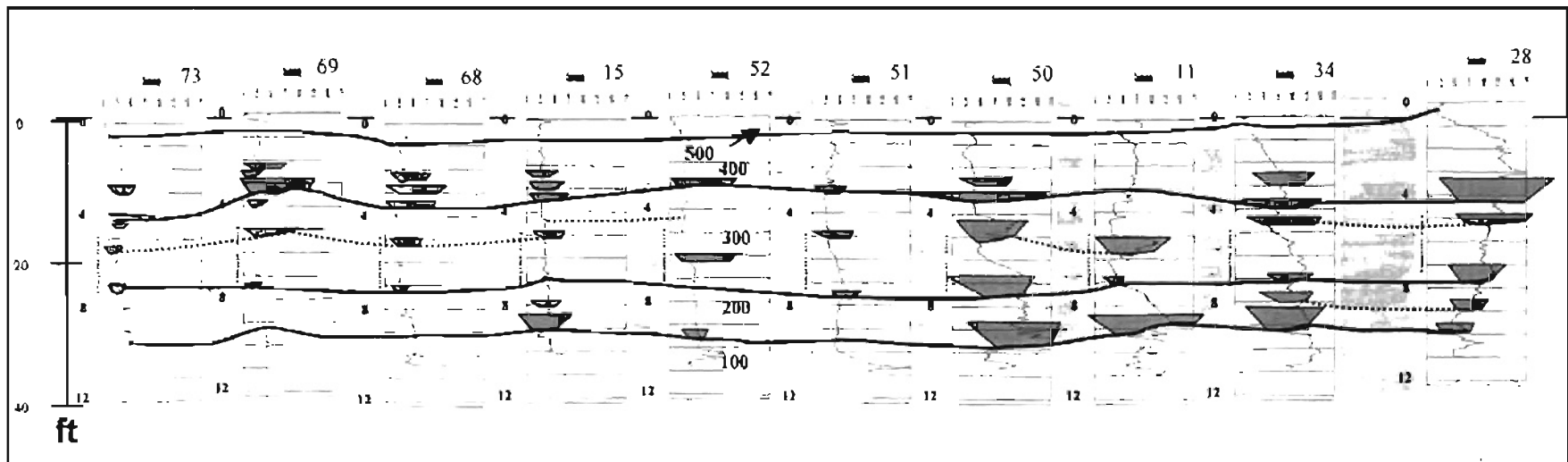
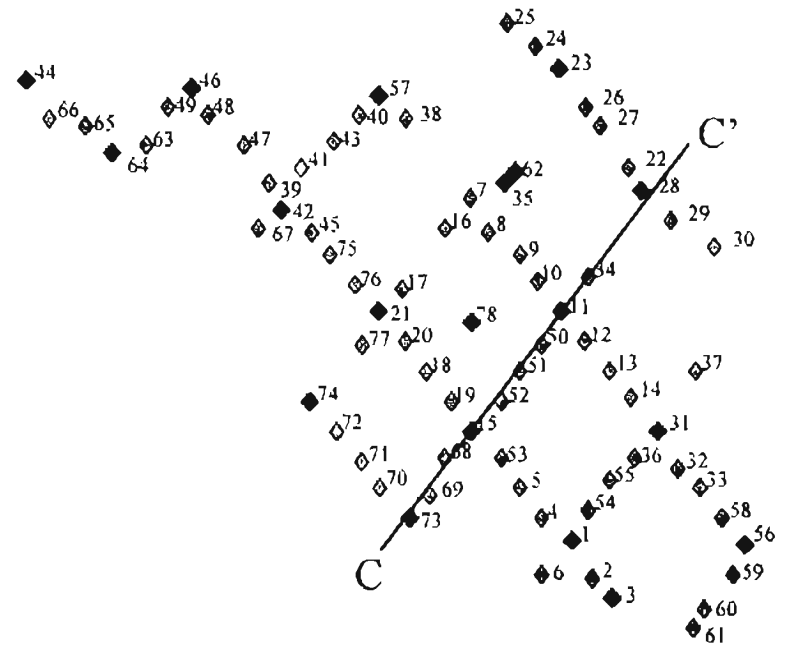
Norman Landfill Cross-Section A-A'



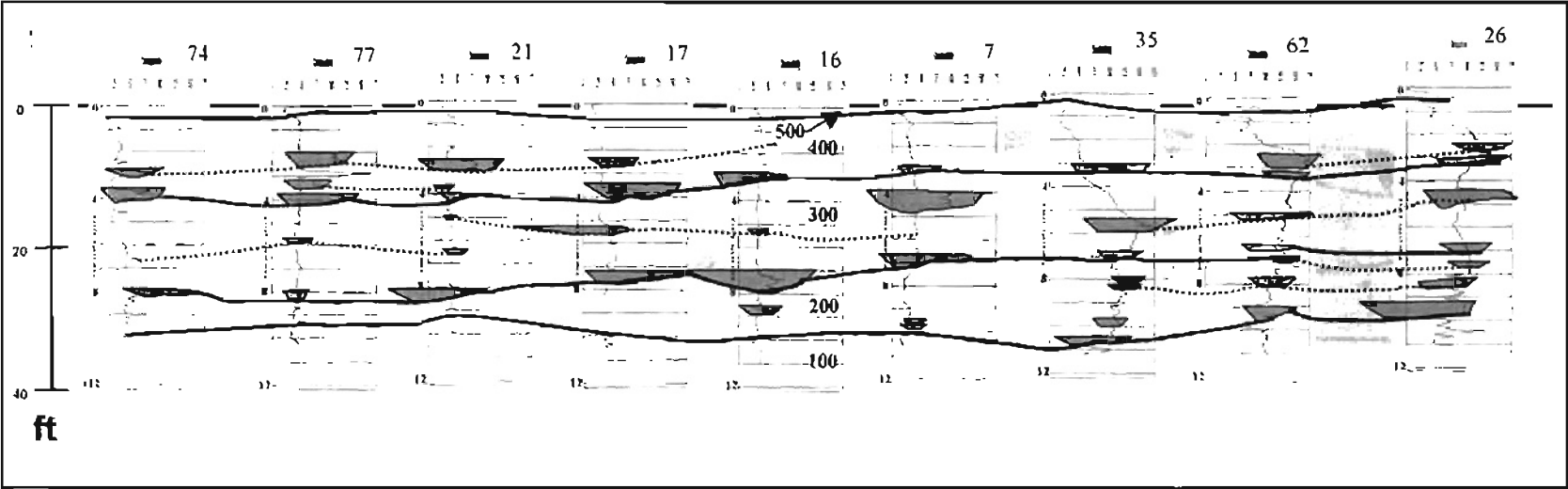
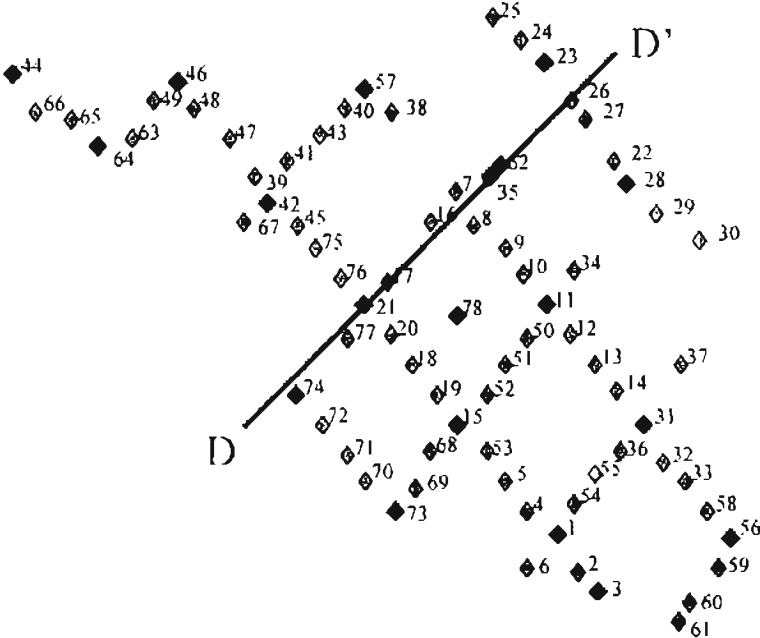
Norman Landfill Cross-Section B-B'



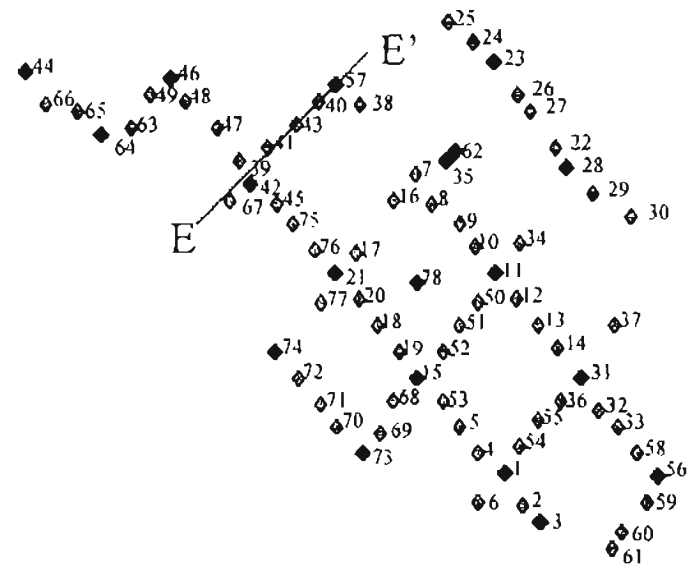
Norman Landfill Cross-Section C-C'



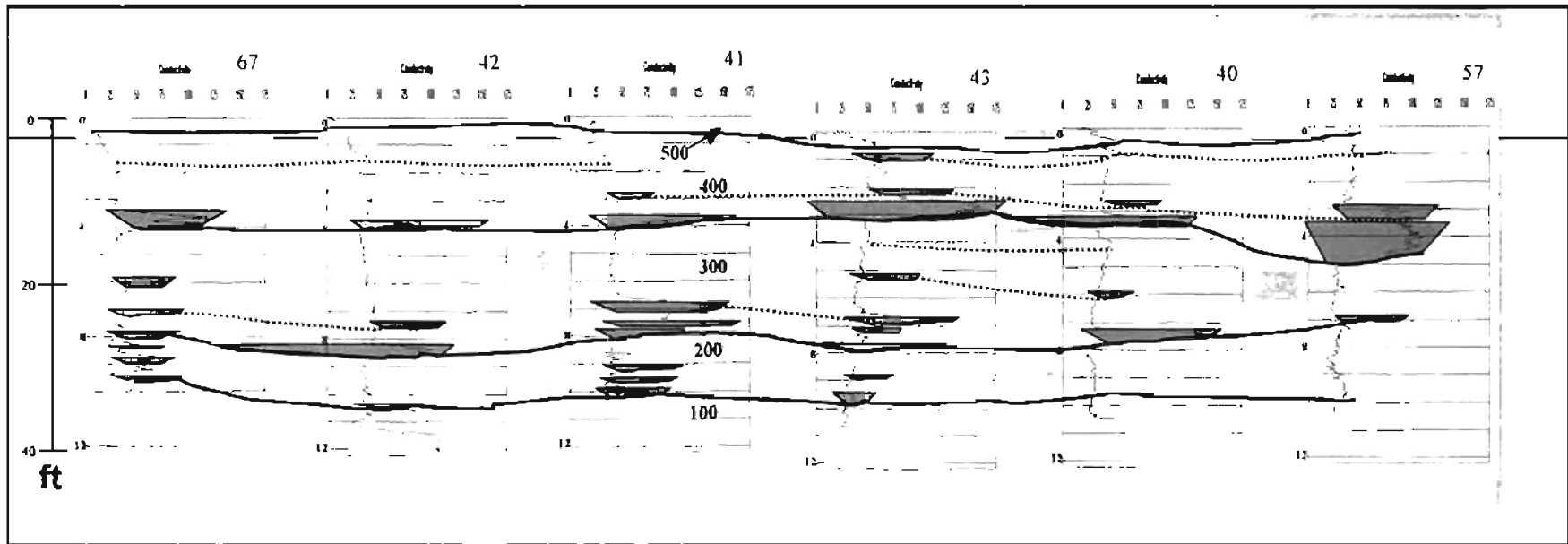
Norman Landfill Cross-Section D-D'



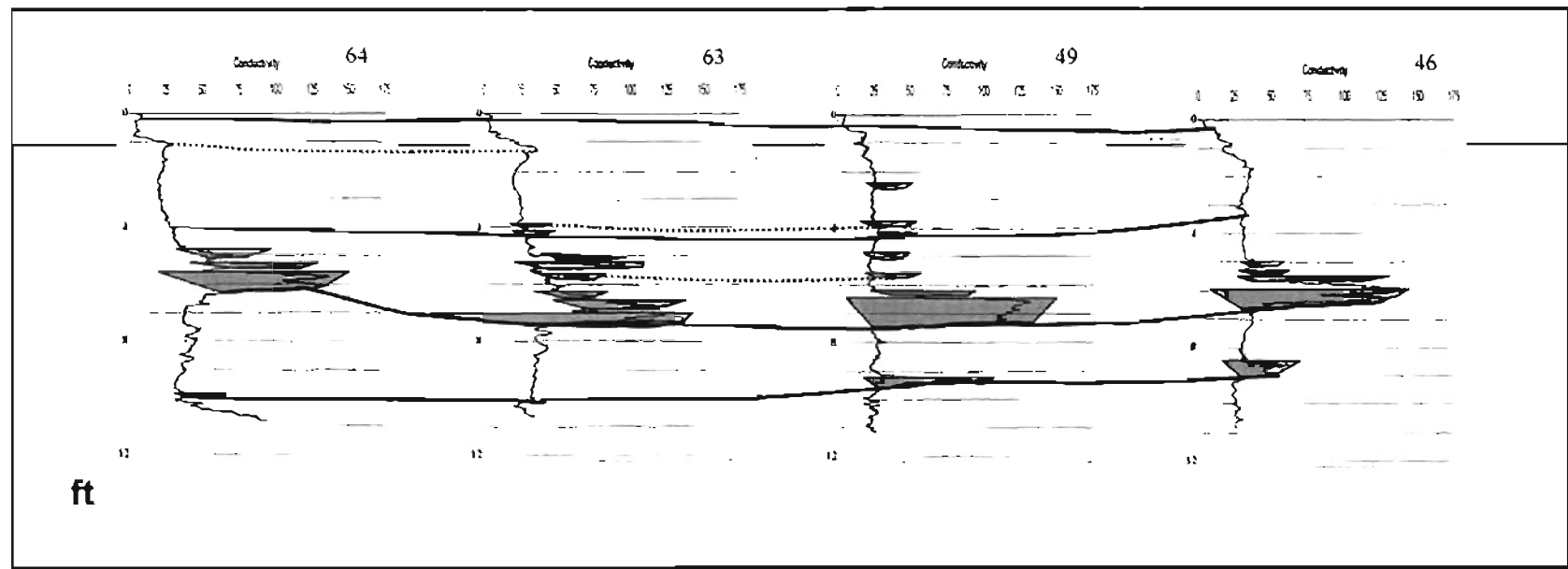
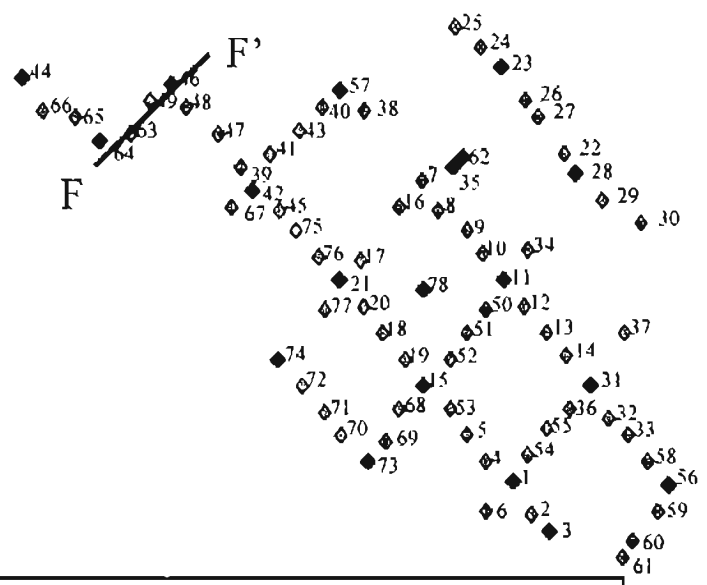
Norman Landfill Cross-Section E-E'



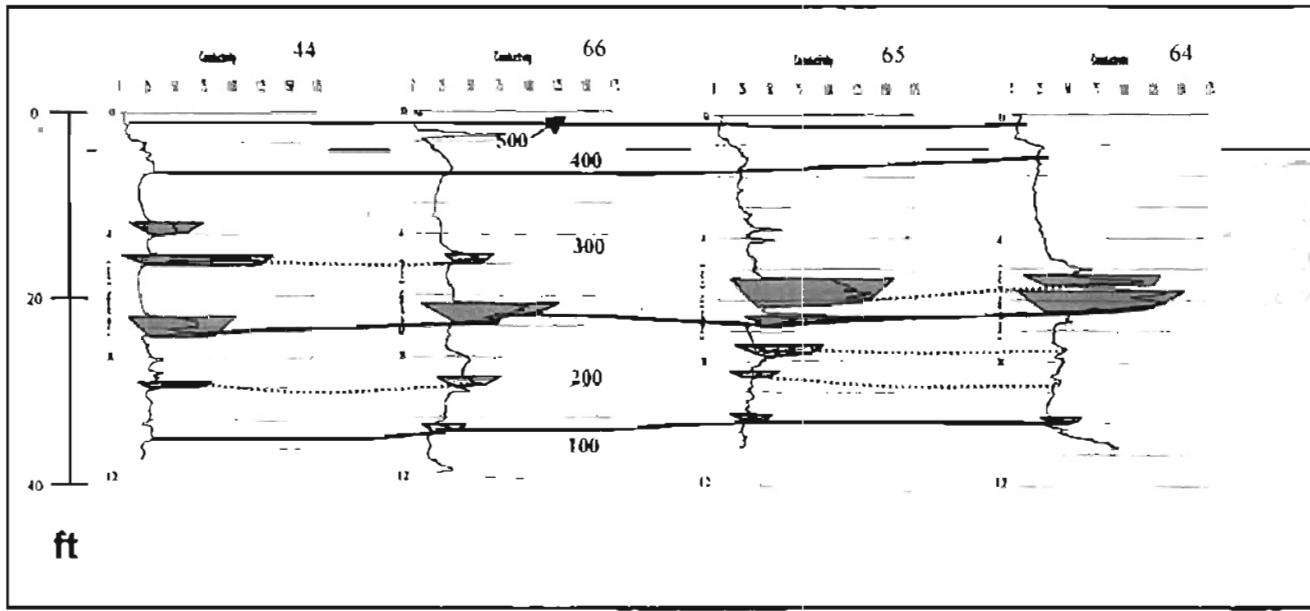
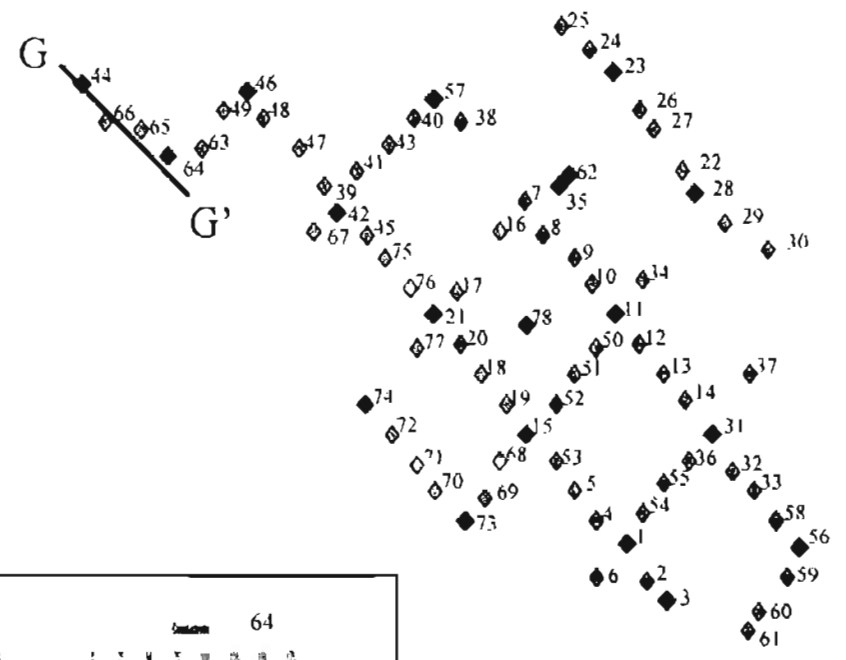
189



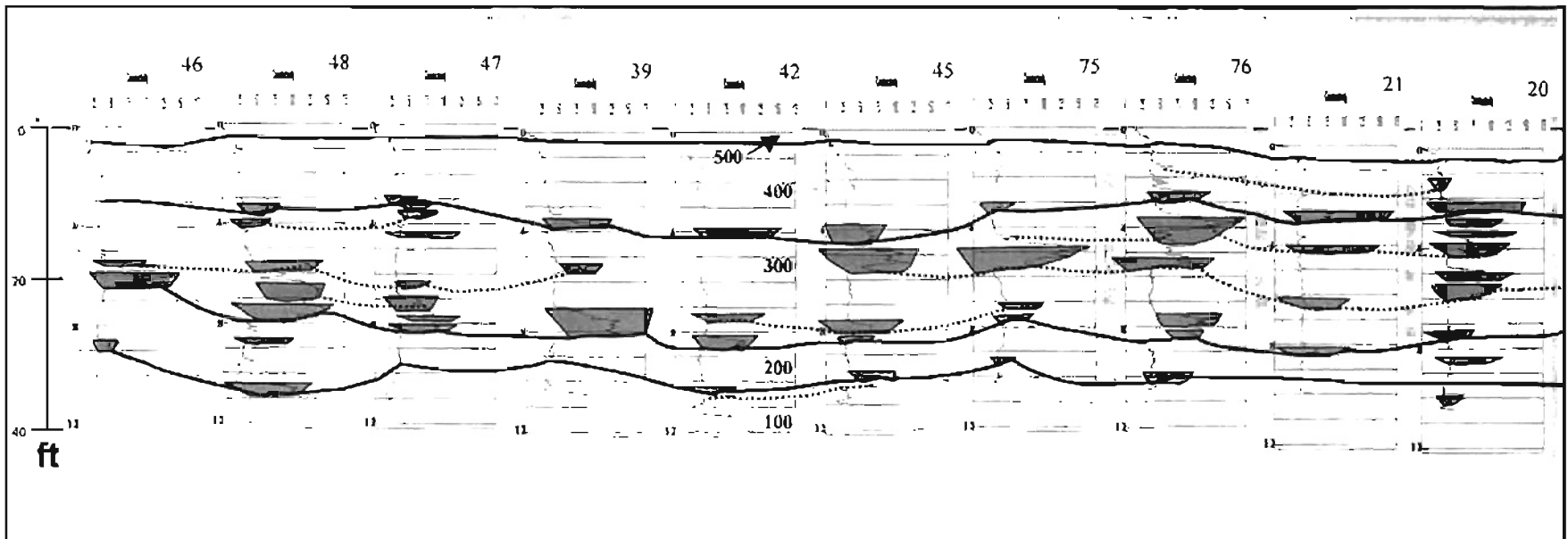
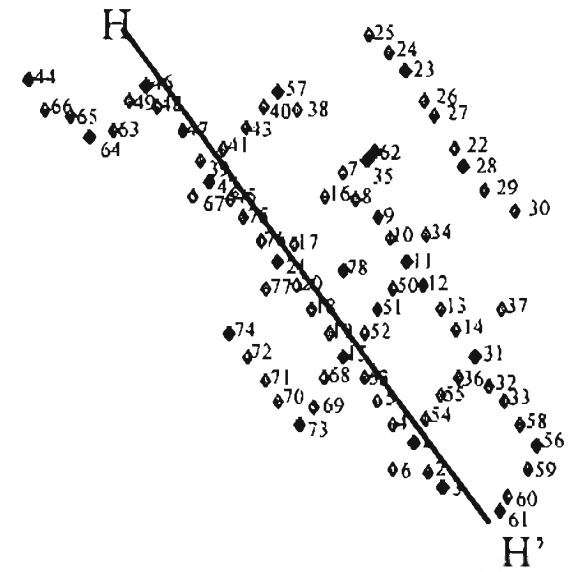
Norman Landfill Cross-Section F-F'



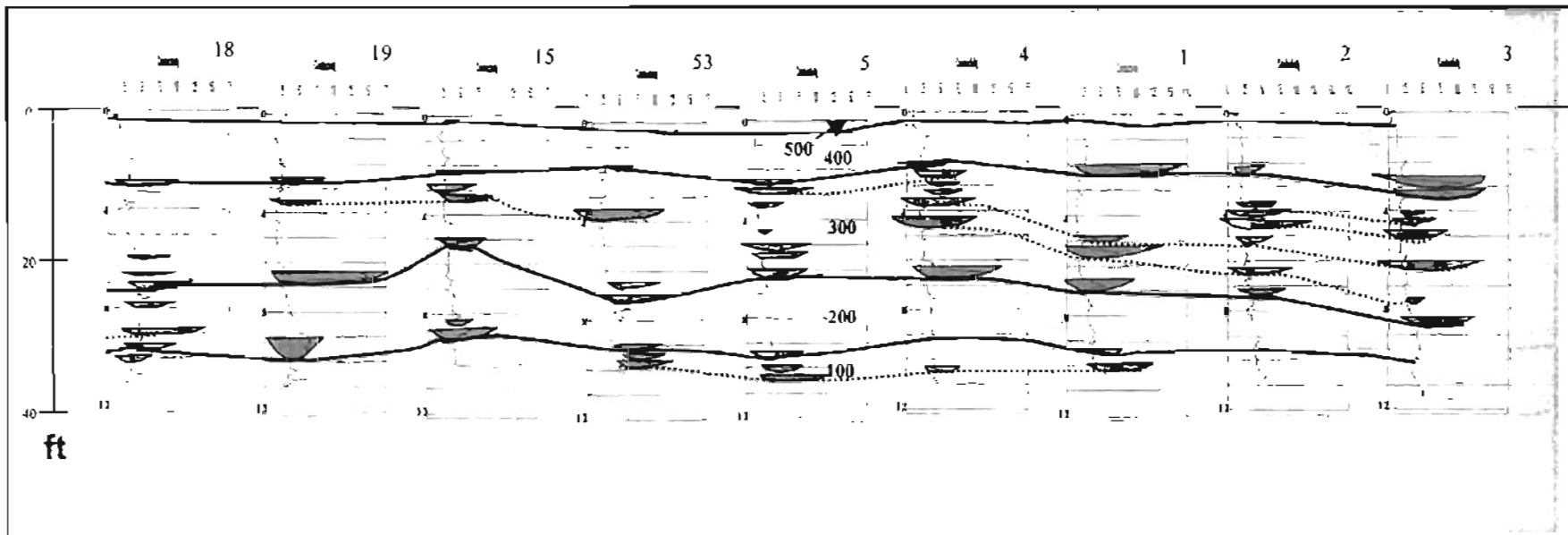
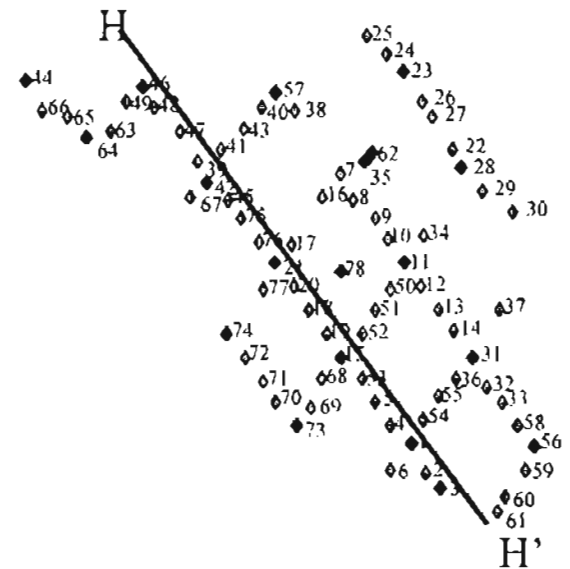
Norman Landfill Cross-Section G-G'



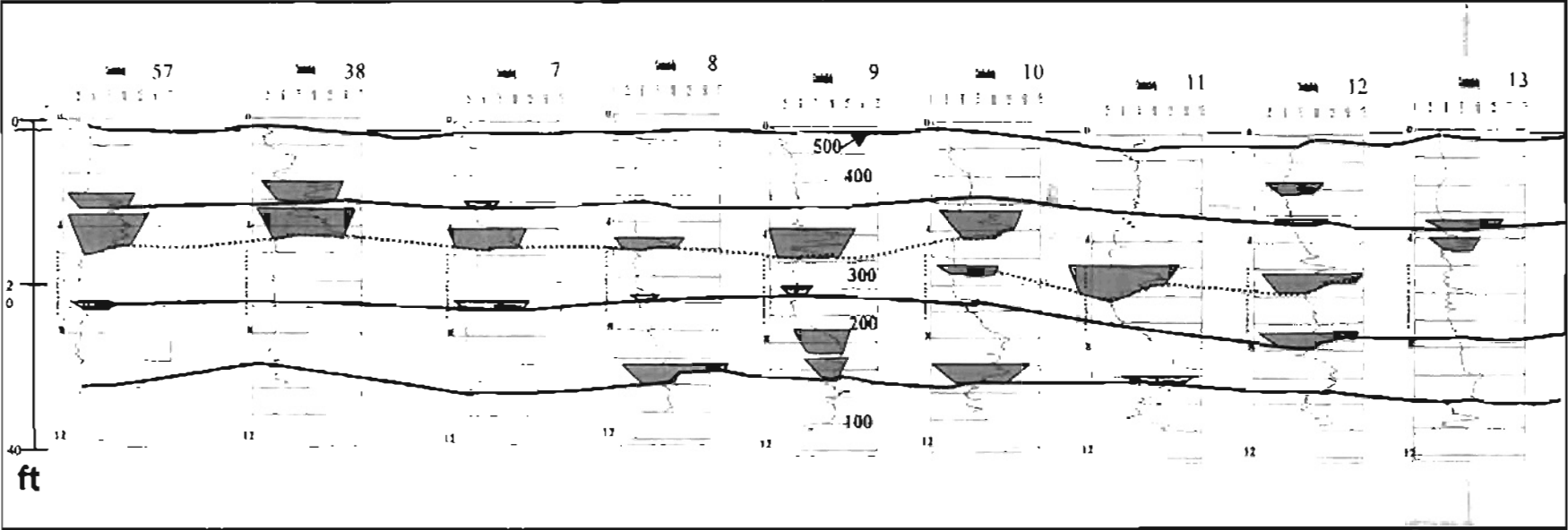
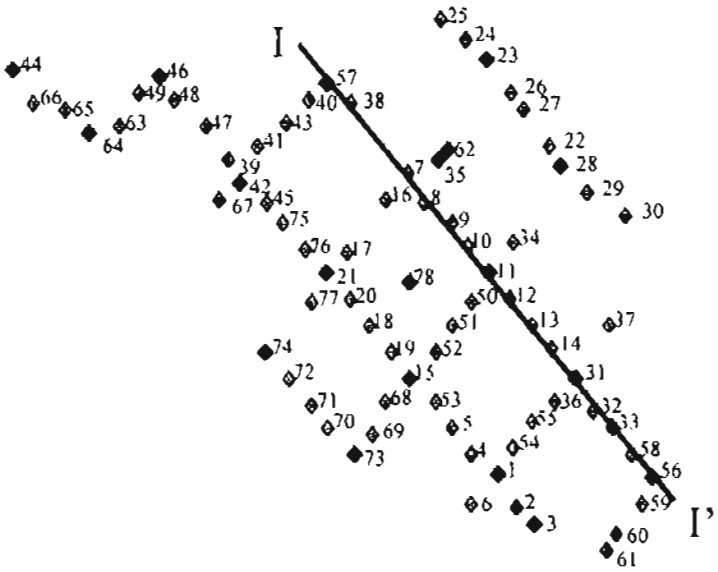
Normal Landfill Cross-Section H-H'



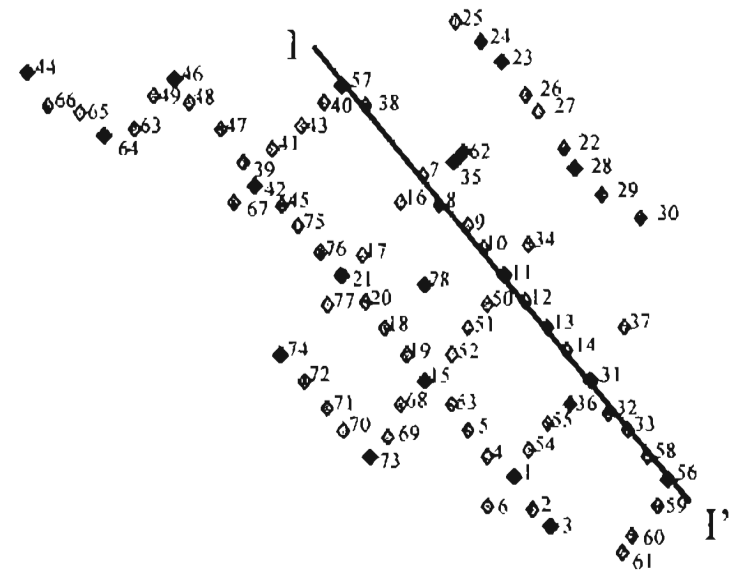
Norman Landfill Cross-Section H-H', cont.



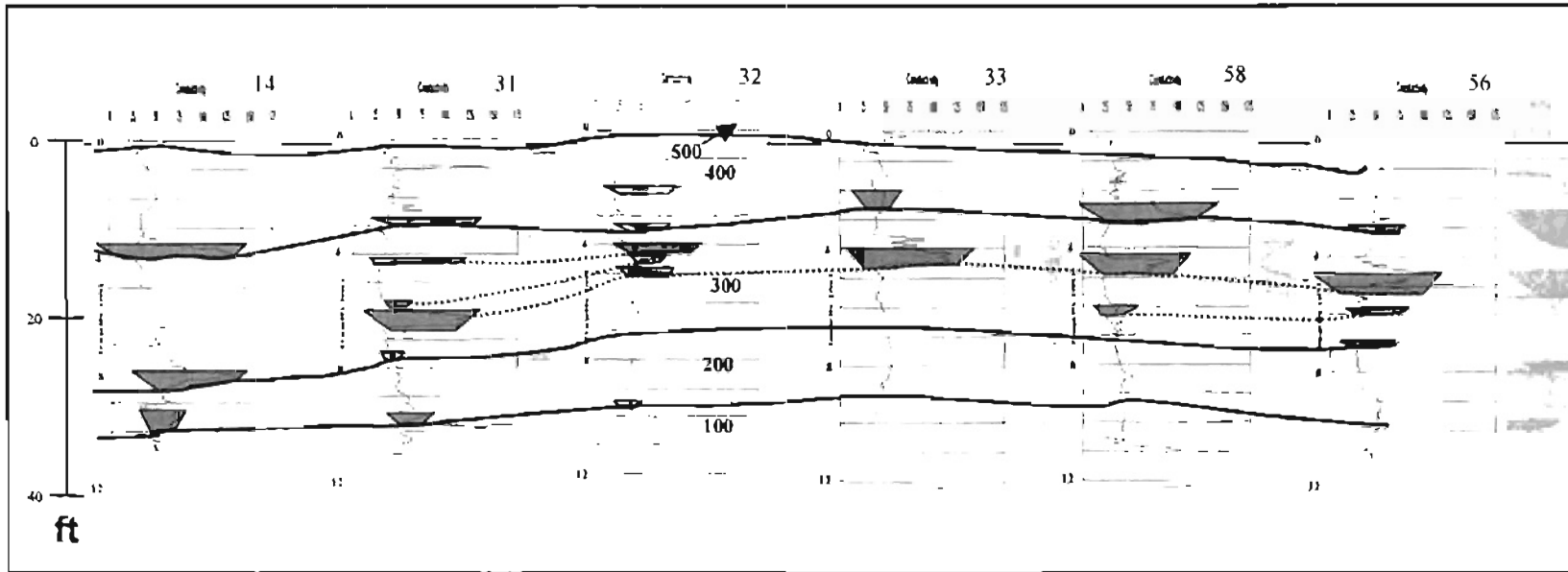
Norman Landfill Cross-Section I-I'



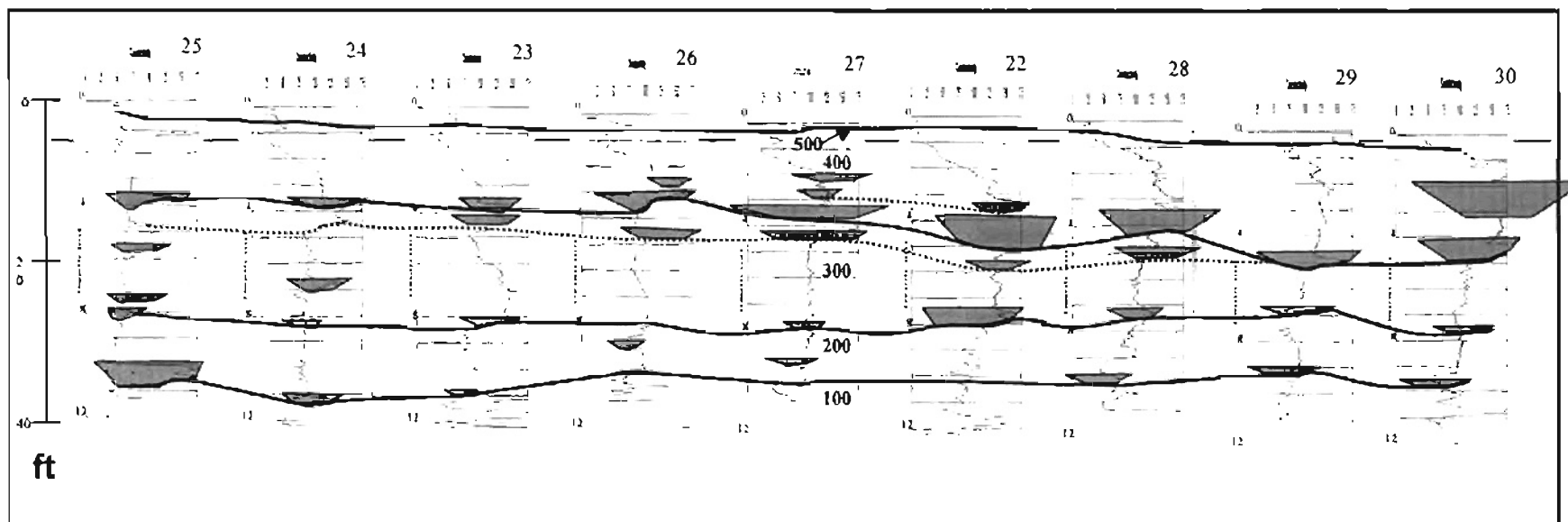
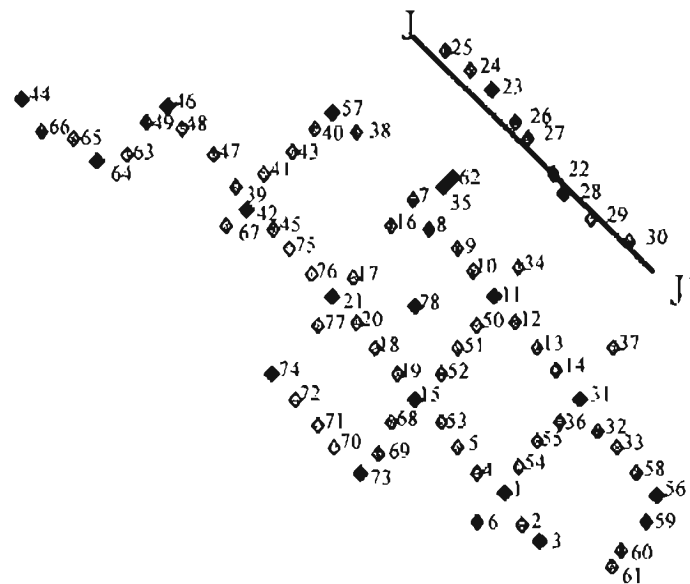
Norman Landfill Cross-Section I-I', cont.



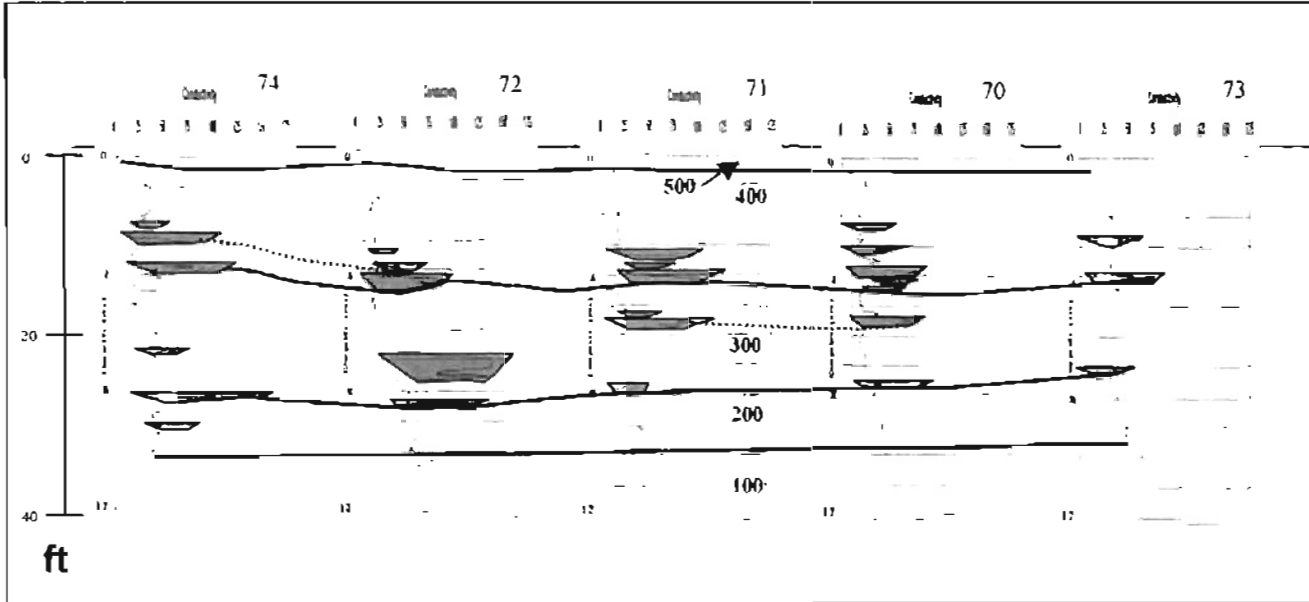
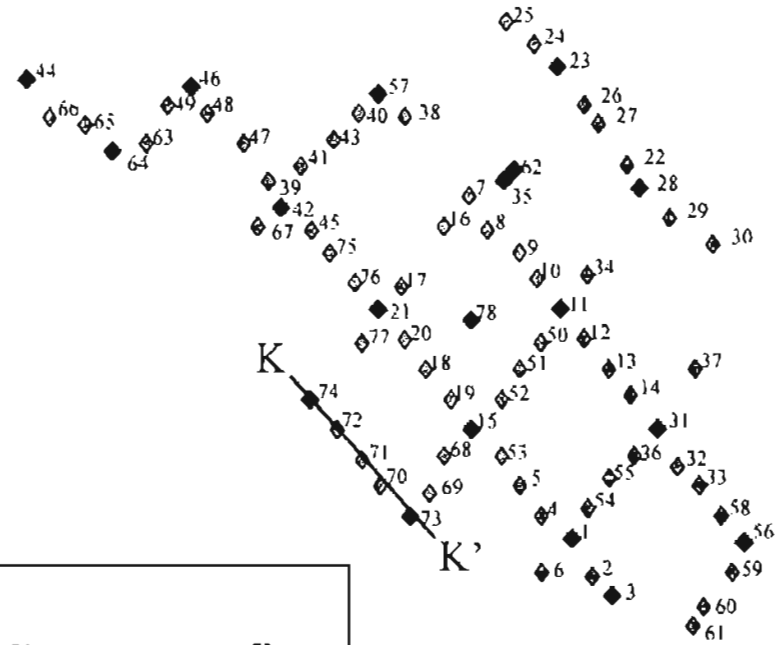
195



Norman Landfill Cross-Section J-J'



Norman Landfill Cross-Section K-K'



APPENDIX E
SIEVE SAMPLE DEPTHS

Well	Interval	Sample #	Depth Interval in Feet
w01	100	1-19	3309-3409 33'09" - 34'09"
w01	100	1-20	3503-3509
w01	200	1-14	2303-2310
w01	200	1-15	2602-2607
w01	200	1-16	2706-2711
w01	200	1-17	2903-3004
w01	200	1-18	3103-3110
w01	300	1-11	1808-1901
w01	300	1-12	1906-1910
w01	300	1-13	2110-2207
w01	300	1-10	1800-1804
w01	300	1-9	1506-1510
w01	300	1-8	1405-1410
w01	300	1-7	1303-1308
w01	300	1-6	1106-1110
w01	300	1-5	0907-1000
w01	400	1-4	0610-0703
w01	400	1-3	0511-0603
w01	400	1-2	0305-0400
w01	500	1-1	0106-0200
w03	100	3-14	3406-3500 34'06" - 35'00"
w03	100	3-15	3505-3510
w03	100	3-16	3702-3800
w03	100	3-17	3806-3811
w03	200	3-10	2908-3001
w03	200	3-11	3006-3011
w03	200	3-12	3105-3110
w03	200	3-13	3300-3400
w03	300	3-6	1303-1403
w03	300	3-7	2109-2202
w03	300	3-8	2306-2310
w03	300	3-9	2603-2702
w03	400	3-3	
w03	400	3-2	0304-0310
w03	400	3-4	0703-0710
w03	400	3-5	0910-1003
w03	500	3-1	0110-0204
w07	100	7-1	3509-3500 35'09" - 35'00"
w07	100	7-2	3402-3408
w07	100	7-3	3307-3311
w07	200	7-4	3100-3165
w07	200	7-5	2900-2903
w07	200	7-6	2609-2707
w07	200	7-7	2510-2604

w07	300	7-8	2108-2111	
w07	300	7-9	1904-1907	
w07	300	7-10	1711-1803	
w07	300	7-11	1305-1308	
w07	400	7-12	0907-0911	
w07	400	7-13	0505-0509	
w07	400	7-14	0307-0310	
w07	400	7-15	0203-0207	
w11	100	11-1	3506-3510	35'06" - 35'10"
w11	100	11-2	3109-3200	
w11	100	11-3	3008-3102	
w11	100	11-4	2909-3003	
w11	200	11-5	2704-2709	
w11	200	11-6	2511-2604	
w11	200	11-7	2304-2309	
w11	200	11-8	2108-2203	
w11	300	11-9	1607-1700	
w11	300	11-10	1404-1409	
w11	300	11-11	1005-1100	
w11	400	11-12	0706-0711	
w11	400	11-13	0603-0608	
w11	400	11-14	0304-0310	
w15	100	15-13	3003-3007	30'03" - 30'07"
w15	100	15-14	3103-3108	
w15	100	15-15	3311-3403	
w15	100	15-16	3405-3408	
w15	100	15-17	3505-3510	
w15	200	15-11	2305-2309	
w15	200	15-12	2706-2710	
w15	300	15-6	1411-1503	
w15	300	15-7	1506-1510	
w15	300	15-8	1709-1801	
w15	300	15-9	1807-1811	
w15	300	15-10	2106-2200	
w15	400	15-2	0304-0308	
w15	400	15-3	0702-0706	
w15	400	15-4	0904-0908	
w15	400	15-5	1106-1110	
w15	500	15-1	0101-0106	
w21	100	21-1	3501-3510	35'01" - 35'10"
w21	100	21-2	3107-3110	
w21	200	21-3	2903-2907	
w21	300	21-4	2607-2610.5	
w21	300	21-5	2206-2211	
w21	300	21-6	1802-1806	
w21	300	21-7	1400-1405	
w21	300	21-8	1302-1306	
w21	300	21-9	1000-1004.5	
w21	400	21-10	0702-0705	

w07	300	7-8	2108-2111	
w07	300	7-9	1904-1907	
w07	300	7-10	1711-1803	
w07	300	7-11	1305-1308	
w07	400	7-12	0907-0911	
w07	400	7-13	0505-0509	
w07	400	7-14	0307-0310	
w07	400	7-15	0203-0207	
w11	100	11-1	3506-3510	35'06" - 35'10"
w11	100	11-2	3109-3200	
w11	100	11-3	3008-3102	
w11	100	11-4	2909-3003	
w11	200	11-5	2704-2709	
w11	200	11-6	2511-2604	
w11	200	11-7	2304-2309	
w11	200	11-8	2108-2203	
w11	300	11-9	1607-1700	
w11	300	11-10	1404-1409	
w11	300	11-11	1005-1100	
w11	400	11-12	0706-0711	
w11	400	11-13	0603-0608	
w11	400	11-14	0304-0310	
w15	100	15-13	3003-3007	30'03" - 30'07"
w15	100	15-14	3103-3108	
w15	100	15-15	3311-3403	
w15	100	15-16	3405-3408	
w15	100	15-17	3505-3510	
w15	200	15-11	2305-2309	
w15	200	15-12	2706-2710	
w15	300	15-6	1411-1503	
w15	300	15-7	1506-1510	
w15	300	15-8	1709-1801	
w15	300	15-9	1807-1811	
w15	300	15-10	2106-2200	
w15	400	15-2	0304-0308	
w15	400	15-3	0702-0706	
w15	400	15-4	0904-0908	
w15	400	15-5	1106-1110	
w15	500	15-1	0101-0106	
w21	100	21-1	3501-3510	35'01" - 35'10"
w21	100	21-2	3107-3110	
w21	200	21-3	2903-2907	
w21	300	21-4	2607-2610.5	
w21	300	21-5	2206-2211	
w21	300	21-6	1802-1806	
w21	300	21-7	1400-1405	
w21	300	21-8	1302-1306	
w21	300	21-9	1000-1004.5	
w21	400	21-10	0702-0705	

w21	500	21-11	0111-0203	
w23	100	23-14	3708-3800	37'08" - 38'00"
w23	100	23-15	3806-3810	
w23	200	23-10	2701-2704	
w23	200	23-11	3006.5-3100	
w23	200	23-12	3108-3111	
w23	200	23-13	3409-3500	
w23	300	23-5	1809-1901	
w23	300	23-6	1906.5-1910	
w23	300	23-7	2107.5-2200	
w23	300	23-8	2307.5- 2310.5	
w23	300	23-9	2508-2511	
w23	400	23-1	0301-0305	
w23	400	23-2	0605.5-0609.5	
w23	400	23-3	1005-1009	
w23	400	23-4	1301-1307	
w28	100	28-1	3700-3709	37'00" - 37'09"
w28	100	28-2	3409-3503	
w28	100	28-3	3310-3405	
w28	100	28-4	3204-3210	
w28	200	28-5	3011-3104	
w28	200	28-6	2900-2907	
w28	200	28-7	2705-2710	
w28	200	28-8	2507-2603	
w28	300	28-9	2210-2303	
w28	300	28-10	2103-2200	
w28	300	28-11	1905-1910	
w28	300	28-12	1706-1711	
w28	300	28-13	1506-1600	
w28	400	28-14	1102-1107	
w28	400	28-15	0706-0800	
w28	400	28-16	0304-0310	
w31	100	31-1	3507-3600	35'07" - 36'00"
w31	100	31-2	3405-3410	
w31	100	31-3	3300-3305	
w31	200	31-4	3102.5-3107	
w31	200	31-5	2906-2909	
w31	200	31-6	2706-2710	
w31	200	31-7	2602.5-2608.5	
w31	200	31-8	2308-2400	
w31	200	31-9	2300-2305	
w31	300	31-10	1806-1810	
w31	300	31-11	1506-1510.5	
w31	300	31-12	1305-1311	
w31	300	31-13	1106-1110.5	
w31	300	31-14	0910.5-1002	
w31	400	31-15	0704-0708	
w31	400	31-16	0605-0609	
w31	400	31-17	0505-0508	

w31	400	31-18	0304-0309	
w31	400	31-19	0204-0210	
w31	500	31-20	0103-0108	
w42	100	42-1	3506-3509	35'06" - 35'09"
w42	100	42-2	3500-3503	
w42	100	42-3	3403-3406	
w42	200	42-4	3107-3110	
w42	200	42-5	3006-3010	
w42	200	42-6	2906-2909	
w42	300	42-7	2608-2611	
w42	300	42-8	2307-2310	
w42	300	42-9	2201-2205	
w42	300	42-10	1810-1902	
w42	300	42-11	1506-1510	
w42	300	42-12	1402-1405	
w42	400	42-13	1106-1110	
w42	400	42-14	0911-1003	
w42	400	42-15	0611-0703	
w42	400	42-16	0305-0310	
w42	500	42-17	0109-0200	
w44	100	44-1	3803-3807	38'03" - 38'07"
w44	100	44-2	3709-3801	
w44	100	44-3	3700-3704	
w44	100	44-4	3500-3505	
w44	200	44-5	3009-3102	
w44	200	44-6	2608-2701	
w44	300	44-7	2106-2110	
w44	300	44-8	1904-1910	
w44	300	44-9	1701-1707	
w44	300	44-10	1401-1407	
w44	300	44-11	1104-1110	
w44	300	44-12	0908-1001	
w44	300	44-13	0705-0710	
w44	300	44-14	0605-0609	
w44	400	44-15	0305-0310	
w44	400	44-16	0201-0206	
w46	100	46-1	3506-3510	35'06" - 35'10"
w46	100	46-2	3405.5-3408	
w46	100	46-3	3308-3311	
w46	100	46-4	3102-3105	
w46	200	46-5	2610-2725	
w46	200	46-6	2305-2309.5	
w46	300	46-7	1500-1505	
w46	300	46-8	1310-1403	
w46	300	46-9	1100-1103	
w46	300	46-10	1000-1004	
w46	400	46-11	0707-0710	
w46	400	46-12	0511-0602	
w46	400	46-13	0502-0507	

w46	400	46-14	0205-0209	
w46	500	46-15	0106-0110	
w56	100	56-1	3508-3600	35'08" - 36'00"
w56	100	56-2	3411-3504	
w56	200	56-3	3106-3111	
w56	200	56-4	2706-2711	
w56	200	56-5	2600.5-2606	
w56	200	56-6	2306-2310.5	
w56	300	56-7	2205.5-2210.5	
w56	300	56-8	2106-2110.5	
w56	300	56-9	1809.5-1900	
w56	300	56-10	1400-1403.5	
w56	300	56-11	1305-1310	
w56	300	56-12	1104-1110	
w56	400	56-13	1003.5-1008	
w56	400	56-14	0808-0810	
w56	400	56-15	0604-0611	
w56	400	56-16	0306-0310	
w56	400	56-17	0201.5-0207.5	
w-57	100	57-1	3504-3509	35'04" - 35'09"
w-57	100	57-2	3311-3405	
w-57	200	57-3	3103-3107	
w-57	200	57-4	3008-3101	
w-57	200	57-5	2705-2709	
w-57	200	57-6	2507-2511	
w-57	200	57-9	2309-2400	
w-57	300	57-7	2211-2303	
w-57	300	57-8	2106-2111	
w-57	300	57-10	1709-1801	
w-57	300	57-11	1003-1007	
w-57	400	57-12	0706-0710	
w-57	400	57-13	0600-0605	
w-57	400	57-14	0306-0310	
w-57	400	57-15	0111-0204	
w-57	500	57-16	0102-0107	
w62	100	62-1	3605-3610	36'05" - 36'10"
w62	100	62-2	3507-3511	
w62	100	62-3	3407-3500	
w62	100	62-4	3300-3306	
w62	200	62-5	3108-3200	
w62	200	62-6	2811-2904	
w62	200	62-7	2705.5-2709	
w62	200	62-8	2507-2600	
w62	300	62-9	2107-2200	
w62	300	62-10	1804-1807	
w62	300	62-11	1504-1509	
w62	300	62-12	1104-1109	
w62	400	62-13	0704-0710	
w62	400	62-14	0305-0309	

w62	500	62-15 0203-0206	
w64	100	64-1 3311-3403	33'11" - 34'03"
w64	100	64-2 3304-3309	
w64	200	64-3 3105-3110	
w64	200	64-4 2705-2710	
w64	200	64-5 2606-2611	
w64	200	64-6 2308-2400	
w64	300	64-7 1505-1510	
w64	300	64-8 1404-1408	
w64	400	64-9 1102-1107	
w64	400	64-10 0704-0709	
w64	400	64-11 0604-0608	
w64	400	64-12 0510-0602	
w64	400	64-13 0305-0310	
w64	500	64-14 0110-0203	
w73	100	73-1 3505-3510	35'05" - 35'10"
w73	100	73-2 3106-3111	
w73	200	73-3 3000-3006	
w73	200	73-4 2705-2710	
w73	200	73-5 2600-2607	
w73	300	73-6 2300-2305	
w73	300	73-7 2106-2200	
w73	300	73-8 1905-1910	
w73	300	73-9 1800-1806	
w73	300	73-10 1311-1404	
w73	400	73-11 1103-1109	
w73	400	73-12 1004-1008	
w73	400	73-13 0909-1001	
w73	400	73-14 0606-0700	
w73	400	73-15 0301-0307	
w73	500	73-16 0105-0111	
w74	100	74-1 3504-3507	35'04" - 35'07"
w74	100	74-2 3409-3500	
w74	200	74-3 3106-3110	
w74	200	74-4 3005-3008	
w74	200	74-5 2908-3001	
w74	200	74-6 2705-2709	
w74	300	74-7 2303.5-2308	
w74	300	74-8 2205-2209.5	
w74	300	74-9 2108-2201	
w74	300	74-10 1907-1911	
w74	300	74-11 1802-1806.5	
w74	300	74-12 1700-1705	
w74	300	74-13 1507-1511	
w74	400	74-14 1301-1305	
w74	400	74-15 1105-1109.5	
w74	400	74-16 0704-0709	
w74	400	74-17 0306-0310.5	
w74	400	74-18 0211-0305.5	

w74	500	74-19 0102.5-0107.5
w78	100	78-1 3406-3400 34'06" - 34'00"
w78	100	78-2 3010-3104
w78	200	78-3 2704-2710
w78	200	78-4 2305-2310
w78	200	78-5 2103-2110
w78	300	78-6 1703-1709
w78	300	78-7 1505-1510
w78	300	78-8 1406-1411
w78	400	78-9 1010-1103
w78	400	78-10 0611-0704
w78	400	78-11 0603-0609
w78	400	78-12 0306-0311
w78	400	78-13 0210-0302

VITA

Kelli Lynn Collins

Candidate for the Degree of

Master of Science

Thesis: PERMEABILITY PATHWAYS IN THE CANADIAN RIVER
ALLUVIUM ADJACENT TO THE NORMAN LANDFILL,
NORMAN, OKLAHOMA

Major Field: Geology

Biographical:

Personal Data: Born in Vinita, Oklahoma on August 18, 1976, the daughter of John A. (Tony) and Jan Collins.

Education: Graduated from Ketchum High School, Ketchum, Oklahoma in May 1994; received Bachelor of Science degree in Geology from Oklahoma State University, Stillwater, Oklahoma in December 1998. Completed the requirements for the Master of Science degree with a major in Geology at Oklahoma State in December, 2001.

Experience: Worked as a teaching assistant for the Department of Geology at Oklahoma State University from January 1999 to May 2000; employed by the U. S. Geological Survey as a student Hydrologic Technician from May 2000 to present.

Professional Memberships: Geological Society of America

